EDUARDO UMARAS

A New Method of Rigid Assemblies Stochastic 3D Tolerance Analysis Including Thermal Performance

São Paulo

2022

EDUARDO UMARAS

A New Method of Rigid Assemblies Stochastic 3D Tolerance Analysis Including Thermal Performance

Revised Version

Ph.D. Thesis presented at the Escola Politécnica da Universidade de São Paulo in partial fulfillment of the requirements for the Doctorate degree in Sciences.

Concentration area: Mechanical Engineering

Advisor:
Prof. Dr. Marcos de Sales Guerra Tsuzuki

São Paulo
2022

This copy has been revised and amended from the original version, with the sole responsibility of the author and with the consent of his advisor. The original of this document is available at EPUSP Mechanical Engineering Library.

Este exemplar foi revisado e alterado em relação à versão original, sob responsabilidade única do autor e com a anuência de seu orientador. O original deste documento está disponível na Biblioteca da Engenharia Mecânica da EPUSP.

São Paulo, June 13, 2022. / São Paulo, 13 de junho de 2022.

Author's signature / Assinatura do autor

Advisor's signature / Assinatura do orientador

Catalogação-na-publicação

Umaras, Eduardo
A New Method of Rigid Assemblies Stochastic 3D Tolerance Analysis Including Thermal Performance / E. Umaras -- versão corr. -- São Paulo, 2022.
186 p.: il. (algumas color.)

Tese (Doutorado) - Escola Politécnica da Universidade de São Paulo. Departamento de Engenharia Mecatrônica e de Sistemas Mecânicos.

1.Tolerância e ajustamento das peças 2.Produção industrial (Otimização) 3.Método de Monte Carlo 4.Processo de fabricação (Engenharia Mecânica) 5.Custo econômico I.Universidade de São Paulo. Escola Politécnica. Departamento de Engenharia Mecatrônica e de Sistemas Mecânicos II.t. III.Tsuzuki, Marcos de Sales Guerra, orient.

Nome: UMARAS, Eduardo

Título:A new method of stochastic 3D tolerance analysis of rigid assemblies including thermal performance

Tese de doutorado apresentada à Escola Politécnica da Universidade de São Paulo como requisito parcial para obtenção do título de Doutor em Ciências.

Aprovado em: 14 de abril de 2022.

Banca Examinadora

Prof. Dr. Marcos de Sales Guerra Tsuzuki (Presidente)

Instituição: Escola Politécnica - Universidade de São Paulo - EP-USP

Julgamento: Aprovado

Prof. Dr. Jonas de Carvalho (Titular)

Instituição: Escola de Engenharia de São Carlos - EESC - USP

Julgamento: Aprovado

Prof. Dr. Roberto Silvio Ubertino Rosso Junior (Titular)

Instituição: Universidade do Estado de Santa Catarina - UDESC

Julgamento: Aprovado

Prof. Dr. Ahmad Barari (Titular)

Instituição: University of Ontario Institute of Technology, UOIT

Julgamento: Aprovado

Prof. Dr. Fernando Humel Lafratta (Titular)

Instituição: Universidade do Estado de Santa Catarina UDESC

Julgamento: Aprovado

To my parents and to my grandparents

Acknowledgements

To my wife Regina for her great patience during all these years,

To Prof. Marcos de Sales Guerra Tsuzuki for his great support during this program.

Simple can be harder than complex: You have to work hard to get your thinking clean to make it simple. But it's worth it in the end ....

Steeve Jobs [2011]

RESUMO

Tolerâncias de posição e orientação são especificadas em componentes de um conjunto mecânico e apresentam grande importância no projeto, pois afetam sua qualidade, confiabilidade e custo. A análise de tolerâncias é um método de acumulação de tolerâncias de peças de um conjunto para obtenção de um valor global em uma direção. A abordagem oposta é a síntese de tolerâncias, ou alocação, onde as tolerâncias dos componentes são ajustadas por determinado critério para o atendimento de restrições de projeto ou para fins de otimização, tais como redução de custo. A síntese de tolerâncias é geralmente realizada quando os resultados do processo de análise de tolerâncias não atingem os requisitos de restrições de projeto. O alvo desta tese é o de propor um novo método de análise de tolerâncias em domínio tridimensional, incluindo simulação de fabricação e a consideração de efeitos térmicos funcionais. Um estudo de caso envolvendo um motor de combustão interna comprova a eficácia do método. A simulação de fabricação, baseada no método de Monte Carlo, fornece uma representação da distribuição estatística da variação do processo ao longo do intervalo especificado de tolerâncias. Esse recurso permite uma otimização do intervalo de tolerâncias do conjunto mecânico em cada uma das direções ortogonais e pode representar um significativo auxílio tanto em decisões de projeto como para a seleção de processos de fabricação. Uma característica do método proposto é a consideração de tolerâncias geométricas de posição como função de tolerâncias de orientação. Essa característica resulta em grande precisão, para grandes volumes de produção. O método também é voltado à aplicação e pode ser efetivamente aplicado na Indústria.

Palavras-chave: Distribuições multivariadas, análise de tolerâncias tridimensionais, Método de Monte Carlo, tolerâncias geométricas, motores de combustão interna.

ABSTRACT

Positional and orientation tolerances are specified in the components of a mechanical assembly and are of great importance in design, as they affect its quality, reliability, and cost. Tolerance analysis is a method of stacking the tolerances parts of an assembly to achieve an overall value in a given direction. The opposite approach is tolerance synthesis, or allocation, where the tolerances of the components are adjusted through a determined criterion for compliance with design constraints or for optimization purposes, such as cost reduction. The tolerance synthesis is generally performed when the results of a tolerance analysis process do not reach a design constraint requirement. The aim of this thesis is to propose a new method for tolerance analysis in a three-dimensional domain, including manufacturing simulation and consideration of functional thermal effects. A case study involving an internal combustion engine shows the efficacy of the method. Manufacturing simulation based on the Monte Carlo method provides a statistical distribution representation of process variation along a specified tolerance range. This resource can lead to optimization of the tolerance range of the mechanical assembly in each orthogonal direction and can also be a significant aid in design decisions and the selection of manufacturing processes. A feature of the proposed method is the consideration of geometric position tolerances as a function of orientation tolerances. The feature results in great accuracy at a high manufacturing volume. The method is application-oriented and can be applied effectively in the industry.

Keywords: Multivariate distribution, 3D tolerance analysis, Monte Carlo method, geometric tolerances, internal combustion engines.

Contents

List of Figures

List of Tables

1 Introduction

The specification of dimensional tolerances (DT) is of utmost importance in the development of mechanical designs. The quality of a product with respect to its functional behavior, reliability, durability, visual appearance, and even environmental sustainability, depends on the adequate DT specification [HOFFENSON et al., 2014]. Another important consideration regarding the concept of DT is its relationship with the cost of the product, that is, the lower the value of DT (the greater the accuracy of the dimensions), the higher the cost of a manufactured component, which affects the price of the product [WANG et al., 2019]. The conventional study of DT started in the unidimensional (1D) and two-dimensional (2D) domains [ANSELMETTI; LOUATI, 2005]. The approach of Geometric Dimensioning and Tolerancing (GD&T) brought a great improvement in the treatment of the DT concept. In addition to the definition and standardization of terms, the GD&T approach allows the expansion of the tolerance concept to the three-dimensional (3D) domain, where the position of a feature can be determined, as well as its conditions in the space, such as orientation, profile, and form [SCHLEICH; WARTZACK, 2015].

Today, and over the past decades, designs have been developed with computer-aided design (CAD) and computer-aided engineering (CAE). The resulting CAD digital data of engineering designs are used in computer-aided manufacturing (CAM) to produce parts not only in material removal/additive processes but also in tooling, such as for cast/injected molded and stamped parts. Any CAD mechanical design is developed considering the nominal or exact conditions of positioning, orientation, and form of the components of an assembly. However, any manufacturing process presents its inherent variation with respect to the intended nominal dimension. Therefore, in the mechanical design of parts, the nominal value of any feature must be linked to tolerances, used to specify a range between minimum and maximum values, allowing the design specification to comply with the process variation of the required features. This tolerance range is represented in different forms and is specified according to some rational design criteria that ensure that the product has adequate functional behavior, since the nominal value cannot be obtained in practice [BJORKE, 1989]. Integrated modules of CAD systems, known as computer-assisted tolerancing (CAT), were developed to allow consideration of manufacturing variations in the design specification. For the development of CAT software, several types of tolerance representation model must be created [ZHANG et al., 2018], the main ones are described in this text.

The specification of the DT of mechanical components is especially important when they are assembled. Generally, due to fit and/or functional purposes, assembly tolerances are considered design constraints and, in most cases, are identified as key product characteristics (KPC) or simply (KC) [MAZUR et al., 2011; WHITNEY, 2006]. Two criteria are used to check whether the assembly specification meets the design constraints: tolerance analysis and tolerance synthesis [LEE; WOO, 1990].

In **tolerance analysis**, the tolerances of the components accumulate in a sequence or in a **tolerance chain**, resulting in the overall tolerance of the assembly. Due to this, the method is also called *tolerance stack-up*. After CAD design modeling of each component in its nominal dimensions, tolerances are specified for its features, generally based on concurrent engineering [PENG; PENG, 2019]. When the assembly tolerance analysis is performed, its overall tolerance can be in compliance with one or more design constraints. If the design constraint of the assembly is attained, the components' tolerances are considered appropriate, and, in principle, no design action is required. In this case, loosening of component tolerances may be considered for other reasons, provided that a new analysis is performed afterwards [RENZI et al., 2018]. If the design constraint of the assembly is not met, the surplus tolerance value resulting from the tolerance analysis must be removed from one or more components of the assembly using some rational criteria. This process is known as **tolerance synthesis**, or *tolerance allocation*. Additionally, as a tool to design constraint compliance, tolerance synthesis can be used with the aim of optimizing implied variables such as cost, quality loss, or other variables. Therefore, in other words, tolerance synthesis can be considered as an adjustment of the tolerance analysis procedure to an adequate assembly tolerance within its dimensions [HALLMANN et al., 2020a].

Another important concept worth noting is that components in mechanical assemblies are in contact with each other **through surfaces**. This contact can be static or movable, as in the case of linkages and mechanisms. The components assembled in such a way form a succession of main dimensions that resemble trees, closed loops, or open loops. The tolerances involved in these main dimensions may also be arranged in series, forming the tolerance chains already cited.

The sources of variation that affect a mechanical assembly and that must be considered in the tolerancing design work are [CHASE et al., 1998]:

1. *The dimensional variation of individual components*, due to inherent variation in manufacturing processes;

2. *The geometric variation of the surface of a component which makes contact with the next component in the chain*, also due to manufacturing inaccuracies;

3. *Variation due to small kinematic adjustments among components*, which occurs due to the interaction of the characteristics of the components at the time of assembly. This occurs when contact between components occurs through small areas. The *tolerance shift* described ahead is an example of kinematic adjustment.

In addition to the sources of variation cited with respect to the fabrication and assembly processes, the causes of functional dimensional variation must be considered: temperature and mechanical loading, which can be evaluated by currently available CAE tools. The consideration of strains due to these variations causes must be considered, depending on each case, according to their magnitude order in relation to the manufacturing variations.

1.1 Motivation

The motivation for the theme of this thesis has been developed during several decades of the author's professional activity in the design of complex mechanical components and the corresponding assemblies, more specifically diesel engines and their application equipment. Despite the availability of powerful CAD and CAE resources, there is a lack of practical design tools to support designers' work, which could result in an effective design environment. The main reasons to mention are the following.

- CAT tools, when available, are considered “black boxes”, that is, design engineers do not know which method(s) have been considered to obtain the results;
- Up to it being known, there is no GD&T module for process variation simulation available in commercial software;
- Statistical analyzes depend on the scheduled production volume. CAT statistical tools, when available, are also black boxes regarding this aspect.
- CAT modules do not consider functional-dimensional variations because they are not integrated with CAE tools. Moreover, CAE dimensional simulation results, although accurate, are fully dependent on good estimates regarding input parameters, such as temperature.

1.2 Objective

The objective of this work is to develop a method for the tolerance analysis of rigid mechanical assemblies in a 3D space, focusing on its design application. The proposed method aims to overcome some observed gaps in the currently available work, described in Section 3, allowing its use in the design phase of a product. It aims to integrate the specification of GD&T requirements, process variation simulation through statistical tolerancing, and the consideration of functional strain caused by temperature gradients into a unique algorithm.

1.3 DT Research Current Status

Several tools used in tolerance analysis have been created in the last decades, in conjunction with the rapid development of computer hardware and software. As noted above, CAD systems work with nominal dimensions and, conversely, manufacturing processes present their innate and unavoidable dimensional variation. As a consequence, tolerance analysis methods need ways to consider the spatial condition of an actual fabricated surface in relation to a theoretical CAD surface.

Figure 1 presents a taxonomy of the theme DT. The approach of the main areas, tolerance analysis and tolerance synthesis, has already been made previously.

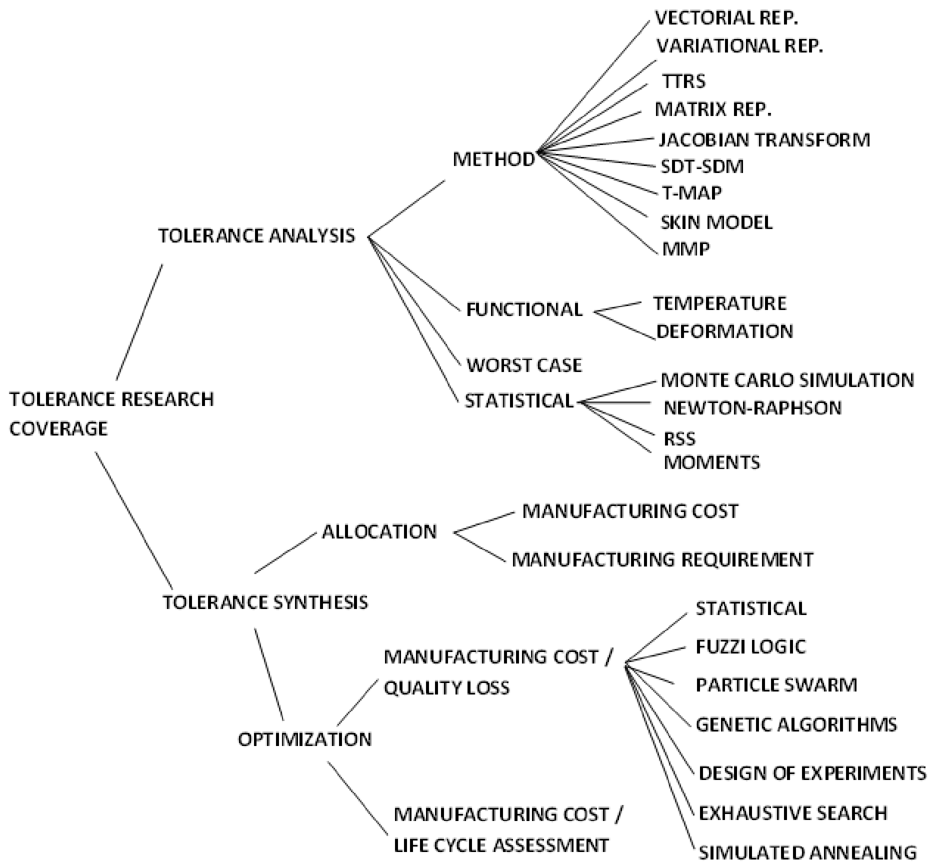

Figure 1 – An overview of the extensive field of DT research. (Source: author).

As cited in the objective, this thesis aims to develop a new approach to tolerance analysis, the content of which can be summarized as follows.

- Method: A new proposal for 3D geometrical stacking for rigid assemblies is presented, which considers the most common form of restraining degrees of freedom (DoF) observed in industrial practice, including tolerance-shift errors. The GD&T orientation variation is considered within the dimensional variation.

- Functional strain: the influence of the effects of the average temperature on the basic dimensions is also considered. Mechanical load deformation can be considered when available using computer-assisted methods. However, since rigid assemblies are concerned, the deformation under load must be considered very small by design principles;

- Worst Case (WC): the WC tolerance values are considered as references in the results;
- Statistical: a simulation using random values is conducted in each tolerance of the considered chain, either positional or orientational, including the assembly shifts.

It can be seen that the current literature on the subject lacks some important aspects with respect to the effective applicability of the developed methods. The main gaps that need to be addressed are the following.

- Some methods consider specific theoretical purposes, and others integrate already developed theories in an attempt to widen their practical applicability. For example, statistical tools are difficult, if not impossible, to be considered concurrently, due to the high mathematical complexity generally involved;
- The great majority of the available methods are aimed at manufacturing variations. Functional variations are not considered at all;
- As can be seen in most of the works, very simple examples are used, and, even so, their solutions involve great complexity. The application to more realistic cases could be very troublesome;
- As mentioned, in practice, components are assembled through surfaces and located by geometric features or mechanical elements, which restrain the remaining DoF. Some methods of tolerance analysis consider a point-to-point tolerance chain. However, assembly shifts (caused by gaps between the hole surfaces and fasteners) can present a significant effect, and it is not clear how they can be considered in these methods. Obviously, assembly shift does not occur in press fits;
- The orientation deviations between two points that restrict one or more DoFs in a surface depend on the orientation of the surface. This is also not clearly considered in the available methods and how the surface orientation tolerance is connected to its position tolerance;
- The theoretical methods are adequate for implementation in CAD and CAT software, as was the case of T-Map in 3D ACISModeler [HE et al., 2016] and CATIA-V5 [ANSELMETTI et al., 2010]. Independent design tools provide much more flexibility to include specific design needs in custom designs.

1.4 Thesis Structure

The text of the thesis is structured as follows. Chapter 2 describes the necessary theoretical background used in the development of the work, consisting of GD&T definitions, such as tolerance of form, tolerance of orientation, tolerance of location, and tolerance of profile. Some concepts related to 3D tolerance analysis and functional tolerances, mainly related to thermal effects, are also included. Other interesting concepts related to the subject of the thesis are found in the Appendix A. Chapter 3 presents a bibliographic review, where the concepts introduced in Chapter 2 are used to facilitate comprehension and comparison between proposals. The review follows the structure presented in Fig. 22: method, functional, worst case, and statistical. Chapter 4 explains the proposed method, where the tolerance analysis process is divided into modules. The proposed method combines GD&T, statistical simulation (considering manufacturing variation), and the effect of thermal functional strain on dimensions. Chapter 5 exemplifies the proposal through a case study of an internal combustion engine, where the results are presented and commented on demonstrating the effectiveness of the method.

Finally, chapter 6 concludes the work with the findings and suggests future work.

2 Theoretical Background

This chapter presents the definitions and concepts necessary for a proper understanding of this thesis. Depending on the familiarity of the reader with the subject approached, the first section can be skipped, since the referenced terms along the text are linked to the corresponding definitions in this chapter. Additional non essential concepts related to the subject can be found in Annex A.

2.1 Geometric Tolerancing

The Geometric Dimensioning and Tolerancing (GD&T) approach has been conceived to address issues in 3D design practice. The main standards referring to this subject are ASME Y14.5.1.M [ASME..., 2009] and ISO 1101 [ISO..., 1983], which establish uniform practices for stating, interpreting, dimensioning, tolerate and providing requirements for use in engineering drawings and related documents. The standards are very similar in content. The ASME consists of a single standard and is preferred in practice. The ISO standard consists of several other standards that cover specific items. Because of this, the ASME standard has been chosen to refer to the concepts and definitions presented in this section, the only ones necessary for understanding this text. As the standards use the metric system, all dimensions shown in the figures are in millimeters.

2.1.1 Definitions

1. Feature: a physical portion of a part such as a surface, pin, hole, or slot, or its representation on drawings, models, or digital data files [ASME..., 2009]. It is worth noting that this definition applies to the GD &T concept - other definitions are expected in different areas.

2. Tolerance: the total amount that a specific dimension can vary. The tolerance is the difference between the maximum and minimum limits [ASME..., 2009, ch. 1].

3. Position: the location of one or more features of size relative to one another or to one or more datums [ASME..., 2009, ch. 7].

4. Orientation: is a geometric notation that references the position of a feature based on a specific direction. Orientation defines the direction of a feature with respect to a given reference - parallel, perpendicular or other angular relationship.

5. Geometric tolerance: the general term applied to the category of tolerances used to control size, form, profile, orientation, location and runout [ASME..., 2009].

6. Datums: theoretically exact points, axes, lines, and planes [ASME..., 2009, ch. 4].

2.1.2 The basic Dimension

Basic dimensions are theoretically exact dimensions [ASME..., 1995, pp 3, 24]. The basic dimensions are specified in parallel to the main axes. These dimensions define the lengths Lx, Ly, Lz of the respective vectors from the datum to any point P, as illustrated in Figure 2. The vectorial sum of the vectors of the components results in a vector of length L.

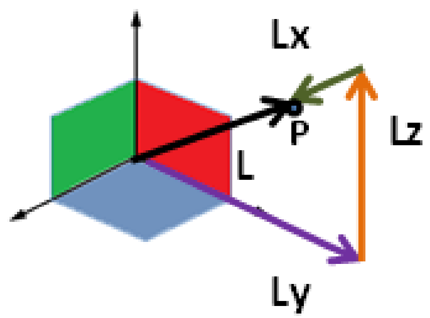

Figure 2 – Vectors Lx, Ly, Lz parallel to main axes represent the basic dimensions of a point on a component, in relation to a reference frame. (Source: the author).

2.1.3 Reference frames

A datum reference frame is three mutually perpendicular intersecting datum planes [ASME..., 2009, p. 48]. When a datum reference frame is specified, the body is impeded in dislocating in any degree of freedom. This occurs with the first component of a mechanical assembly, which is immobilized in space. When a datum for a component is established, three orthogonal planes $A - B - C$, with intersections being the axes of the three directions $X - Y - Z$ and an origin **o** are defined, as shown in Figure 3.

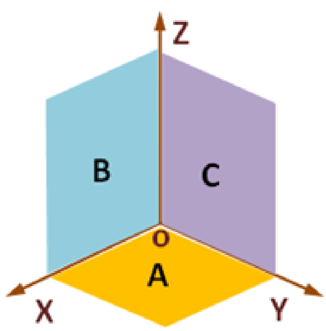

Figure 3 – A datum defined by three axes and three orthogonal planes. (Source: the author).

2.1.4 Tolerance Zone

The tolerance zone is the distance between two boundaries disposed equally or unequally about the true (nominal) profile [ASME..., 2009, ch. 8]. The tolerance zone is a delimited area or region of the tolerance field considered for a specific purpose, for example, a flatness tolerance zone of 0.1 mm and a flatness tolerance zone of 0.05 in 100 mm of length. When positional tolerances are specified in each of the orthogonal planes A, B and C, their neighboring point P in space assumes an ellipsoidal shape, as illustrated in Figure 4.

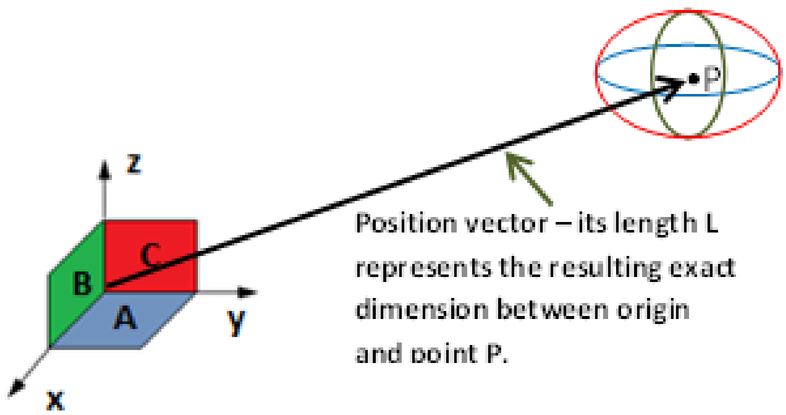

Figure 4 – A 3D tolerance zone positioned in relation to a reference frame. (Source: the author).

2.1.5 Tolerance of Position

One of the major contributions of GD&T approach is the concept of position tolerances. Figure 5 illustrates the position dimensioning of the conventional non-geometric case. The range of tolerances in the directions x and y is given by

$$|x| \leq t_x/2 \quad \text{and} \quad |y| \leq t_y/2. \tag{2.1}$$

Holes are the main features used to position and fasten mechanical elements. The concern about the conventional position dimensioning case is caused by the material removal processes of holes, such as drilling and reaming. In Figure 5, the areas between the edges of the tolerance square and a circumscribed circle are specified but not used in practice, as the cutting process is round-shaped.

The GD&T approach has solved this problem as illustrated in Figure 6. There is a relationship between the variates x and y to accomplish the specification, that is,

$$\sqrt{x^2 + y^2} \leq d/2. \tag{2.2}$$

.

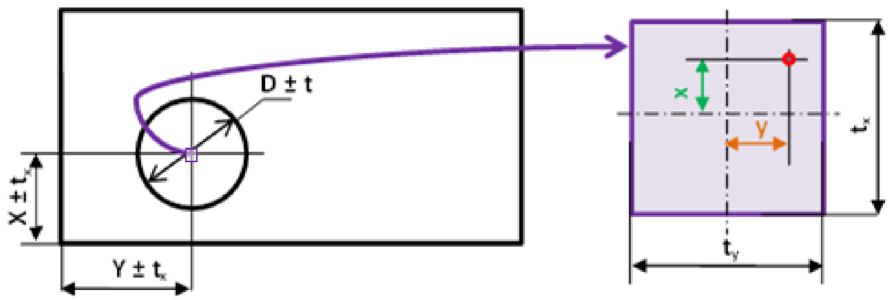

Figure 5 – Tolerance of a feature in a plane for non-geometric tolerancing. The position tolerance fields are rectangular or square shaped. (Source: the author).

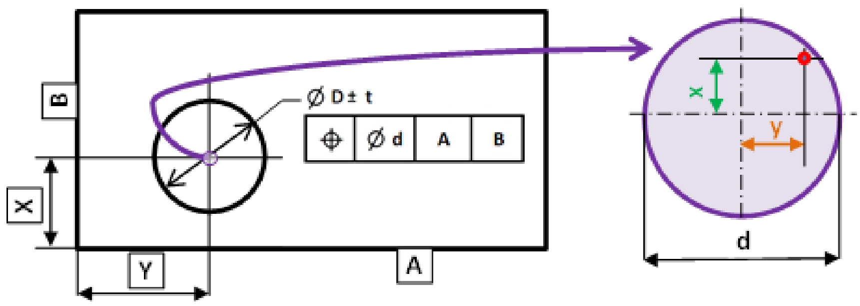

Figure 6 – Positional tolerance of a feature in a plane – the shaded circle limits the permissible position allowed for the displacement of the center of the feature. (Source: the author).

2.2 Tolerance of Form

Tolerances of form control straightness, flatness, circularity, and cylindricity. Each of the tolerances is described in sequence.

2.2.1 Straightness

Straightness is a condition where an element of a surface, or the derived median line, is a straight line. A straightness tolerance specifies a tolerance zone within which the considered element of a surface or the derived median line must lie. A tolerance of straightness is applied in the view where the elements to be controlled are represented by a straight line [ASME. . . , 2009, p. 91]. Figure 7 illustrates the tolerance.

2.2.2 Flatness

Flatness is the condition of a surface or a derived median plane having all elements in one plane. A flatness tolerance specifies a tolerance zone defined by two parallel planes

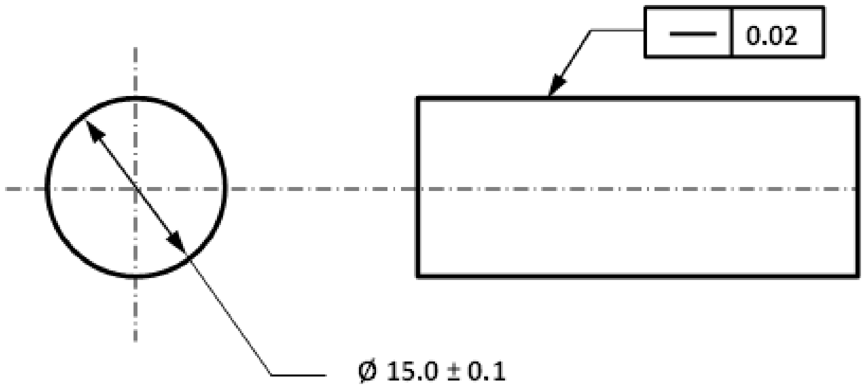

Figure 7 – Each longitudinal element of the surface must lie between two parallel lines (0.02 mm apart) where the two lines and the axis of the unrelated actual mating envelope share a common plane. The feature must be within the specified limits of size and the boundary of perfect form at maximum material condition (MMC) (15.1 mm). (Source: based on [ASME..., 2009, p. 92]).

within which the surface or the derived median plane must lie. When a flatness tolerance is specified on a surface, the feature control frame is attached to a leader directed to the surface or to an extension line of the surface. It is placed in a view where the surface elements to be controlled are represented by a line, as shown in Figure 8.

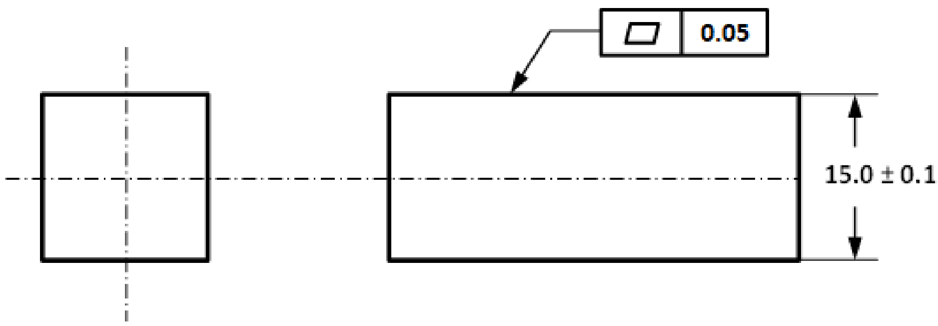

Figure 8 – The surface must lie between two parallel planes 0.05 mm apart. The surface must be within the specified limits of size $15 \pm 0.1mm$. (Source: based on [ASME..., 2009, p. 94]).

2.2.3 Circularity

Circularity, or roundness, is a condition of a surface [ASME..., 2009, p. 94]:

1. for a feature other than a sphere, all points of the surface intersected by any plane perpendicular to an axis or spine (curved line) are equidistant from that axis or spine;

2. for a sphere, all points of the surface intersected by any plane passing through a common center are equidistant from that center.

A circularity tolerance specifies a tolerance zone bounded by two concentric circles within which each circular element of the surface must lie and is applied independently at any plane described in the previous surface conditions. Figure 9 shows its representation.

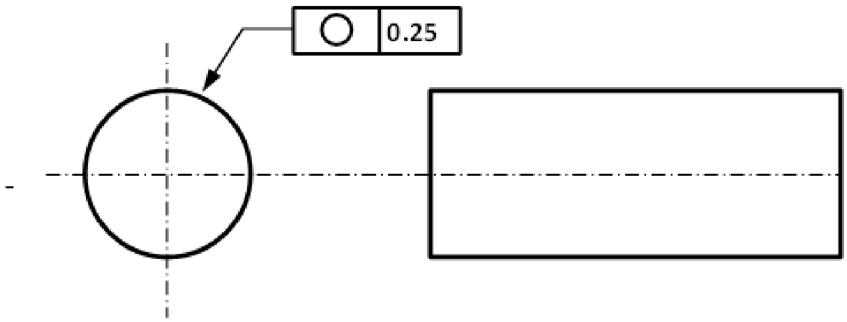

Figure 9 – Each circular element of the surface in a plane perpendicular to an axis must lie between two concentric circles, one having a radius 0.25 mm larger than the other. Each circular element of the surface must be within the specified limits of size. (Source: based on [ASME..., 2009, p. 96]).

2.2.4 Cylindricity

Cylindricity is a condition of a surface of revolution in which all points of the surface are equidistant from a common axis.

A cylindricity tolerance specifies a tolerance zone bounded by two concentric cylinders within which the surface must lie. In the case of cylindricity, unlike that of circularity, the tolerance applies simultaneously to both circular and longitudinal elements of the surface (the entire surface) [ASME..., 2009, p. 95]. Figure 10 illustrates the representation.

2.3 Tolerances of Orientation

An orientation tolerance controls parallel, perpendicular, and all other angular relationships. The specification of an orientation tolerance must consider that the feature is related to one or more datums. Orientation tolerances are restricted only in the rotational DoF relative to the referenced datums; they are not restricted in the translational DoF.

2.3.1 Angularity

Angularity is the condition of a surface, the center plane of the feature, or the axis of the feature at any specified angle from a datum plane or the datum axis [ASME..., 2009, p.

99] (see Figure 11).

2.3.2 Parallelism

Parallelism is the condition of the center plane of a surface or feature, equidistant from all points of a datum plane; or the axis of a feature, equidistant along its length from one or more datum planes or datum axes [ASME..., 2009, p. 99] (see Figure 12).

2.3.3 Perpendicularity

Perpendicularity is the condition of a surface, the center plane of the feature or the axis of the feature at a right angle to a datum plane or datum axis [ASME..., 2009, p. 99] (see Figure 13).

2.4 Tolerances of Location

Location tolerances include position, concentricity, and symmetry, which are used to control the following relationships [ASME..., 2009, p. 108]:

- Center distance between features of size such as holes, slots, bosses, and tabs;
- location of features of size, such as described in the former item above, as a group of datum features, such as plane and cylindrical surfaces;
- coaxiality of features of size;
- concentricity or symmetry of features of size-center distances of correspondingly located feature elements, equally disposed about a datum axis or plane.

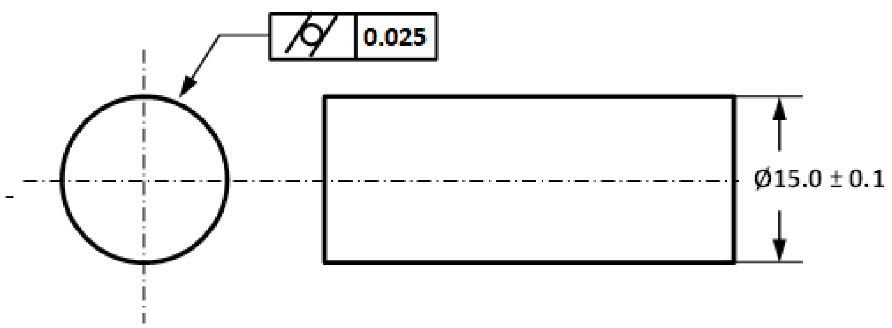

Figure 10 – The cylindrical surface must lie between two concentric cylinders, one having a radius 0.025 mm larger than the other. The surface must be within the specified limits of size (15 ± 0.1 mm). (Source: based on [ASME..., 2009, p. 96]).

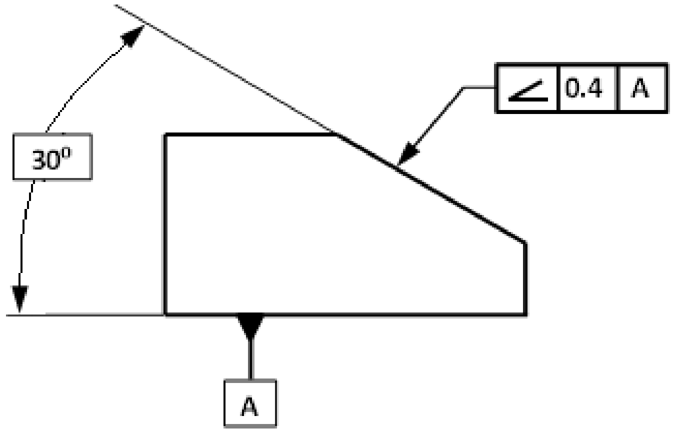

Figure 11 – The surface must lie between two parallel planes 0.4 mm apart which are inclined at 30° to datum plane A. (Source: based on [ASME..., 2009, p. 100]).

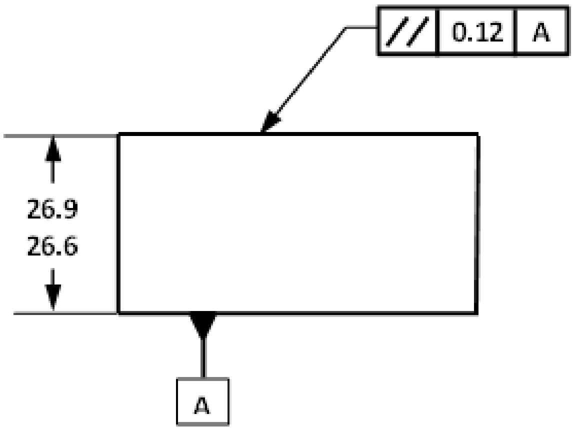

Figure 12 – The surface must lie between two parallel planes 0.12 mm apart which are parallel to datum plane A. The surface must be within the specified limits of size. (Source: based on [ASME..., 2009, p. 100]).

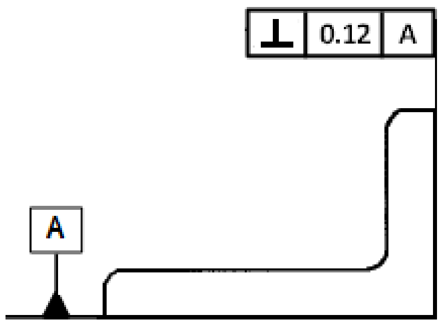

Figure 13 – The surface must lie between two parallel planes 0.12 mm apart which are perpendicular to datum plane A. (Source: based on [ASME..., 2009, p. 100]).

In this text, only position tolerances are addressed. Coaxiality and concentricity are not used because they are not referenced in its content.

Position is the location of one or more features of size relative to each other or to one or more datums. A positional tolerance defines either of the following:

1. A zone within which the center, axis, or center plane of a feature of size is permitted to vary from a true (theoretically exact) position;

2. a boundary (where specified on an MMC or least material condition (LMC) basis), defined as the virtual condition, located at the true (theoretically exact) position that may not be violated by the surface or surfaces of the considered feature of size.

The basic dimensions establish the true position from the specified datums and between the interrelated features. A positional tolerance is indicated by the position symbol, a tolerance value, applicable material condition modifiers, and appropriate datum references placed in a feature control frame, as shown in Figure 14.

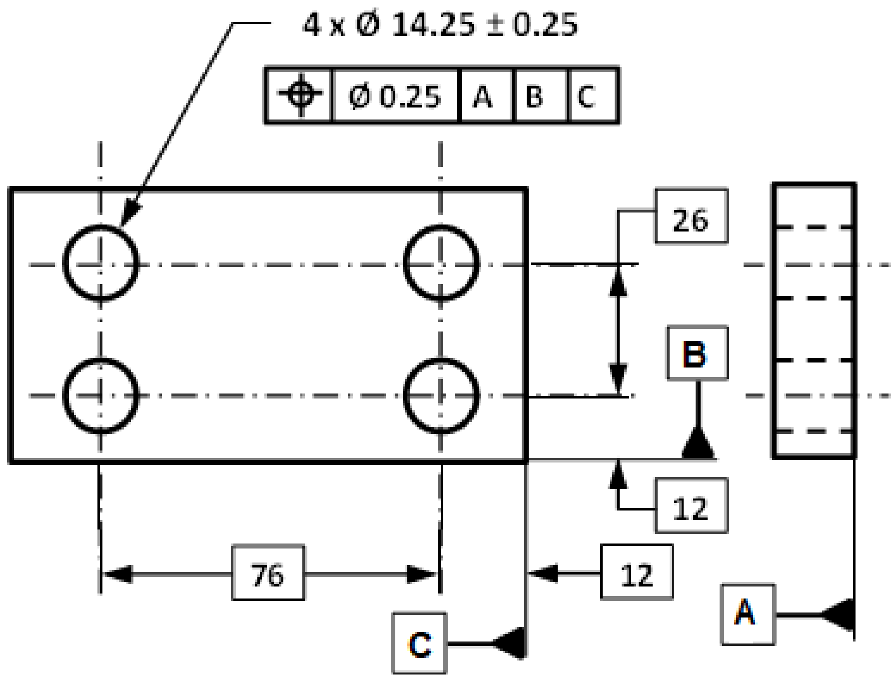

Figure 14 – The position of the centers of the four holes must lie within a circle of diameter 0.25 mm in relation to datums A, B, and C. The center distances of the holes are basic dimensions. (Source: based on [ASME..., 2009, p. 113]).

2.5 Tolerances of Profile

A profile is an outline of a surface, a shape made up of one or more features, or a 2D element of one or more features. Profile tolerances are used to define a tolerance zone to control the form or combinations of size, form, orientation, and location of feature(s) relative to a true profile. Depending on the design requirements, the profile tolerance zones may or may not be related to datums. A digital data file or an appropriate view of a drawing shall define the true profile. A true profile is a profile defined by a basic radius, a basic angular dimension, basic coordinate dimensions, basic size dimensions, undimensioned drawings, formulas, or mathematical data, including design models. When used as a refinement of a tolerance of size created by tolerance dimensions, the tolerance of profile must be within the size limits [ASME. . . , 2009, p. 158]. Figure 15 illustrates an example of common profile tolerance. Other specific cases are found in the cited reference.

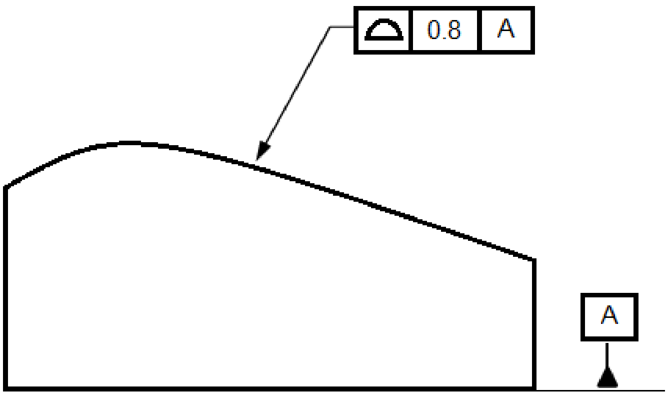

Figure 15 – 0.8 mm wide tolerance zone equally disposed about the true profile (0.4 mm each side). (Source: based on [ASME. . . , 2009, p. 161]).

2.6 Concepts Regarding 3D Tolerance Analysis

The aim of this section is to present a synthesis of the theoretical concepts used in the development of this thesis. A sequence of applicable concepts is presented to facilitate the explanation of the method.

2.6.1 Degrees of Freedom

DoF describes the number of independent motions that are allowed to a body. All bodies can move in six DoFs in a 3D space, three in linear parallel displacement to each of the main orthogonal axes, and three in rotation in relation to these axes, as illustrated in Figure 16. The referenced names of the movements of a rigid body [CRAIG, 2014, p.41] are mentioned in this text. *Regarding geometric tolerances, in principle displacement DoFs represent positional tolerances and rotational DoFs represent orientation tolerances.*

Figure 16 – DoF in a 3D space. (Source: the author).

2.6.2 3D Tolerance Chains

The thesis proposal considers a representative system of the vast majority of applications of mechanical assemblies in industry where rigid components are assembled in a chain. Compliant (non-rigid) components must consider the theory of elasticity as applicable and are not referenced in this text. The exact length vectors of the former component define the position of a tolerance zone, where the origin of the datum frame of the next component is placed, as shown in Figure 17. This configuration resembles a frame mapping in robotics [CRAIG, 2014, p. 23]. The difference is that, in our case, the tolerance zones are considered.

The tolerance zone of the former component affects the position of the next component by displacing its datum frame (exact form and dimensions) in orthogonal directions X, Y and Z. The position vector of the next component moves in a parallel direction in relation to the former component if only its positional tolerance zone is considered. The present method also accounts for the orientation variations specified in the design and considers the angular displacements of the contact surfaces due to the orientation tolerance effect. The method considers a simple geometric treatment to achieve the desired results.

2.6.3 Assembly Shift

The datum of the subsequent component is placed through a surface contact within the tolerance zone of the former. The shape and dimensions of the tolerance zone are a function of statistically distributed manufacturing variation. When accurate placement is required, the positioning between components is restrained through tight-fit elements, such as guide pins (dowel). If the positioning between the contact components is not

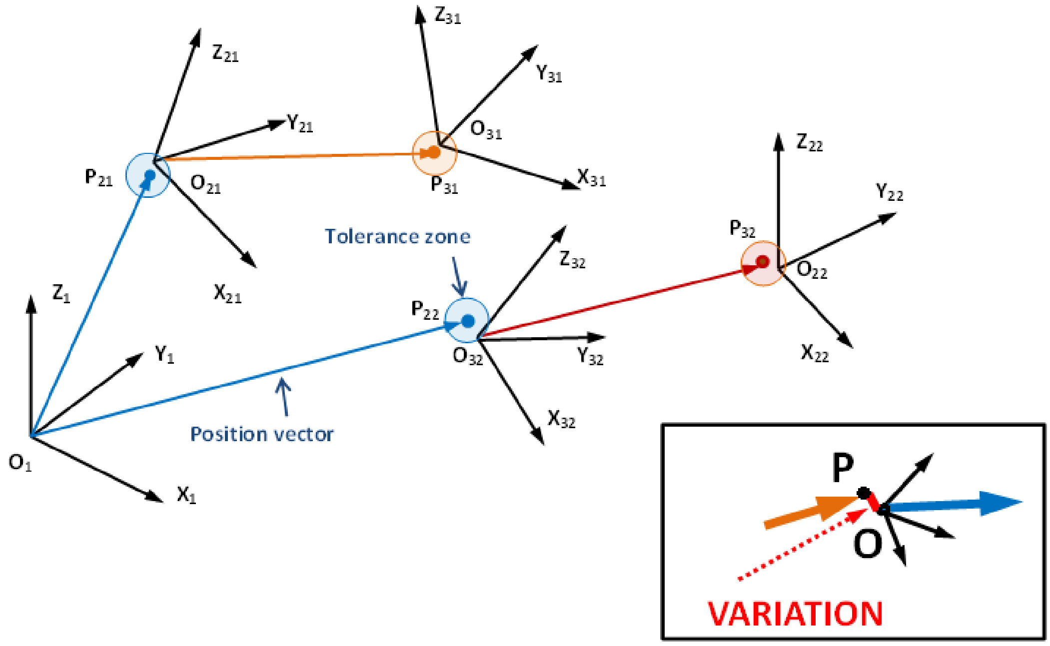

Figure 17 – Datum frames of components of a rigid mechanical assembly positioned at the tolerance zones of the former components. (Source: the author).

restricted, a assembly shift [FISCHER, 2011, p. 62] must be considered. This occurs, for example, when parts are fastened by bolts or studs, in the floating fastener case [ASME..., 2009, p. 191]: the clearance between their diameters and their respective holes causes the positioning of the parts to vary, regardless of positional tolerance. Figure 18 illustrates an example of a WC assembly shift. Assembly shift values are independent of positional tolerances, so both must be added.

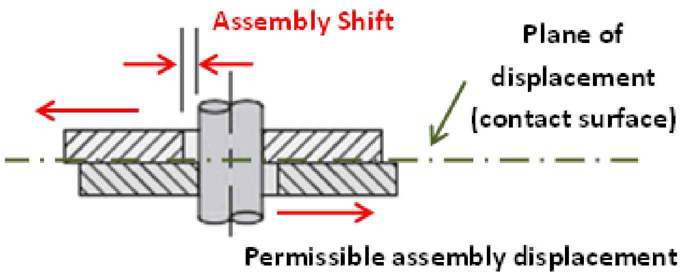

Figure 18 – Section showing an assembly shift between parts (WC displacement in one direction). (Source: the author).

2.6.4 Tolerance Zone Including an Assembly Shift

In mechanical assemblies, in most cases in practice, a circular positional tolerance and an orthogonal straight zone are commonly observed in practice. This feature arises from the rotational behavior of the material removal processes used to manufacture internal and external diameters. This condition occurs when the surface of parts is fastened with bolts or studs and is restricted or not by guide pins. The positional tolerance of the surface in each part is a volume limited by the shape of the surface and the straight tolerance zone. Orientation tolerances, such as parallelism, generally are an additional constraint, which will be discussed later in the text. Figure 19 illustrates a situation involving flat surface contact between parts and an assembly shift condition.

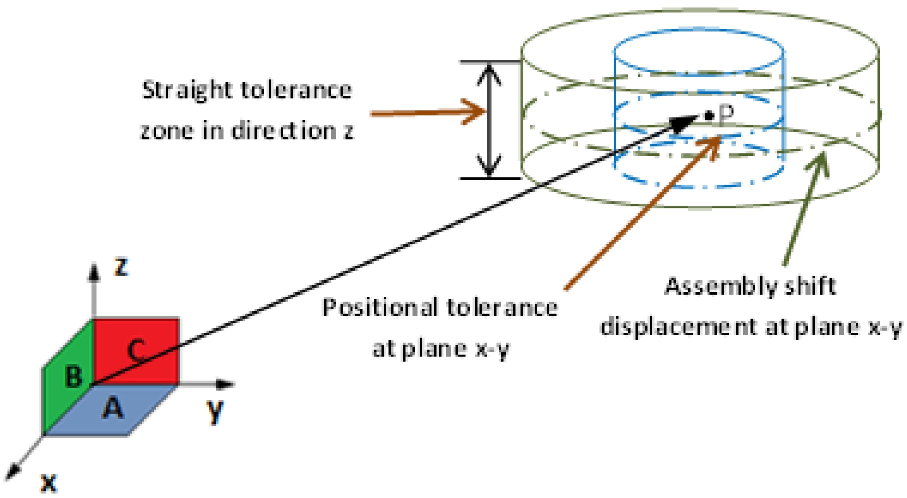

Figure 19 – A 3D positional tolerance zone and assembly shift in relation to a datum. (Source: the author).

2.6.5 The WC Method

The WC method assumes that all dimensions in the tolerance stackup may be at their worst-case maximum or minimum, regardless of the improbability. No study is necessary as the limits are already defined. [FISCHER, 2011, p. 57]. Let the assembly tolerance T_{ASM} be determined by linearly adding the tolerances of the component T_i. Each component dimension is assumed to be at its maximum or minimum specified limit simultaneously, resulting in the worst possible assembly limits [CHASE; GREENWOOD, 1988, p. 4]. The unique feature of the WC method is that all assemblies will meet the specified assembly limit. However, a consequent big issue is that, as the number of parts in the assembly increases, the component tolerances must be greatly reduced to meet the assembly limit, leading to higher or even impracticable production costs.

For 1D assemblies

$$T_{ASM} = \sum T_i. \tag{2.3}$$

For multidimensional assemblies

$$T_{ASM} = \sum (|\partial f / \partial x_i| T_i) \tag{2.4}$$

where x_i are the nominal dimensions of the components and $f(x_i)$ is the assembly function that describes the resulting dimension of the assembly. This output can be a clearance (positive value) or interference (negative value). The partial derivatives represent the sensitivity of the assembly tolerance to variations in the dimensions of individual components.

According to Evans [1974, p. 189], another way to state the WC policy is that tolerances must be assigned to the components of the mechanical assembly in such a way that *the probability that the assembly will not assemble or will not function properly is zero.*

As the limits present fixed values, generally the inspection of parts specified by this method can be inspected by a go/no-go or high/low calipers [JACK, 2020], [EVANS, 1974]: if the dimension passes through the go (high) aperture, it means that the dimension is lower than the maximum specified; the opposite also applies.

The major concern with this method, as already cited, is the manufacturing cost involved, due to the accuracy of the process required to ensure the specified tolerance limits.

2.6.6 Tolerance Analysis and Tolerance Synthesis

The concepts of tolerance analysis and tolerance synthesis are crucial in the study of DT. A brief comment on the approach has already been made in Section 1.

One of the original works that dealt with these concepts was developed by Chase and Greenwood [1988]. Figure 20 illustrates the comparison between the concepts. In tolerance analysis, the component tolerances are accumulated to form the final tolerance of the assembly, which must be within the assembly constraint specification. In tolerance synthesis, the opposite happens, i.e., the assembly tolerance restricted by the specified constraint must be allocated among the components by means of a determined criterion.

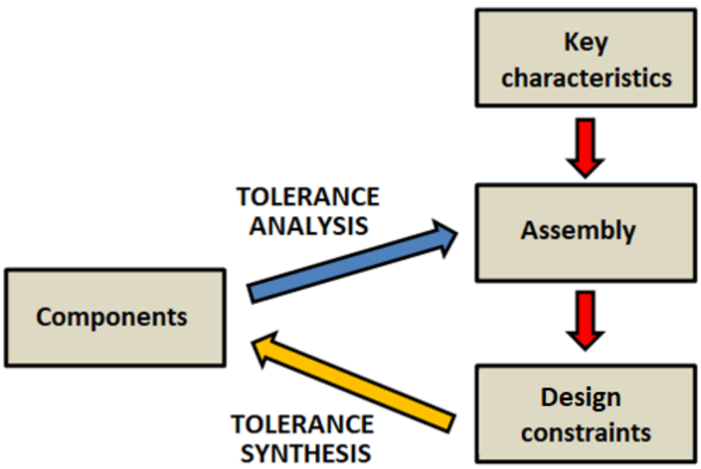

Figure 20 – Tolerance analysis and synthesis processes. (Source: the author).

Tolerance Analysis

In the tolerance analysis process, also called *tolerance stacking* or *tolerance accumulation*, the tolerances of the components are known (specified) and the resulting assembly tolerance is calculated [CHASE; GREENWOOD, 1988, pp. 2-3]. Its basis in design is an analytical model for the accumulation of tolerances in a mechanical assembly of components. The two most common models used in engineering design are the WC and the root sum of squares (RSS). Other general cases are described by Chase and Greenwood [1988].

Tolerance Synthesis

In tolerance synthesis, also known as *tolerance allocation* or *tolerance distribution*, the tolerance of the assembly is specified by the design requirements, while the tolerances of the components must be determined. The available assembly tolerance must be distributed or allocated among the components in some rational way [CHASE; GREENWOOD, 1988, p. 3]. The rational allocation of component tolerances requires the establishment of some rules which are not described, since tolerance synthesis is beyond the scope of our work. The procedure is performed when the output of the tolerance analysis does not meet the design requirements or when an optimization study is required. They are allocated by:

- proportional scaling;
- constant precision factor;
- using optimization techniques;
- Lagrange multipliers.

2.6.7 Statistical Tolerances

Statistical distributions can be used to predict the "yield" of an assembly, that is, the number or fraction of assemblies that are likely to fall within the specified limits [CHASE; PARKINSON, 1991]. In the tolerance analysis in the WC, the probability that the assembly will not assemble or function properly is null, since, as the name WC indicates, the worst case of assembly possibilities is contemplated. The *statistical tolerance* (ST) is used to relax this requirement and to allow the probability to be greater than zero, but is usually very small. However, when the probability is allowed to be nonzero, that is, when the tolerances are such that a certain percentage of assembly production may be out of specification, this statement must be quantified. This quantification allows component tolerances to be defined as probability distributions. Thinking about the consequences of a certain little percentage of components being out of dimensional specification, this can lead to an assembling interference or even to a product failure. However, assembly concerns can be managed by simply replacing one component. Failures, on the other hand, can also occur due to a myriad of other causes, such as material failure due to porosity, lack of lubrication holes, etc. According to Evans [1974, p. 189], a portion between 0.1 and 1.0% would be acceptable with respect to product failures. If the range of 6σ is considered ($\sigma =$ the standard deviation), representing a probability of 99.7% in a normal distribution, this can be considered coherent. Only in cases in which personal safety and/or high monetary amounts are involved, this procedure may not be applicable. To demonstrate the effectiveness of the use of ST, the same author replicates a classic example of Shewhart's classic work [SHEWHART, 1931]: he compares a stack assembly of ten identical discs, where the height must present a tolerated plus/minus dimension:

- Surely, in the WC, the tolerated thickness of each disc is exactly the tolerated height of the stack divided by ten;
- If the ST method is applied to the same stack of discs with a centralized mean and a range of $\pm 3\sigma$, the probability that the stack would be outside the tolerated dimension is of the order of 10^{-12}, that is, in practice it would not occur. In the case of mass production, this percentage can be used to estimate the number of rejected assemblies.

However, the cost due to the additional precision of machining the discs in the WC is much higher than in the ST one. For a high production volume, the cost penalty would be very high.

In another work Evans [1975b, p. 73] treats the test (inspection requirement) difference between the WC and ST methods:

- In the WC (high/low tolerancing), each single component must be accepted or not;
- In the ST, the acceptance is based on the statistical distribution of the lot (sampling).

Chase and Parkinson [1991] present a very detailed work on ST in tolerance analysis. They identify the different models described below.

The Root-Sum-of-Squares Method

In the root-sum-of-squares (RSS) method, the component's RSS tolerances are added. The low probability that the WC combination occurs is statistically taken into account, assuming a normal or Gaussian distribution for component variations. It is commonly assumed that the tolerance ranges correspond to six standard deviations (6σ or $\pm 3\sigma$) (see Figure 21).

Consequently, the component tolerances may be significantly increased in relation to the WC method, since they add RSS. For 1D assemblies:

$$T_{ASM} = [\sum T_i^2]^{1/2}, \tag{2.5}$$

where T_{ASM} is the tolerance of the assembly and T_i are the tolerances of the components. For multidimensional assemblies

$$T_{ASM} = [\sum(\partial f/\partial x_i)^2 T_i^2]^{1/2}. \tag{2.6}$$

RSS analysis generally predicts too few rejects compared to real assembly processes. This is because the normal distribution is only an approximation of the true distribution, which may be flatter or skewed. The mean of the distribution may also be shifted from the midpoint of the tolerance range. To account for these uncertainties, a more general form of the RSS model is frequently used [CHASE; PARKINSON, 1991]:

$$d(U) = C_f \cdot Z \left[\sum \left(\frac{\delta f}{\delta x_i} \right)^2 \left(\frac{T_i}{Z_i} \right)^2 \right]^{(1/2)} \leq T_{ASM}, \tag{2.7}$$

where Z is the number of standard deviations desired for the specified assembly tolerance; Z_i describes the expected standard deviations for each component tolerance; C_f is a correction factor added to account for non-ideal conditions. The typical values for C_f range from 1.4 to 1.8.

Regarding Z_i, a conservative value may be taken as $\sqrt{3}$ [CHASE; PARKINSON, 1991, p. 24]. For a normal truncated distribution due to inspection, a value of $\sqrt{3} < Z_i < 3$ may be considered [SPOTTS, 1983].

Estimated Mean Shift

Simple RSS analysis assumes that the variation of each component dimension is symmetrically distributed about the mean or nominal dimension. This is a theoretical concept that, in most practical cases, does not apply (see Figure 21).

In real processes, the mean is shifted due to:

- Setup errors or drift: ignoring mean shifts can be very detrimental, resulting in large errors in estimates of the number of assemblies within specification limits [EVANS, 1975b].
- Time-varying parameters, such as tool wear [SPOTTS, 1983, p. 98].

Further modifications to the RSS model were proposed to take into account mean shifts or biased distributions, where tolerance accumulation is represented as a sum of WC plus an RSS sum [CHASE; PARKINSON, 1991]. Greenwood and Chase [1987], and Chase and Greenwood [1988] introduced an *estimated mean shift factor m_i varying between* 0 *and* 1.0, which quantifies the expected mean shift as a fraction of the specified tolerances. The following is defined.

$$dU = \sum \left| m_i \frac{\delta f}{\delta x_i} T_i \right| + \left[\sum (1 - m_i)^2 \frac{\delta f^2}{\delta x_i} T_i^2 \right]^{1/2} \leq T_{ASM}. \tag{2.8}$$

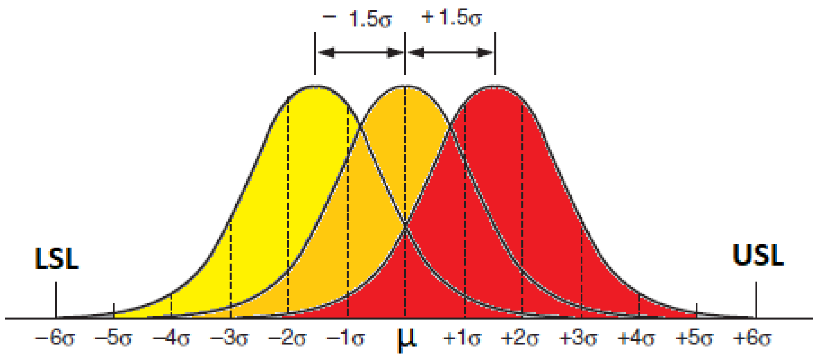

Figure 21 – The effect of a 1.5 σ shift of the normal distribution mean (LSL = lower specification limit / USL = Upper specification limit). (Source: based on [BREYFOGLE, 2003, p. 14]).

Six sigma

According to Linderman et al. [2003, p. 194], the Six Sigma is a management tool, which concept originated by Motorola Inc. in the USA about 1985, due to the threat they were facing from Japanese competition in the electronics industry. At that time, they needed to make drastic improvements in quality levels. Six Sigma is considered in the tolerance study due to the statistical parameters used in its formulation.

Taking into consideration the manufacturing processes, a versatile feature of the Six Sigma model is its ability to distinguish the process capability behavior [CHASE; PARKINSON, 1991, p. 25]:

- In the short term, the process capability quantifies the spread of the process, defined as 6.0 times its standard deviation ($6\sigma_i$);

- Over the long term, the mean of a process may drift from a lot to a lot for many reasons, such as due to tool wear or due to the setup conditions. This mean drift can result in *an apparent increase* in the process capability. The expression

$$\sigma_i = \frac{T_i}{3Cp_i(1 - m_i)} \tag{2.9}$$

  shows the resulting modified standard deviation of a component process.

Where

$$Cp_i = \frac{\text{USL} - \text{LSL}}{6\sigma_i}. \tag{2.10}$$

is the process capability of a component i between the specification limits LSL and USL and m_i is the estimated mean shift factor, as already cited.

When $m_i = 0$, σ_i describes the process short-term variation; when $0 < m_i < 1.0$, σ_i approximates the long-term variation of the process. For the standard Six Sigma model, the target values of $Cp_i = 2$ and $m_i = 0.25$ result in long-term tolerance limits of $\pm 4.5\sigma_i$

over the long term. It is also worth noting that other values Cp_i and m_i can be selected to account for the degree of uncertainty in an individual process. Regarding tolerance analysis, the Six Sigma model for tolerance accumulation is represented by

$$dU = Z \left[\sum \left(\frac{df}{dx_i} \right)^2 \left(\frac{T_i}{3Cp_i(1-m_i)} \right)^2 \right]^{1/2} \leq T_{ASM}. \tag{2.11}$$

It considers the process mean shift variation by using an effective standard deviation as expressed in Equation (2.9). When the value of σ_i for a specific process is known from experience, it can be replaced in the equation.

In summary, the method proposes an increase in the process capability equivalent to a variation of $\pm 6\sigma$ in relation to the distribution mean. Furthermore, a shift in the mean position of $\pm 1.5\sigma$ is allowed [BREYFOGLE, 2003, p. 14], as aforementioned. Figure 21 illustrates the concept. Table 2.1 presents the data shown in Figure 21. Data regarding standard deviations show the percent probabilities of both product acceptance percent and the rejection fraction in parts per million (ppm) for centered and shifted distributions. It can be seen that the data for the centered distribution are the same (not rounded) as those in Figure 21.

It is important to mention that the Six-Sigma tolerance analysis model is just one of the requisites of the management system of the same name. The summary of its features is as follows:

1. The low rejection rates;
2. Production cost reduction;
3. Product quality improvement.

Table 2.1 – Data from centered and shifted 6σ distributions

specified limit	conformity [%] centered	defective [ppm] centered	conformity [%] shifted $\pm 1.5\sigma$	defective [ppm] shifted $\pm 1.5\sigma$
$\pm 1\sigma$	68.27	317,300	30.23	697,700
$\pm 2\sigma$	95.45	45,500	69.13	308,700
$\pm 3\sigma$	99.73	2,700	93.32	66,810
$\pm 4\sigma$	99.9937	63	99.3790	6210
$\pm 5\sigma$	99.999943	0.57	99.97670	233
$\pm 6\sigma$	99.9999998	0.02	99.999606	3.4

Source: based on [BREYFOGLE, 2003, p. 14].

A full description of the Six Sigma concept propositions can be found in Linderman et al. [2003]. Joglekar [2003] presents a practical book on the application of Six Sigma in research and development (R&D) and manufacturing. Pande et al. [2000] make a detailed description on how great companies improved their market performance by adopting the Six Sigma management system. Willyard and McClees [1987] present a "roadmap" on the Six Sigma implementation process adopted by Motorola. Liu and Li [2011] present a case study describing a Six Sigma methodology: *DMAIC (Define, Measure, Analysis, Improve, and Control)*. Karthi et al. [2012] proposed an integration between the global concepts of Six Sigma and the requirements of the ISO 9001 standard. Aboelmaged [2010] presented a comprehensive review of a period of seventeen years from 1992 to work referencing Six Sigma. Another review paper was developed by Tjahjono and Ball [2010].

2.7 Functional Tolerances

Functional tolerances are especially important when mechanical assemblies are subjected to thermal and/or stresses due to static or dynamic loading. In this section, the effects on dimensions as a result of temperature and stresses are considered, although only thermal stresses are in the scope of our work.

The most complete work on the thermal expansion of metallic materials in our research is that of Touloukian et al. [1975], the 12th volume of a series of thermophysical properties of matter. The book includes theoretical development, measurement methods, and comprehensive numerical data. For nonmetallic solid materials, the 13th volume of the series is applicable [TOULOUKIAN et al., 1977].

2.7.1 Theoretical Concepts

The concepts of this section are based on the reference cited [TOULOUKIAN et al., 1977]. When there is a change in temperature $T_1 \Rightarrow T_2$ due to the addition of heat to a material, a corresponding $V_1 \Rightarrow V_2$ change occurs in its volume from its initial value V_1 to its final value V_2. This change can be described by *mean coefficient of volumetric thermal expansion* of the material, defined by

$$\beta_m = \frac{V_2 - V_1}{V_1(T_2 - T_1)}. \tag{2.12}$$

The definition of the exact value of this coefficient can be made taking a limiting value of its ratio at constant pressure P as the temperature changes by a differential amount dT. Thus, the true coefficient of volumetric thermal expansion, or just *coefficient of thermal expansion*, is

$$\beta = \frac{1}{V}\left(\frac{\delta V}{\delta T}\right)_P. \tag{2.13}$$

The corresponding definitions of these coefficients for the linear (unidirectional) case are as follows.

$$\alpha_m = \frac{L_2 - L_1}{L_1(T_2 - T_1)} \tag{2.14}$$

and

$$\alpha = \frac{1}{L}\left(\frac{\delta L}{\delta T}\right)_P. \tag{2.15}$$

For an isotropic substance, the coefficient of thermal expansion is equal to three times the coefficient of linear thermal expansion.

$$\beta = 3\alpha. \tag{2.16}$$

Note that the values of the coefficients cited vary with temperature. Weisskopf and Bernstein [1985] developed equations for an estimation of their values based on the atomic binding energy of the material and compared the resultant values with those reported in the tables. The authors also consider that the variations of the thermal coefficients are very small in the temperature ranges of 100 °C. Ahrens [1995, p. 29] describe a theoretical model based on the energy of lattice vibrations to demonstrate the phenomenon of thermal expansivity of solids and compare the theoretical proposal with experimental values.

Another interesting feature of some solid materials, such as complex metal oxides, polymers, and zeolites, is the presence of a negative thermal expansion coefficient (NTE). Miller et al. [2009] present a comprehensive review on the subject and state that NTE is generally derived from supramolecular structural mechanisms and see composites as a potential application field. Evans [1999] describes the NTE in some materials. In our work, a mean value of the coefficient of linear expansion is considered, since the dimensions are taken in the three space coordinates independently and between the standard measurement temperature in the room and the functional temperature considered of the specific component in the assembly. The measured values obtained from the tables are used to deal with temperature-level variation. For temperatures lower than 0°C, instead of a thermal expansion, a shrinkage of the material is observed. For negative temperatures, specific coefficients are used in this work.

2.7.2 Consideration of the Thermal Effects on DT

Thermal effects affect the dimensions of the components of an assembly, as cited in the former item. According to Benichou and Anselmetti [2011, p. 1585], “the impact of the temperature variation on the deviation can be higher of the same order than the geometric defaults” and must be considered if the temperature variation over the standard one is significant. Expansion has a direct impact on the clearance and dimensions of a mechanism and can seriously affect its functional behavior. The authors cited present a case study of a simple assembly, where a tolerance synthesis is performed through a finite element analysis (FEA) at nominal dimensions: the objective is to study the clearance of a shaft-bearing loose fit to check the lubrication oil film condition at higher temperatures. The paper considers only a 2D WC condition and does not make statistical considerations.

Jayaprakash et al. [2012] use the Bjorke [1989] classic gearbox example to consider thermal and inertia effects on functional tolerances using FEA. The vector loop method is used to represent the Björke tolerance chain. As this is a simple shaft housing example, the solution was used and FEA software resources were only used to obtain the numerical results. The same author in another work [JAYAPRAKASH et al., 2014] describes another example (a motor crank system) in which the same FEA software is used to obtain the solution and a neural network algorithm is used to address a cost-based tolerance function.

Spruegel et al. [2014] describes a case of an assembly of three washers of different materials in a pin. The assembly is locked through a slotted spring pin. A design constraint, the gap between washers, is analyzed with respect to the clearance. The functional variable is the temperature of the ambient season in different regions in the range of −50 to +40°C world temperature. The analysis consisted of applying the dimensional variation due to temperature and a simple statistical analysis considering a normal distribution. Joint distributions are not considered.

Mayr et al. [2015] analyze the effect of temperature on a three-axis machine tool. A mathematical model is used to locate the tip of the machining tool in a 3D space. Measurements of position and temperature are made and comparative plots between the model and measurements are drawn with the collected data.

2.7.3 Consideration of the Mechanical Load Effects on DT

Mechanical assemblies can be subject to dimensional variation caused by load effects. The loads acting on parts can be classified into static and dynamic. The loads can also be caused by external and internal forces.

The weight of the parts on their own and supported basis is generally not significant enough to cause any variation in conventional mechanical assemblies. The loads that cause the dimensional variation of the parts are generally those that result from the performance of the product, by means of surface pressure, contact forces, or mass inertia.

Compliant (non-rigid) parts are widely used in automotive, aerospace, electronics, and home appliance manufacturing. These parts mainly consist of sheet metal and plastics. In these cases, in addition to variation due to application loads, the dimensional variation of the assembly is caused by the manufacturing variation of the components, the variation of the tooling, and the deformation of the part due to clamping, joining, and springback.

Some researched works on this subject are briefly described as follows:

Barari [2012b] proposed the evaluation of the total combination of design tolerances allocated and deformations due to various loadings on the final product, using a unified methodology in which minimum deformation zones for various types of loading in an assembly of parts are considered. In this way, the optimum tolerances for the geometric parameters of mechanical structures are found. The implementation of the methodology is made by means of a beam-frame model, in which a Finite Element Analysis determines nodal deflection of the design structure due to applied loading condition using equations developed in the method. Once the deflections for all possible loading events have been found, other developed equations are used to allocate the optimum tolerances for the structural components. In the work, a 3D frame structure of a vehicle is analyzed as an example.

Korbi et al. [2018] developed a new approach for tolerance analysis of non-rigid parts assemblies, consisting on a CAD/tolerancing integration. The method considers modeling of realistic mating constraints, between rigid and non-rigid parts. Planar and cylindrical joints are used for method description.

Tebby et al. [2012] developed a method that uses beam elements to represent the structure of a vehicle, using a numerical finite element method. Based on Simple Structural Surfaces, a method that utilizes planar sheets to model the vehicle structure and allows the determination of the forces in each sheet, the proposed method is able to determine unknown deflections and reaction forces, as well as the internal loading on each member of the structure. Moreover, the method can also be readily adapted to allow parametric optimization of the bending stiffness.

Forslund et al. [2018], focusing on aerospace components, proposed a modeling based on the parametric point method, an approach that allows point-scanned data to be transferred to parameterised CAD models in a way that maintains the design intent, providing forward applicability. The capability of the methodology is demonstrated through applications in which the effects of geometric variation on the aerodynamic, thermal, and structural performance of a load bearing turbofan component are analyzed.

Xie et al. [2007] presented a new methodology based on finite elements, developed to predict components and the propagation of tooling variation in an assembly process of sheet metal parts.

Hu et al. [2006] presented models to analyze the propagation of dimensional variation in multistage compliant assembly systems and the use of such models for robust design and adaptive control of assembly quality. The models combine engineering structure analysis with advanced statistical methods to consider the effect of part variation, tooling variation, as well as part deformation due to clamping, joining, and springback.

An analysis of all the methods investigated leads to the conclusion that the use of CAE tools is essential to determine the mechanical deformation of the product parts, since the material strain-stress behavior must be evaluated through the Theory of Elasticity.

3 Review on current research

The description of the main existing tolerance analysis methods is developed in sequence, according to the scope of this thesis. Figure 22 is an extract of Figure 1 and illustrates the overview of this section. A discussion of the features of the items listed for comparison with the proposal of this work is made, and specific shortcomings are highlighted.

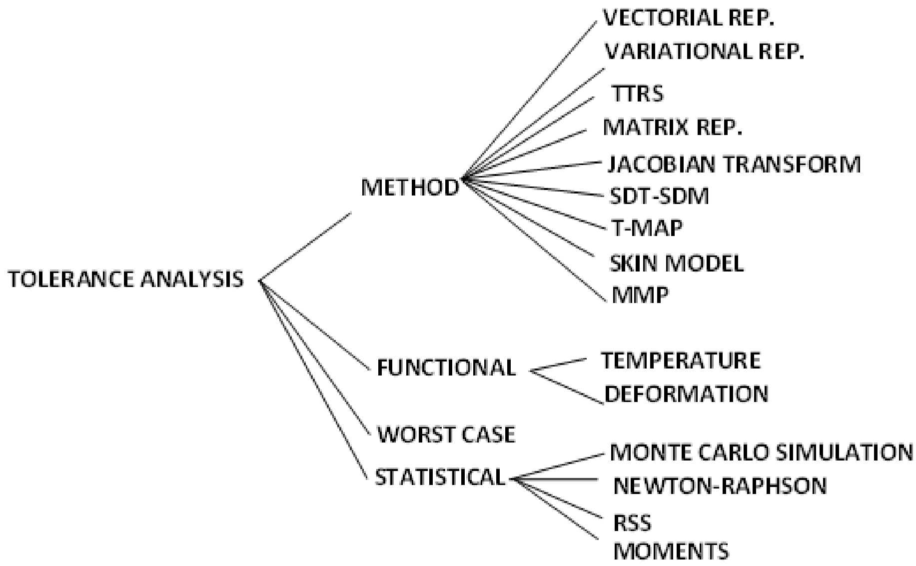

Figure 22 – An overview of the tolerance analysis study. (Source: the author).

3.1 Methods

In this section, the methods of 3D tolerance analysis currently available in the literature are explained. As can be seen, the methods present very different approaches. Insofar as possible, the methods follow a chronological order of publication. Their descriptions are summarized, but an effort has been made in an attempt to preserve their conceptual content.

3.1.1 Small Displacement Torsor

Regarding kinematic joints (one of the sources cited for the process variation), the main contribution seems to be **Small Displacement Torsor** (SDT). The SDT concept was developed in the 1970s of the last century by Bourdet and Clément [1988] with the objective of solving the general problem of fitting a feature to sets of available points. This concept was introduced in the metrology area as **Small Screw Displacement Model** (SDM)

[BOURDET; CLéMENT, 1988] and has been widely used in 3D metrology software for coordinate measuring machines (CMM). Its main idea is that the displacement of a rigid body or a surface should be small [LEGOFF et al., 1999].

An application of the SDT model was proposed by Teissandier et al. [1999] as **Proportioned Assembly Clearance Volume** (PACV), where an ideal surface represented by a set of points is displaced through SDT to generate another ideal (fabricated) surface. This small displacement can then represent a tolerance field, as illustrated in Figure 23.

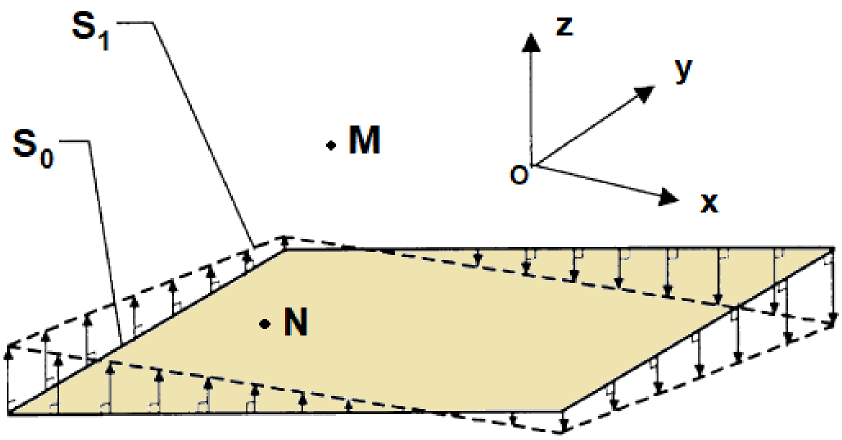

Figure 23 – A field of small displacements. (Source: based on [TEISSANDIER et al., 1999]).

The mathematical development of the SDT is made when considering the position and orientation of an ideal surface S_1 in relation to another ideal surface S_0, at a given point N of S_0, and with the hypothesis that the topology of these surfaces is maintained and given by

$$[D_{1/0}]_N = [\rho_{1/0}, \epsilon_{1/0,N}], \tag{3.1}$$

where $[D_{1/0}]_N$ represents the SDT, $\rho_{1/0}$ is a rotation vector and $\epsilon_{1/0,N}$ is a translation vector.

An expression of relative translation between two surfaces at any point M in the Euclidean space $[x, y, z]$ can be deduced by linearizing the relative rotations between two ideal surfaces (see Figure 23) relative to the point N using a transport rule.

$$\epsilon_{1/0,M} = \epsilon_{1/0,N} + \rho_{1/0} \wedge \delta_{NM} \tag{3.2}$$

where $\epsilon_{1/0,M}$ is a translation vector.

δ_{NM} is the transport vector of a cross product whose components are deduced from the coordinates of the points $N(N_x, N_y, N_z)$ and $M(M_x, M_y, M_z)$.

$$\delta_{NM} = \begin{bmatrix} d_{NMx} = x_M - x_N \\ d_{NMy} = y_M - y_N \\ d_{NMz} = z_M - z_N \end{bmatrix} \tag{3.3}$$

A PACV is composed by six intervals, which set small displacement limits between two ideal surfaces in a tolerance zone. A tolerance zone is a region of Euclidean space where a nominal surface (an ideal surface by definition) and a fabricated surface (an ideal surface by hypothesis) can move. Any relative position between two ideal surfaces can be formalized by SDT. Therefore, a PACV characterizes an infinite number of SDTs [TEISSANDIER et al., 1999]. Figure 24 shows a nominal surface S_{in} and an actual surface, modeled by an ideal surface S_{id}. Since the SDT departs from ideal surfaces, when a real surface (defined through measured points) is related to these surfaces, it can be positioned in the generated tolerance zone.

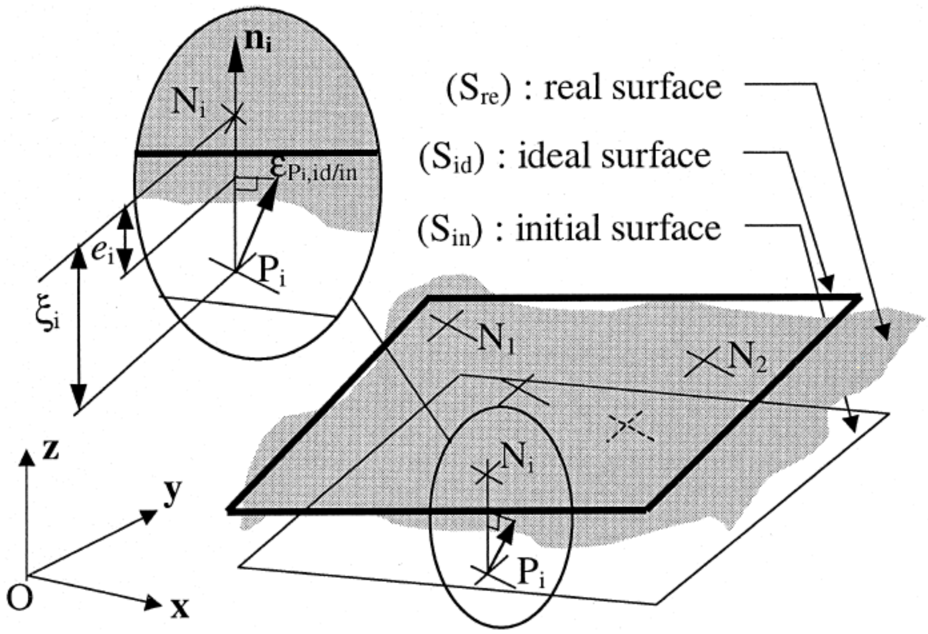

Figure 24 – Association of an ideal surface with a finite number of measured points. (Source: based on [TEISSANDIER et al., 1999]).

The concept of "screw model" used by other authors [LEGOFF et al., 1999] uses a similar mathematical development of SDT.

For ease of use of the screw model, Desrochers et al. [2003] proposed an inventory of all standard tolerance zones, together with their corresponding "torsor representations" and geometric constraints. The torsors of a functional element have various possible dispersions in translation (u, v, w) and rotation (α, β, δ). The remaining DoFs are represented by zeros in the torsor matrix. For the rotation vector,

$$\rho = \begin{bmatrix} 0 & -\gamma & \beta \\ \gamma & 0 & -\alpha \\ -\beta & \alpha & 0 \end{bmatrix}. \tag{3.4}$$

3.1.2 Virtual Joints

The concept of **virtual joints** [LAPERRIèRE; LAFOND, 1999] consists in associating a set of six virtual DoF, three for small translations and three for small rotations, to every pair of functional elements (FE)s of a tolerance chain. A FE can be a point, a curve or surface, or a part, real or imaginary. A functional requirement (FR) is influenced by FEs in an assembly chain, generally in terms of gaps, clearance, and fit between pairs of FEs. Figure 25 illustrates the concept, where the boxes represent translational dispersions.

The cylinders represent rotational dispersions, and the virtual joints simulate the effects of the positional and orientation process variation between two FEs of the same component, chosen according to an FR of the assembly.

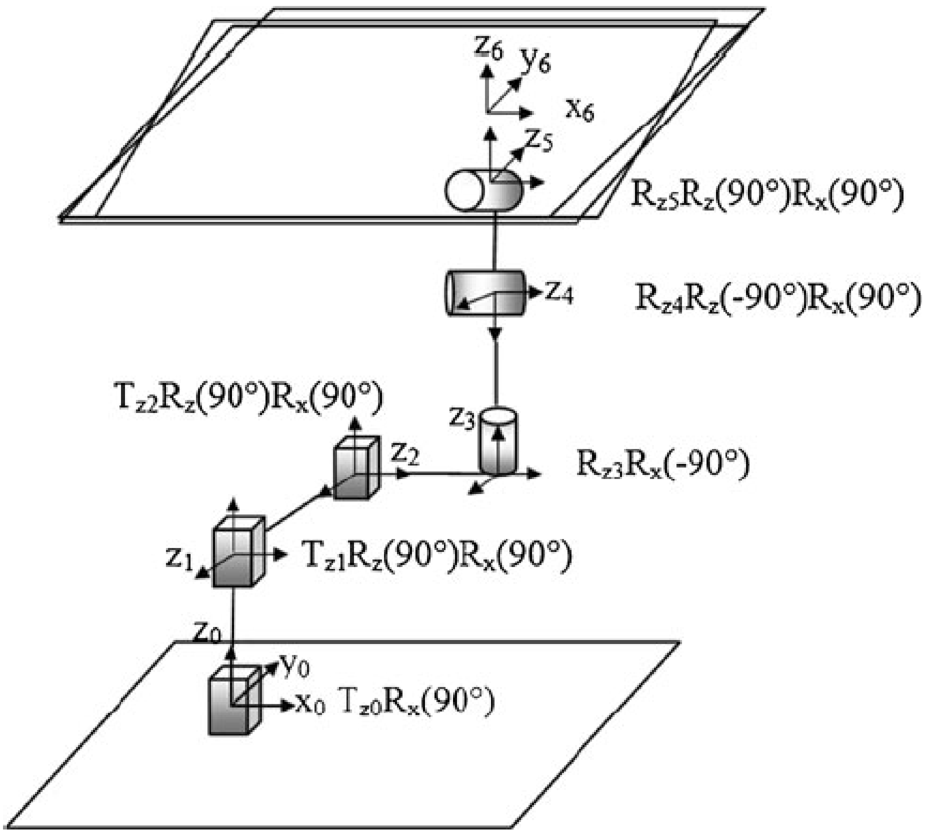

Figure 25 – Six possible dispersions modeled for a pair of FEs identified by planes in a same part. (Source: based on [LAPERRIèRE; LAFOND, 1999]).

3.1.3 The Unified Jacobian Torsor

The mathematical model of the virtual joints presented in the previous subsection is obtained by associating a coordinate frame to every virtual joint, which is positioned and oriented with respect to the base frame. In sequence, the computation of the global position and orientation of each frame is performed by means of transformation matrices, or **Jacobian transform matrices**.

The method of integrating the two concepts is known as **Unified Jacobian torsor** [DESROCHERS et al., 2003; TING et al., 2018] and was first introduced by Laperrière and Lafond [1998], Laperrière and Lafond [1999]. Figure 26 can help explain this and shows a closed kinematic tolerance chain, with identification of the FEs that influence the FR. The problem task is to mathematically quantify the functional relationship between the FE dispersion values FEs_d and the FR dispersion value FR_d, that is,

$$\mathrm{FR}_d = \mathcal{F}(\mathrm{FEs}_d) \tag{3.5}$$

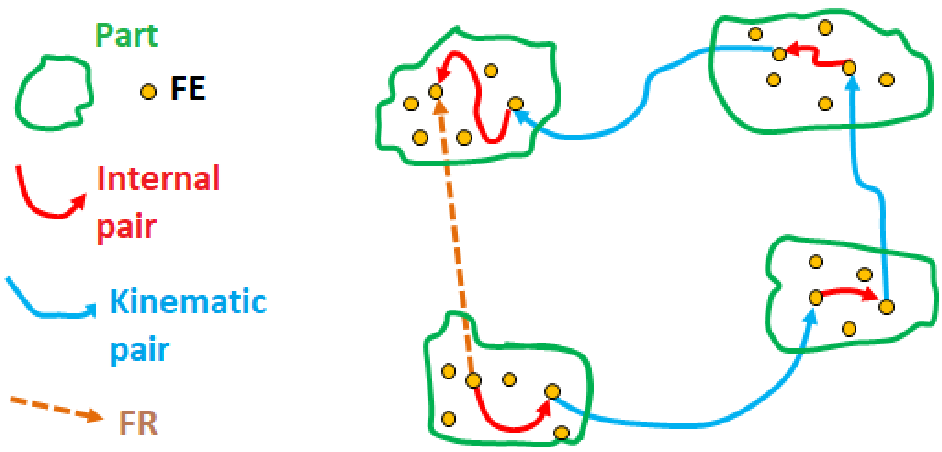

Figure 26 – Graph model representation of a tolerance chain around the FR of a four part assembly. (Source: based on [LAPERRIèRE; LAFOND, 1998]).

The Jacobian model approach uses homogeneous matrix transforms and their partial derivatives in terms of a Jacobian matrix to relate $\mathrm{FE}'s_d$ to $\mathrm{FR}'s_d$ in a tolerance chain. In modeling virtual joints for tolerating purposes, coordinate frames are associated with the tolerated FE in a pair, assuming that there exists a set of virtual joints that can make the tolerated FE of the pair move relative to the other FE of the pair, to simulate manufacturing inaccuracies. The essence of the method is to consider consecutive virtual joints **each with a single DoF**. Therefore, the tolerated FE in a pair will be modeled with six virtual frames attached to the six virtual joints to account for the six possible dispersions that it can perform (three small translations and three small rotations).

The mathematical development of the method can be found in the work of the three cited authors [LAPERRIèRE; LAFOND, 1998; LAPERRIèRE; LAFOND, 1999; LAFOND;

LAPERRIèRE, 1999]. The general equation that results for the model is

$$\begin{bmatrix} \delta \vec{s} \\ \delta \vec{\alpha} \end{bmatrix} = \begin{bmatrix} \begin{bmatrix} J_1 \\ J_2 \\ J_3 \\ J_4 \\ J_5 \\ J_6 \end{bmatrix}^T_{\mathrm{FE}_1} & \cdots & \begin{bmatrix} J_1 \\ J_2 \\ J_3 \\ J_4 \\ J_5 \\ J_6 \end{bmatrix}^T_{\mathrm{FE}_n} \end{bmatrix} \cdot \begin{bmatrix} \vec{\delta}_{\mathrm{FE}_i} \\ \cdot \\ \cdot \\ \cdot \\ \vec{\delta}_{\mathrm{FE}_{n-1}} \\ \vec{\delta}_{\mathrm{FE}_n} \end{bmatrix}$$

where $\delta \vec{s}$ is a 3-vector of small translations of the point of interest, $\delta \vec{\alpha}$ is a 3-vector of point of interest's small rotations, $\begin{bmatrix} J_1 & J_2 & J_3 & J_4 & J_5 & J_6 \end{bmatrix}_{\mathrm{FE}_i}$ is a 6×6 Jacobian matrix associated with the toleranced FE of the i-th FE pair, $\vec{\delta}_{\mathrm{FE}_i}$ is a 6-vector of small dispersions associated with the tolerated FE of the i-th FE pair.

Using standard Jacobian-based computations, it becomes possible to model the effects of such small dispersions of each element in a kinematic chain around a point of interest on an assembly, in particular around the desired FR.

Other relevant works on the model are the following:

- Laperrière et al. [2002] proposed unified CAT system based on the Jacobian model that integrates both WC and ST. However, an issue is the great computation involved. According to the authors, "after solving the constraint equations for every FE, instead of performing an interval-based multiplication operation, randomly distributed real values can be generated over each interval using the real multiplication operator with J. When a large number of such multiplications are performed using a large number of randomly generated values within each interval, the resulting distribution can be discovered". They presented a simple case result, but did not mention anything about the difficulty of obtaining it;

- Desrochers et al. [2003] presented a proposal for a unified representation of the Jacobian model and tolerance zones based on torsors, such as planar discs, parallelepiped, and hollow cylinder. As can be seen, the construction of the model for each case is very difficult and time consuming;

- Nejad et al. [2008] combined the Jacobian model with the manufactured part model, described in this text;

- Ghie et al. [2007] proposed the use of the Jacobian model to redesign existing mechanical assemblies, instead of performing a tolerance synthesis. The purpose of tolerance redesign is to verify and adjust the tolerances assigned in the design stage to meet a given FR target at the assembly level, such as a gap or clearance;

- Guie [2009] described a statistical tolerance analysis using the Monte Carlo method (MCM) similar to the one proposed by Laperrière et al. [2002] and developed application examples;
- Guowei et al. [2010] proposed a tolerance analysis using the Jacobian model to forecast and analyze assembly performance during operation and exemplified the proposal with case studies;
- Zuo et al. [2013] used the Jacobian torsor model not for the usual intention, tolerance analysis, but rather to preview error propagation in machining processes. Instead of components, they considered the workpiece, fixtures, machine tool, and tool for analysis;
- Zeng et al. [2017] proposed the use of the Jacobian model in the WC tolerance analysis of a spiral bevel gearbox application. The innovation in this article is that tolerance analysis considers parallel chains instead of a unique serial chain;
- Peng and Wang [2017a] proposes a redesign of an assembly, similar to how Ghie et al. [2007] works. A statistical analysis using the MCM is applied;
- Peng and Wang [2017b] used the same work of Peng and Wang [2017a] including a surface graph.

3.1.4 The concept of Skin Model Representation

The **Skin model representation** considers geometric deviations that are expected, predicted, or already observed in real manufacturing processes. The concept of skin model representation was first considered as a discrete representation and simulation of shapes. This initial approach enabled the model the form, orientation, and position deviations employing second-order shapes and different methods for obtaining randomly deviated geometry. In general, the skin model is imagined as a continuous surface, but shape defects are considered at different scales of observation, i.e., macro, micro, and nanoscales. Due to this, a great number of parameters are required in computer calculations, and discrete models are used to allow its application in practice due to the high processing time. The representation level of the model is the same as a solid model, but with a larger number of description parameters, requiring a tremendous volume of data for its computation. To cope with this barrier, algorithms for discrete geometry have been created [ANWER et al., 2013]. Figure 27 illustrates the skin model process development of a design.

Applications of the representation of the skin model can be found in [CORRADO; POLINI, 2017].

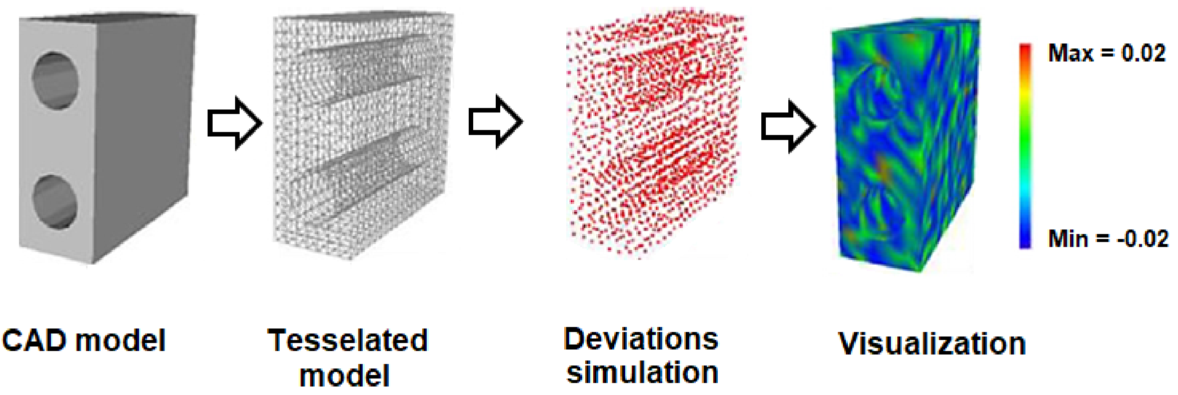

Figure 27 – The skin model process development. (Source: based on [ANWER et al., 2013]).

3.1.5 The Variational Representation

In the subject bibliography, perhaps the original works on geometric tolerances representation are those known as **Variational representation**. The objective of these Requicha's works [REQUICHA, 1980; REQUICHA, 1986] was the representation of rigid solid objects in computer-based systems, as a means to enable GD&T tolerancing resources for nominal geometry of CAD systems, that is, an early attempt to develop a CAT system. Concepts of constructive solid geometry (CSG) and variational graph (V-graph) were originally developed, where trees and subtrees of geometric tolerances could be represented, resembling tolerance chains. A mathematical model for Requicha's proposal was developed by Boyer and Stewart [1991]. As already discussed, a CAD model is an idealization of certain geometric properties of a part or an assembly of parts, works with theoretical exact dimensions, and does not support actual manufacturing process variations regarding size, location, orientation, and form of their features. Variational modeling involves applying variations to a computer model of a part or assembly of parts and can be classified according to the representation used as either procedural or declarative [GUPTA; TURNER, 1993].

The procedural modeling systems store a step-by-step plan for constructing the geometric elements that comprise the part or assembly. Two types can be mentioned:

1. In solid CSG modelers, the system builds a sequential procedure to build a part or assembly model in the form of a tree, as illustrated in Figure 28. In such modelers, variations can be induced in two ways:

    a) The model variables associated with both the shape and location parameters of the primitives can be changed, and the construction procedure to produce a new model instance can be reevaluated;

    b) Variations to the boundaries of primitives can be applied.

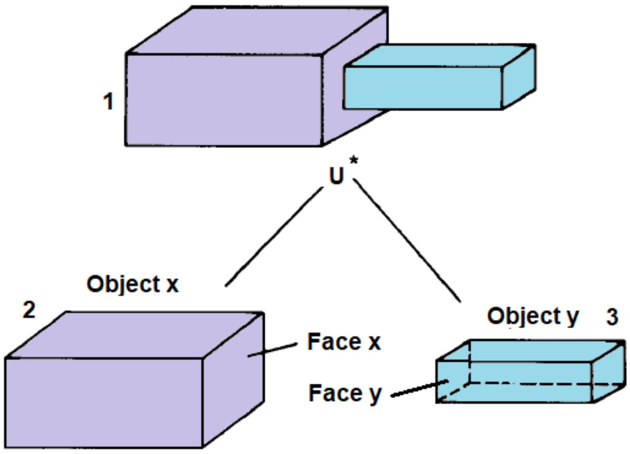

Figure 28 – Complex object constructed using the union regularized set operator. (Source: based on [ALAGAR et al., 1990]).

2. In feature-based systems, a part model is expressed in terms of base features and certain feature-forming operations. The location and shape parameters associated with the geometry of the feature can vary. The choice of features used and the sequence in which they are applied determine the variational coverage of the model. Figure 29 shows an example.

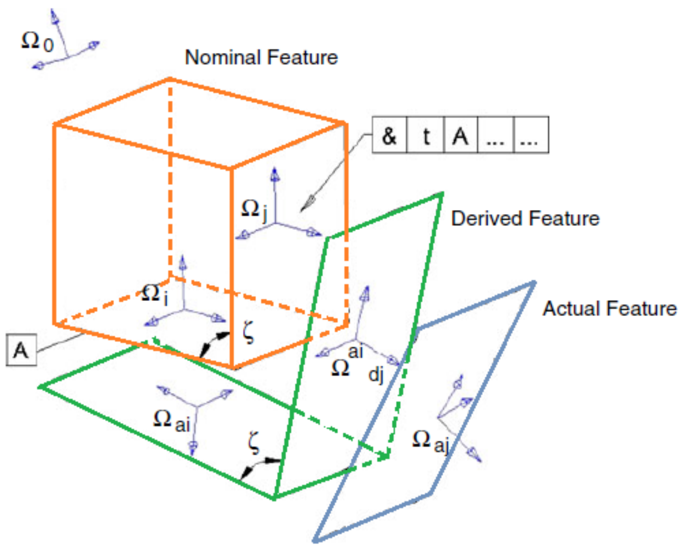

Figure 29 – Feature modeling. A coordinate reference frame is attached to each feature. (Source: based on [FRANCIOSA et al., 2010]).

In declarative solid modelers, the system builds a representation of each geometric element together with information about interconnections. However, it does not store the sequence of steps used to construct the model. Figure 30 illustrates the modeling concept. Variations can be introduced by varying the coordinates of vertices or the positions and orientations of surfaces after declarative modeling in pure boundary representation (B-rep) modelers.

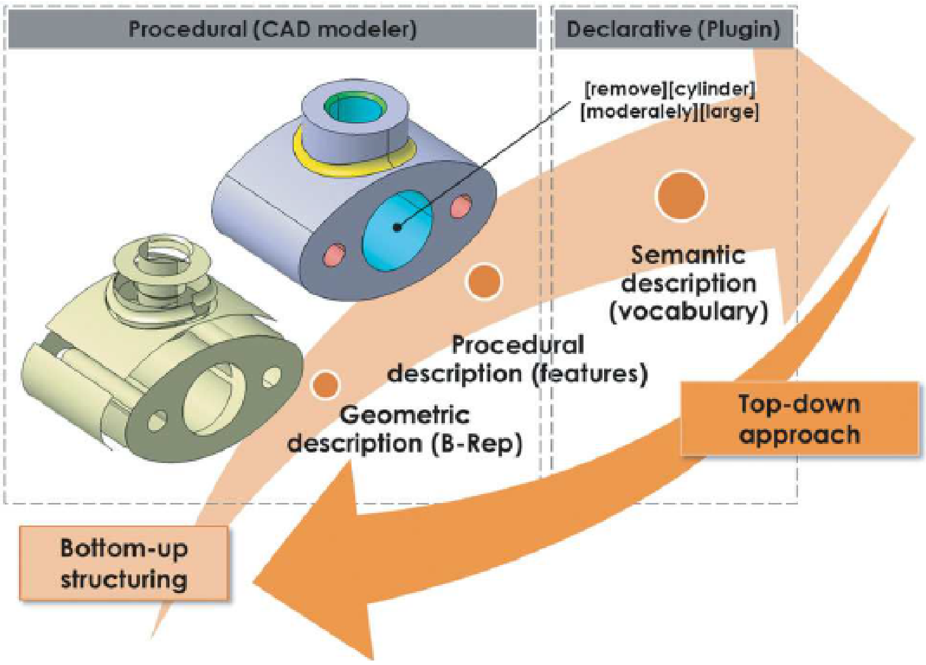

Figure 30 – Declarative modeling approach built on top of a procedural CAD modeler. (Source: based on [DéCRITEAU et al., 2016]).

3.1.6 The Realistic Geometrical Solid Model

The Realistic Geometrical Solid Model (RGSM) is a representation of part geometry considering the superposition of the surface geometric error with the nominal solid model. Current CAD systems establish a nominal solid model of parts that belongs to the ideal geometry hierarchy and is defined by driving dimension parameters. The CAD surface model of geometric errors belongs to the non-ideal geometry hierarchy and is determined by Non-Uniform Rational B-Spline (NURBS) surface parameters. NURBS is a standard format for CAD, supported by international information exchange formats, and can be considered an additional improvement over the previous variational representation models [ZHANG et al., 2018]. Figure 31 shows the comparison of RGSM with other representation models. The geometric errors described by the authors refer to form deviations, as referenced by GD&T standards, additionally to position and orientation variations. The use of the NURBS surface model by RGSM comes from its widespread use in the CAD system, because it provides a uniform mathematical representation for standard and free-form surfaces. The NURBS method uses surface reconstruction *based on measured points on a machined surface*, where the surface is defined through the tensor product of two NURBS basis functions in two orthogonal directions u and v, to construct the representation of the surface model. Therefore, the inverse algorithm for the control points on the NURBS surface is the key to surface reconstruction.

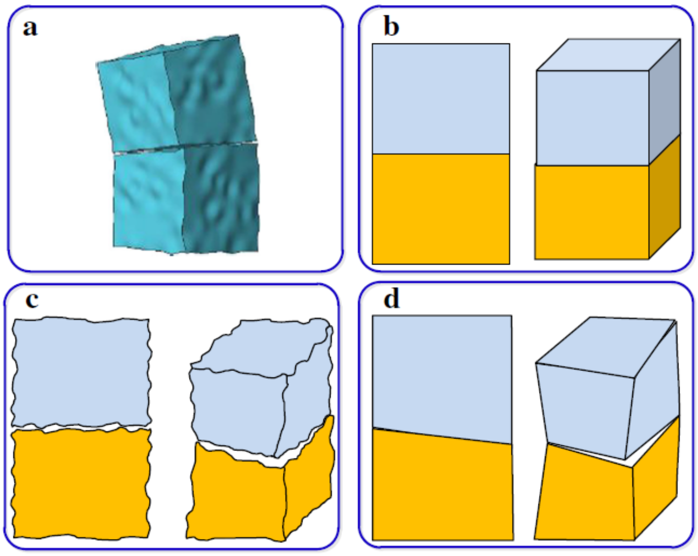

Figure 31 – Geometric error representation of machined parts for computer-aided tolerance analysis and assembly simulation: a) Actual parts; b) Nominal model; c) RGSM; d) Variational geometric solid model. (Source: based on [ZHANG et al., 2018]).

3.1.7 The Vectorial Representation

The **3D vectorial tolerance representation**, or vectorial tolerancing, originally from Wirtz [1988], aims to cope with quality control regarding metrology and manufacturing. The method uses up to four vectors to describe the position, orientation, form, and dimension of a geometrical feature. To each of these vectors are associated two parameters: one for the nominal state and the other for the deviation, and then the model can represent a real surface by adding the nominal characteristics and their deviations by vectorial addition [DESROCHERS et al., 2003]. Figure 32 illustrates the representation. As the representation was developed from metrology and manufacturing origins, the best-fit plane cited was derived from measurements of an actual surface by means of a statistical procedure, such as RSS. It should be noted that the ASME Y14.5.1.M-1994 standard [ASME. . . , 1995], a mathematical representation of the ASME GD&T standard [ASME. . . , 2009] uses vectors to conceptualize the tolerance of geometric features.

Another vectorial representation of tolerances is the vector assembly model [CHASE et al., 1997], where a chain of vectors is placed in a 2D space, representing open or closed loops. The sum of the vectors results in the tolerance for assembly in each direction. Critical dimensions, such as gaps, can be calculated in an open loop. Figure 33 shows an example of a vectorial 2D model.

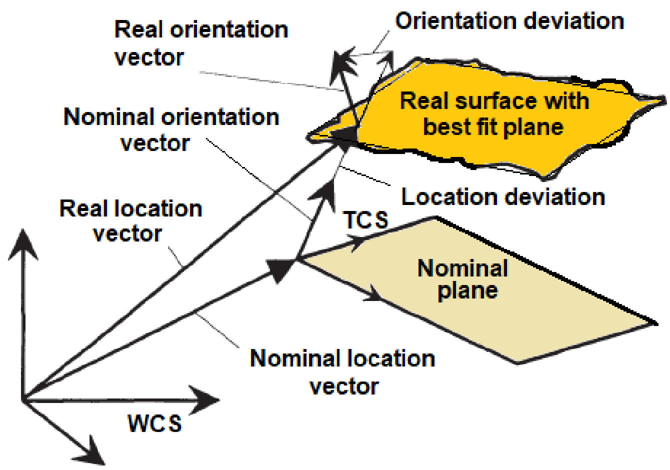

Figure 32 – Vectorial tolerance model indicating the positional and orientation of both nominal and real conditions of a flat surface. The tolerance coordinate system (TCS) is referenced from the workpiece coordinate system (WCS). (Source: based on [MARTINSEN; KOJIMA, 1997]).

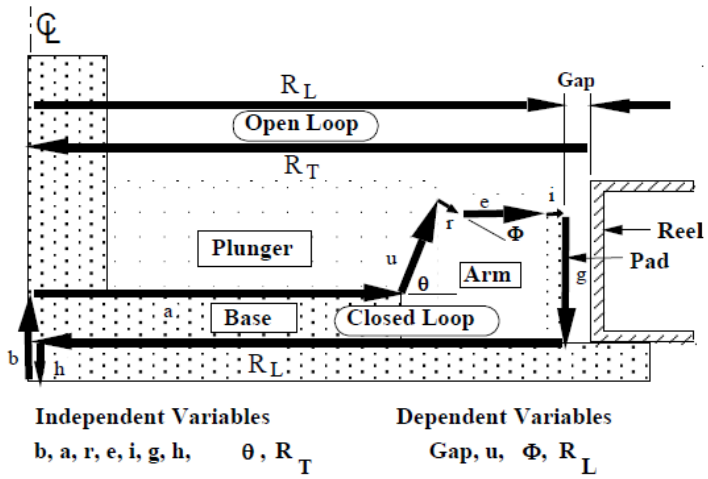

Figure 33 – Vector assembly model showing an open and a closed loop representing a locking hub assembly. (Source: based on [CHASE; MAGLEBY, 1997]).

3.1.8 The Model of Manufactured Part

The Model of Manufactured Part (MMP) was conceived by Villeneuve et al. [2001]. It is constructed around the nominal model of a component. This nominal model can be placed on a set of ideal surfaces that are associated with real surfaces by a criterion such as least squares. The deviations of these surfaces are described by SDTs (refer to Subsection 3.1.1). The parameters of these torsors depend on the positioning and machining deviations, and the limits on these parameters are expressed by design constraints. The purpose of the model is to “virtually simulate the machining processes” and include them in a CAD platform. Consider the variation (in relation to the nominal part dimensions) produced in each machining setup. By machining setup, we mean the preparation and adjustment of equipment for each different task by shifting fixtures and tools [MERRIAN-WEBSTER, 2020]. Thus, the influence of each set-up is taken into account in the next phase, and eventually a "virtual manufactured part" is created. Nejad et al. [2010] proposed a model with the combined approach of the MMP with the Unified Jacobian Torsor model.

As the model description is not straightforward, a brief explanation of its development is the following:

1. The method is applicable to a single component;
2. Determine the effect of a given manufacturing process in terms of deviation of the surfaces of the part for a machine setup;
3. The variation is taken as the deviation from the nominal dimension and is measured through a "virtual gauge";
4. From the record of the setup variation, consider the part repositioning on the next machine setup. The variation of the raw material part (stock), fixtures and tools must be considered. Figures 34 and 35 illustrate the nominal and the actual processes conditions, respectively;
5. Proceed with the next steps until the last setup;
6. At the end of this sequence, the MMP model - including all the variation - is generated;
7. Analyze the MMP regarding its functional features, that is, the features that affect the assembly, such as contact surfaces, and record the results;
8. Express the variation by SDT, added to the variations of the intrinsic characteristics of the surfaces, such as the diameter for a cylinder or a sphere;
9. Consider the domain of variation of the parameters representing the 3D capabilities of the manufacturing parameters (machine-tool, cutting tools, part holders) used during the machining process.

The MMP has been used in other works:

- Vignat et al. [2010] used MMP to simultaneously analyze the deviations of the casting and machining process. They also used MCM to simulate the dimensions of a production;
- Nejad et al. [2010] combine the MMP and Jacobian–Torsor model for the analysis of the tolerance of a machined part taking into account geometrical defects that occur in a multistage machining process;
- Nejad et al. [2012] used MMP in a multistage machining process and performed a tolerance analysis to compare the results with WC and statistical methods.

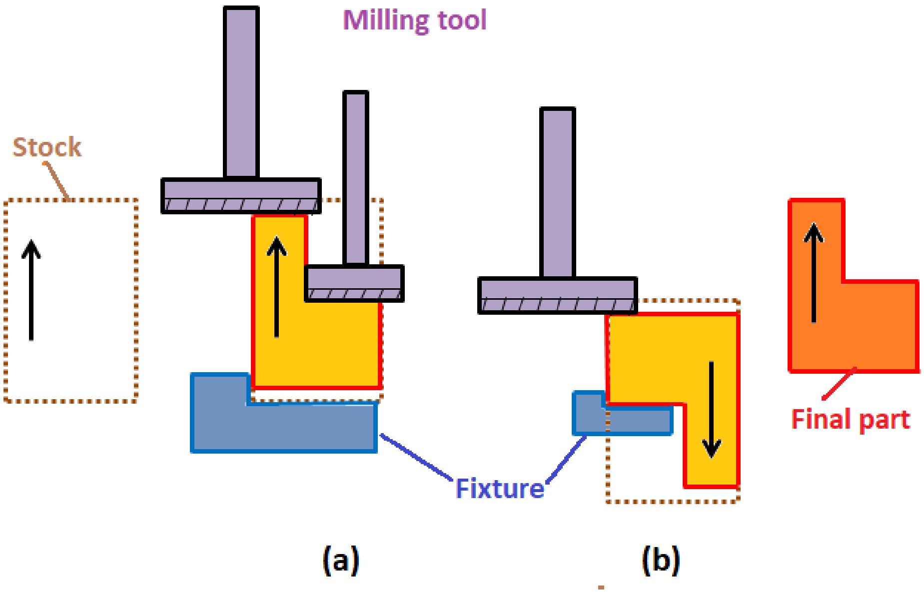

Figure 34 – Nominal process: (a) setup 1 and (b) setup 2. (Source: the author).

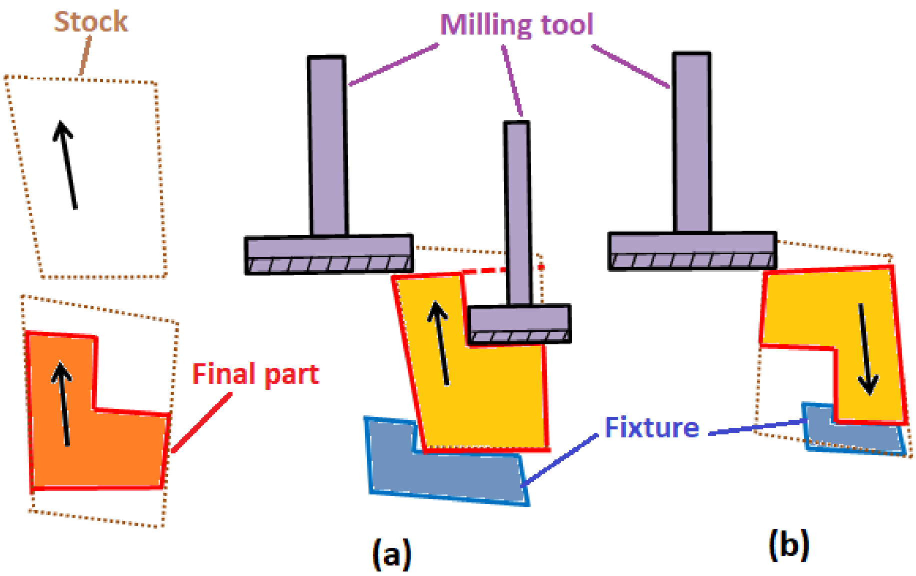

Figure 35 – Actual process: (a) setup 1 and (b) setup 2. (Source: the author).

3.1.9 The TTRS

The approach **TTRS**, or Technologically and Topologically Related Surfaces, was conceived by Desrochers and Clément [1994]. TTRS is based on successive binary associations of elementary surfaces and includes a method to generate partial or complete datum systems (or reference frames) that represent the various surface associations. The association is always unbalanced since it links several levels in one single end result. These reference frames are known as *minimum geometric datum elements* (MGDE) [CLéMENT et al., 1998], [AMETA et al., 2011]. This combined approach enables both the design and the process plan specifications by allowing a basis for establishing a general dimensioning and tolerating assistance scheme. At the end of the association procedure, all functional surfaces and all TTRS's are related in a hierarchical fashion to form an association of either separate or combined trees or graphs in 3D space.

The authors had proposed their own definition of surface, which can be stated as: "Any surface can be defined and classified by its degrees of invariance". In this way, *a degree of invariance can be seen as a translation or a rotation under which a given geometry remains unchanged*. In summary, the authors proposed only three basic MGDEs:

- A spherical surface represented by a point;
- A planar surface represented by a plane and;
- A line represented by a line.

The main properties of the TTRS are as follows:

1. The concept is based on the notion of surfaces. To allow mathematical representation in CAD/CAE systems, elementary surfaces based on their degree of freedom are established;
2. The association process is binary. The association is made two by two, either between two surfaces or between a surface and other TTRSs, or also between two TTRSs;
3. The process of association is recursive. The entire TTRS is a hierarchical association of several TTRSs, as illustrated in Figure 36;
4. Kinematic loops guide the associations. Functional surfaces present critical dimensions for the mating and functioning of the systems. Functional surfaces are represented by solid lines, as shown in Figure 36 and their identification enables visualization of the illustrated kinematic loops. These loops are equivalent to 3D tolerance chains.

Therefore, according to the TTRS model, parts will be represented by successive surface associations forming a tree, and each surface association, or TTRS object, will be

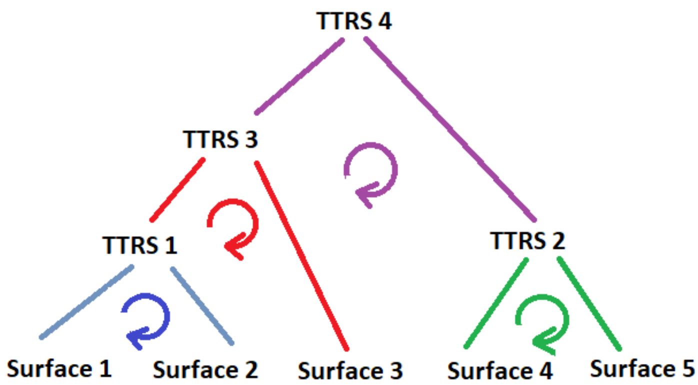

Figure 36 – A TTRS association tree. (Source: based on [DESROCHERS; CLéMENT, 1994, p. 354]).

represented by the MGDEs already cited. MGDEs are equivalent to actual representations of theoretical reference frames that are intended to represent real surfaces or TTRS according to the ASME standard [ASME. . . , 2009].

An example of a block with two perpendicular drilled holes is shown in Figure 37. The association of two parallel cylinders $S1$ and $S2$ leads to the creation of a prismatic $TTRS1$, which in turn is suitable represented by an axis and a plane such as MGDE. The plane of the flat surface $S3$ associated with $TTRS1$ makes the final $TTRS2$.

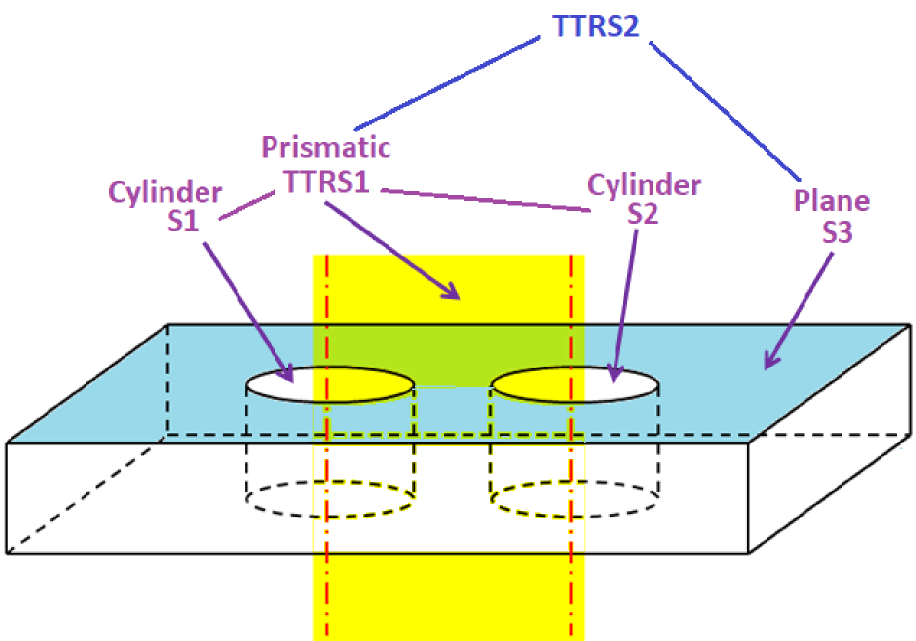

Figure 37 – A block with a milled flat surface and two drilled holes showing the association of MGDEs. (Source: based on [DESROCHERS; CLéMENT, 1994, p. 355])

In summary, this is a description of the main aspects of the TTRS concept. In the paper cited [DESROCHERS; CLéMENT, 1994], a full description of the method is developed. Desrochers and Maranzana [1996] presented the same concept with examples in the book chapter. Clément et al. [1998] describes TTRSs as 13 constraints on dimensioning and tolerancing in another book chapter. The TTRS concept is also presented as a methodology for the transfer of 3D tolerance by Desrochers and Verheul [1999]. Ameta et al. [2011] make a comparison between TTRS and two other spatial mathematical models for tolerance analysis. Jaballi et al. [2011] uses the TTRS concept in an algorithm for tolerance synthesis called *R3DMTSyn*. Salomons et al. [1999] presented an application of the TTRS method in the tolerance specification of industrial practice for a water pump. According to Lafond and Laperrière [1999], TTRS has been partially adopted in the tolerating module of CATIA CAD software [DASSAULTSYSTEMES, 2020].

3.1.10 The T-Map

The T-Map, or Tolerance-Map, is a hypothetical volume of points that corresponds to all possible locations and variations of a segment of a plane that can arise from tolerances of size, form, and orientation. The T-map is a patented method [METHOD..., 2005] and represents a mathematical model of geometric tolerances that can incorporate the GD&T rules. It is a one-to-one mapping of points from all variational possibilities of a feature within its tolerance zone.

The mathematical model of T-Map can represent any combination of tolerances on a feature and is constructed on a tetrahedron basis described by *areal coordinates* (also *area coordinates* and *barycentric coordinates*) [BHIDE et al., 2001]. Referencing Figure 38, the four base points σ_1, σ_2, σ_3, and σ_4 of the tetrahedron are placed as shown. The points $(\sigma_1, \sigma_2, \sigma_3)$ and $(\sigma_1, \sigma_2, \sigma_4)$ form two congruent isosceles triangles joined at right angles and of unity of the aspect ratio, that is, their heights and base length σ_1, σ_2 are the same. Masses with positive or negative values are placed at the four basis points σ_1, σ_2, σ_3, and σ_4. When considering a unitary total mass, $\lambda_1 + \lambda_2 + \lambda_3 + \lambda_4 = 1$, the position of the centroid of these masses σ is determined uniquely by linear combination.

$$\sigma = \lambda_1\sigma_1 + \lambda_2\sigma_2 + \lambda_3\sigma_3 + \lambda_4\sigma_4. \tag{3.6}$$

Therefore, the centroid can assume any position in the 3D space as a function of the values of the mass and, additionally, all positive values of the mass position of the centroid inside the tetrahedron.

In summary, the masses $\lambda_1, \lambda_2, \lambda_3, \lambda_4$ represent the areal coordinates of σ, which are used to describe the T maps of planar surfaces, such as the faces of a part. Figures 39 and 40 illustrate tolerance zones of the T-map for rectangular and circular section bars, respectively.

The T-map was conceived by a team of researchers at Arizona State University. Some works treat specific applications:

- Davidson and Shah [2000] referred the application for line geometry and screws;

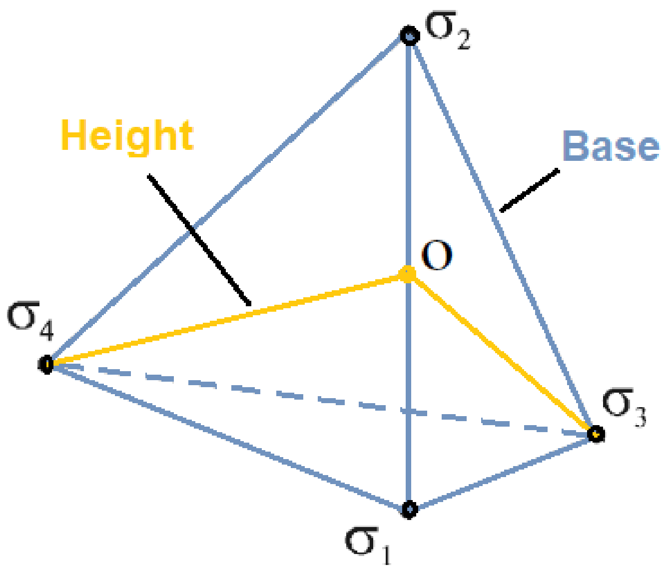

Figure 38 – The reference tetrahedron. $\sigma_1\sigma_2 = O\sigma_3 = O\sigma_4 = t$. (Source: based on [BHIDE et al., 2001]).

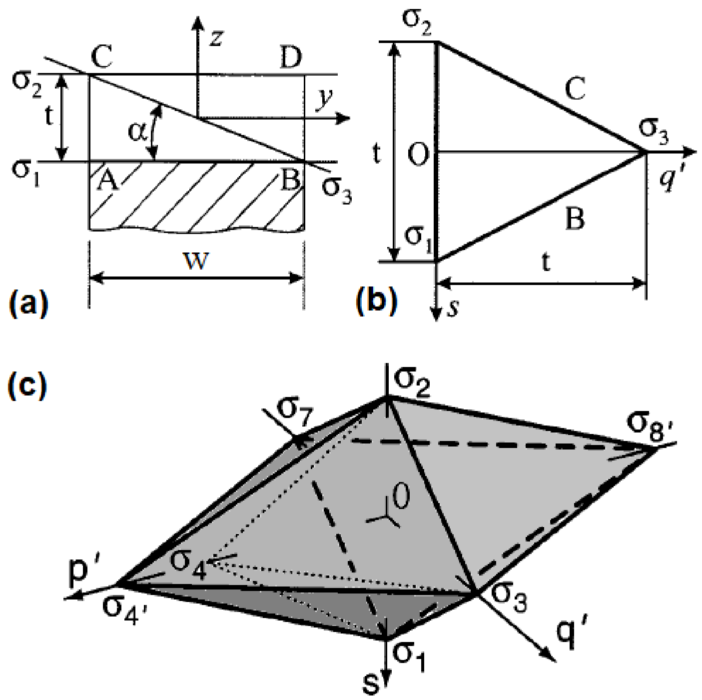

Figure 39 – The Tolerance-Map for the tolerance-zone t of a rectangular cross section bar. (Source: based on [BHIDE et al., 2001]).

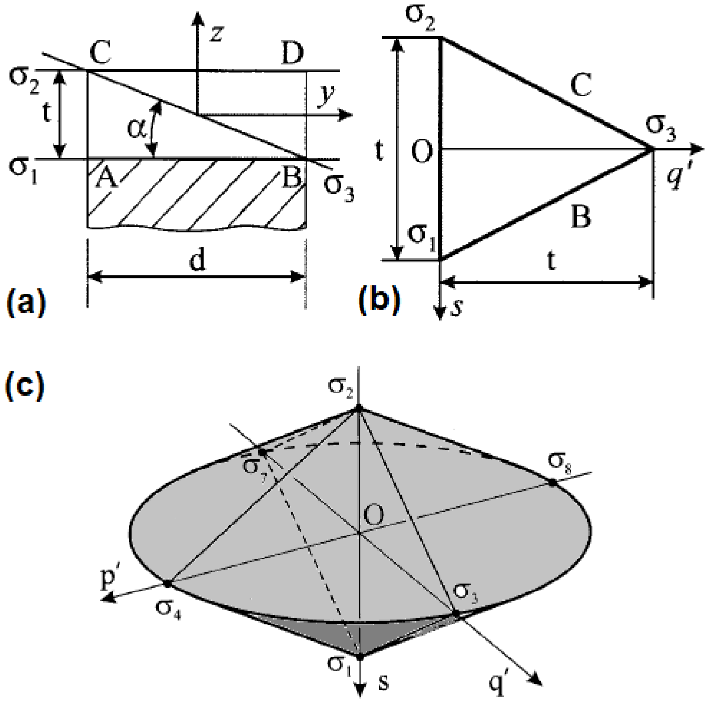

Figure 40 – The Tolerance-Map for the tolerance-zone t of a round cross section bar. (Source: based on [BHIDE et al., 2001]).

- Davidson et al. [2002] developed a mathematical model for round faces;
- Mujezinovic et al. [2004] considered a mathematical model for polygonal faces;
- Ameta et al. [2011] used the T-Map in a power saw assembly example;
- Jiang et al. [2014] referred to the T-map method to validate machining tolerances for the transfer of cylindrical datum in the manufacturing process;
- He et al. [2016] referred to the T-map for the Boolean intersection between line profiles and primitive T-Map elements.

Other authors also used the method.

3.1.11 The Matrix Representation

The approach **Matrix representation** is based on the use of 3D standardized tolerance zones constructed around the theoretical surfaces of a part. The method was originally proposed by Desrochers and Rivière [1997], and is described in sequence.

Among numerous methods for representing a displacement, the matrix method uses homogeneous transforms. A homogeneous transform matrix is composed of a rotation matrix 3×3 and a translated column vector 3×1. A displacement depends on six independent parameters: three for rotation and three for translation parameters. Each of these parameters defines a displacement itself, called *elementary displacement*. Rotation displacements are expressed by the rotation angles around the coordinate system axis, that is, α, β, and γ around the axes x, y, and z. Translation displacements are expressed by components u, v, and w representing translations along axes x, y and z, respectively.

A tolerance zone is a surface or volume space limited by one or several definition elements of the surface or line. Nine tolerance zones are defined, four for surface elements and five for volume elements.

Surface:

1. defined by a planar disk;
2. defined by a planar annulus;
3. defined by a straight planar strip;
4. resulting from the offsetting of a line.

Volume:

1. Inside a square section prism;
2. inside of a cylinder;
3. inside of a cylindrical annulus;
4. resulting from the offsetting of a plane;
5. resulting from the offset of a surface.

The common representation of the tolerance zone defined by the inner volume of a cylinder, as illustrated in Figure 41. The diameter cylindrical zone t is constructed around the line element A, B that represents the axis of a cylindrical surface. The reference frame $(0, x, y, z)$ is defined with 0 as the middle point of the segment A, B and $\vec{X}$ oriented along the vector $\vec{AB}$. The application of the tolerance zone is represented by the positional tolerance of a cylindrical surface with respect to a complete set of data. The set of displacements that do not leave the segment A, B globally invariant is represented by the homogeneous transform matrix $D(v, w, \beta, \gamma)$ expressed in the reference frame $(0, x, y, z)$ as

$$D(v, w, \beta, \gamma) = \begin{bmatrix} C\gamma C\beta & -S\gamma & C\gamma S\beta & 0 \\ S\gamma C\beta & C\gamma & S\gamma S\beta & v \\ -S\beta & 0 & C\beta & w \\ 0 & 0 & 0 & 1 \end{bmatrix}. \tag{3.7}$$

Marziale and Polini [2009] compared the matrix method with the vector loop method. Using a case study, they concluded that the vector loop presents advantages over the matrix model. The matrix model also gives underestimated responses.

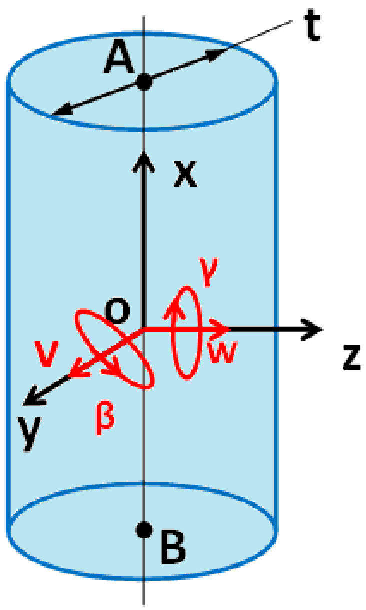

Figure 41 – A cylindrical tolerance zone. (Source: based on [DESROCHERS; RIVIèRE, 1997]).

Salomons et al. [1996] used the matrix representation model for the development of a CAD module for tolerance analysis, called FROOM. This software is explained in Section 3.3.

Yan et al. [2016] developed statistical tolerance analysis based on a homogeneous transform matrix. In their work, the homogeneous transform matrix is used to describe the assembly function. As the work also involves statistical analysis, it is commented on in Section 3.4.

3.2 Functional Tolerancing

Functional tolerancing is classically based on dimension chains with respect to functional requirements (FR) [BENICHOU; ANSELMETTI, 2011]. Dimensional variations or strains can occur in mechanical assemblies during their functional performance due to temperature or mechanical loading. Relative to the general coverage of the current literature on DT, few papers are available on functional tolerancing.

As this thesis considers only rigid assemblies in its scope, the main focus of this text is on the impact of temperature on dimensions. However, in this section a brief presentation about the effect of mechanical loading is made.

Jeang et al. [2007] presented a statistical tolerance design under thermal impact. The authors used the response surface methodology (RSM). RSM has the ability to produce an approximating function using a small number of experimental runs and is adopted to analyze measurement scores. According to the authors, an efficient solution can be reached with the method in terms of cost, quality, and time spent during design activities for simultaneous optimization of parameters and tolerance design. The classical example of a gearbox was used, first presented by [BJORKE, 1989]. The thermal calculations for each component of the assembly were calculated using the classical thermal expansion equation.

Pierre et al. [2009] described an example of tolerance design in a helicopter turboshaft engine to study the thermal effects of shaft bearing clearance. They used the skin model method to calculate tolerances and the FEM for thermal strain evaluation.

Benichou and Anselmetti [2011] developed an example of an electric motor shaft supported by two bearings, where the implications of shaft alignment and bearing clearance were considered. A meshed model was calculated using FEM for thermal design.

Jayaprakash et al. [2012] used also Bjorke's gearbox example for tolerance and thermal design. A FEM simulation was used to calculate both the thermal dilatation and inertia loads of parts. The tolerance design used the WC and was based on critical clearance points. The same authors [JAYAPRAKASH et al., 2014] used FEM to study the behavior of a mechanism subjected to thermal impact.

Spruegel et al. [2014] developed an interesting study of the functional behavior that affects the quality of products under the effect of global temperature. They illustrate the case of a bolt connection of three plates and reported its application in different countries at different seasons.

Sigmetrix [2016] described the integration of CETOL software technology 6σ with CAD technology to create an accurate model of assembly variation and introduced thermal expansion into the CAD / CETOL system 6σ to analyze the fit and function of assemblies that operate at any feasible operating temperature.

3.3 Worst Case

Few papers have been found that specifically treat the WC method. The reason for this finding is that all works that do not mention the statistical treatment of tolerances consider the WC approach. In some cases, the WC approach is compared to the statistical treatment of tolerances.

Dantan and Qureshi [2009] compared WC and statistical approaches in a work based on quantified constraints satisfaction problems. The authors used a mathematical formulation to simulate the influence of geometrical deviations on the geometrical behavior of the mechanisms. The notion of a quantifier (existential quantifier: "there exists"; universal quantifier: "for all") was integrated into the method. The influence of geometrical deviations and the influence of the types of contacts on the geometrical behavior were also taken into account.

Salomons et al. [1996] developed tolerance analysis using WC in a CAD tool module in development at that time *FROOM*. FROOM is an acronym for *feature and relation based object oriented modeling*. The method used a matrix-based development.

Askri et al. [2018] also compared WC and statistical approaches not in a tolerance analysis, but in a tolerance synthesis example for the propagation of uncertainties. The authors stated that the use of a reduced finite element model of fastened metal composite joints and a strategy to reduce the number of calculations ensure a low cost in time. The example considered the application of a single-lap metal-composite four-bolt joint, where several sources of variability were introduced, such as hole location error, pin/hole clearance, and fastener preload.

3.4 Statistical Simulation

The objective of statistical tolerancing (ST) is to avoid the conservative approach of WC, which results in a high product cost due to the small tolerance range of components required.

Several works dealing with ST are found in the literature for which a full description would be impracticable. Some works are commented on in this section; those whose content is more close to the thesis topic and more recently published.

Perhaps the most comprehensive study of statistical tolerances was conducted by Evans [1974], in several works [EVANS, 1975a], [EVANS, 1975b].

Yan et al. [2016] developed a statistical tolerance analysis based on a good set of points and a homogeneous transform matrix. In the work, the Newton-Raphson iterative procedure was adopted to solve the assembly constraint equations after the iterative formula had been deduced. The method is based on statistics, where the first n samples are generated based on *good point set* according to the distribution of each dimension. Then, for every sample, one functional requirement sample is computed according to the assembly constraint equations.

According to Fischer [2011, p. 99], *There are very powerful tools and are great for solving 3D tolerance stackups, as these tools allow the tolerance analyst to look at many combinations of translational and rotational variation. These tools are also fairly expensive and can be difficult to learn and use. 3D simulation tools are becoming easier to use with each release, but are still complex enough to warrant having dedicated staff to use them effectively.* The same author also cites commercial software *CETOL 6 Sigma* as a powerful 3D tolerance analysis modeling tool that does not use MCM and solves for WC and statistical variation.

Movahedi et al. [2016] used a method named the percentile method (PM) to estimate statistical distribution parameters and the generalized lambda distribution for design and analysis of tolerances of the assembly components. According to the authors, the findings indicated that when the distribution of the component data is unknown, the proposed method could be used to accelerate the design of the tolerance of the component. Furthermore, in the case of assembled sets, a more extensive tolerance for each component with the same target performance could be utilized.

Ledoux and Teissandier [2013] described a tolerance analysis method using a reliability-based approach to ensure that a functional condition is satisfied. According to the authors, a particular feature of the method is that it defines the combined effects of geometric and dimensional ISO specifications for product parts and the architectural parameters that define the relative positions of parts in contact.

3.5 Discussion on the Current Methods

Current 3D tolerance analysis methods that are used in CAT software mainly rely on parameterized geometry. Such a geometry is defined in 3D by means of a variational or parametric CAD model. In general, the objective is to determine the relationships between the variations in the parameters used to describe the geometry and the variations in the variables associated with the functional conditions. A functional condition is most often described by limits imposed on variables as a result of parameters, such as clearance or distance between two points on two functional surfaces [MANSUY et al., 2011].

An analysis of the currently available representation models leads us to the following considerations.

- No work considering general application-oriented examples is found at all. In many cases, the same example is used for a comparison among methods;
- Most of the models consider components. Although the variations of the contact surfaces between parts are accurately previewed, the overall variation of the assembly is not defined, as the positioning between parts is unclear. Kinematic adjustments are generally not taken into account;
- The tolerance simulation in the available models is difficult, if not impossible, to carry out. The works referencing statistical treatment of tolerances do not effectively consider the production simulation;
- The assembly shift variation observed in practice in actual assemblies, when precise fits are not specified, is not considered in all described methods;
- Few methods include functional dimensional variations.

4 A New Proposal for 3D Tolerances Analysis of Mechanical Assemblies Including Functional Effects

The DT approach, with fundamental importance in industrial applications, presents a very complex treatment and involves many theoretical ramifications. As discussed in the literature review, the several methods developed by different researchers are more prone to be used in the development of CAD tolerance modules software (CAT) rather than being useful for direct application. Moreover, CAT modules are considered “black boxes”, i.e., no indication of the method used is provided to the user, who has to rely on the results without any discussion about what is being effectively considered. So, the aim of this proposal is to present a new method for geometric tolerance analysis that can reach an effective result. It is based on the current GD&T standards applicable to mechanical designs. The proposed algorithm is simple and can be modified according to the design specific needs: the features of the geometric tolerances can be modified as required for attainment of the desired result. Manufacturing of high production volumes are contemplated and functional effects are considered, except for those ones regarding kinematic and dynamic behaviors.

To facilitate the understanding of the proposal, Figure 42 shows a diagram of the design sequence of a product, covering only its relevant items of interest. This is a step-by-step visualization identifying the items of this and of the next chapter as well.

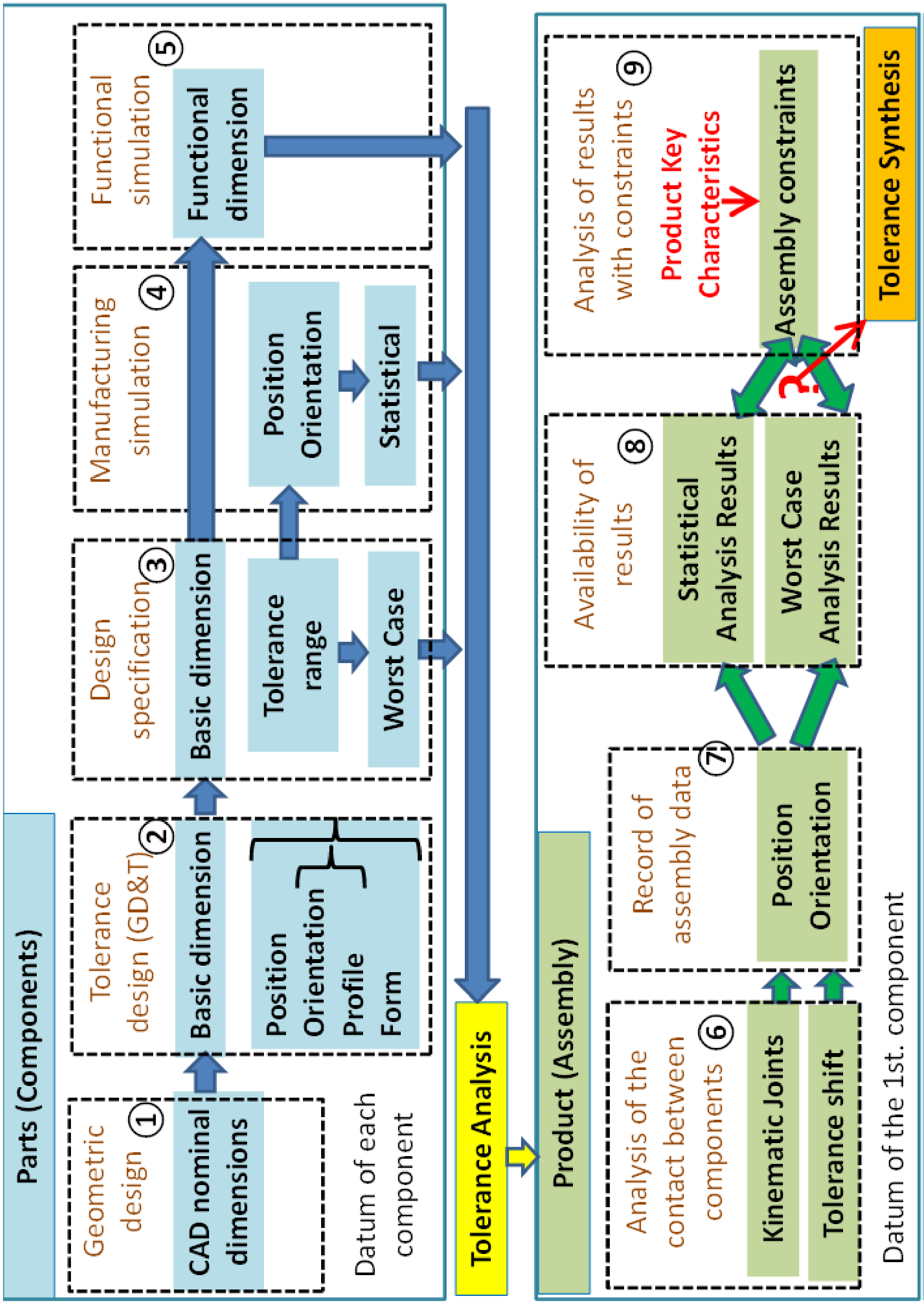

Figure 42 – Proposed scheme. (Source: the author).

The scheme is divided in different design activities, identified by numbered boxes, just to allow a better explanation. During the algorithm run, some activities are performed in a different order, such as the manufacturing simulation, all ones in each simulation step.

Before starting with the explanation of the method, a rough illustration of it is provided in Figure 43, summarizing its main characteristics:

- The main datum of the assembly is the the same one of the first component, which references all features position and orientation tolerances;
- The target feature, the end of the tolerance chain of the assembly, is located at the last component;
- The contact of all surfaces between all components in the chain is affected by position and orientation variations. All variations are subjected to random simulation.

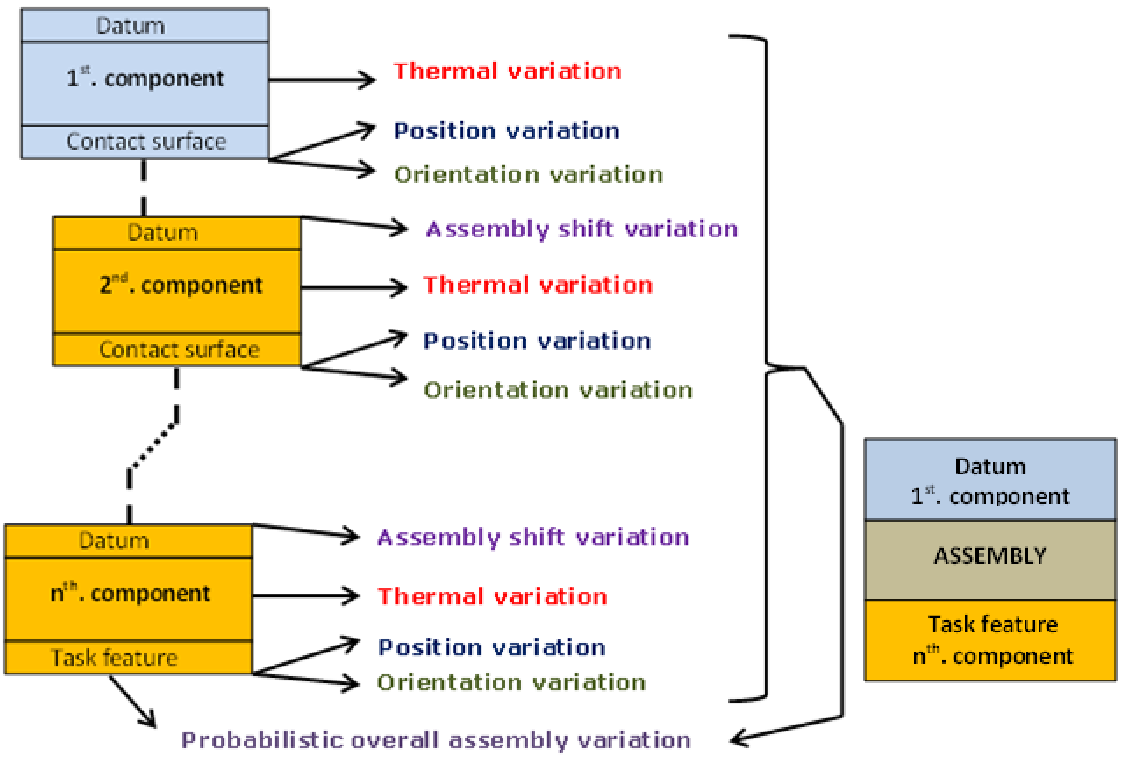

Figure 43 – Assembly's target feature probabilistic overall variation as function of components' variation. The assembly datum frame is located at the first component. (Source: the author).

The sections ahead follow the numbering of the boxes in Figure 42. The respective subsections detail the development of the proposal regarding each topic.

4.1 Geometric Design

The geometric design of the product is developed in a CAD platform, based on the product conceptual design, where the principle of solution is elaborated. It is generally originated from a mock-up. After the conceptual phase, the following part of the product design is the *embodiment design, when designers must determine the overall layout design (general arrangement and spatial compatibility), the preliminary form designs (component shapes and materials) and the production processes, and provide solutions for any auxiliary functions* [PAHL et al., 2007, p. 227].

The product production volume and its proposed cost are taken into account on the design decisions. The knowledge acquired from former designs are also considered. All dimensions are nominal and all shapes are perfect.

From the main assembly nominal model, the models of each component are defined by means of different criteria, such as:

- main and auxiliary functions;
- safety;
- process feasibility and cost;
- life-cycle (wear, fatigue) and replacement timing when applicable;
- direction of flow, motion, position, etc;
- material-determining requirements, such as resistance to corrosion, service life, strength, temperature, etc.;
- assembly feasibility and easiness, and maintainability (such as tool access and need of special tools);
- finishing;
- material recycling requirements.

The CAD models of the components can be used for CAE simulations, such as material strength dimensioning and flow performance. The interfaces between consecutive components are defined, as well as their locating and fastening elements. Although the components' surfaces are generally not specifically identified with this purpose on the respective detail drawings, which are used primarily for manufacturing and inspection purposes, they are important for material strength calculation and for the assembly design.

4.2 Tolerance Design

The tolerance design of each component is performed. The components' CAD model are extracted from the assembly layout and the basic (nominal) dimensions are preserved. Tolerances for each dimension and feature are specified based on concurrent engineering (CE) with other areas, such as manufacturing and quality.

The CE approach aims to improve communication among the several areas involved in a new project and to reduce their interfaces rigidity. An example of this approach can be found in [BARARI; POP-ILIEV, 2009], consisting of a novel model of product lifecycle management (PLM) in which, instead of studying engineering activities exclusively with respect to a temporal variable, the processes are deliberately managed to form closed loops of two or more activities with respect to two independent dimensions: time and rigidity. The model was referred to as closed-loop engineering (CLE), in which flexible interfaces are generated by real-time analysis of respective actions and the reactions between them, and eliminates the need to specify solid interfaces between the engineering activities.

In this design step, the datum frame of each component is defined, following the order of precedence of the assembly tolerance chain. In the detail drawings, all dimensions depart from the component's specified datum frame origin.

4.2.1 The Treatment of the Location Tolerances

In case of mechanical rigid assemblies, as defined in the scope of this work, their parts are joined through finished contacting surfaces. A flat surface restrains one linear displacement DoF and two rotational DoF. The remaining three DoF - two linear displacement and one rotational in the surface plane - are generally restrained by two holes: one of them restrains the linear displacement in orthogonal directions and the other one restrains the rotation, as illustrates Figure 44.

The restraining of DoF obeys an order of precedence [ASME..., 1995, p. 49]: in this case, the flat surface (plane $X - Y$), the first hole (plane $X - Z$) and finally the second hole (plane $Y - Z$) defines a datum frame $X - Y - Z$. Naturally, other forms of DoF locking in space can be used, such as curved surface-hole, flat surface-flat surface- flat surface, flat surface-line-surface (as is the case of positioning with a key). However, in mechanical design practice, the feasibility of manufacturing, cost and need of fastening are of utmost importance. For this reason it is observed that the surface-hole-hole restraining design is the preferred one, except for the special cases.

4.2.2 The Treatment of Orientation Tolerances

The orientation deviation may be small and its significance must be checked before being considered in the tolerance calculation.

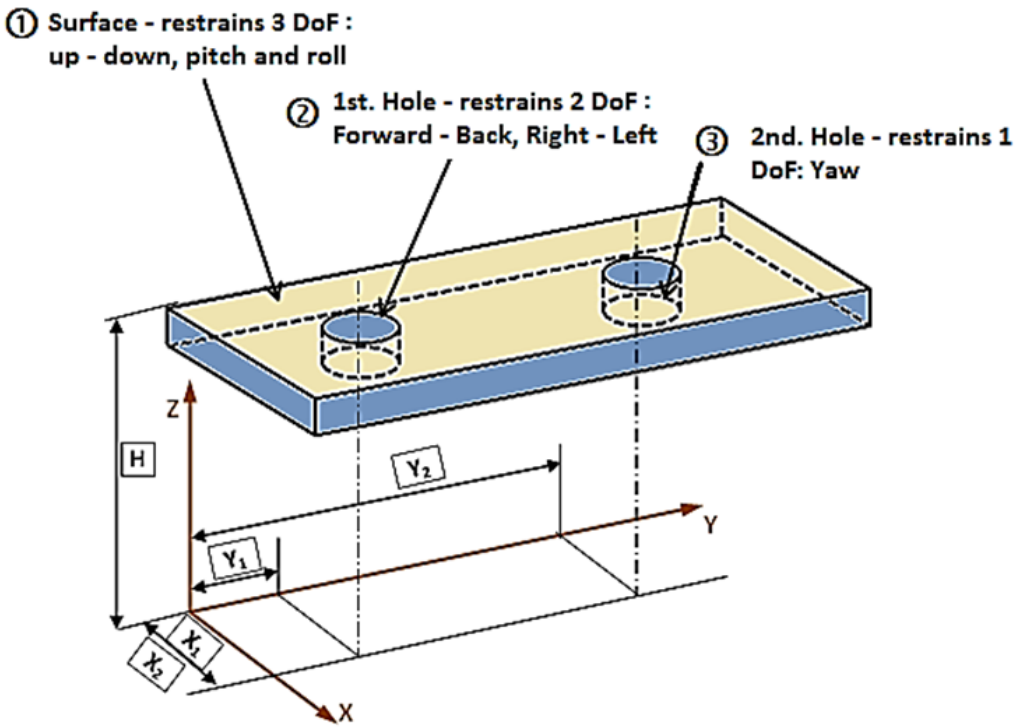

Figure 44 – Datum referencing with 1 surface and 2 holes. DoF are restrained in a sequence and Frame $X - Y - Z$ is defined. (Source: the author).

An example is the parallelism between surfaces: an usual parallelism of 0.2 mm in a surface width of 400 mm, in the WC, gives a deviation of

$$\tan \alpha = \frac{0.2}{400} \rightarrow \alpha = \arctan\left(\frac{0.2}{400}\right) \cong 0.03°. \tag{4.1}$$

However, in this work the approach regarding orientation deviation is addressed as deep as needed in order to the attainment of the best result in function of the design specified accuracy.

In this explanation, four-sided surfaces (see Figure 45) are considered because they are useful to represent surfaces **of any shape** since just the main orthogonal directions (X, Y, Z) are considered in the calculations. Indeed, four-sided surfaces are also the most common ones found in industrial applications. Figure 45 illustrates the concept for a single orientation variation direction for simplification. However, the same applies to an orthogonal direction and also for a composition of directions.

4.2.3 Surface Orientation

In a tolerance chain, the orientation deviation of a component is affected by both the orientation and the profile tolerances of the contact surface of the former component [ASME, 2005, pp. 99, 158]. These tolerances are angularity, parallelism, perpendicularity and profile of any shape. The last ones may be used optionally [ASME, 2005, p. 166].

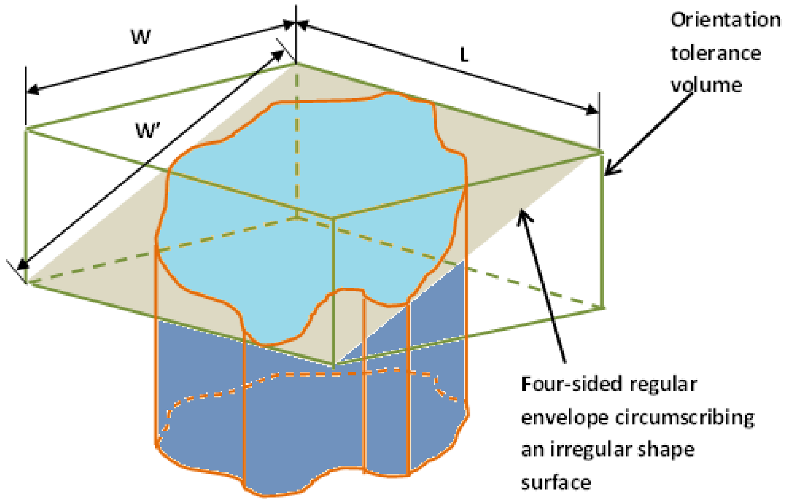

Figure 45 – An irregular shape surface can be treated as circumscribed in a regular four-sided envelope through its maximum length L and width W'. (Source: the author).

The best way for explaining the method of treatment of the orientation tolerances is by means of an example, in which a parallelism tolerance is considered. However, the same concept is valid for tolerances of angularity and perpendicularity, because all of them involve angles: the only difference is their angle direction and/or magnitude.

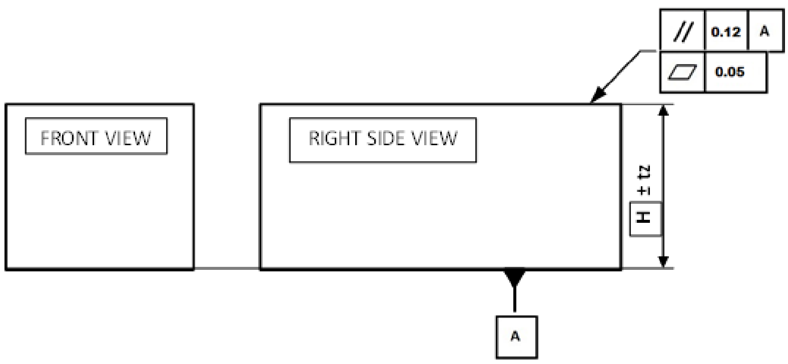

Figure 46 – A drawing of a block with specification of a tolerated height, a parallelism (0.12 mm) and a flatness (0.05 mm) tolerances. (Source: the author).

Let's consider a single block illustrated in Figure 46. The height of the block is specified by a non geometric tolerance $\pm tz$ in a basic dimension H. The bottom face is taken as datum A for the top surface tolerance of orientation (a parallelism of 0.12 mm). A form tolerance is additionally specified on the top face (a flatness of 0.05 mm). The meaning of the specification is illustrated by Figures 47 to 50:

1. In Figure 47, the full height tolerance range $\pm tz$ is represented by a height $2tz$ in a volume containing all possibilities of positioning the block top face, including

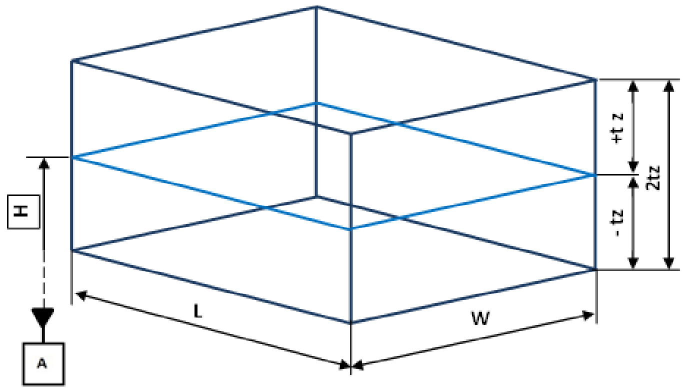

Figure 47 – A volume containing the full tolerance range of the specified height dimension (position). (Source: the author).

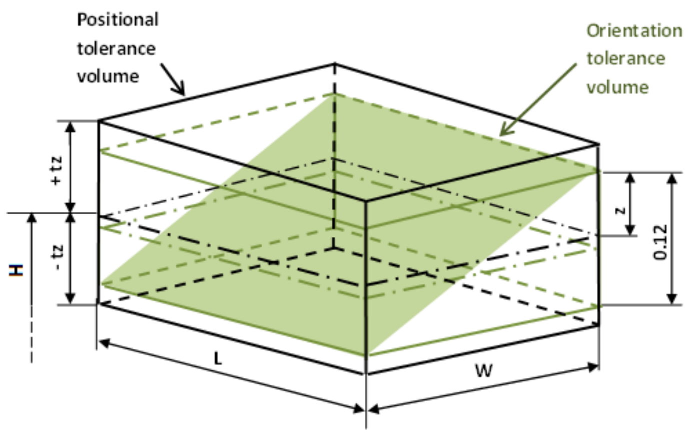

Figure 48 – A volume containing the maximum orientation tolerance ($to = 0.12mm$). The orientation tolerance volume must be contained within the position tolerance volume $L \times W \times 2tz$. (Source: based on [ASME..., 1995, p. 100]).

all possibilities of pitch and/or roll variation. The top face, when positioned with its four edges at the same distance $2tz$ from A (maximum volume), represents the maximum material condition (MMC) in this direction and limits all the tolerances of form [ASME, 2005, pp. 6, 91] and orientation [ASME, 2005, p. 100], that is, the top face in this condition must present a perfect form and no orientation deviation is allowed (this is a theoretical approach, impossible in practice). Inversely, the same occurs when the surface is at the minimum positional value, the least material condition (LMC). The variate z may take any value in the range $\pm tz$ in relation to the basic value H;

2. In Figure 48, an orientation tolerance volume is shown at a random portion of the height position tolerance volume, at a given value z (any value within $\pm tz$). The plane illustrates the orientation (maximum roll position) at the shown direction (maximum parallelism tolerance range). However, infinite positions of the plane

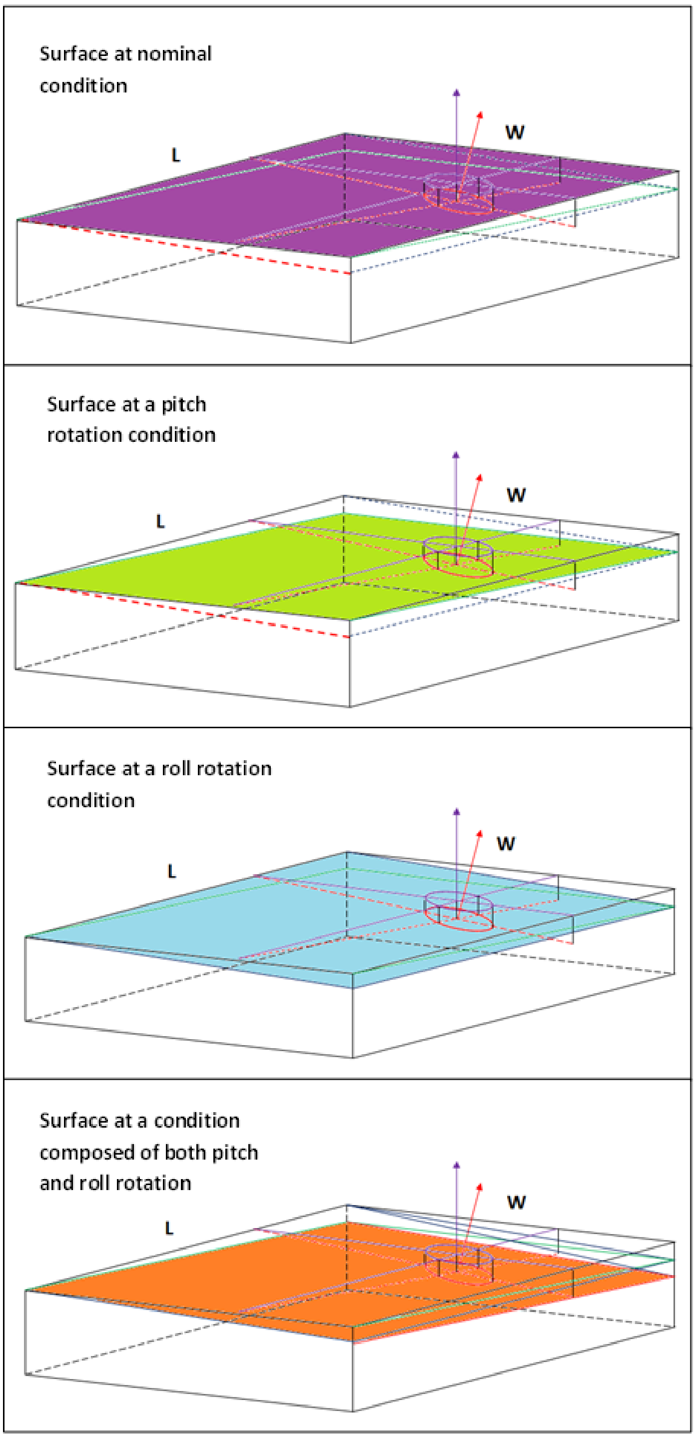

Figure 49 – Possibilities of orientation of a surface. (Source: the author).

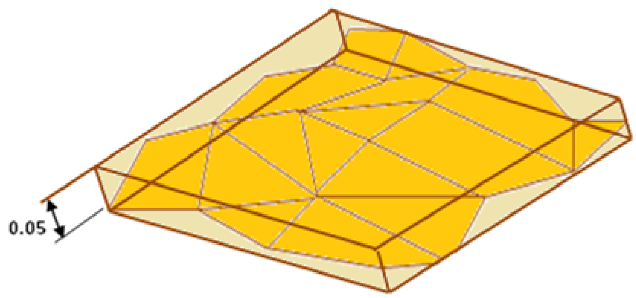

Figure 50 – A volume containing the flatness tolerance of 0.05mm. When the part surface coincides with either MMC or least material condition (LMC), no flatness tolerance is allowed. (Source: the author).

are possible within the orientation tolerance *to*, within the tolerance range volume defined by values of height from 0 to 0.12 mm. For a better understanding, Figure 49 shows some orientation possibilities among several other alternatives;

3. Figure 50 shows an additional design constraint regarding a form tolerance (flatness) of 0.05 mm in the same rotation condition (roll) of Figure 48. Form tolerances, such as orientation tolerances, may not go beyond either MMC or LMC, i. e., beyond the upper or lower limits of the positional tolerance [ASME, 2005, p. 91];

4. In mechanical assemblies, flatness tolerances are usually specified in two cases:

   (1) when sealing elements are fit or poured between components' surfaces to prevent leakage of fluids; in these cases, solid gaskets are designed to squeeze along the flatness tolerance and liquid sealants are supposed to occupy voids between surfaces and to withstand the service fluid pressures after curing;

   (2) when a solid contact is made between surfaces, the compression pressure allowed by fastening elements tightening torque results in deformation by material compression (above the yielding limit) of the high regions of the materials' contact.

   In practice, flatness deviations may be disregarded regarding position and orientation deviations because: a) its order of magnitude is very low in relation to the considered dimensions and; b) in average, the flatness deviation value is zero, otherwise it would either be considered as an orientation deviation or the surface would be warped;

5. It is also important to stress that no misunderstanding must occur between form tolerances and rugosity. Rugosity is defined in a micro order of magnitude and does not apply in the range of dimensions considered in geometrical tolerances;

6. In this proposal, the orientation tolerance of a component's surface, in a specific direction, is treated as a random variable. This variable defines the spatial orientation

of positioning the datum of the next component in the assembly chain, i.e., the orientation tolerance angle defines the orientation of a normal vector of the surface where the next component datum is positioned, as shows Figure 51. As already cited, orientation tolerances restrain two rotational DoFs.

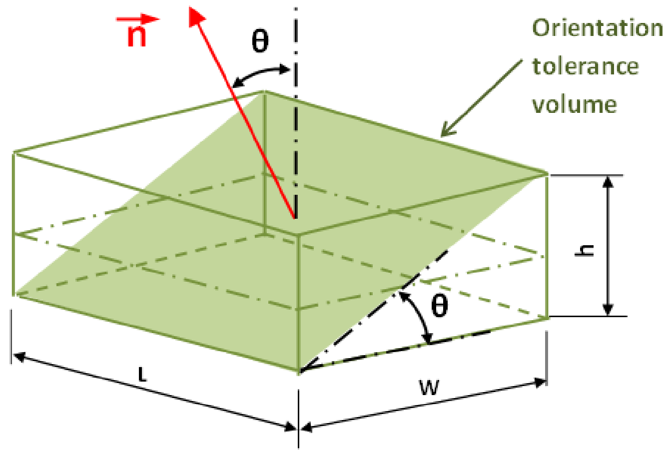

Figure 51 – The angle defined by the orientation tolerance in a given direction positions the datum of the next component in the assembly chain. (Source: the author).

4.2.4 Position Displacement Due to Orientation Tolerances

1. The original concept of GD&T resulted from the need to represent tolerances in a 3D space, where not only dimensional tolerances are considered, but also other ones needed to represent the specification of other manufacturing deviations. The effect of an orientation variation (angular displacements) can present a significant impact when components are assembled in a chain, since their surfaces must fit to each other through a best contact in an equilibrium condition. This fact leads to a resulting target feature that presents both position and orientation variations, as illustrates Figure 52.

2. A very important issue regarding the location tolerances of a mechanical assembly component is how to consider its orientation tolerances in the tolerance chain, that is, the effect of the orientation variation of a surface where the next component of the assembly will make contact, positioned, and fastened. Positioning is generally made by drilled and reamed holes and fastening by threading. Figure 53 illustrates the direction of the center lines of the holes in relation to both a nominal and an actual surface affected by an orientation variation.

   Figure 54 illustrates a nominal surface, containing points Q_0, P_0, R_0 and S_0 positioning a hole in relation to the component datum. The points Q_E, R_E, and S_E are located at the edges of the surface. The surface may assume any infinite orientation

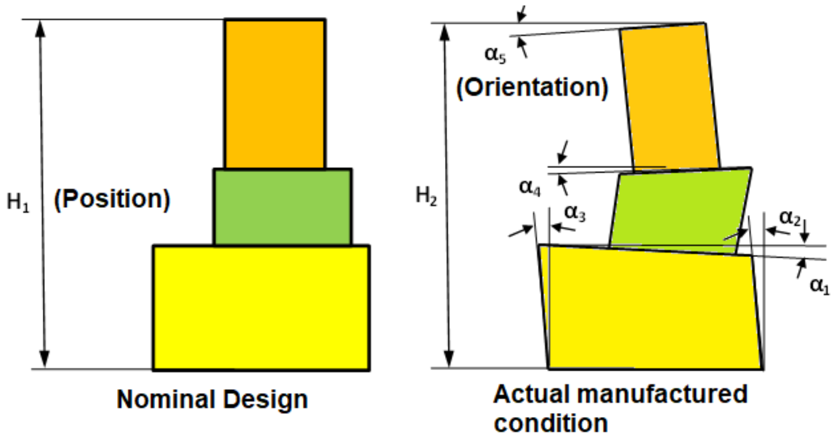

Figure 52 – The effect of orientation variation on the position variation. (Source: the author).

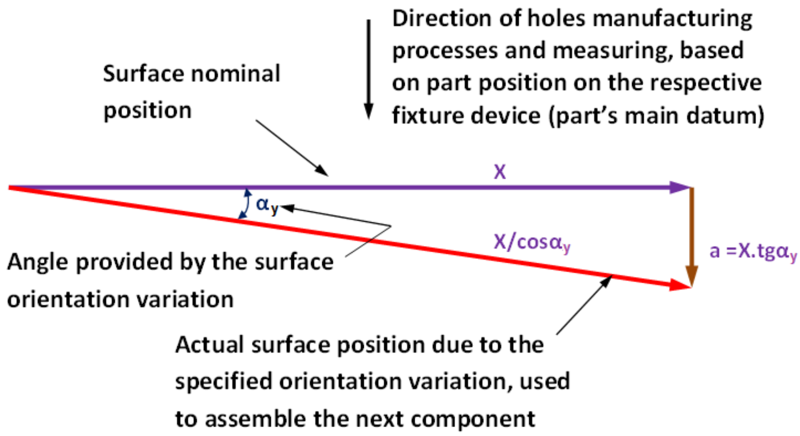

Figure 53 – The effect of a surface orientation variation on the manufacturing process of holes. (Source: the author).

direction and inclination (defined by variation Δto within the orientation tolerance volume defined by specified height to, width W and length L).

As can be seen in Figures 53 and 54, the centers of the locating/fastening holes are not theoretically perpendicular to the actual flat surface, and this characteristic affects the assembly condition of the next component. However, this angular error is small and is compensated by assembly shift clearances in fastening and mechanical deformation in the case of locating elements.

3. The horizontal directions shown for the basic dimensions X and Y in Figure 54 are parallel to the datum surface, which is used to position the part on the machine fixture device. The reason for this is due to the features of the usual manufacturing processes, as follows:

a) Material removal processes, such as drilling and reaming, are performed in either three-axis or five-axis machines, where no adjustment regarding the orientation position of the processed surface is made and all dimensions depart from a fixed

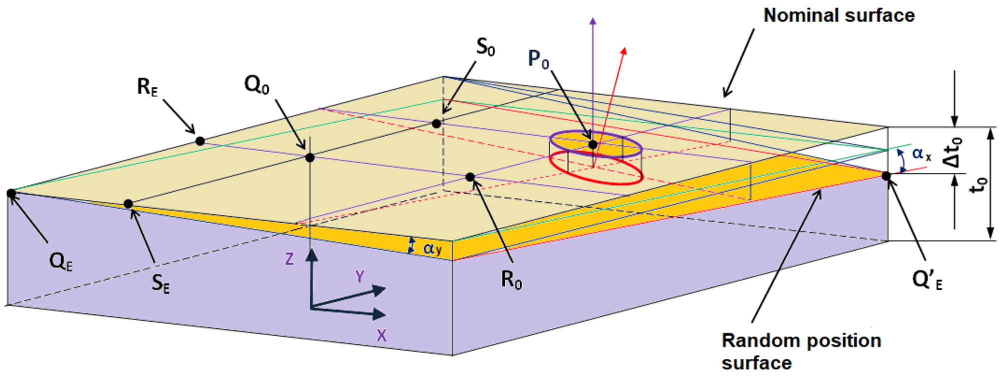

Figure 54 – A random position of a surface within an orientation volume. (Source: the author).

reference, generally a bottom face, through which the part is positioned and held. The same occurs with the milling and grinding processes;

b) The additive process of the materials is carried out using a nozzle fitted to a moving head. The part starts from a first layer deposited over a table, its datum surface. The head must be accurately adjusted to move flatten to the table; otherwise material voids would occur. In this case, the position and orientation of the variates (random variables) x and y are theoretically linked to the datum surface.

The necessary mathematical treatment can be better understood with an analysis of Figure 55, which is a magnification of Figure 54. The points P, Q, R, and S are located on the surface rotated at a random position within the orientation volume.

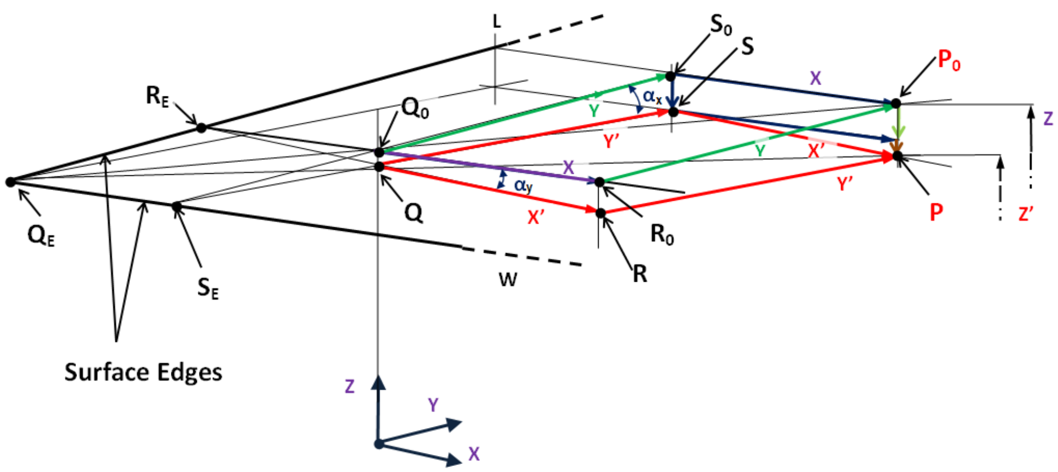

Figure 55 – Geometric representation of a surface orientation variation. The points shown are the same of the ones of Figure 54. (Source: the author).

For the development of the algorithm of the proposed method, some simple rules must be placed:

(a) As default, the basic dimension X and the variate x are associated to the width W, respectively. In the same way Y and y are associated to length L. As already cited, the *roll* rotation occurs in relation to axis Y, and *pitch* in relation to axis X;

(b) An analysis of Figure 55 leads to four possibilities of the plane orientation for non null angle values, limited by orientation variation Δto:

1. Right / Forward (R/F), as shown;
2. Left / Back (L/B);
3. Right / Back (R/B);
4. Left / Forward (L/F).

(c) The possibilities of the plane inclination are driven by the alternative signs of the angles of the surface inclination about the axes X and Y, regardless the angle magnitude α_y (roll) and α_x (pitch). Obviously, the plane's opposite sides must be parallel, otherwise the surface would be deformed (warped) - *this condition is also ensured by a specified flatness condition*. Figure 56 is a magnified detail of the system, showing some possibilities.

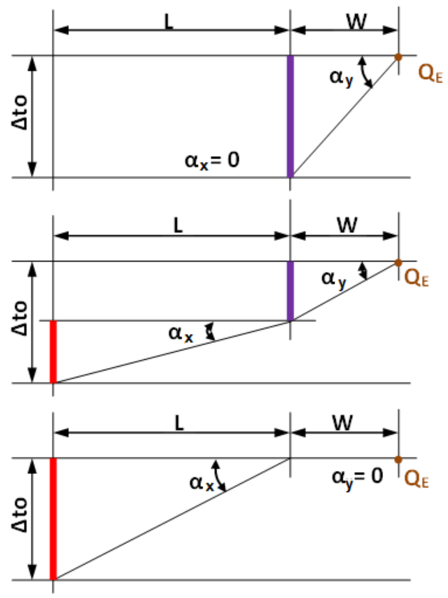

Figure 56 – Some orientation possibilities for angles α_x and α_y. (Source: the author).

The absolute value of the sum of the variations in each direction must be equal to the orientation variation Δto, the problem constraint, as

$$|L \cdot \tan\alpha_x + W \cdot \tan\alpha_y| = \Delta to. \tag{4.2}$$

4. Regarding the location of a generic point P pertaining to the inclined plane with dimensions $W \times L$, Figure 57 illustrates one of the possible orientation configurations

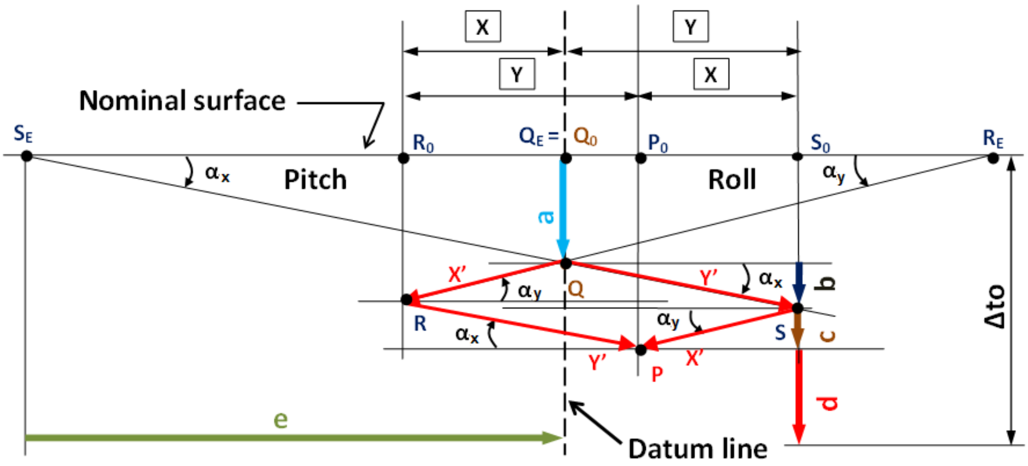

Figure 57 – Determination of point P position. (Source: the author).

for the plane of Figure 55, folded in relation to point Q. Point P belongs to plane $Q - R - S$;

5. From Figure 57, the following equations are developed:

$$\tan \alpha_y = \frac{c}{X} \rightarrow c = X \cdot \tan \alpha_y \tag{4.3}$$

$$\tan \alpha_x = \frac{a}{e} \rightarrow a = e \cdot \tan \alpha_x \tag{4.4}$$

$$\tan \alpha_x = \frac{b}{Y} \rightarrow b = Y \cdot \tan \alpha_x \tag{4.5}$$

As can be seen, at least one dimension from one of the edges of the surface is necessary to determine the position of the point P. This results from the definition of the constraint Δto.

6. Equation

$$d = \Delta to - a - b - c \tag{4.6}$$

gives the value of the positional deviation d due to the orientation variation, which can be summed with the vertical dimension $H \pm z$. In the algorithm, in each iteration, both the constraint Δto and one of the angles (α_x), are chosen within their limits (Δto within to and α_x within Δto).

The algorithm routine for the above calculation is straightforward, based on Equations 4.2 to 4.6.

Figure 58 illustrates the effect of orientation variation on the position of the next component in a tolerance chain. The datum frame of the next component is positioned and oriented as a function of the surface variation of the former component.

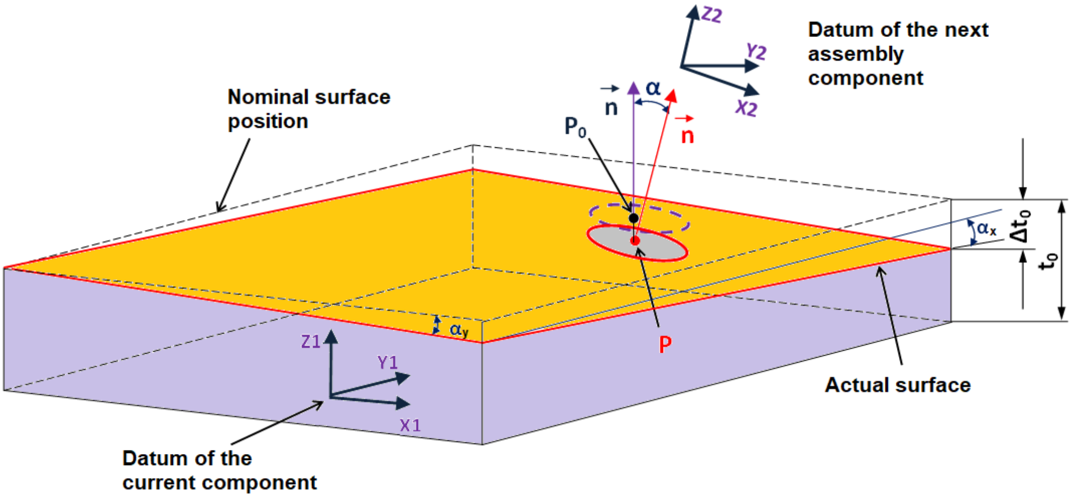

Figure 58 – The effect of the orientation variation on the position of the next component in a tolerance chain. (Source: the author).

4.2.5 Orientation Variation on a Flat Surface due to Assembly Shift

The orientation variation may also be affected by the assembly shift between fasteners and holes, although this deviation may be considered very small. However, it is taken into account in our work. This deviation affects mainly the positioning of the datum of a component in relation to the fastening threads on the surface of a predecessor component in the assembly chain when guide holes are not considered in the design. Indeed, this procedure is not applicable to the first component of an assembly since it defines the main datum. Figure 59 shows the centered offset conditions and one of the thread-hole contact. Infinite offset positions between a fastener thread and a hole are possible in each direction and at infinite direction possibilities as well.

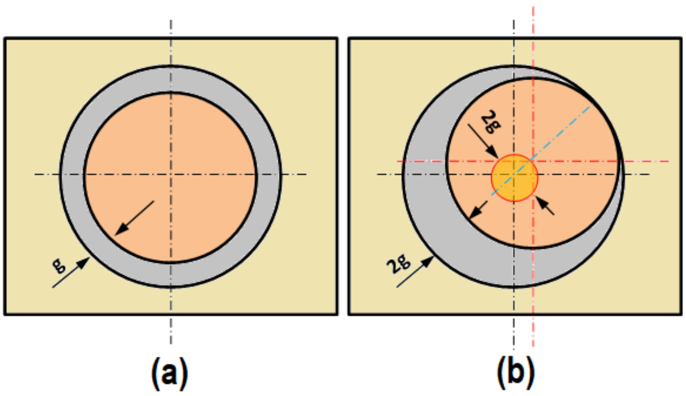

Figure 59 – Position variation due to a gap g between fastener and hole: a) centered condition; b) maximum offset condition in one direction. (Source: the author).

Figures 60 and 61 illustrate two of the three possibilities of center positions of the first and second fasteners. The range of variation is restricted to a circle of diameter $2g$, that is, twice the value of the gap between the thread and the hole. The position tolerances of the holes are considered separately.

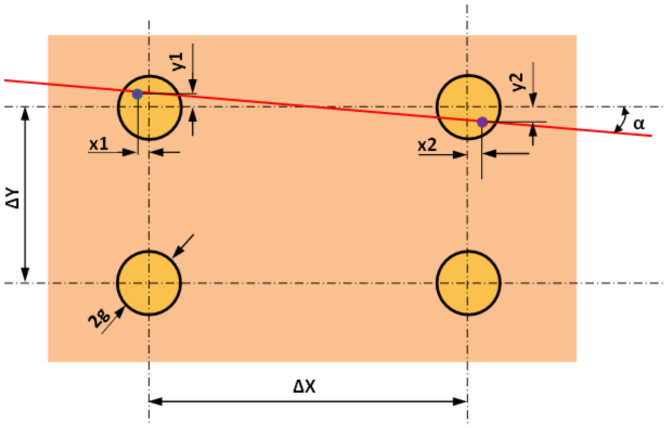

Figure 60 – Orientation variation generated by a hole-thread gap - aligned holes. (Source: the author).

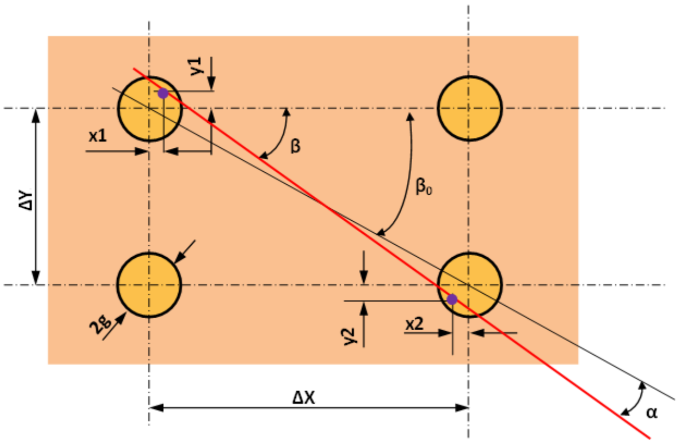

Figure 61 – Orientation variation generated by a hole-thread gap - opposite holes. (Source: the author).

As already mentioned, a datum surface immobilizes three DoFs (two rotational and one translational). The first hole, secondary in the datum sequence, with index (x_1, y_1) locks the other two (translational) DoFs. The second hole, with index (x_2, y_2), locks the remaining rotational DoF. The other holes, due to their design positional tolerances, do not interfere or participate in component positioning. This feature is provided by a good design.

The algorithm developed to calculate the orientation deviation is described below, according to the elements referenced in Figures 60 and 61.

```
% Data input
    deltax = value;
    deltay = value;
```

```
    x1 = value;
    x2 = value;
    y1 = value;
    y2 = value;
if deltax>0
    beta0 = atand(deltay ./deltax);
    beta = atand((deltay-y1+y2)./(deltax-x1+x2)) - beta0;
else
    beta0 = atand(deltax ./deltay);
    beta = atand((deltax-x1+x2)./(deltay-y1+y2)) - beta0;
end
```

As can be seen, the values of $deltax$, $deltay$, and $beta0$ are positive or null. The input values x_1, x_2, y_1, y_2 and the result value $beta$ can be positive, negative, or null. Furthermore, since this algorithm is included in the main program, the values of x_1, x_2, y_1, y_2 are the result of a previous random generation in each iteration. For a null value of $deltax$, the secondary hole aligns with the primary in a lower vertical position, not shown in the figure. The calculation is inverted in relation to the case of $deltay = 0$.

4.3 Design specification

After the selection of tolerances, the design specification is concluded. The tolerance range for each dimension is recorded, allowing the calculation of the WC tolerance analysis.

4.4 Manufacturing simulation

On the basis of both the tolerance range and the production volume, a manufacturing statistical simulation is conducted for each position and orientation. The algorithm routine for calculation of random values amid a range of any position or orientation tolerance can be constructed using the subroutine *rand* of the software, which generates random values between 0 and 1, as follows:

```
x1wcma=  value;             % (WC maximum value)
x1wcmi= -value;             % (WC minimum value)
x1 = rand;                  % (random number between 0 and 1)
if x1 >= 0.5                % (a positive value)
   x1 = (x1-0.5).*x1wcma;
else
   x1 = x1.*(x1wcmi);       % (a negative value)
end
```

The manufacturing simulation approach is based on the use of random variables. The joint distribution of two discrete random variables x and y is an expression $p(x_i, y_i)$ that gives the probability associated with all possible pairs of the random variable for all possible combinations of x_i and y_i [HAHN; SHAPIRO, 1967, p. 52]. The validity of a joint distribution $p(x_i, y_i)$ requires that x_i and y_i be independent [HAUGEN, 1968, p. 19].

In a mechanical assembly, the positional tolerances of its components are evidently independent because they are produced by independent processes and, in most cases, by different suppliers.

However, an issue could be raised regarding the independence of variates in the same component of the assembly when the design involves the geometric tolerance approach. Consider, for example, the general case illustrated in Figure 6 in Chapter 2.

As geometric tolerances are considered in 3D designs, the positional tolerance d in a plane is contained in a circle with a specified diameter [ASME..., 1995], and this fact could induce a supposed dependence between x and y. However, in non-geometric tolerancing, the relationship given by Equation (2.1) is not observed and the variates are fully independent from each other, which proves the independence of the variables in geometric tolerancing. Figure 5 in Chapter 2 illustrates the configuration.

The algorithm routine regarding the positional tolerance of a guide hole with a location tolerance (diameter) $= 2 \times value$, can be constructed as follows:

```
x1wcma =  value;                    % (WC maximum value of x1)
x1wcmi = -value;                    % (WC minimum value of x1)
y1wcma =  value;                    % (WC maximum value of y1)
y1wcmi = -value;                    % (WC minimum value of y1)
x1 = VALUE;  % (VALUE >> value) % (value that forces the while loop)
y1 = VALUE;  % (VALUE >> value) % (value that forces the while loop)
while (sqrt(x1^2 + y1^2) > value)
x1 = rand;
if x1 >= 0.5                        % (a positive value)
x1 = (x1-0.5).*x1wcma;
else
x1 = x1.*(x1wcmi);                  % (a negative value)
end
y1 = rand;
if y1 >= 0.5                        % (a positive value)
y1 = (y1-0.5).*y1wcma;
else
y1=y1.*(y1wcmi);                    % (a negative value)
end
end
```

4.5 Functional Simulation

In this work, the functional-dimensional variation considered by the method considers the thermal effects of the assembly application. The dimensional variation due to the effect of the mechanical loads, if applicable, can be calculated using CAE tools, as mentioned in Subsection 2.7.3. Furthermore, since the scope of the work refers only to rigid assemblies, the dimensional variation due to mechanical loading is not significant regarding its degree of magnitude in relation to the other ones addressed.

Functional thermal simulation is conducted on components affected by significant operational temperatures. Mean temperatures are estimated for discrete segments of significant length, based on either previous experience or available reliable data.

The consideration of thermal effects

Thermal effects can have an influence on the DT of a mechanical assembly, depending on the magnitude of both the temperature variation and the dimensions of the components. A representative example may be found in [UMARAS et al., 2020].

The thermal effect also follows a path inside the component where its material is present. In components manufactured in metallic materials, which present good thermal conduction, steady-state is generally considered in most cases. Figure 62 illustrates a component subject to an overall temperature gradient, represented by discrete segments. There is supposed to be a lower temperature gradient at each segment. This is an approximation used in our proposal to allow the representation of different material regions, for example, affected by cooling flows. When a computer flow design (CFD) analysis is available, it can be used to improve accuracy. However, measurements are generally made in these cases to validate the results.

The approximation by discrete segments allows for the calculation of the dimensional variation on the length of each one in the main algorithm. Equations

$$\Delta l_i = l_i \cdot \alpha_m \cdot \Delta T_i \tag{4.7}$$

$$\Delta l = \sum_{0}^{i} \Delta l_i, \tag{4.8}$$

are used in this procedure, where Δl = variation in length due to the temperature gradient; Δl_i = difference in dimension between the functional temperature of the component and the ambient temperature of a material segment subject to a temperature gradient ΔT_i; l_i = dimension under the difference in functional temperature ΔT_i; α_m = Component material coefficient of expansion; ΔT_i = Difference in temperature between functional and ambient conditions for the material segment.

The values of the thermal expansion coefficient are usually very small and the basic dimensions are very large compared to their tolerance ranges. Therefore, **only basic**

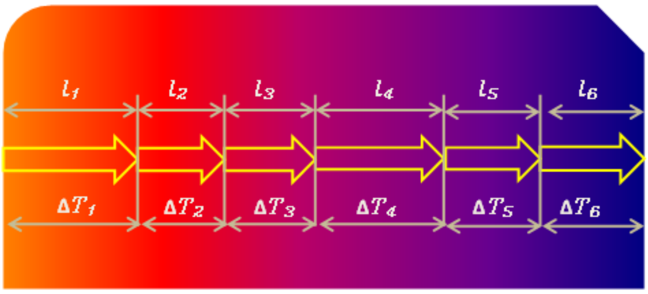

Figure 62 – Discrete segments at constant temperature representing an overall temperature gradient inside a component. (Source: the author).

dimensions are considered to be affected by thermal effects, as the dimensional variations in the tolerances are exceptionally small and must be considered in another magnitude order and can be neglected. However, the method does not restrain any special condition in which thermal effects over tolerances could be considered, since the described approach is also valid with applicable adjustments.

The algorithm routine for the thermal dilatation is straightforward, based on the equations 4.7 and 4.8.

4.6 Analysis of the Contact Between Components

When the assembly tolerance analysis is initiated, the contact surfaces between consecutive components (kinematic joints) are affected by the position and orientation variations determined by the simulation values. The tolerance shift, as applicable, can also affect the orientation variation. This item represents a major novelty with respect to the current available methods of tolerance analysis, as cumulative variations of both position and orientation at each joint of components in the assembly chain can affect the overall result of the analysis. There is no evident finding of such features in other existing models.

4.7 Record of Assembly Data

The position and orientation values for each component contact are registered for each simulation step. This is also a distinctive characteristic of the method in terms of its statistical behavior, mainly for high production volumes.

4.8 Availability of Results

The results of the tolerance analysis are presented. The statistical results are displayed as 3D clouds of points. The software allows for visualization of the values of each simulated point. The WC results are displayed for maximum and minimum values in the 3D space, allowing comparison with the simulation results.

4.9 Analysis of Results with Constraints

The results of the assembly analysis can be compared with the intended design constraints. In the event of non-compliant values with the design intent, a tolerance synthesis must be performed to reduce the tolerance values of one or more components. In general, a cost-quality balance is considered in the process. As mentioned above, tolerance syntheses processes are not within the scope of this work.

4.10 Proposed Algorithm

The algorithm of the proposed method is summarized in the flow charts illustrated in Figures 63, 64, and 65. The splitting of the algorithm into parts intends to facilitate the explanation with the corresponding enumerated items of the step-to-step procedure described in sequence:

1. Data entry

   a) input the number m of components;

   b) Address the datum frame of the first component: $X_0, Y_0, Z_0 = 0$, as well as the datum frames of all other components. Make sure that the specified directions are consistent with those of the first component of the assembly;

   c) For the output surface of each component, where the next component of the assembly chain is positioned and fastened, retrieve the specified orientation tolerance, the tolerances of the specified positioning features, and the tolerance of the fastening features;

2. Check whether orientation and/or profile tolerances referencing position are specified. An example of this tolerance is found in the thrust face of the case study presented ahead;

3. Recall and record the WC values of the tolerance for the orientation of the surface, according to Section 4.2.3. Values are used to determine the position tolerance of other features;

4. Determine and record the position of the first positional feature, according to Section 4.2.1;

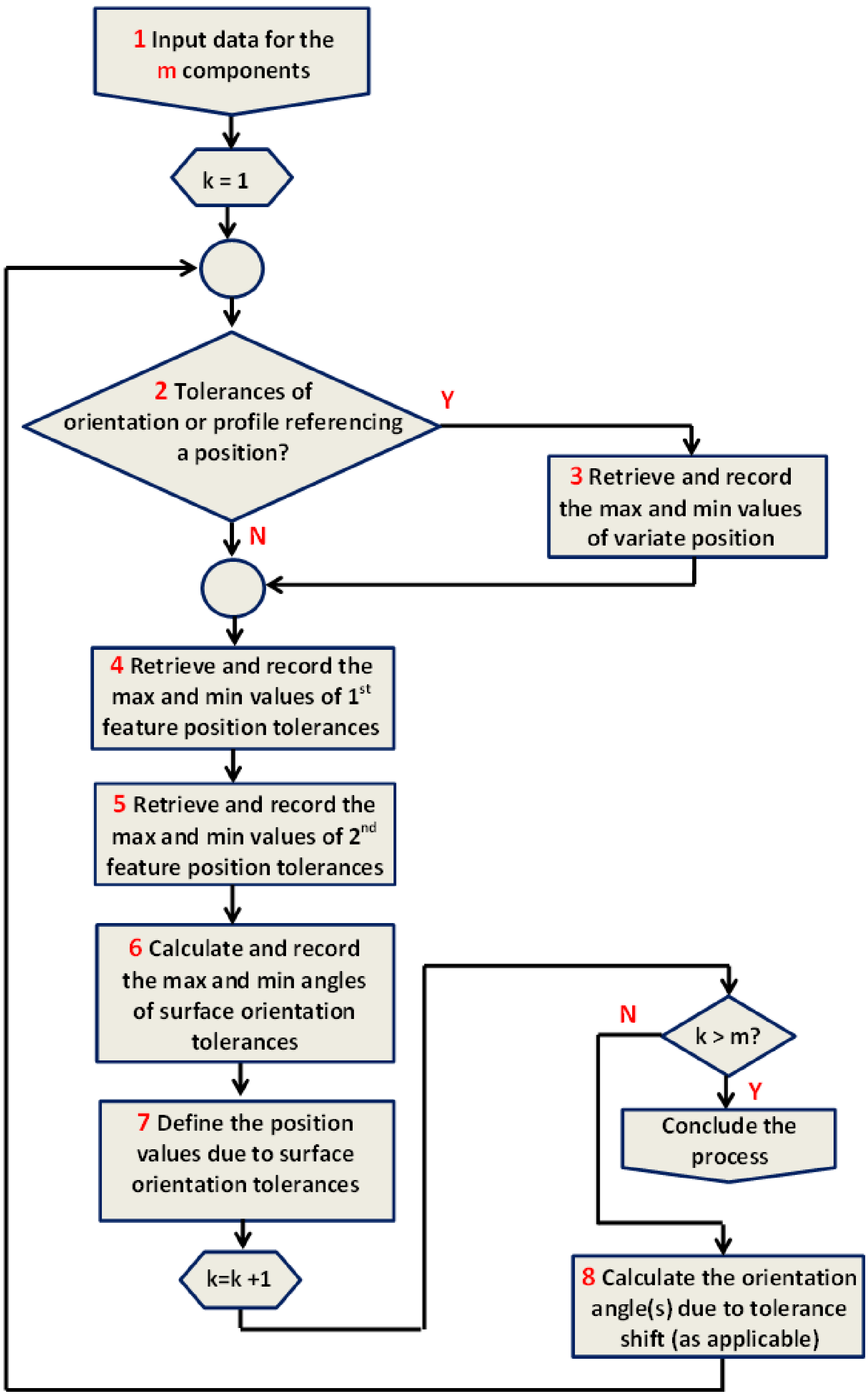

Figure 63 – Process for calculation of WC tolerance values. Position and orientation tolerances of all components of the assembly are contemplated. This process corresponds to item 10 of the flowchart of Figure 64. (Source: the author).

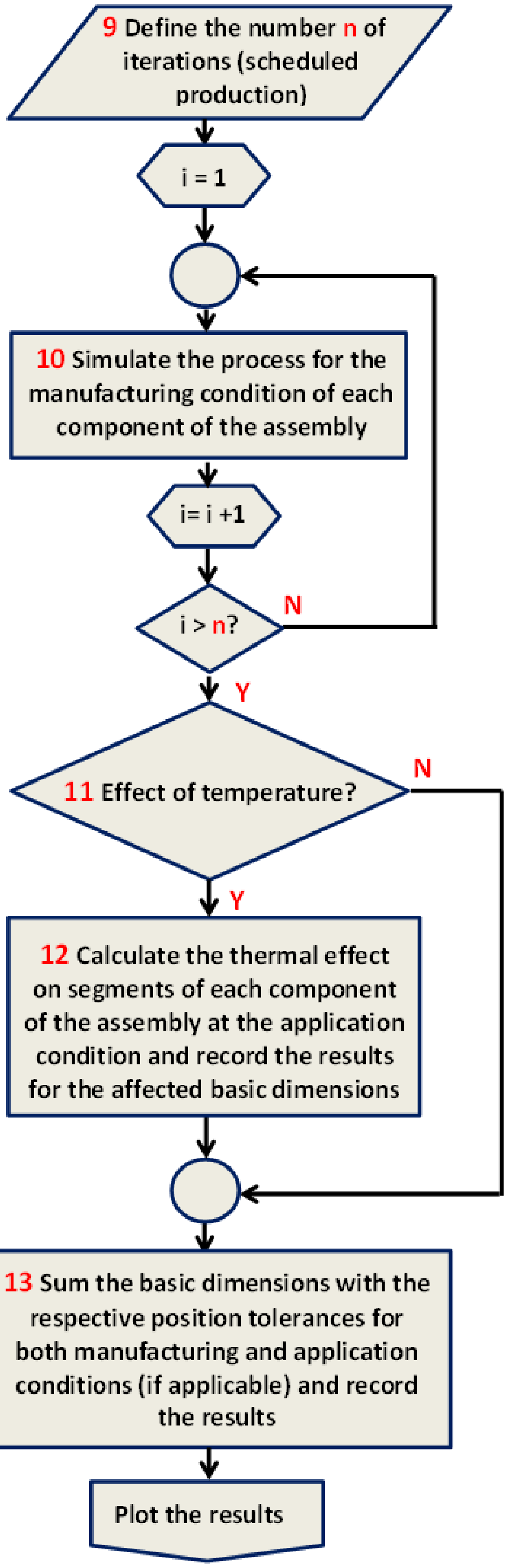

Figure 64 – The flowchart of the main algorithm including both the assembling and the application conditions. (Source: the author).

5. Determine and record the position of the second positional feature, according to Subsection 4.2.1;

6. Calculate and record the orientation angles according to Section 4.2.3;

7. Determine the position value due to the tolerance of the surface orientation, according to Subsection 4.2.4;

8. Calculate the orientation variation due to the tolerance shift, as applicable, according to Section 4.2.5. Repeat the process for all components of the assembly;

9. Define the number n of iterations of the stochastic simulation of the product scheduled production;

10. Call the routine described in Figure 63 for each iteration until the number n is attained;

11. Check whether the application behavior of the assembly components must take into account significant thermal effects. This verification can consider both temperature values and linear lengths. It is worth noting that only the basic dimensions are used in the calculation, since the strains are very small even at elevated values of temperature;

12. Calculate the thermal dilatation on the basis of the mean estimated temperature of the linear segments in the dimensions of the components. Refer to Section 4.5 for more details.

13. Calculate the sum of basic dimensions with the calculated variations in the WC and in the production simulation under manufacturing and application conditions for all components' dimensions. Finally, plot the results;

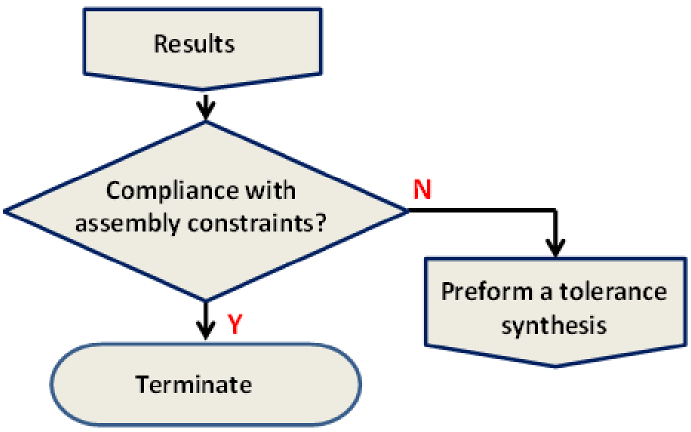

Figure 65 – The scheme considering the results of the 3D tolerance analysis simulation and their comparison with the task design constraints. (Source: the author).

Graphic representations of the position of the characteristic are a three-variate function representation of the dependent variates x, y, and z. The same approach is used for the feature orientation graphs of the variates α_x, α_y, and α_z.

The 3D tolerance analysis process can be used in two different ways:

1. Generally, the results are checked against the target design value(s) and/or design constraints. If the resulting values exceed the intended values, a tolerance synthesis process must be performed to decrease the tolerance range of one or more components, at a cost penalty. This happens when stringent design conditions are specified;

2. In other cases, as the one used in the case study, the process is conducted as a design aid either for specifying dimensions or to enable alternative design solutions. As both manufacturing and application situations are considered in a large production volume, the adoption of an appropriate solution is indirectly validated before product performance tests, which can greatly improve its reliability.

5 Statistical 3D Tolerance Analysis of an Internal Combustion Engine

The objective of this example is to demonstrate the feasibility of the application of the thesis proposal described in Chapter 4. Differently from the several available studies already cited, where only geometrical analysis are performed at specific conditions, this proposal has an economic differential, since it uses a random simulation of a large production volume. Furthermore, the dimensional and form tolerances are based on similar data of actual internal combustion engines (ICEs). The usual approach of a product 3D tolerance analysis referencing only WC leads to an inappropriate conclusion on the assembly configuration when a large production amount is considered, with expected cost penalties and, in some cases, the design can be considered unfeasible due to unmanageable constraints. Even so, WC is considered in this case for comparison with the statistical simulation. Moreover, as the chosen example deals with significant thermal variation, its dimensional effects on the results are also included. The objective function of this problem is the probability distribution of the dimensional variation in the 3D space of one specific feature. This variation is computed in relation to the main assembly datum frame. Although just one feature is considered, the same approach can be used for any other one, as the procedure is the same for any other case. The result is comprehensive, considering the manufacturing statistical variation, either positional or regarding spatial orientation, of all involved components of the assembly and variation due to thermal effects as well.

For simplification, only the features and details needed for the development of the proposal are shown, otherwise the figures would be very complex, and the search for data and the drawings interpretation would be very difficult and time consuming for the reader. Initially, datum references are presented in a logic order, following the assembly sequence of each component. These datum references are used for an accurate positioning in the engine assembly. Irrelevant fastening elements, holes, and threads are not shown, but their influence is considered where necessary to allow the calculation of kinematic adjustments. Leak tightening items, such as gaskets are considered in the as-assembled condition, with a mean tightening value usually measured in practice. All dimensions in the figures are given in millimeters and not often mentioned, as usually occurs in detail drawings.

Regarding the design sequence diagram [42] illustrated in Chapter 4, the development of this example starts at item 3, since the specification of all components is considered complete in this design phase and ready for the tolerance analysis.

5.1 Description of the Assembly Components and Their Main Features

This case study is based on data searched on several actual ICEs of different manufacturers, to provide representative results. A large displacement engine model was considered to magnify the thermal effects in relation to its dimensions. Figure 66 shows a diesel engine assembly and identifies the components used in this study. The procedure described in Chapter 4 is developed with this example. The software MatLab was used for running the algorithms. The thermal effects were based on the normal operating temperatures of cooling and lubricating fluids developed from components. Steady state mean temperatures were used and an average wall temperature was considered appropriate since cast iron presents a high heat conduction coefficient.

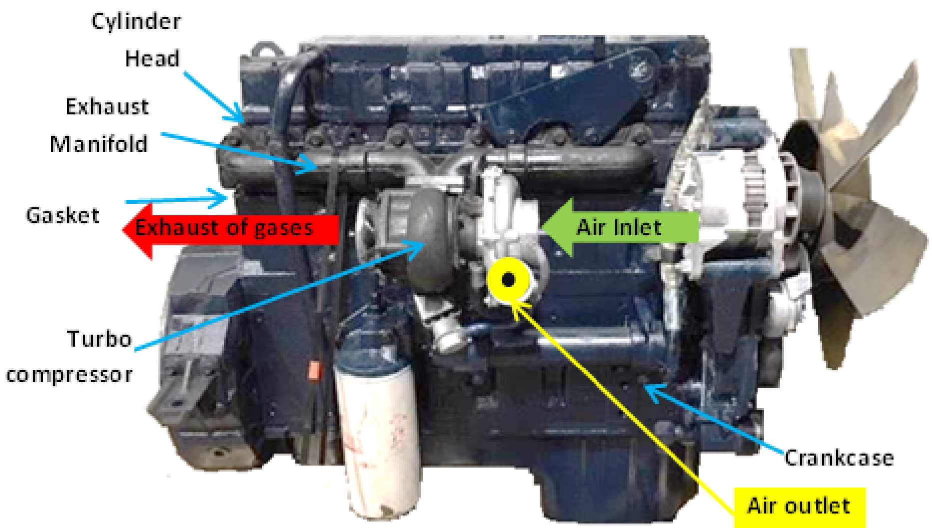

Figure 66 – A diesel engine and some components. (Source: the author, based on commercial catalog).

The chosen feature to represent the case results is the turbo-compressor air outlet port, as illustrates Figure 67. The reason for this choice was based on a design constraint: as the compressed air exits above $120°C$ from this port, generally it is cooled before entering the combustion chamber for thermodynamic efficiency purposes. This is done by means of an after-cooler (an air-liquid heat exchanger) connected to the intake manifold, both not shown. The significant functional dimensional variation between these components must be known in order that a flexible joint can be properly dimensioned. Other concerns are the stresses that can be generated due to significant strains caused by different dimensional variation among components. The position (yellow) vector, shown in Figure 67, locates the references of all results of this example. The configuration is referenced again ahead in this chapter by means of a more detailed figure.

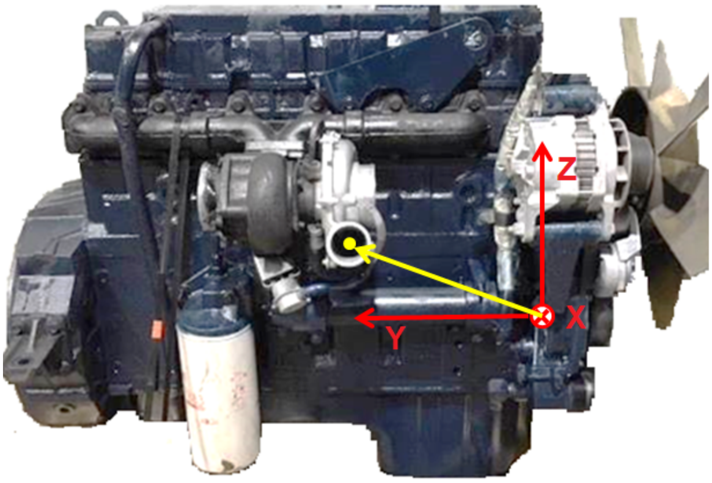

Figure 67 – The chosen target feature for the case study. The datum frame of the assembly referencing all components is located on the crankcase, the first component. (Source: the author).

Figure 68 shows an exploded view of the engine with the referenced components. The diagram in Figure 69 displays the assembly chain sequence as well as the algorithm flow.

5.1.1 Crankcase

The crankcase, or engine block, is the main structural component of the assembly, which datum references are defined according to the assembly's functional requirements (FRs). The main engine's functional component is the crankshaft, whose cast bearing housings must be machined into the crankcase, the component under discussion (see Figure 70). Bearing housings are accurately bored and aligned for fitting the crankshaft bearing shells. However, due to the manufacturing implications, the machining process is started from other features – the crankcase bottom surfaces, which are used to position this heavy part in all other tooling devices.

Due to its importance, this is a component in which the design and the manufacturing process plan must be carried out together. As cited before, the main datum of the entire engine assembly is defined in the crankcase. Intermediate references are used to define the surface and other features which will position the datum reference of the following components in the assembly chain. Therefore, the sequence below is used for explaining the intermediate references, as illustrate Figures 71 to 75:

1. Due to process implications, the first process operation is the machining (milling) of the bottom surfaces (reference **D1**) (see Figure 71), because they are used to position the part in all other operations. The flatness specification is necessary for oil sealing purpose. The seats of the crankshaft bearings are also milled in sequence and the threads are made. Four process auxiliary holes are drilled to position the

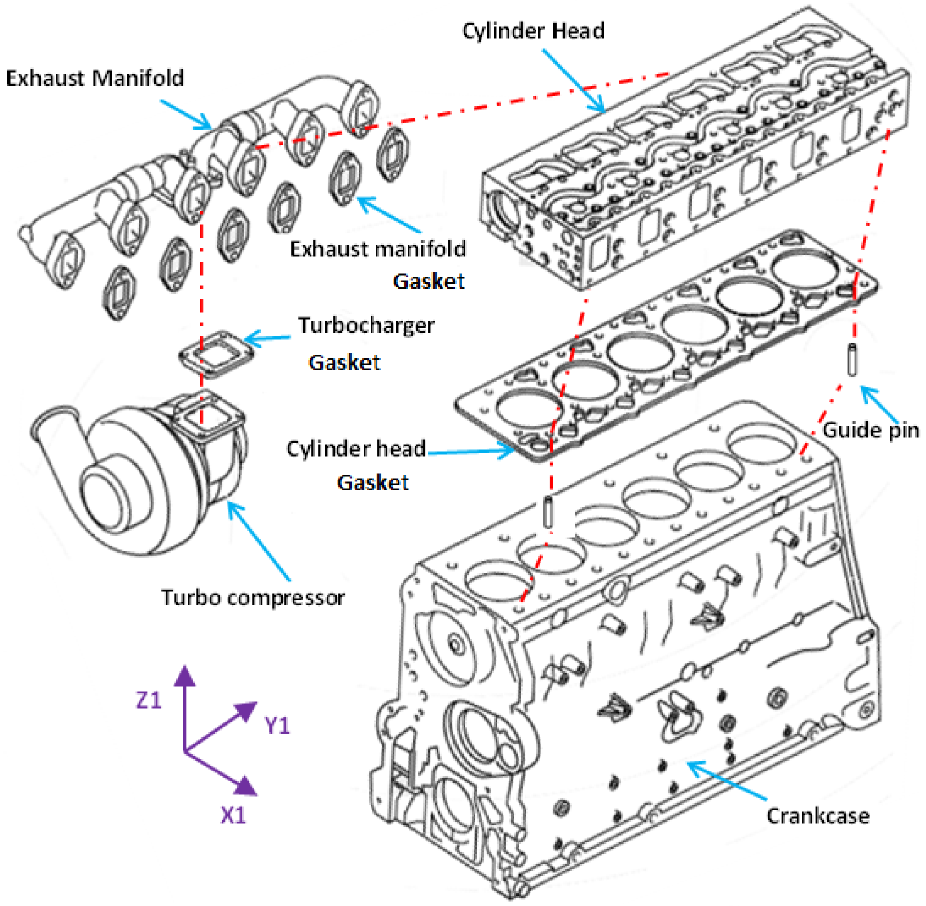

Figure 68 – An exploded view of the engine showing some components. (Source: the author, based on a workshop manual).

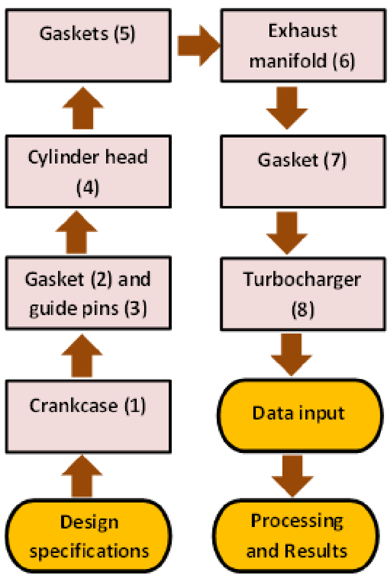

Figure 69 – Diagram for the case study development. (Source: the author).

part in relation to the casting surfaces to assure adequate machining allowances in all further operations;

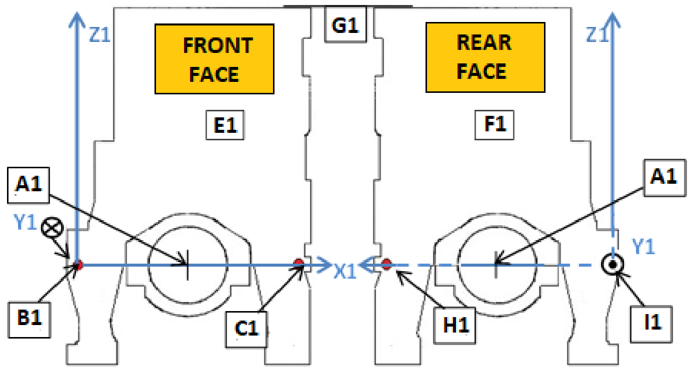

Figure 70 – Definition of crankcase orthogonal axes, the component datum frame. (Source: the author).

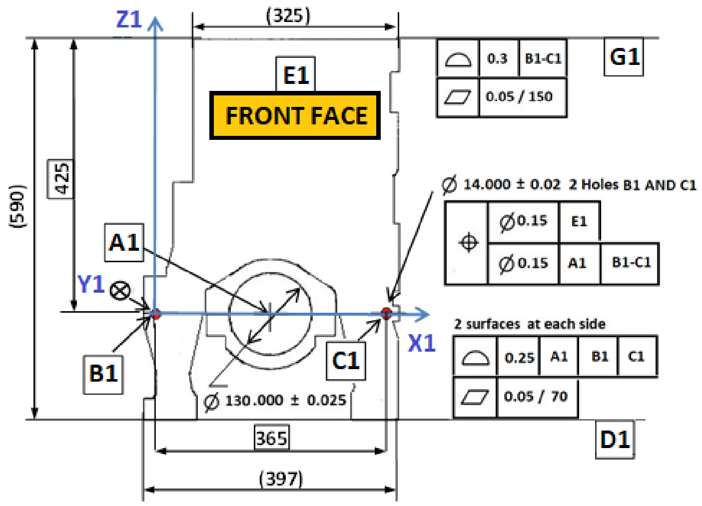

Figure 71 – Datum features of the crankcase front face – crankshaft main bearings, dowel pins and bottom and top faces. (Source: the author).

2. The front surface (Ref. **E1**) is milled to meet the flatness requirement, as illustrated in Figure 72;

3. Guide holes (Refs. **B1** and **C1**) are drilled at the same time and reamed to ensure the accuracy of the distance between the centers (see Figure 71). The two-spindle drilling device is also designed to ensure the specified profile tolerance (parallelism) of the bottom surface;

4. Pre-machined bearing caps are assembled at their locations. The fastening bolts are tightened to the specified torque. All bearing diameters are then drilled in the same operation. The machining device uses the bottom face **D1** and the holes **B1** and **C1** as references. With this operation, the reference **A1** is defined, as well as the

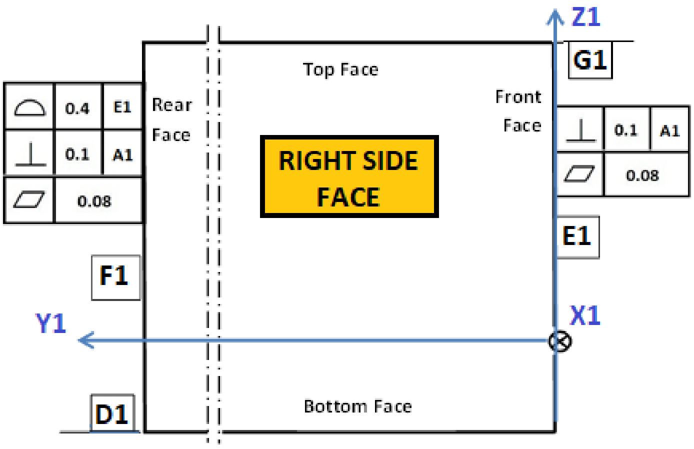

Figure 72 – Datum features of the crankcase side face – main faces. (Source: the author).

component datum: **X1** on the surface **E1**, passing through the centers of the holes **B1** and **C1**; **Z1** also on the surface **E1**, orthogonal to **X1**; **Y1**, orthogonal to the plane **X1** - **Z1**;

5. The surface **F1** is milled according to references **A1** and **E1**;
6. Guide holes **H1** and **I1** (see Figure 73) are drilled at the same time and reamed, according to references **F1** and **A1**;

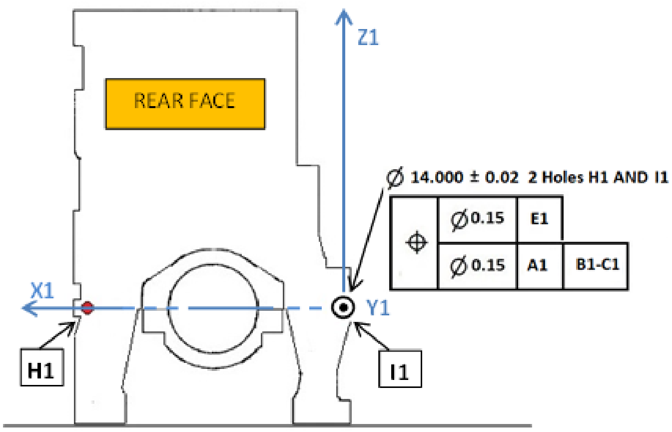

Figure 73 – Datum features of the crankcase rear face – dowel pins. (Source: the author).

7. The thrust face **J1** (Figure 74 locates the crankshaft axially and bears the axial load transmitted by the flywheel for power take-off. It is located in relation to the rear face **F1** and ensures the position of the pistons relative to their respective cylinders;

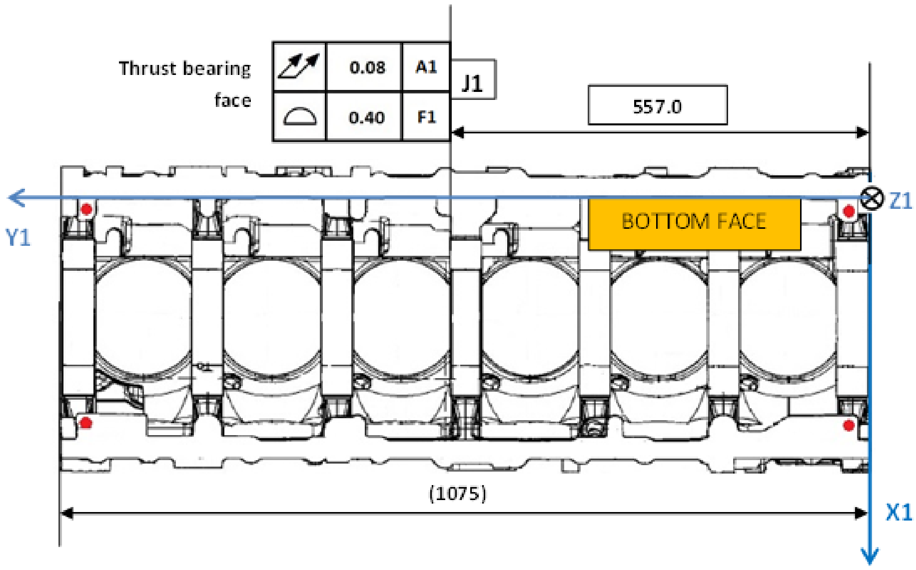

Figure 74 – Datum features of the crankcase bottom face. Only the thrust face is shown. (Source: the author).

8. The upper face **G1** is milled using as a reference the plane **X1-Y1**;
9. The cylinders are bored at the same time using references **A1**, **J1**, and **G1**. Finishing (honing) is performed in sequence;
10. Finally, guide pin holes **M1** and **N1** (Figure 75) are also drilled and reamed in relation to the first and sixth cylinders and the top face **G1** as well;
11. Additional operations are performed, but do not influence our study, such as drilling and thread machining for the cylinder head fastening bolt assembly.

This is a complex example showing the features involved in referencing the datum of a component and the position used to locate the next component in the assembly chain. Several geometric 3D location and position tolerances must be considered.

These features are used for the boring operation of the crankshaft bearing housings ($A1$) (together with pre-machined bearing caps and bolted to the specified tightening torque). Because of this, the datum references may seem inverted in relation to the machining sequence. Figures 71 to 75 show the datums and the position and form the characteristics used in this example.

5.1.2 Guide Pins and Cylinder Head Gasket

The guide pins and the cylinder head gasket play a minor role in the tolerance chain. Pins are used to position the bottom face of the cylinder head on the top face of the crankcase. Two different types of guide pin can be used, as shown in Figure 76:

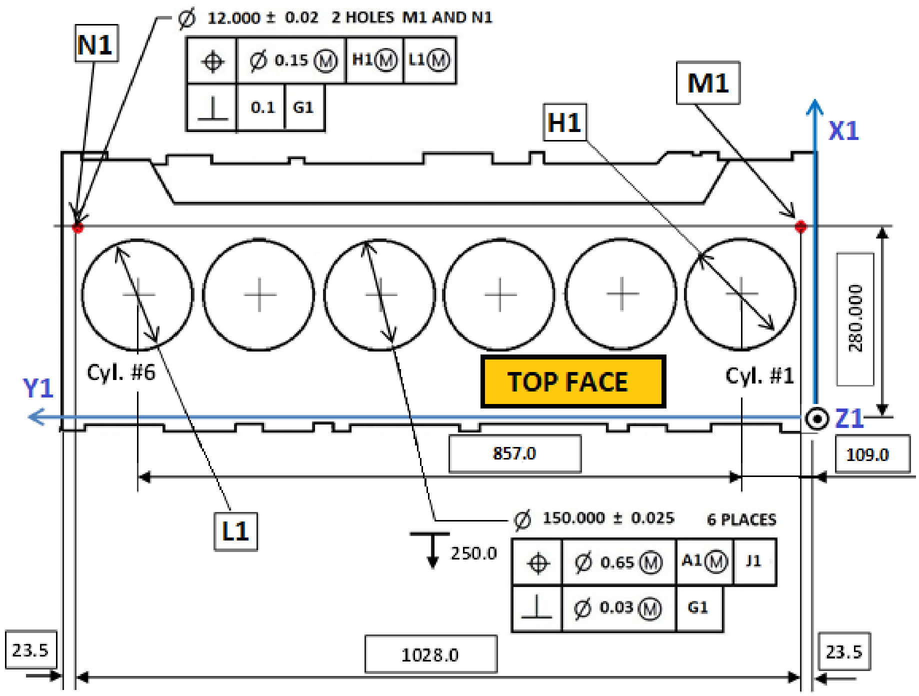

Figure 75 – Datum features of the crankcase top face. The surface and guide holes are used to position the cylinder head. (Source: author).

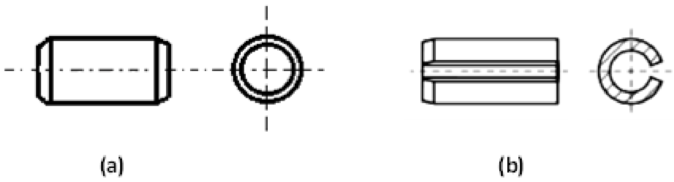

Figure 76 – Types of guide pins used to locate mechanical components: (a) dowel pin and (b) spring pin. (Source: the author).

- The solid (dowel) pin ensures a more accurate positioning but induces lateral stresses and can bring difficulty to both assembly and maintenance;
- The spring type prevents stresses, facilitates assembly and maintenance, but lessens the positioning accuracy.

Although it may seem indifferent, the fit of the guide pins on the cylinder head obeys the order of precedence defined in the design: The first locks two displacement DoFs $(x - y)$ and the second locks one (yaw) rotational DoF, defining the part datum, as shown in Figures 77 and 78. Furthermore, due to assembly and logistics requirements, only one type can be chosen, provided that the characteristics cited are observed in the design requirements.

In this example, solid pins are considered. The specified diameter is $12.000 + 0.007 + 0.018$ mm, according to ISO... [1997]. When assembled at the top of the guide holes of the crankcase 12.000 ± 0.02 mm, in practice an interference fit is expected. With the bottom face guide hole of the cylinder head 12.063 ± 0.02 mm, a loose fit can be considered.

The cylinder head gasket is assembled between the top face of the crankcase and the bottom face of the cylinder head. It does not need special positioning since it only has the function of sealing. Generous gaps are provided in the holes through which fluid, pins, and fastening elements pass. A relatively large thickness is necessary to compensate for the flatness errors on the contact surfaces of the crankcase and the cylinder head. The tightening torque on the fastening bolts of the cylinder head also obeys a cross-sequence in the transverse direction and starts from the center to the extremities to prevent warping. This torque ensures a relatively constant compressed thickness after assembly. For the engine size in this example, a thickness of 1.5 ± 0.1 mm (as assembled) is specified.

5.1.3 Cylinder Head

The cylinder head is assembled on top of the cylinder head gasket. Its position in the Z direction on the upper surface of the crankcase is a function of the compressed thickness of the gasket. In the $X - Y$ plane, its position is determined by the guide pins mounted on the top surface of the crankcase.

Similarly to the crankcase, the process sequence skipping operation is not applicable to the case study (see Figures 77 and 78):

1. The first operation is the milling of the bottom face **A2** with the flatness tolerance specification;

2. The guide pin holes **B2** and **C2** are drilled at the same time and reamed. The component's datum $X2 - Y2 - Z2$ is then defined;

3. The right side face is milled in relation to references **A2**- **B2** and **C2**, at the specified flatness tolerance;

4. Finally, the holes and threads are machined to fasten the exhaust manifold. As the exhaust manifold position is not critical, guide pins are not used, and a generous positional tolerance is specified for cost reasons. The $M10$ threads used to fasten the exhaust manifold are specified by ISO 965 [ISO965..., 1998], with an external diameter varying between 9.968 and 9.732 mm. The maximum material condition (MMC) 9.968 mm is used in position and orientation calculations due to assembly shift.

5.1.4 Exhaust Manifold Gaskets

Exhaust manifold gaskets are used to seal the contact between the cylinder head and the exhaust manifold surfaces against leakage. Currently, different designs are used, as

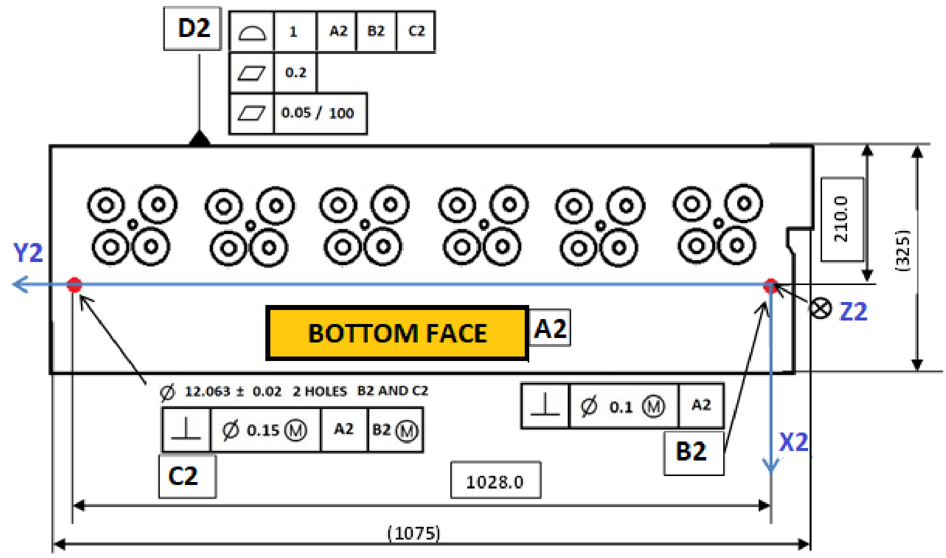

Figure 77 – The cylinder head viewed from its bottom face. Guide holes $B2$ and $C2$ define the part's datum and position the cylinder head on crankcase. (Source: the author).

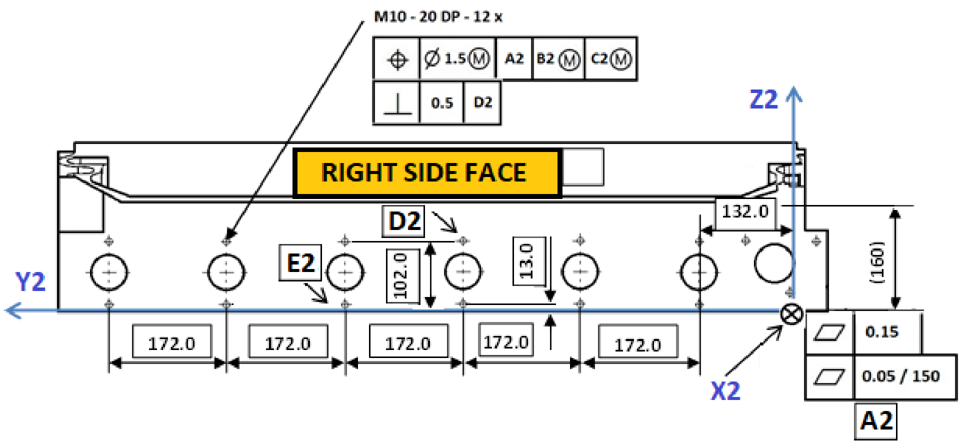

Figure 78 – The cylinder head viewed from its right side face. Threads $D2$ and $E2$ position the central part of the exhaust manifold. (Source: the author).

described in Dischaw and Kobayashi [1989], Nakasone... [1991]. The compressed thickness considered in the case study is based on Nakasone... [1991], which provides a more accurate value of 1.2 ± 0.01 mm. Exhaust manifold gaskets have characteristics similar to those of the cylinder head gasket but are designed to seal only combustion gases. As the area involved is smaller, the necessary thickness is also smaller.

5.1.5 Exhaust Manifold

The exhaust manifold is split into three parts due to its length and the high temperatures it reaches in service. The joints between parts are designed to allow sealing at high temperatures. In this example, only the central part is considered for simplification, since it is the positioning link between the cylinder head and the turbocompressor, and the inclusion of the other parts would not add any benefit.

The holes used to fasten the manifold to the cylinder head provide significant gaps in the fastening elements, allowing displacement at high temperatures. Two of them are oblong to allow alignment of the assembly. Figure 79 illustrates these characteristics.

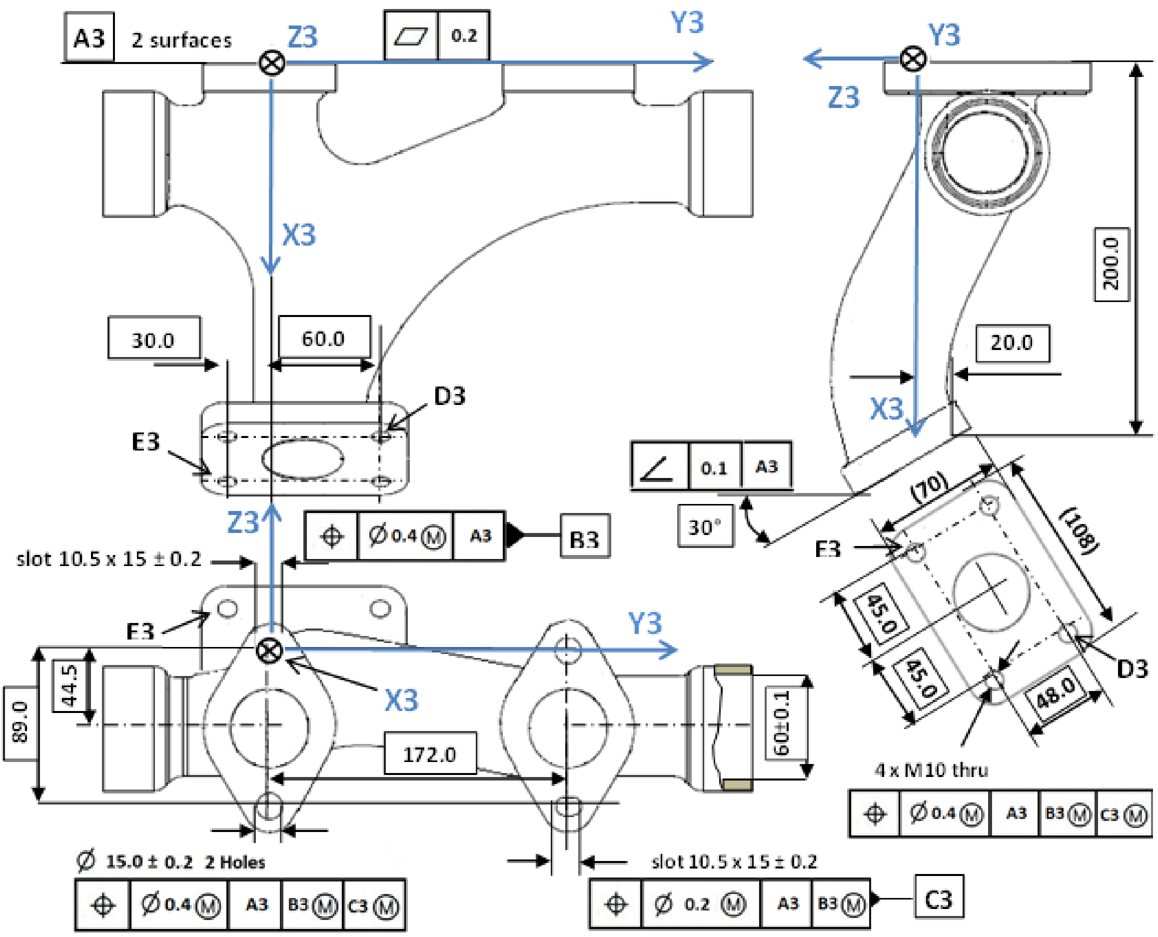

Figure 79 – The exhaust manifold central part. (Source: the author).

5.1.6 Turbocompressor gasket

The turbo-compressor gasket is used to seal the contact between the exhaust manifold and the turbo-compressor surface against leakage. Its design is the same as that of the exhaust manifold gaskets. The turbo-compressor gasket is also designed to withstand high temperatures and allow some displacement on contact surfaces through its compressed thickness.

5.1.7 Turbocompressor

The turbo-compressor is the last component of the example. It is subject to a temperature gradient between the outlet of compressed air and the inlet and outlet of exhaust gases. This functional behavior affects assembly dimensioning. Figure 80 illustrates the component.

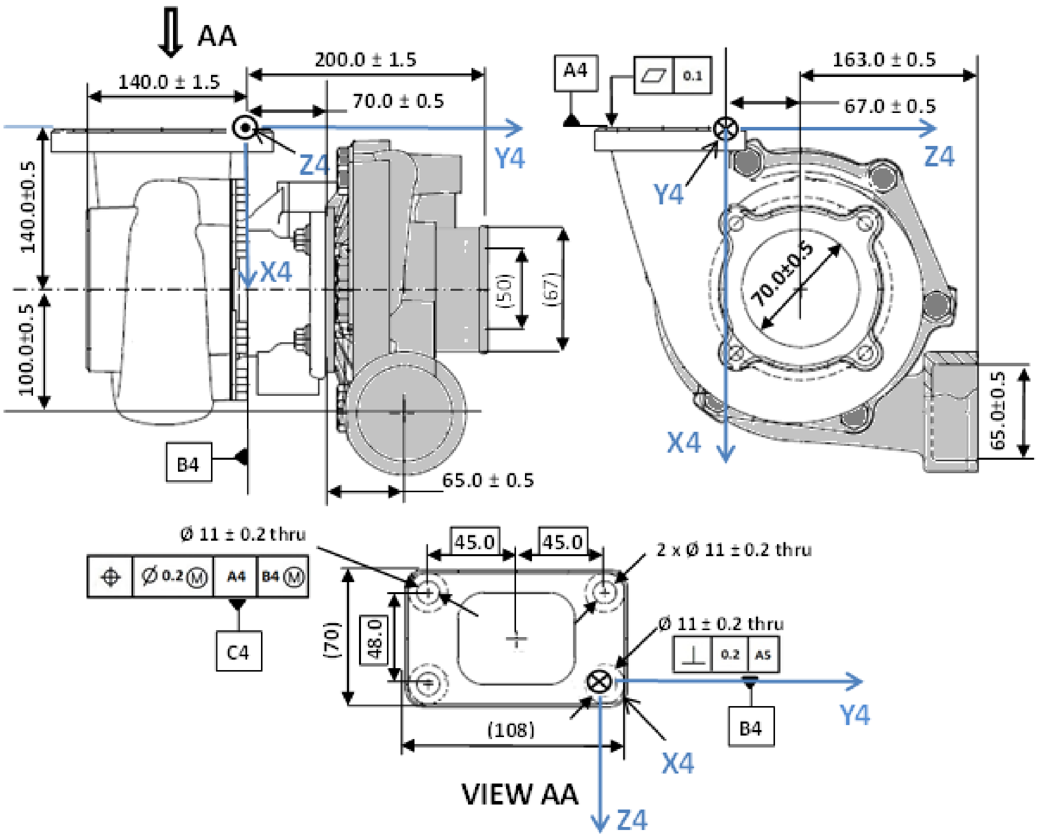

Figure 80 – The turbocompressor. The gray part identifies the compressor. (Source: the author).

5.2 The Functional Variation Approach

This section is related to item 5 of Figure 42 in Chapter 4.

Comment about Mechanical Loading

As mentioned in Section 4.5, the dimensional variations with respect to mechanical loads in rigid assemblies are usually very small and calculated by CAE. In this specific case study, they had not to be considered at all due to the following mechanical loading identified:

1. The deformation (compressed thickness) of each gasket is individually referenced and

included in the algorithm. Their values are obtained by experiments as a function of the tightening torques of the fastening elements and are considered accurate;

2. the internal inertial loads originating from the reciprocating movement of the subassembly *pistons-pins-connecting rods-crankshaft webs* are transferred to the crankshaft bearings through the bearing shells. Bearing surfaces are properly dimensioned for low-wear shells and adequate lubrication, without significant deformation. Furthermore, they do not affect the tolerance analysis process because they are inside the crankcase;

3. the inertial load due to the engine mass is born by its supports, also CAE dimensioned for the function. The deformation of the supports due to inertia loads and static loads, if any, is beyond the algorithm scope, as they are outside the tolerance chain;

4. the components subjected to fuel injection and combustion pressures are properly CAE dimensioned for strength. The oil, air, and exhaust gases pressures are comparatively low.

The comments above can also be applied, with the due considerations, for other similar applications.

The Variation due to Thermal Load

To consider the effect of functional thermal load on the dimensional variation of the case study, a specific investigation was conducted on the subject, since the manufacturers' applicable data are considered proprietary and thus unavailable. Data acquisition with respect to this item would be costly and time consuming and, additionally, it is not in the scope of this work. Fortunately, comprehensive and applicable works on automotive applications were found, from which relevant information was acquired and are described below.

As mentioned above, temperature affects common materials by expanding (or contracting) their dimensions. Regarding GD&T, this feature is only considered in basic dimensions, since the thermal variation is small in the temperature range generally considered. The variation regarding DT is exceptionally small and may be disregarded even in more accurate calculations because of their order of magnitude; a simple analysis of the tables presented in sequence in the text can demonstrate this statement. Furthermore, vectors considering average discrete temperature variations may be used for simplification; considering a continuous variation would require the integration of an estimated function, which could lead to great complexity and unpredictable errors. In the case of an available computer fluid design (CFD) analysis in a similar application, it can be used instead, but even so some estimation is required.

5.2.1 The Crankcase and Cylinder Head

The wall temperatures of the engine crankcase and the cylinder head were taken from Parra [2008], under full load conditions. A summary of the data is shown in Figures 81 and 82. The data refer to each cylinder, but are displayed just once for simplification.

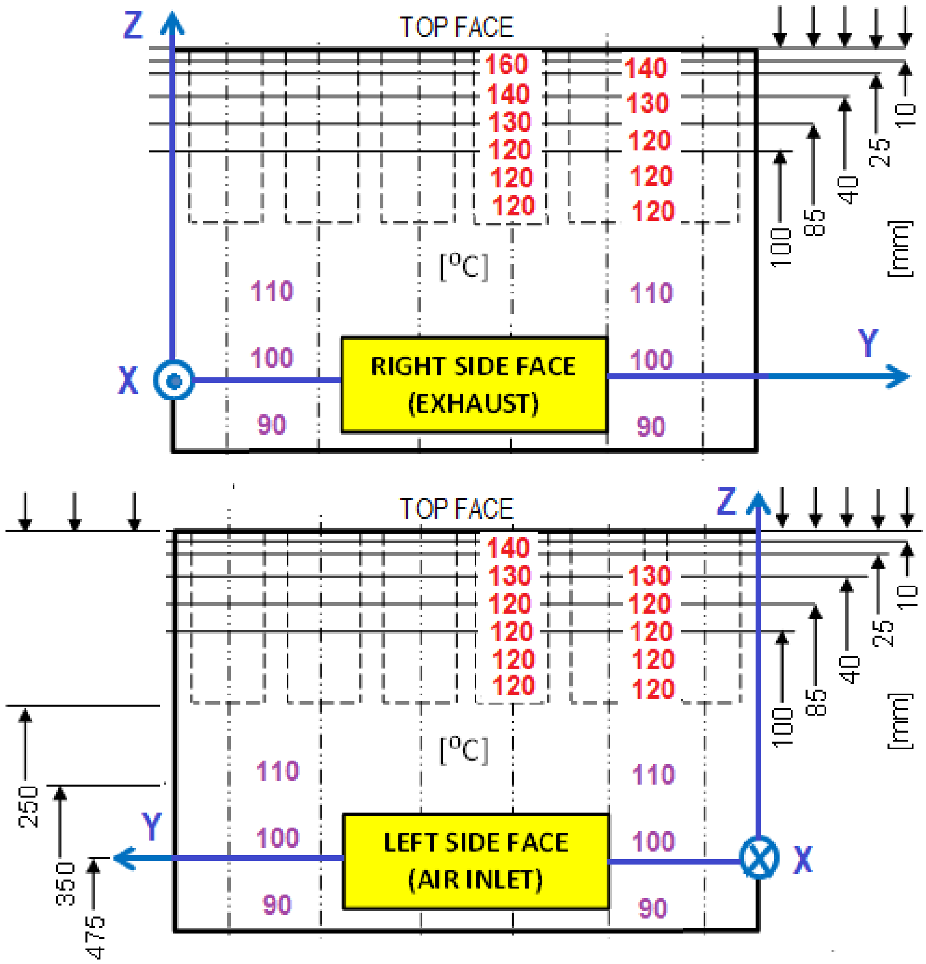

Figure 81 – The crankcase wall temperatures (degrees Celsius, in red). The violet color temperatures were estimated. (Source: based on Parra [2008, p. 107]).

The crankcases (or engine blocks) and cylinder heads are cast in gray iron according to SAE J431 - G3000 or G3500 grades [ASM, 1990, p. 55]. The thermal expansion coefficient of the material (CTE), according to ASM [1990, p. 85] is about 13 $\mu m/(m.°C)$ in the temperature range of 0 to 500 °C and approximately 10.5 $\mu m/(m \cdot° C)$ between 0 and 100°C. These values are in agreement with the most accurate ones found in Zieher et al. [2005], illustrated in Figure 83 and used in this work. For −10 °C the linear shrinkage is approximately −0.03% [TOULOUKIAN et al., 1975, p. 157].

In the crankcase, the affected basic dimensions are those related to the guide holes $M1$ and $N1$ from the component datum reference (see Figures 71, 74 and 75). For the calculation of the thermal variation of holes $M1$ and $N1$, some assumptions are made

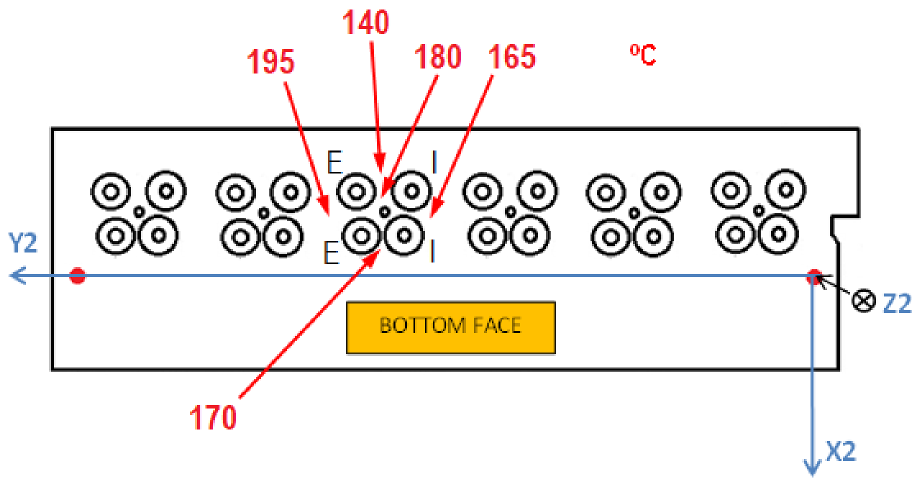

Figure 82 – The cylinder head wall temperatures (degrees Celsius, in red). Exhaust valve (E) Intake valve (I). (Source: based on Parra [2008, p. 116]).

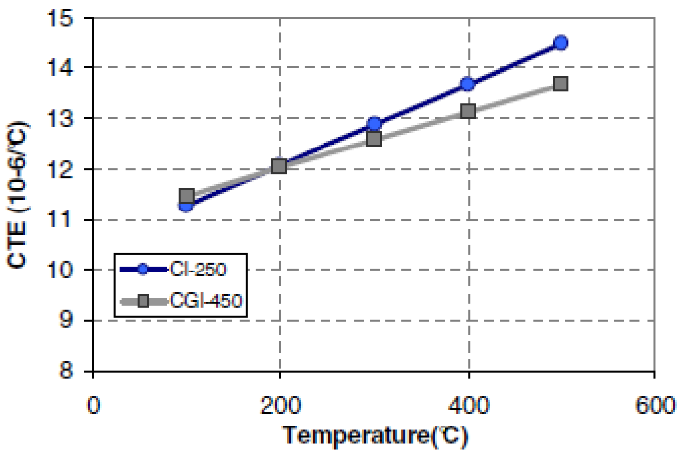

Figure 83 – The coefficient of thermal expansion for gray cast iron (CI) and ductile cast iron (CGI). (Source: based on Zieher et al. [2005]).

about the mean values of the application temperatures in the three main directions, as illustrated in Figure 81.

- X, 140°C;
- Y, 140°C;
- Z, $100, 110, 120, 135$°C in segments of $125, 100, 150, 100$ mm, respectively.

The corresponding calculated basic dimensions for both ambient and application temperatures are shown in Table 5.2.

In the cylinder head, the affected basic dimensions are those related to the threads $D2$ and $E2$ from the component datum reference (see Figures 77 and 78). For the calculation of the thermal variation of the threads $D2$ and $E2$, some assumptions are made about the

Table 5.2 – Top surface dimensions and basic dimensions from the main datum to holes $M1$ and $N1$ in ST (standard temperature of 20°C), in LT (low temperature of −10°C) and AT (application temperatures).

Dim.	X ST	X LT	X AT	Y ST	Y LT	Y AT	Z ST	Z LT	Z AT
Width	325.0	—	—	—	—	—	—	—	—
Length	—	—	—	1,075.0	—	—	—	—	—
$\rightarrow M1$	280.0	279.92	280.39	23.5	23.49	23.53	425.0	424.86	425.53
$\rightarrow N1$	280.0	279.92	280.39	1,051.5	1,051.2	1,053.00	425.0	424.86	425.53

mean values of the application temperatures in the three main directions. The cylinder head is internally cooled by the flow of cooling fluid. The threads are located on the exhaust side. Based on Figure 82, the temperatures of 170 and 200°C are assumed for directions X and Y, Z, respectively. The corresponding calculated basic dimensions for both ambient and application temperatures are shown in Table 5.3.

Table 5.3 – Basic dimensions from the main datum to the threads $D2$ and $E2$ in ST (standard temperature of 20°C), in LT (low temperature of −10°C) and AT (application temperature).

Thread	X ST	X LT	X AT	Y ST	Y LT	Y AT	Z ST	Z LT	Z AT
$\rightarrow D2$	-210.0	-209.94	-210.48	476.0	475.86	477.09	102.0	101.97	102.14
$\rightarrow E2$	-210.0	-209.94	-210.48	648.0	647.80	649.49	13.0	12.99	13.02

5.2.2 The Exhaust Manifold

Exhaust manifolds currently designed for high-performance diesel engines are prone to thermal fatigue as a result of cracks that initiate in the deformation range of the plastic material. Due to this, malleable cast irons resistant to high temperatures are mainly used as materials [YANG et al., 2013; LIU et al., 2018]. Another design solution to address the thermal fatigue issue is to provide a generous gap between the manifold flange fastening holes and their fastening elements. This feature is adequately described by Kim et al. [2006].

The average temperature of the combustion gases (T_g) at full load through the exhaust manifold was also obtained in the work of Parra [2008, p. 137], in conformity with the results. The approximate value of $T_g = 640$°C was considered. The temperature of the manifold wall was estimated from measurements in the works of Cardoso and Andreatta [2016] and He et al. [2006] as $T_w = 380$°C. The thermal expansion ratio of the material, which varies with temperature, was obtained in Yang et al. [2013] and is shown in Figure 84. Therefore, the thermal variation of the manifold material can be taken as $\Delta L/L_0 = 0.005$.

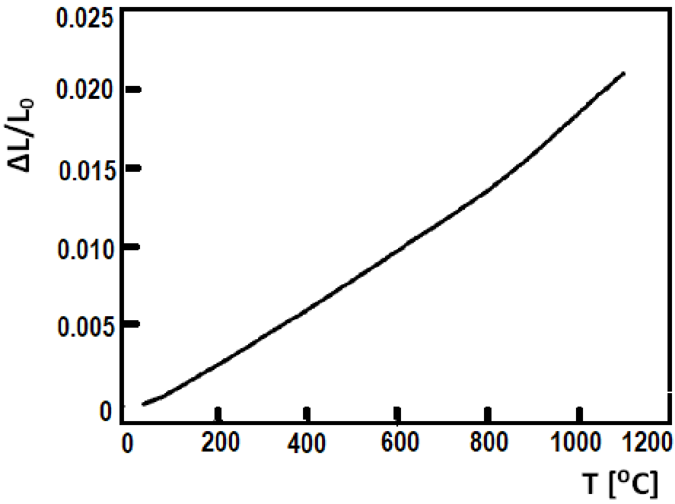

Figure 84 – The coefficient of thermal expansion ratio for malleable cast iron. Source: based on Yang et al. [2013].

In the exhaust manifold, the basic dimensions affected are those related to the threads $D3$ and $E3$ from the component datum reference (see Figure 79). The corresponding calculated basic dimensions for both ambient and application temperatures are shown in Table 5.4.

Table 5.4 – Basic dimensions from the main datum to the threads $D3$ and $E3$ in ST (standard temperature of 20°C), in LT (low temperature of -10°C) and AT (application temperature).

Thread	X ST	X LT	X AT	Y ST	Y LT	Y AT	Z ST	Z LT	Z AT
$\rightarrow D3$	-200.0	-199.94	-200.83	60.0	59.98	60.23	-20.0	-19.99	-20.08
$\rightarrow E3$	-224.0	-223.93	-224.93	-30.0	-29.99	-30.15	21.57	21.56	21.66

5.2.3 The Turbocompressor

Turbocompressors are mechanical assemblies made up of two main parts: the turbine and the air compressor. Turbines are subject to high exhaust gases temperatures and have the same basic material as used in the exhaust manifold [LI, 2013; GUO; LONG, 2018]. In this case study, the wall temperatures of the exhaust manifold and the turbine housing are considered the same, although the gas flow presents a decrease between the inlet and outlet ports.

Air compressors are statically connected to the turbine housing with a common shaft. The compressor housing is cast in an aluminum alloy $Al - Si - Mg$ such as the alloy AA

365.0 / UNS A03650 [KAUFMAN; ROOY, 2004, p. 18]. The material CTE varies between 17.6 and 24.7 $\times$ 10^{-6}/°C in the range of 20 − 100°C [KAUFMAN; ROOY, 2004, p. 2]. In the case study, compressed air at full engine load reaches temperatures between 100 and 150°C, leading to the use of the CTE value of 24.7 $\times$ 10^{-6}/°C. The temperature of the wall of the compressor housing is assumed to be 120°C.

Based on the dimensions shown in Figure 80, the basic dimensions of the turbine housing and the compressor housing in each direction (in the condition of the engine assembly) are given in Table 5.5:

Table 5.5 – Basic dimensions of the turbo compressor (TC) in ST (20°C) in LT (low temperature of −10°C) and AT (application temperature). I = iron; Al = aluminum

TC	X ST	X LT	X AT	Y ST	Y LT	Y AT	Z ST	Z LT	Z AT
I	-121.24	-121.21	-121.84	-70.00	-69.98	-70.35	58.02	58.00	58.31
Al	-86.60	-86.53	-86.81	-65.00	-64.95	-65.16	141.16	141.06	141.51
Sum	-207.84	-207.74	-208.65	-135.00	-134.93	-135.51	199.18	199.06	199.82

5.3 The 3D Tolerance Analysis of the Engine Assembly

The example tolerance analysis considers three different simulation approaches:

- First, a production simulation is performed with the components under the manufacturing condition, that is, at the standard temperature of 20°C. This and the subsequent simulations are based on the Monte Carlo method. In this approach, a new 3D tolerance analysis proposal is applied.

  The statistical approach is one of the objectives of this work and has followed the proposal presented in the previous chapter. Its task is to find the statistical variation of the manufacturing condition (at the standard temperature) of a target feature in relation to the assembly's main datum. The datum is located in the crankcase, and the feature is the air outlet of the turbocompressor.

- In the sequence, a WC analysis is also performed on the components at standard temperature, based on a 3D vector summation. The WC simulation used the limit values of the specified geometric tolerances for the manufacturing conditions, for comparison analysis only;

- Then, a simulation is performed considering the cold start of the engine at low temperature (−10°C). This procedure is useful for comparing the behavior of basic dimensions at different temperature conditions;

- Finally, the proposed simulation method is used to highlight the functional behavior of the assembly under full load condition in the application, with the respective temperatures of each component at a substantially higher level.

These different simulations were performed using MatLab software (version 2021b) to compare the magnitude of their results. To obtain the best accurate final results, the algorithm construction considered a sequential randomization of tolerances involving all components at each iteration, rather than considering the sum of the means and variances of the tolerances of the assembly's components. This practice resulted in a greater time consumption on running the program, but also in a more realistic approach by considering the random variation regarding the individual tolerance of each component.

5.4 The Results

In this section, the results of the case study are presented. As mentioned in the beginning of this chapter, the chosen target feature is the air outlet port of the turbocharger, shown in Figure 67, revisited in Figure 85 with the detailed information needed for the interpretation of the results.

The tolerance zone shown in Figure 85 is represented by a cloud of points in the results. Three conditions have been considered for **positional variation**:

1. Manufacturing and assembly under ambient temperature conditions (20°C);
2. Engine cold starting condition at -10°C and
3. Engine operating temperatures in the application (significantly higher than the standard manufacturing temperature).

The position of the outlet port of the turbocharger compressor is illustrated below.

In Figures 86 and 87 at **assembly condition**.

In Figures 88 and 89 in **cold start condition**.

In Figures 90 and 91 in **application condition**.

In all cases, a production simulation with 100 and $10,000$ iterations was considered, respectively. WC results are also included to facilitate analysis.

With respect to orientation variation, the angles in each orthogonal direction are also represented by a cloud of points in the figures to display the statistical dispersion and the WC values. It must be noted that, in both the cold starting and the application conditions, the orientation variation is not referenced, since only the basic dimensions are considered in the thermal calculation and, consequently, do not affect orientation.

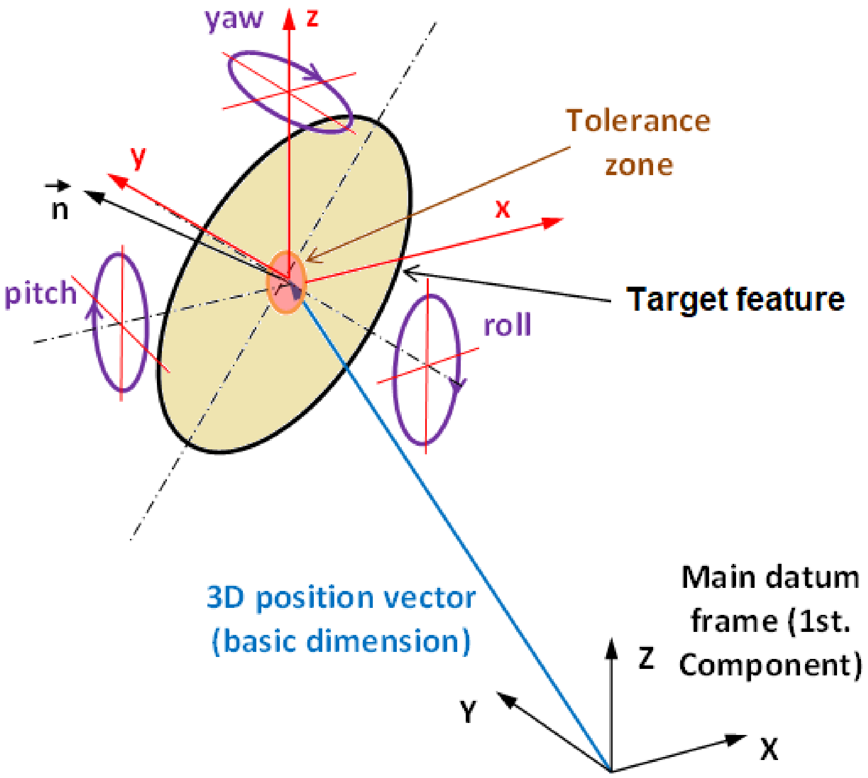

Figure 85 – The case study target feature and its position and orientation references. (Source: the author).

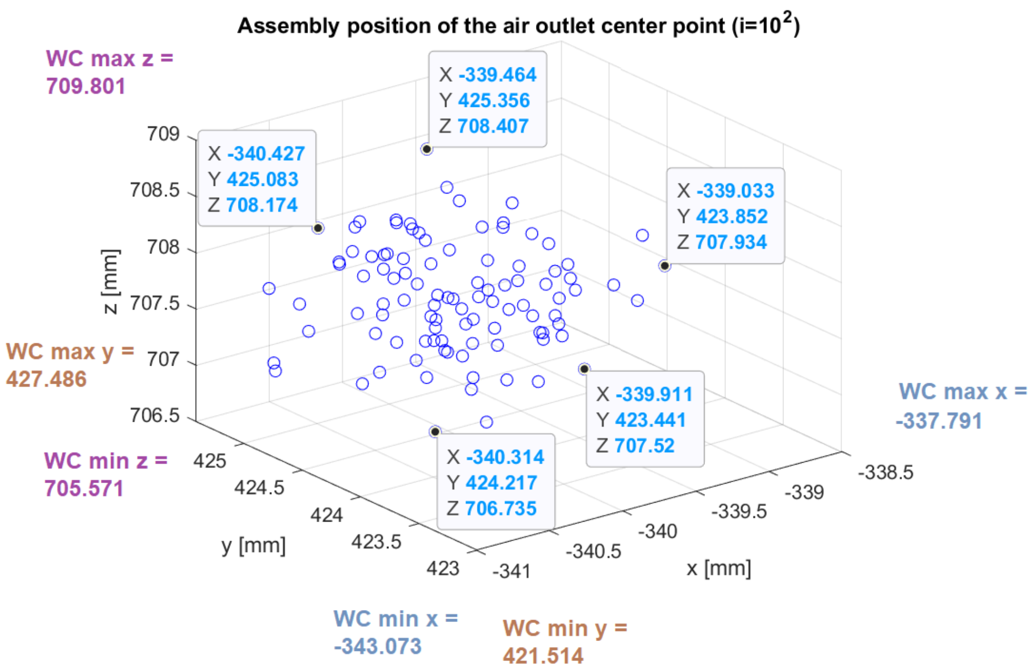

Figure 86 – The statistical variation of the center point position of the turbocharger compressor outlet port for 100 iterations.

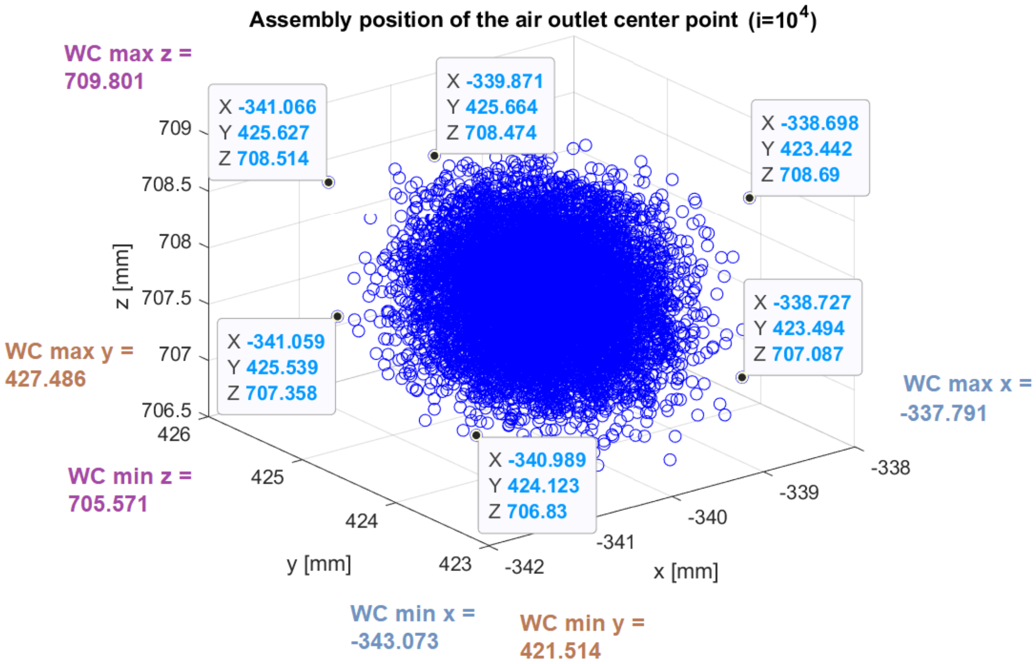

Figure 87 – The statistical variation of the center point position of the turbocharger compressor outlet port for 10, 000 iterations.

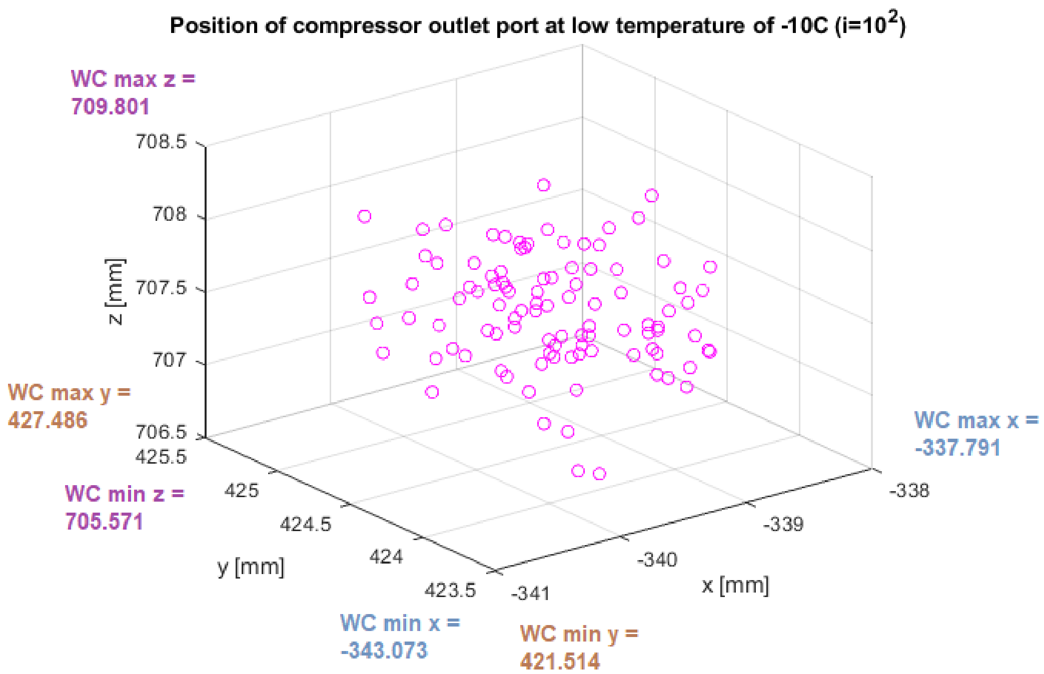

Figure 88 – The statistical variation of the center point position of the turbocharger compressor outlet port for 100 iterations at cold start condition.

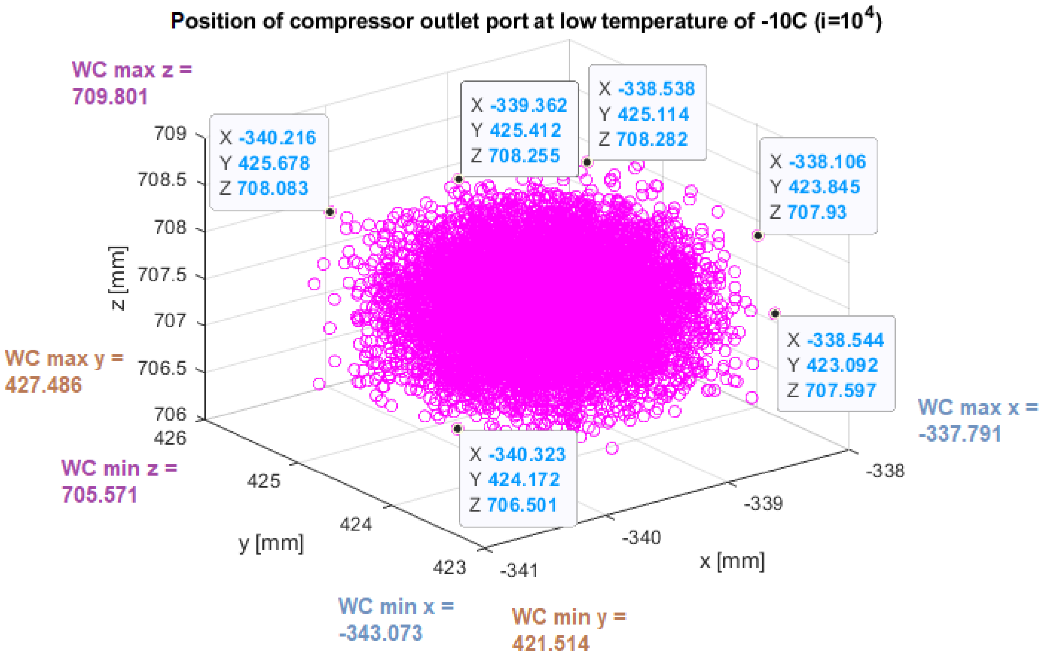

Figure 89 – The statistical variation of the center point position of the turbocharger compressor outlet port for 10, 000 iterations at cold start condition.

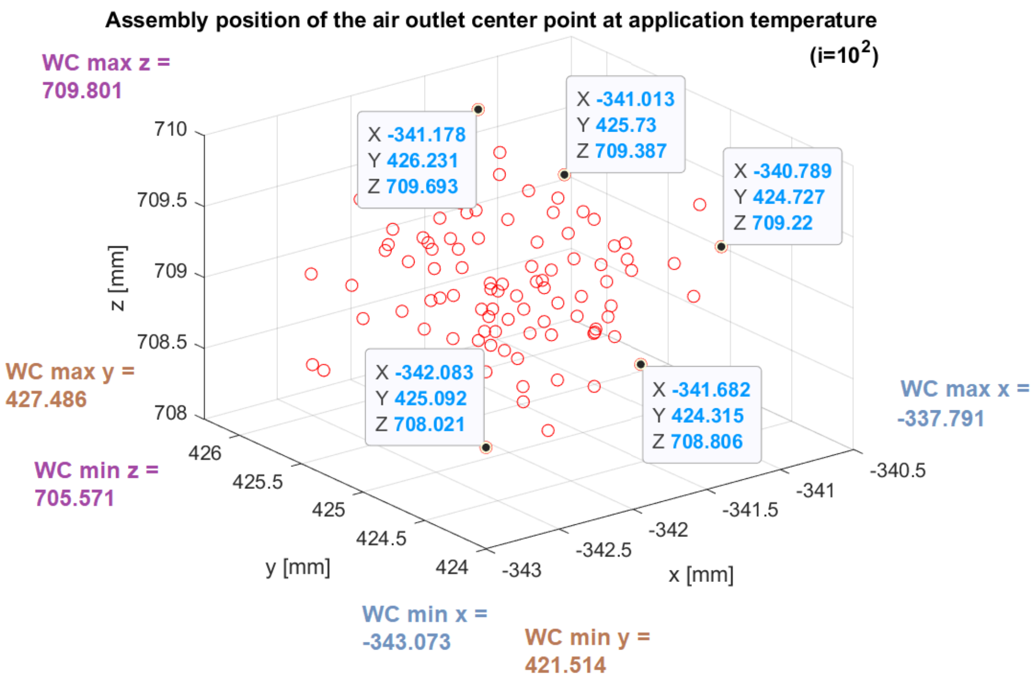

Figure 90 – The statistical variation of the center point position of the turbocharger compressor outlet port for 100 iterations at application condition.

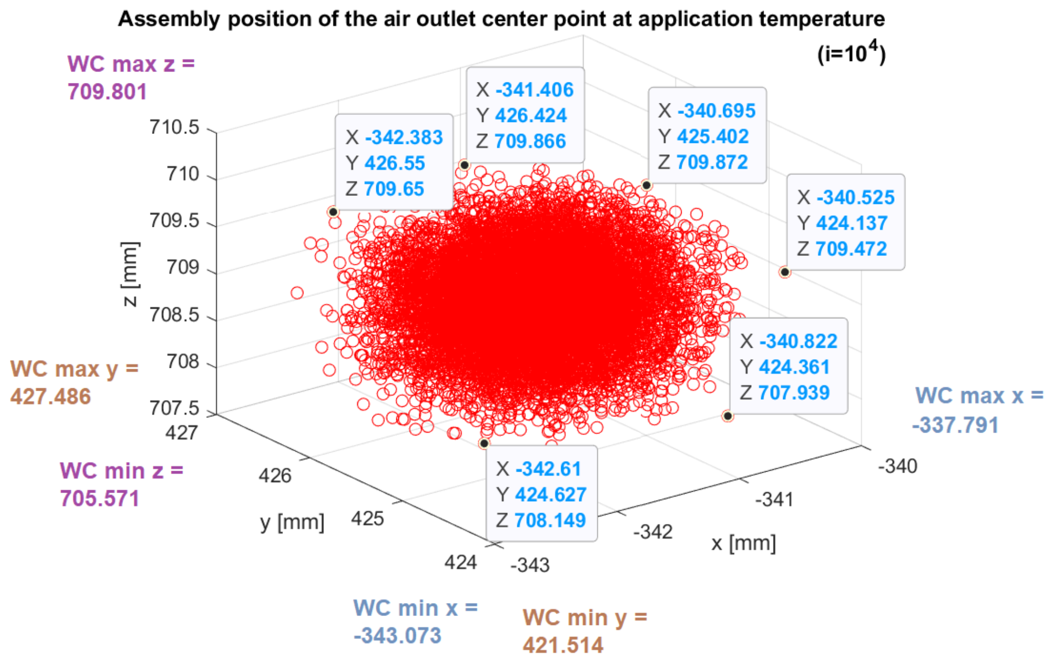

Figure 91 – The statistical variation of the center point position of the turbocharger compressor outlet port for 10, 000 iterations at application condition.

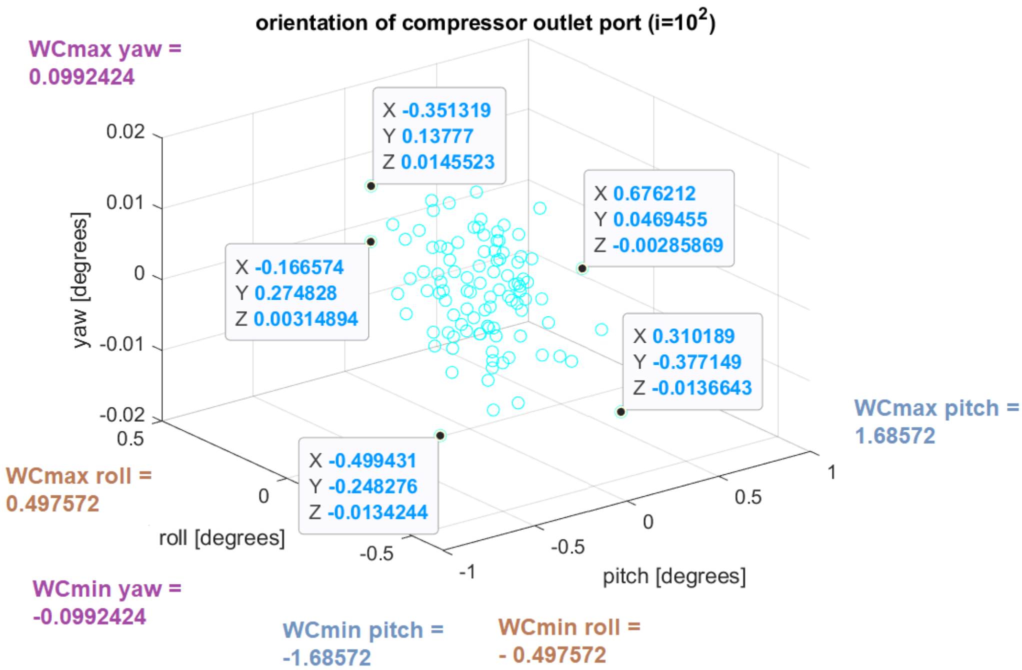

Figure 92 – The statistical variation of the center point orientation of the turbocharger compressor outlet port for 100 iterations.

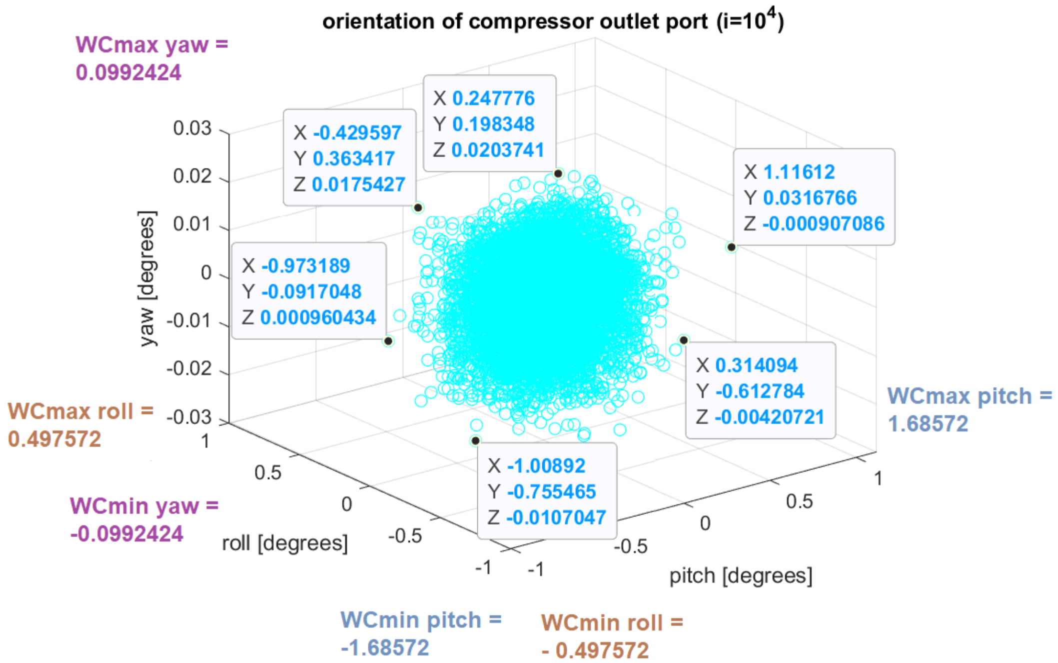

Figure 93 – The statistical variation of the center point orientation of the turbocharger compressor outlet port for 10, 000 iterations.

The potential use of the method

The results of the stochastic manufacturing data displayed under the real application condition allow important design information to be used in different ways.

1. Verification of compliance with predetermined design constraints.

2. Provide a solution to design problems during its development, such as the dimensioning of matching components;

The first item is obviously considered if a value is previously specified for comparison. Therefore, the second element is developed to exemplify the method.

The design problem is to dimension the parts to be connected to the air outlet port of the turbocompressor, which must function in the full range of the engine working condition. These parts are the aftercooler and the connecting tube, as illustrated in Figure 94.

The connection design between the matching parts is illustrated in Figure 95, where the dotted line represents the nominal position and the blue shadow regions represent the variation fields.

The algorithm provides detailed data on the upstream tolerance chain, as summarized in Figure 96, and information on the design of the parts involved. The red dots represent the displacement as a result of the thermal effect of the application. The cold starting conditions at low temperatures are not included for figure simplification. The design configuration allows the aftercooler to be fastened to the left-hand side face of the cylinder head, the location variation highlighted in yellow.

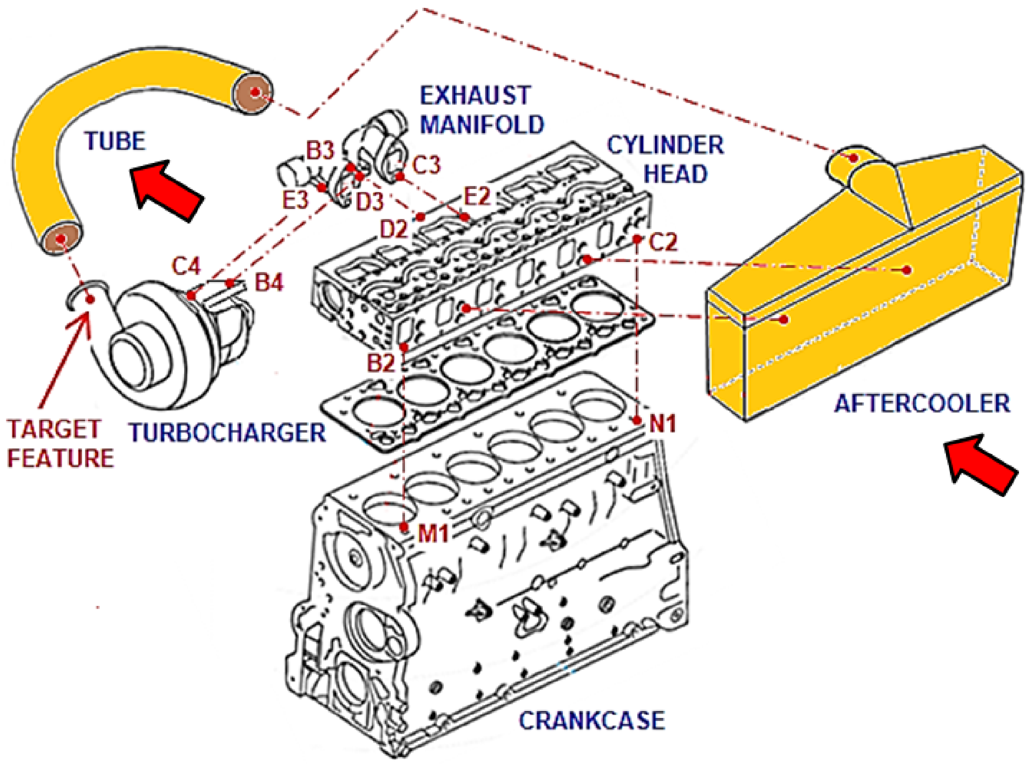

Figure 94 – Parts connected to the turbocharger air outlet port. Source: the author.

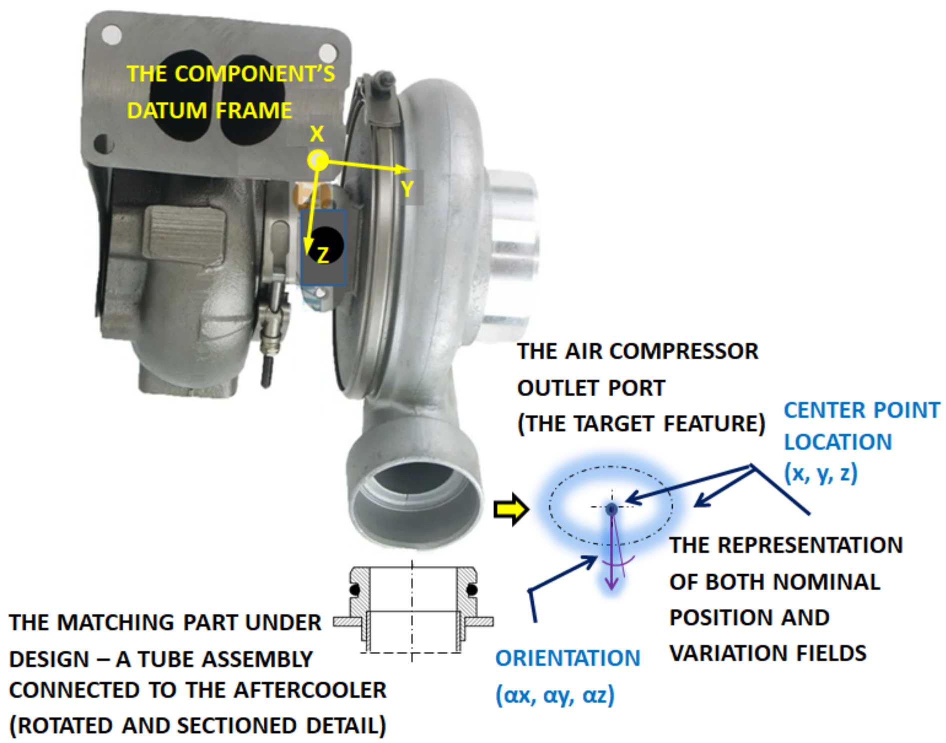

Figure 95 – Design of the connection between the turbocompressor air outlet port and the tube. Source: the author.

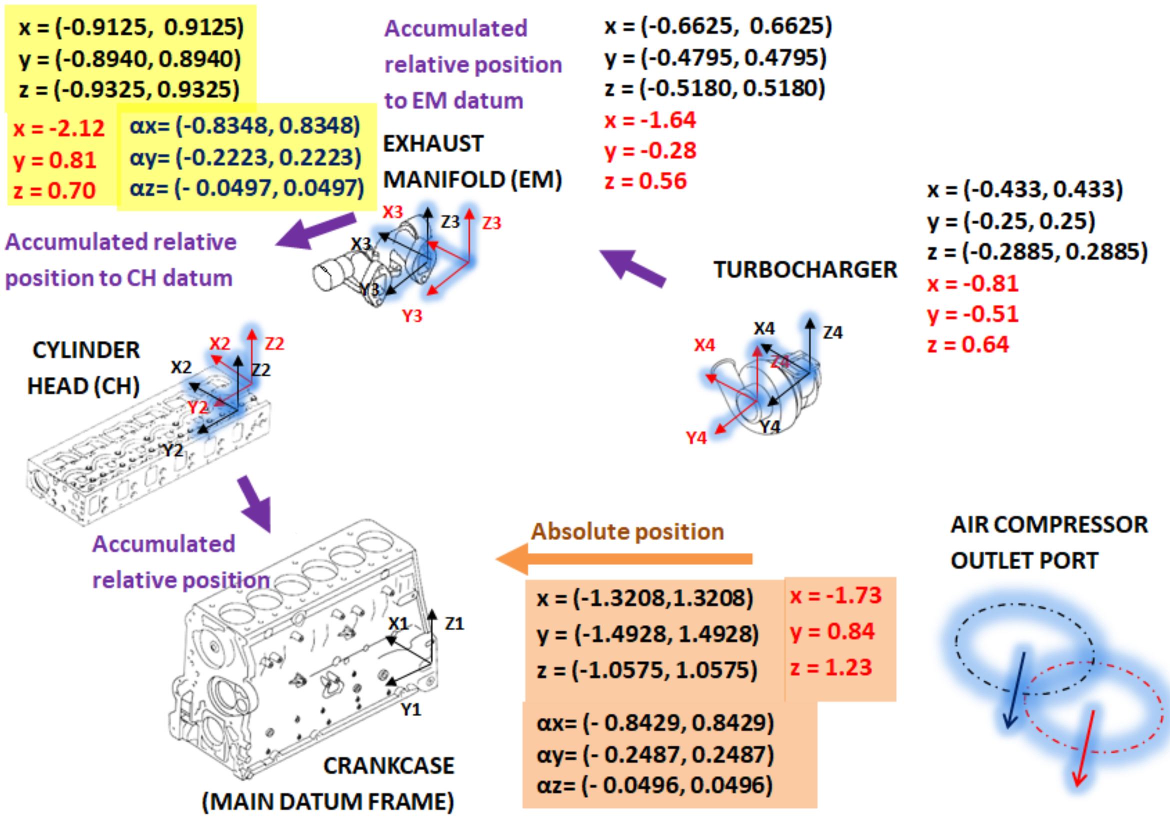

Figure 96 – Summary of the absolute and relative positions among parts. Source: the author.

Discussion of the results

In the conclusion of this chapter, on the basis of the results presented, some conclusions can be drawn from them.

1. The WC condition is very conservative: the full range of WC position tolerance is found in the main directions (Figures 86 to 93):

    - X: $[-337.791 - (-343.073)] = 5.282$ mm;
    - Y: $[427.486 - 421.514] = 5.972$ mm;
    - Z: $[709.801 - 705.571] = 4.230$ mm

    Values are expected due to both the dimensions and the process costs of the components involved in assembly in relation to a commercial product. However, as commented before, the example target feature refers to an intermediate value needed for the design of a paired component. This coupling component must connect the compressor outlet port (the target feature) to the inlet port of an aftercooler (an air-coolant heat exchanger, already cited). Some issues can be raised:

    a) The aftercooler must be fastened to some other part of the engine and assumes the accumulated tolerances of the main reference frame plus its own position tolerances;

b) this coupling component is exposed to significant radiant heat flux. Its material must have adequate heat resistance;

c) a leak tightness design is involved with respect to the internal hot air pressure;

d) due to both the thermal strain and assembly requirements, a flexible and/or rigid material with a flexible joint must be considered in the design.

On the basis of these issues, a prior specified value for the position of the connecting component would lead to the need for a tolerance synthesis of the referenced components in this example. This tolerance synthesis should reduce the above tolerances (around 5 mm), which is impracticable for economic and technical reasons;

2. A simple observation of Figures 86 and 87 shows that the results of the production simulation with both numbers of iterations present a significantly lower range of values compared to the WC case in all main directions. The software resources allow the joint calculation of the main moments of the statistical distribution, that is, its mean μ and its variance σ^2. The standard deviation σ allows important inferences about the assembly rejection rate. The values of some program runs with $10,000$ iterations in standard temperature assembly are shown in Table 5.6.

Table 5.6 – Approximate values of mean μ, variance σ^2 and standard deviation σ for the results of $10,000$ iterations at standard temperature assembly

	X	Y	Z
μ	-340.43	424.50	707.68
σ^2	0.2056	0.1857	0.1597
σ	0.4534	0.4309	0.3997

However, an analysis of Table 2.1 in Chapter 2 shows that a specified limit of $\pm 3\sigma$ leads to an acceptance rate of 99.73% or a defective number of 2,700 ppm. In the production of $10,000$ engines, this results in only 27 rejected assemblies. If this condition is considered for the values in Table 5.6 and considering that the WC range occurs (in practice) for $\pm 6\sigma$ (see Table 2.1), the positional variation will be half of the WC range, that is,

(WC)

$\mathrm{X} = -340.43 \pm (-5.282/2) = -340.43 \pm 2.64$ mm

$\mathrm{Y} = 424.50 \pm (5.972/4) = 424.50 \pm 2.99$ mm

$\mathrm{Z} = 707.68 \pm (4.230/4) = 707.68 \pm 2.12$ mm

(STATISTICAL)

X $= -340.43 \pm (-5.282/4) = -340.43 \pm 1.32$ mm

Y $= 424.50 \pm (5.972/4) = 424.50 \pm 1.49$ mm

Z $= 707.68 \pm (4.230/4) = 707.68 \pm 1.06$ mm

This is a much better condition provided by the method and can simplify the design of the compressor outlet port connection counterpart. The conduction of a tolerance synthesis process is also facilitated if these new tolerance ranges are considered as design constraints.

3. The dimensional variation caused by the thermal loads (affecting the basic dimensions as already cited) described in Tables 5.2, 5.3, 5.4, and 5.5 is summarized in Table 5.7 for comparison with engine data, where these components are found under both as-assembled and application conditions.

Table 5.7 – Summary of the variation (Δ) of the position of the target feature (Σ) under standard manufacturing conditions (ST) with respect to cold starting at low temperature (LT) and application conditions (AT). Engine components: Crankcase (Cc); Cylinder Head (CH); Exhaust Manifold (EM); Turbocharger (Tc);

	X ST	X LT	X AT	Y ST	Y LT	Y AT	Z ST	Z LT	Z AT
Cc	280.00	279.92	280.39	23.50	23.49	23.53	425.00	424.86	425.53
CH	-210.00	-209.94	-210.48	476.00	475.86	477.09	102.00	101.97	102.14
EM	-200.00	-199.94	-200.83	60.00	59.98	60.23	-20.00	-19.99	-20.08
Tc	-207.84	-207.74	-208.65	-135.00	-134.93	-135.51	199.18	199.06	199.82
Σ	-337.84	-337.70	-339.57	424.50	424.40	425.34	706.18	705.90	707.41
Δ		-0.14	1.73		0.10	-0.84		0.28	-1.23

An analysis of Table 5.7 shows that the differences between the standard temperature condition and the application condition, that is, the dilatation of the material, present *a significant percentage of the entire ($\pm$) statistical positional variation, in the same degree of magnitude* of the same characteristic. As the WC limits are determined for the standard temperature conditions considered for both the component fabrication and the assembly of them, it can be seen (Figures 90 and 91) that the clouds of points in the application condition are displaced in each orthogonal direction toward one of the WC limits compared to the assembly condition (Figures 86 and 87). This behavior is due to the fact that the tolerance variation is the same (in practice, as already cited), and the position vectors in each direction increase in length with temperature. This observation leads to a possible design solution: the specification of a distribution mean shift on one side, to compensate the thermal variation when the materials are subject to critical application temperatures.

Regarding the variation in orientation of the target feature, Figures 92 and 93 show the effectiveness and accuracy of the method. The orientation variation values are those that result exclusively from the manufacturing orientation variations (e.g. profile tolerances) on the surfaces that contact components and from the tolerance shift between the fasteners and the passage of the holes. In this case study, the values can be considered irrelevant due to the product characteristics, but can be useful in applications where the need for accurate alignment is important, for example.

In summary, the method provides an important design tool in terms of the design of the connection between the air outlet port and the aftercooler inlet port for this specific case study. Although the design of parts is not within the scope of this work, all the necessary dimensional information has been developed in this work, considering all sources of variation, and with a high accuracy level.

The same approach can be applied to other designs with due consideration.

6 Conclusion and Future Work

This thesis has proposed a new method of 3D dimensional tolerance analysis with the incorporation of functional thermal effects. The main differential of the proposal over the existing methods is the consideration of the influence of orientation variation on the position tolerances, not only regarding the inclination of surfaces but also due to the kinematic adjustment on occasion of the assembly of consecutive components. The tolerance shift caused by the clearance between the fastening elements and the holes is the main factor that leads to the kinematic adjustment. The proposed method also aims to be applied concurrently with the CAD-CAE tools used in engineering design, in an application-oriented approach, rather than as a pure theoretical development. Although the current technological development is high, current CAD-CAE systems are not able to aggregate the characteristics of the new proposal. As the case study results have shown, the cited features provide very accurate results, since very little angular variation is contemplated along the tolerance analysis calculation. The prior accessibility of the angular variation, depending on the case, is fundamental to the design development and/or assembly feasibility, due to the likelihood of misalignment concerns. Another contribution of the method is the stochastic simulation of the manufacturing and assembling processes, leading to an economic differential, mainly when it is used in design decisions. As the simulation of a high production volume involves not only the dimensioning of each component, but also the assembly behavior between consecutive components, the results can be considered very reliable regarding a design decision. The case study chosen reflects an actual application, with the usual values of dimensional tolerances found in practice that demonstrate, as much as possible, a real performance condition and a decision aid for the choice of an alternative design for a matching part. Furthermore, consideration of the functional thermal effect on the basic dimensions has shown its influence on the overall result, although it could not be significant in some cases. In summary, the method, due to its simple programming work, can be an effective tool for 3D tolerance analysis in a myriad of different applications and for the evaluation of design alternatives as well.

The concepts addressed in this work can be used in the further development of algorithms seeking integration with CAD systems, due to its geometric nature regarding the treatment of position and orientation of geometric features. A link with CAE systems to import mechanical loading effects can also be considered. The approaches of dimensional variation with thermal loads and production simulation are also prone to be considered in new design tools. Finally, an extension of the tolerance analysis method can also consider tolerance synthesis, with the due increase in complexity regarding algorithm construction.

Bibliography

ABOELMAGED, M. G. Six sigma quality: a structured review and implications for future research. *International Journal of Quality & Reliability Management*, v. 27-3, p. 268–317, 2010. Cited in page 45.

AHRENS, T. J. E. *Mineral Physics & Crystallography: Vol. 2 - A Handbook of Physical Constants*. Washington DC, USA: American Geophysical Union, 1995. Cited in page 46.

ALAGAR, V. S.; BUI, T. D.; PERIYASAMY, K. Semantic csg trees for finite element analysis. *Computer-Aided Design*, v. 22-4, p. 194–198, May 1990. Cited 2 time in page 13 and 57.

AMETA, G.; SERGE, S.; GIORDANO, M. Comparison of spatial math models for tolerance analysis: Tolerance-maps, deviation domain, and TTRS. *Journal of Computing and Information Science in Engineering*, v. 11, p. 1–8, Jun. 2011. Cited 3 time in page 63, 65, and 67.

ANDOLFATTO, L.; LAVERNHE, S.; MAYER, J. R. R. Evaluation of servo, geometric and dynamic error sources on five axis high-speed machine tool. *International Journal of Machine Tools and Manufacture*, v. 56-10-11, p. 787–796, Oct. 2011. Cited in page 164.

ANDRáSSYOVá, Z.; PAULICEK, T.; PICHNA, P.; KOTUS, M. Improving quality of statistical process control by dealing with non-normal data in automotive industry. *Management Systems in Production Engineering*, v. 3-7, p. 26–30, 2012. Cited in page 176.

ANSELMETTI, B.; CHAVANNE, R.; YANG, J.-X.; ANWER, N. Quick GPS: A new CAT system for single part tolerancing. *Computer-Aided Design*, v. 42, p. 768–780, 2010. Cited in page 24.

ANSELMETTI, B.; LOUATI, H. Generation of manufacturing tolerancing with ISO standards. *International Journal of Machine Tools & Manufacture*, v. 45, p. 1124—1131, 2005. Cited in page 20.

ANWER, N.; BALLU, A.; MATHIEU, L. The skin model, a comprehensive geometric model for engineering design. *CIRP Annals - Manufacturing Technology*, v. 62, p. 143–146, 2013. Cited 3 time in page 13, 55, and 56.

ARMILLOTTA, A. Selection of parameters in cost-tolerance functions: review and approach. *The International Journal of Advanced Manufacturing Technology*, v. 108, n. 1, p. 167–182, 2020. Cited in page 159.

ASKRI, R.; BOIS, C.; WARGNIER, H.; GAYTON, N. Tolerance synthesis of fastened metal-composite joints based on probabilistic and worst-case approaches. *Computer-Aided Design*, v. 100, p. 39–51, 2018. Cited in page 71.

ASM. *Handbook Vol. 1 - Properties and selection: Irons, steels and high performance alloys*. ASM International, 1990. 2521 p. Cited in page 112.

ASM. *Handbook Vol. 17 - Nondestructive Evaluation and Quality Control - 2nd. Edition.* ASM International, 1992. 1608 pp. p. Cited 3 time in page 17, 155, and 156.

ASME. *Metric Screw Threads: M Profile*. New York, NY, 2005. Cited 3 time in page 78, 80, and 82.

ASME Y14.5-2009 - Dimensioning and Tolerancing Engineering drawings and related documentation practices. New York, NY, 2009. Cited 16 time in page 12, 13, 26, 27, 28, 29, 30, 31, 32, 33, 34, 35, 37, 59, 64, and 154.

ASME Y14.5.1.M-1994 - Mathematical definition of dimensioning and Tolerancing principles. New York, NY, 1995. Cited 6 time in page 14, 27, 59, 77, 80, and 91.

BARARI, A. Profile tolerance allocation for rapid prototyping of sculptured surfaces in a direct slicing process. In: *Proceedings of the ASME 2012 International Design Engineering Technical Conferences & Computers and Information in Engineering Conference*. ASME, 2012. p. 1–6. Cited in page 159.

BARARI, A. Tolerance allocation for structures subject to various loading events. In: *Proceedings of the ASME 2012 International Design Engineering Technical Conferences & Computers and Information in Engineering Conference*. ASME, 2012. p. 1–8. Cited in page 47.

BARARI, A.; ELMARAGHY, H. A.; ORBAN, P. Nurbs representation of estimated surfaces resulting from machining errors. *International Journal of Computer Integrated Manufacturing*, v. 22-5, p. 395—410, May 2009. Cited in page 163.

BARARI, A.; POP-ILIEV, R. Reducing rigidity by implementing closed-loop engineering in adaptable design and manufacturing systems. *Journal of Manufacturing Systems*, v. 28, p. 47–54, 2009. Cited in page 77.

BARDENET, R. Monte Carlo methods. In: *EPJ Web of Conferences*. France: EDP Sciences, 2013. p. 1–21. Cited in page 184.

BECKWITH T., G.; MARANGONI R., D.; LIENHARD, J. H. *Mechanical Measurements Sixth Edition*. Pearson Learning Solutions, 2011. Cited 3 time in page 17, 153, and 154.

BELLE, G. van. *Statistical Rules of Thumb*. 2nd. ed. New Jersey, USA: John Wiley & Sons, Inc., 2008. Cited in page 176.

BENDAT, J. S.; PIERSOL, A. G. *Random Data: Analysis and Measurement Procedures*. 4th. ed. New Jersey, USA: John Willey & Sons, Inc., 2010. Cited 3 time in page 18, 181, and 182.

BENICHOU, S.; ANSELMETTI, B. Thermal dilatation in functional tolerancing. *Mechanism and Machine Theory*, v. 46, p. 1575—1587, 2011. Cited 3 time in page 46, 69, and 70.

BHIDE, S.; DAVIDSON, J. K.; SHAH, J. J. Areal coordinates: The basis of a mathematical model for geometric tolerances. In: BOURDET, P.; MATHIEU, L. (Ed.). *Geometric Product Specification and Verification: Integration of Functionality*. Cachan, France: Springer Science + Business Media, B. V.,, 2001. p. 35–44. Cited 4 time in page 14, 65, 66, and 67.

BJORKE, O. *Computer Aided Tolerancing*. 2nd. ed. ASME Press, 1989. Cited 3 time in page 20, 46, and 70.

BLACK, J. T.; KOHSER, R. A. *DeGarmo's Materials and Processes in Manufacturing – Tenth Edition*. New Jersey, USA: John Wiley & Sons, Inc, 2008. Cited 7 time in page 17, 150, 158, 169, 170, 172, and 175.

BOURDET, P.; CLéMENT, A. a. A study of optimal-criteria identification based on the small-displacement screw model. *Annals of the CIRP*, v. 37-1, p. 503–506, 1988. Cited 2 time in page 49 and 50.

BOYER, M.; STEWART, N. F. Modeling spaces for toleranced objects. *The International Journal of Robotics Research*, v. 10–5, p. 570–582, 1991. Cited in page 56.

BREYFOGLE, F. W. *Implementing Six Sigma: smarter solutions using statistical methods*. New Jersey, USA: John Wiley & Sons, Inc., 2003. Cited 3 time in page 13, 43, and 44.

BRYAN, J. International status of thermal error research (1990). *Annals of the CIRP*, v. 39-2, p. 645–656, 1990. Cited in page 160.

BUESCHER, P. A. Sampling and measurement errors - part i - sampling errors. *State Center For Health Statistics*, p. 1–7, May 1984. Cited in page 175.

BURY, K. *Statistical Distributions in Engineering*. Cambridge University Press, 1999. Cited in page 150.

BURY, K. V. *Statistical Models in Applied Science*. New Jersey, USA: John Willey & Sons, 1975. Cited in page 173.

CARDOSO, A. A.; ANDREATTA, E. C. Thermomechanical analysis of diesel engine exhaust manifold. *SAE Technical Series*, v. 2016-36-0258, p. 1–8, Oct. 2016. Cited in page 114.

CHASE, K. H.; PARKINSON, A. A survey of research in the application of tolerance analysis to the design of mechanical assemblies. *Research in Engineering Design*, v. 3, p. 23–37, Mar. 1991. Cited 4 time in page 40, 41, 42, and 43.

CHASE, K. W.; GREENWOOD, W. H. Design issues in mechanical tolerance analysis. *Manufacturing Review, ASME*, v. 1-1, p. 50–59, Mar. 1988. Cited 4 time in page 38, 39, 40, and 42.

CHASE, K. W.; MAGLEBY, S. P. A comprehensive system for computer-aided tolerance analysis of 2-D and 3-D mechanical assemblies. In: *Proceedings of the 5th International Seminar on Computer-Aided Tolerancing Toronto, Canada*. 1997. p. 1–16. Cited 2 time in page 14 and 60.

CHASE, K. W.; MAGLEBY, S. P.; GAO, J. Tolerance analysis of 2-D and 3-D mechanical assemblies with small kinematic adjustments. *ADCATS Report*, v. 97-5, p. 1–27, 1997. Cited in page 59.

CHASE, K. W.; MAGLEBY, S. P.; GAO, J. Generalized 3-D tolerance analysis of mechanical assemblies with small kinematic adjustments. *IEE Transactions*, v. 30, p. 367–377, 1998. Cited in page 21.

CHIANG, J.-Y.; TSAI, T.-R.; LIO, Y. L.; LU, W.; SHI, D. An integrated approach for the optimization of tolerance design and quality cost. *Computers & Industrial Engineering*, v. 87, n. 1, p. 186–192, 2015. Cited in page 159.

CHOUDHURY, S. K.; SRINIVAS, P. Tool wear prediction in turning. *Journal of Materials Processing Technology*, v. 153-154, p. 276—-280, 2004. Cited in page 164.

CLéMENT, A.; RIVIèRE, A.; SERRé, P.; VALADE, C. The TTRSs: 13 constraints for dimensioning and tolerancing. In: ELMARAGHY, H. A. (Ed.). *Geometric Design Tolerancing: Theories, Standards and Applications*. Springer Science+Business Media Dordrecht 1998, 1998. p. 122–131. Cited 2 time in page 63 and 65.

COLOSIMO, B. M.; SENIN, N. *Geometric Tolerances - Impact on Product Design, Quality Inspection and Statistical Process Monitoring*. Springer-Verlag London Limited, 2011. Cited 2 time in page 154 and 174.

CORRADO, A.; POLINI, W. Manufacturing signature in variational and vector-loop models for tolerance analysis of rigid parts. *International Journal of Advanced Manufacturing Technology*, v. 88, p. 2153–2161, 2017. Cited in page 55.

CRAIG, J. J. *Introduction to Robotics: Mechanics and Control*. 3rd. ed. Pearson Education Limited, 2014. Cited 2 time in page 35 and 36.

CURRAN, R.; KUNDU, A.; RAGHUNATHAN, S.; EAKIN, D.; MCFADDEN, R. Influence of manufacturing tolerance on aircraft direct operating cost (doc). *Journal of Materials Processing Technology*, v. 138, n. 1, p. 208–213, 2003. Cited in page 159.

CURTIS, M. A.; FARAGO, F. T. *Handbook of Dimensional Measurement*. Industrial Press Inc., 2014. Cited 3 time in page 154, 173, and 174.

DANTAN, J.-Y.; QURESHI, A. J. Worst-case and statistical tolerance analysis based on quantified constraint satisfaction problems and monte carlo simulation. *Computer-Aided Design*, v. 41, p. 1–12, 2009. Cited in page 70.

DARWISH, S. M. Effect of tool bit insert-holder assembly on dimensional accuracy and geometrical tolerances of machined workpieces. *Int. J. Mach. Tools Manufact.*, v. 35-6, p. 841–849, 1995. Cited in page 164.

DASSAULTSYSTEMES. *CATIA V5*. 2020. Last accessed 30 October 2020. Disponível em: <https://www.3ds.com/products-services/catia/>. Cited in page 65.

DAVIDSON, J. K.; MUJEZINOVIC, A.; SHAH, J. J. A new mathematical model for geometric tolerances as applied to round faces. *ASME Journal of Mechanical Design*, v. 124, p. 609–622, Dec. 2002. Cited in page 67.

DAVIDSON, J. K.; SHAH, J. J. Geometric tolerances: A new application for line geometry and screws. In: *Proceedings of a Simposium Commemorating the Legacy, Works and Life of Sir Robert Stawell Ball Upon the 100th Anniversary of A Treatise on The Theory of Screws*. University of Cambridge, 2000. p. 1–17. Cited in page 65.

DEMING, W. E. *Some theory of sampling*. New Jersey, USA: John Wiley & Sons Inc., Chapman & Hall, London, 1950. Cited 2 time in page 173 and 175.

DESROCHERS, A.; GHIE, W.; LAPERRIèRE, L. Application of a unified Jacobian—torsor model for tolerance analysis. *Transactions of the ASME*, v. 3, p. 2–14, Mar. 2003. Cited 4 time in page 51, 53, 54, and 59.

DESROCHERS, A.; MARANZANA, R. Constrained dimensioning and tolerancing assistance for mechanisms. In: KIMURA, F. (Ed.). *Computer-aided Tolerancing - The 4th CIRP Design Seminar on Computer-aided Tolerancing*. Chapman & Hall - CIRP, 1996. p. 17–30. Cited in page 64.

DESROCHERS, A.; RIVIèRE, A. A matrix approach to the representation of tolerance zones and clearances. *International Journal of Advanced Manufacturing Technology*, v. 13, p. 630–636, 1997. Cited 3 time in page 14, 67, and 69.

DESROCHERS, A.; VERHEUL, S. A three dimensional tolerance transfer methodology. In: HOUTEN, F. van (Ed.). *Global Consistency of Tolerances - The 6th CIRP International Seminar on Computer-Aided Tolerancing*. The Netherlands: Springer Science+Business Media Dordrecht, 1999. p. 83–92. Cited in page 65.

DESROCHERS, A. A.; CLéMENT, A. A dimensioning and tolerancing assistance model for CAD/CAM systems. *International Journal of Advanced Manufacturing Technology*, v. 9, p. 352–361, 1994. Cited 3 time in page 14, 63, and 64.

DIMITRELLOU, S. C.; DIPLARIS, S. C.; SFANTSIKOPOULOS, M. M. Cost-competent tolerancing in cad. *International Journal of Advanced Manufacturing Technology*, v. 35, p. 519—-526, 2007. Cited in page 158.

DISCHAW, R. D.; KOBAYASHI, M. Multi-layer steel gasket technology for engine cylinder head and manifold applications. *SAE Technical Papers*, Paper 890270, p. 1–11, Mar. 1989. Cited in page 108.

DONMEZ, M. A.; BLOMQUIST, D. S.; HOCKEN, R. J.; LIU, C. R.; BARASH, M. M. A general methodology for machine tool accuracy enhancement by error compensation. *Precision Engineering*, v. 8-4, p. 187–196, Oct. 1986. Cited in page 165.

DOOLEN, G. D.; HENDRICKS, J. Monte Carlo at work. *Los Alamos Science*, p. 142–143, Special issue 1987. Cited in page 184.

DORNFELD, D.; LEE, D.-E. *Precision Manufacturing*. Springer Science+Business Media, LLC, 2008. Cited 4 time in page 17, 151, 160, and 161.

DUNCAN, A. J. *Quality control and industrial statistics - revised edition*. Richard D. Irwin, Inc., 1959. Cited in page 173.

DéCRITEAU, D.; PERNOT, J.-P.; DANIEL, M. Towards a declarative modeling approach built on top of a CAD modeler. *Computer-Aided Design and Applications, Taylor & Francis Online*, v. 13-6, p. 737–746, 2016. Cited 2 time in page 13 and 58.

ECKHARDT, R. Stam Ulam, John von Neumann and the Monte Carlo method. *Los Alamos Science*, p. 131–137, Special issue 1987. Cited in page 182.

EL-HOFY, H. A.-G. *Fundamentals of Machining Processes - Conventional and Nonconventional Processes*. CRC Press, 2014. Cited 2 time in page 17 and 158.

ELHAKIM, M. A. M.; ABAD, M. D.; ABDELHAMEED, M. M.; SHALABY, M. A.; VELDHUIS, S. C. Wear behavior of some cutting tool materials in hard turning of hss. *Tribology International*, v. 44, p. 1174–1181, 2011. Cited in page 164.

ETIENNE, A.; DANTAN, Y.; SIADAT, A.; MARTIN, P. Activity-based tolerance allocation (abta) – driving tolerance synthesis by evaluating its global cost. *International Journal of Production Research*, v. 47, n. 18, p. 4971–4989, 2009. Cited in page 159.

EVANS, D. H. Multiplex sampling. *The Annals of Mathematical Statistics*, v. 34-4, p. 1322–1346, Dec. 1963. Cited in page 176.

EVANS, D. H. Statistical tolerancing: The state of the art part I. Background. *Journal of Quality Technology*, v. 6-4, p. 188–195, 1974. Cited 3 time in page 39, 41, and 71.

EVANS, D. H. Statistical tolerancing: The state of the art part II. Methods for estimating moments. *Journal of Quality Technology*, v. 7-1, p. 1–12, 1975. Cited in page 71.

EVANS, D. H. Statistical tolerancing: The state of the art part III. Shifts and drifts. *Journal of Quality Technology*, v. 721, p. 72–76, 1975. Cited 4 time in page 41, 42, 71, and 173.

EVANS, J. S. O. Negative thermal expansion materials. *The Royal Society of Chemistry*, p. 3317–3326, 1999. Cited in page 46.

FIGLIOLA, R. S.; BEASLEY, D. E. *Theory and Design for Mechanical Measurements - Fifth Edition*. New Jersey, USA: John Wiley & Sons, Inc., 2011. Cited in page 152.

FISCHER, B. R. *Mechanical tolerance stackup and analysis 2nd. Edition*. CRC Press, 2011. Cited 3 time in page 37, 38, and 71.

FISCHER, H. *A History of the Central Limit Theorem - From Classical to Modern Probability Theory*. Springer Science + Business Media, LLC, 2010. Cited in page 173.

FISCHER, R. A.; YATES, F. *Statistical Tables for Biological, Agricultural, and Medical Research - 2nd. edition*. Oliver and Boyd Edinburgh Tweedalle Court, 1943. Cited in page 183.

FLEISCHER, J.; MUNZINGER, C.; HERDER, S.; WEIS, M. Adaptronical compensation of geometrical machine errors. *Prod. Eng. Res. Devel.*, v. 6, p. 303–309, May 2012. Cited in page 165.

FORSLUND, A. A.; SöDERBERG, J. M. R.; ISAKSSON, O.; LööF, J.; FREY, D. Evaluating how functional performance in aerospace components is affected by geometric variation. *SAE Int. J. Aerosp.*, v. 11-1, p. 5–26, 2018. Cited in page 48.

FRANCIOSA, P.; GERBINO, S.; PATALANO, S. Variational modeling and assembly constraints in tolerance analysis of rigid part assemblies: planar and cylindrical features. *International Journal of Advanced Manufacturing Technology*, v. 49, p. 239–251, 2010. Cited 2 time in page 13 and 57.

FRIDMAN, A. E. *The Quality of Measurements -A Metrological Reference*. Springer Science + Business Media, LLC, 2012. Cited in page 152.

GHIE, W.; LAPERRIèRE, L.; DESROCHERS, A. Re-design of mechanical assemblies using the unified jacobian-torsor model for tolerance analysis. In: DAVIDSON, J. K. (Ed.). *Models for Computer Aided Tolerancing in Design and Manufacturing*. Springer, 2007. p. 95–104. Cited 2 time in page 54 and 55.

GREENWOOD, W. H.; CHASE, K. W. A new tolerance analysis method for designers and manufacturers. *Transactions of the ASME*, v. 109, p. 112–116, May 1987. Cited in page 42.

GREWAL, S. *Manufacturing Process Design and Costing*. Springer-Verlag, 2011. Cited in page 157.

GROOVER, M. P. *Fundamentals of modern manufacturing materials, processes, and systems - fifth edition*. New Jersey, USA: John Wiley & Sons, Inc., 2013. Cited 4 time in page 167, 169, 178, and 179.

GRZESIK, W. *Advanced machining processes of metallic materials - Theory, Modelling and Applications -Second Edition*. Elsevier B.V., 2017. Cited 3 time in page 17, 166, and 168.

GUIE, W. Statistical analysis tolerance using jacobian torsor model based on uncertainty propagation method. *Int. Jnl. of Multiphysics*, v. 3-1, p. 11–30, 2009. Cited in page 55.

GUO, H.; LONG, H. Effect of mesh size in numerical simulation of turbine housing in turbocharger. *SAE Technical Papers*, v. 2018-01-1715, p. 1–5, Sep. 2018. Cited in page 115.

GUOWEI, L.; WEIMIN, Z.; CAN, C. Tolerance analysis considering the impact of working conditions on product performance. In: *2nd International Conference on Industrial Mechatronics and Automation*. IEEE, 2010. p. 47–51. Cited in page 55.

GUPTA, S.; TURNER, J. U. Variational solid modeling for tolerance analysis. *IEEE Computer Graphics and Applications*, v. 13-3, p. 64 – 74, May 1993. Cited in page 56.

HAHN, G. J.; SHAPIRO, S. S. *Statistical Models in Engineering*. New Jersey, USA: John Wiley & Sons, 1967. Cited 5 time in page 18, 91, 177, 180, and 185.

HALLMANN, M.; SCHLEICH, B.; WARTZACK, S. From tolerance allocation to tolerance-cost optimization: a comprehensive literature review. *The International Journal of Advanced Manufacturing Technology*, v. 107, p. 4859–4912, 2020. Cited in page 21.

HALLMANN, M.; SCHLEICH, B.; WARTZACK, S. Sampling-based tolerance-cost optimization of systems with interrelated key characteristics. *Procedia CIRP*, v. 91, n. 1, p. 87–92, 2020. Cited in page 159.

HAMMERSLEY, J. M.; HANDSCOMB, D. C. *Monte Carlo Methods*. Methuen & Co. Ltd., London, 1964. Cited 2 time in page 174 and 183.

HAMMERSLEY, J. M.; MAULDON, J. G. General principles of antithetic variates. In: *Mathematical Proceedings of the Cambridge Philosophical Society*. Cambridge Core, 1956. p. 476–481. Cited in page 183.

HAMMERSLEY, J. M.; MORTON, K. W. Poor man's monte carlo. *Journal of the Royal Statistical Society. Series B -Methodological*, v. 16-1, p. 23–38, 1954. Cited in page 183.

HAMMERSLEY, J. M.; MORTON, K. W. A new monte carlo technique: antithetic variates. In: *Mathematical Proceedings of the Cambridge Philosophical Society*. Cambridge Core, 1956. p. 449–475. Cited in page 183.

HAUGEN, E. B. *Probabilistic approaches in design*. New Jersey, USA: John Wiley & Sons, 1968. Cited 3 time in page 91, 173, and 185.

HE, Y.; BATTISTON, P. A.; ALKIDAS, A. C. Thermal studies in the exhaust manifold of a turbocharged v6 diesel engine operating under steady-state conditions. *SAE Technical Papers*, v. 2006-01-0688, Apr. 2006. Cited in page 114.

HE, Y.; DAVIDSON, J. K.; KALISH, N. J.; SHAH, J. J. Tolerance-maps for line-profiles formed by intersecting kinematically transformed primitive tolerance-map elements. *Journal of Computing and Information Science in Engineering*, v. 16, p. 1–14, Jun. 2016. Cited 2 time in page 24 and 67.

HOCKEN, R. J.; PEREIRA, P. H. *Coordinate Measuring Machines and Systems*. CRC Press, 2012. Cited 4 time in page 18, 152, 155, and 174.

HOFFENSON, S.; DAGMAN, A.; SöDERBERG, R. Tolerance optimisation considering economic and environmental sustainability. *Journal of Engineering Design*, v. 25-10-12, p. 367–390, 2014. Cited in page 20.

HU, S. J.; CAMELIO, J.; ARBOR, A. Modeling and control of compliant assembly systems. *Annals of the CIRP*, v. 55-1, p. 1–4, 2006. Cited in page 48.

ISO 1101 Technical drawings – Geometrical Tolerancing – Tolerancing of form, orientation, location and run-out – Generalities, definitions, symbols, indications on drawings. 1983. Cited in page 26.

ISO 8734 - Parallel pins of hardened steel and martensitic stainless steel - Dowel pins. 1997. Cited in page 106.

ISO965:2 general purpose metric screw threads - Tolerances - Part 2 Limits of sizes for general purpose external and internal screw theads - Medium quality. 1998. Cited in page 107.

ITO, Y. Fundamentals in design of structural body components. In: ITO, Y. (Ed.). *Thermal Deformation in Machine Tools*. McGraw-Hill, 2010. p. 18–45. Cited 2 time in page 160 and 162.

JABALLI, K.; BELLACICCO, A.; LOUATI, J.; RIVIERE, A.; HADDAR, M. Rational method for 3d manufacturing tolerancing synthesis based on the ttrs approach r3dmtsyn. *Computers in Industry*, v. 62, p. 541–554, 2011. Cited in page 65.

JACK, H. *35.6.6 Limit (GO & NO GO) Gauges (Internet Archive)*. 2020. Last accessed 25 September 2020. Disponível em: <https://web.archive.org/web/20080410203043/http://claymore.engineer.gvsu.edu/~jackh/eod/manufact/manufact-124.html>. Cited in page 39.

JAGADEESH, R.; BABU, A. S. Process capability assessment with tool wear: An investigative study. *International Journal of Quality & Reliability Management*, v. 11-2, p. 51–62, 1994. Cited in page 176.

JAYAPRAKASH, G.; SIVAKUMAR, K.; THILAK, M. A numerical study on effect of temperature and inertia on tolerance design of mechanical assembly. *Engineering Computations: International Journal for Computer-Aided Engineering and Software*, v. 29, n. 7, p. 722–742, 2012. Cited 2 time in page 46 and 70.

JAYAPRAKASH, G.; THILAK, M.; SIVAKUMAR, K. Optimal tolerance design for mechanical assembly considering thermal impact. *International Journal of Advanced Manufacturing Technology*, v. 73, p. 859–873, 2014. Cited 2 time in page 47 and 70.

JEANG, A.; CHEN, T.-K.; HWAN, C.-L. A statistical dimension and tolerance design for mechanical assembly under thermal impact. *International Journal of Advanced Manufacturing Technology*, v. 20, p. 907–915, 2007. Cited in page 69.

JEANG, A.; CHUNG, C.-P. Process mean, process tolerance, and use time determination for product life application under deteriorating process. *Int. J. Adv. Manuf. Technol.*, v. 36, p. 97—-113, 2008. Cited in page 176.

JIANG, K.; DAVIDSON, J.; LIU, J.; SHAH, J. J. Using tolerance maps to validate machining tolerances for transfer of cylindrical datum in manufacturing process. *International Journal of Advanced Manufacturing Technology*, v. 73, p. 465–478, 2014. Cited in page 67.

JOBS, S. Steeve jobs quote in businessweek, 1998. In: THOMAS, A. K. (Ed.). *The Business Wisdom of Steve Jobs: 250 quotes from the Innovator Who Changed the World*. New York, NY: Skyhorse Publishing, 2011. p. 23–23. Cited in page 6.

JOGLEKAR, A. M. *Statistical Methods for Six Sigma In R&D and Manufacturing*. New Jersey, USA: John Wiley & Sons, Inc., 2003. Cited in page 44.

KALOS, M. H.; WITHLOC, P. A. *Monte Carlo Methods*. Wyley VcH Verlag GmbH & Co. KGaA, 2004. Cited 2 time in page 174 and 184.

KALPAKJIAN, S.; SCHMID, S. R. *Manufacturing Engineering and Technology*. Pearson Prentice Hall, 2010. Cited 5 time in page 17, 18, 167, 169, and 180.

KARTHI, S.; DEVADASANA, S. R.; MURUGESHB, R.; SREENIVASAC, C. G.; SIVARAM, N. Global views on integrating six sigma and iso 9001 certification. *Total Quality Management*, p. 1–26, 2012. Cited in page 45.

KAUFMAN, J. G.; ROOY, E. L. *Aluminum Alloy Castings Properties, Processes, and Applications*. ASM International, 2004. 321 pp. p. Cited in page 116.

KENDALL, M. G.; SMITH, B. B. *Tables of Random Sampling Numbers*. Cambridge University Press, 1939. Cited in page 183.

KEYENCE. *How to Measure - Understanding displacement sensors and measurement systems*. Keyence Corporation of America, 2019. 24 pp. p. Cited in page 156.

KEYENCE. *Key Technology and Application - Profile Measurement*. Keyence Corporation of America, 2019. 12 pp. p. Cited 2 time in page 17 and 156.

KIM, B.; LEE, S. B.; LEE, E. Effect of a fastener hole design of inlet flanges on the durability of the exhaust manifold for a turbo-diesel engine. In: *Proc. IMechE, Vol. 221 part D*. J. Automobile Engineering, 2006. p. 327–333. Cited in page 114.

KLIR, G. J. *Uncertainty and information : foundations of generalized information theory*. New Jersey, USA: John Wiley & Sons, Inc., 2006. Cited in page 149.

KOCH, K.-R. Monte carlo methods. *Int J Geomath*, v. 9, p. 117–143, 2018. Cited in page 181.

KONKEL, B. P.; ZIPTER, E. C.; KIRKHAM, E. E. Improved parallelism measurement using a laser interferometer. *IEEE Transactions on Industry Applications*, v. 27-4, p. 606–610, Jul. 1991. Cited 3 time in page 17, 155, and 156.

KORBI, A. A.; TLIJA, M.; LOUHICHI B. ANS BENAMARA, A. Cad/tolerancing integration: a new approach for tolerance analysis of non-rigid parts assemblies. *The International Journal of Advanced Manufacturing Technology*, v. 98, p. 2003–2013, 2018. Cited in page 48.

KRAFT, R.; WENSRICH, C. J. *Monte Carlo Methods – A bibliography covering the period 1949 – 1963*. Stanford University Computer Science Library – digitized by Google, 1964. Cited in page 183.

KRAUSE, P.; CLARK, D. *Representing Uncertain Knowledge: Artificial Intelligence Approach*. Springer Science+Business Media Dordrecht, 1993. Cited in page 149.

KROESE, D. P.; TAIMRE, T.; BOTEV, Z. I. *Handbook for Monte Carlo methods*. New Jersey, USA: John Wiley & Sons, Inc, 2011. Cited in page 184.

KUNDRAK, J. J.; KARPUSCHEWSKI, B.; GYANI, K.; BANA, V. Accuracy of hard turning. *Journal of Materials Processing Technology*, v. 202, p. 328–338, 2008. Cited in page 163.

KUZNETS, S. Random events and cyclical oscillations. *Journal of the American Statistical Association*, v. 24-167, p. 258–275, Sep. 1929. Cited in page 181.

KUZNETSOV, A. P. Evolution of methods of assessing the accuracy of metal-cutting machines. *Russian Engineering Research*, v. 37-3, p. 171–179, 2017. Cited 2 time in page 17 and 151.

LAFOND, P.; LAPERRIèRE, L. L. Jacobian-based modeling of dispersions affecting pre-defined functional requirements of mechanical assemblies. In: *Proceedings of the 1999 IEEE*. IEEE, 1999. p. 20–25. Cited 3 time in page 53, 54, and 65.

LAPERRIèRE, L.; GHIE, W.; DESROCHERS, A. Statistical and deterministic tolerance analysis and synthesis using a unified Jacobian-torsor model. *CIRP Anals*, v. 51-1, p. 417–420, 2002. Cited 2 time in page 54 and 55.

LAPERRIèRE, L.; LAFOND, P. Modeling of dispersions affecting pre-defined functional re uirements of mechanical assemblies using jacobian transforms. In: *Integrated design and manufacturing in mechanical engineering '98: Proceedings of the 2nd IDMME Conference held in Compiegne, France, 27-29 May 1998*. Springer-Science+Business Media, B.V., 1998. p. 381–388. Cited 3 time in page 13, 53, and 54.

LAPERRIèRE, L.; LAFOND, P. Tolerance analysis and synthesis using virtual joints. In: *Proceedings of the 6th CIRP International Seminar on Computer-Aided Tolerancing*. Springer Science+Business Media Dordrecht, 1999. p. 405–414. Cited 4 time in page 13, 52, 53, and 54.

LEDOUX, Y.; TEISSANDIER, D. Tolerance analysis of a product coupling geometric and architectural specifications in a probabilistic approach. *Res. Eng. Design*, v. 24, p. 297—311, 2013. Cited in page 72.

LEE, W.; WOO, T. C. Tolerances: Their analysis and synthesis. *Journal of Engineering for Industry*, v. 112, p. 113–121, May 1990. Cited in page 21.

LEGOFF, O.; VILLENEUVE, F.; BOURDET, P. Geometrical tolerancing in process planning: a tridimensional approach. *Proc Instn Mech Engrs*, v. 213B, p. 635–640, 1999. Cited 2 time in page 50 and 51.

LI, D. High-alloy ferritic cast irons with different graphite microstructures for exhaust manifolds and turbocharger housings. *International Journal of Materials Research*, v. 101-6, p. 794–800, May 2013. Cited in page 115.

LI, J.; XIE, F.; LIU, X.-J. Geometric error modeling and sensitivity analysis of a five-axis machine tool. *Int J Adv Manuf Technol*, v. 82, p. 2037–2051, 2016. Cited in page 164.

LI, X. P.; NG, H. H.; LIM, S. C. A predictive mapping system for tool wear in metal cutting. *Journal of Materials Processing Technology*, v. 89-90, p. 279–286, 1999. Cited in page 164.

LIANG, Y.; MORONUKI, N.; Y., F. Calculations of the effect of mater al an sotropy on microcutting processes. *Precision Engineering*, v. 16-2, p. 132–138, Apr. 1994. Cited in page 163.

LINDERMAN, K.; SCHROEDER, R. G.; ZAHEER, S.; CHOO, A. S. Six sigma: a goal-theoretic perspective. *Journal of Operations Management*, v. 21, p. 193–203, 2003. Cited 2 time in page 43 and 44.

LISTEWNIK, K.; GRZECZKA, G.; KLACZYNSKI, M.; CIOCH, W. An on-line diagnostics application for evaluation of machine vibration based on standard iso $10816-1$. *Journal of Vibroengineering*, v. 17-8, p. 4248–4258, Dec. 2015. Cited in page 163.

LIU, Y.; CHEN, H.-S.; SAWKAR, N.; XU, N.; GAIKWAD, S.; SEATON, P.; SINGH, K. A thermomechanical fatigue analysis on a ductile cast iron exhaust manifold. *SAE Technical Papers*, v. 2018-01-1215, p. 1–11, Apr. 2018. Cited in page 114.

LIU, Y.; LI, K. Application of six sigma methodology dmaic in hr project management- a case study of motorola sc hr dss project. *IEEE*, p. 1341–1343, 2011. Cited in page 45.

MAGMA. *Casting Design Case Studies – Engine Blocks Full of Stress*. 2020. Last accessed 01 September 2020. Disponível em: <https://www.magmasoft.com/en/solutions/casting-design/casestudy/Engine-Blocks-Full-of-Stress/>. Cited 3 time in page 17, 18, and 171.

MANSUY, M.; GIORDANO, M.; HERNANDEZ, P. A new calculation method for the worst case tolerance analysis and synthesis in stack-type assemblies. *Computer-Aided Design*, v. 43, p. 1118–1125, 2011. Cited in page 72.

MARTINSEN, K.; KOJIMA, T. Express definition of vectorial tolerancing in product modelling. In: *Information Infrastructure Systems for Manufacturing - Proceedings of the IFIP TC5IWG5.3IWG5.7 international conference on the Design of Information*

Infrastructure Systems for Manufacturing, DIISM '96 Eindhoven, the Netherlands. Springer-Science + Business Media, B.V., 1997. p. 313–324. Cited 2 time in page 14 and 60.

MARZIALE, M.; POLINI, W. A review of two models for tolerance analysis of an assembly: vector loop and matrix. *International Journal of Advanced Manufacturing Technology*, v. 43, p. 1106–1123, 2009. Cited in page 68.

MATHé, P.; NOVAK, E. Simple monte carlo and the metropolis algorithm. *Journal of Complexity*, v. 23, p. 673—696, 2007. Cited in page 184.

MAYR, J.; ESS, M.; PAVLICEK, F.; WEIKERT, S.; SPESCHA, D.; KNAPP, W. Simulation and measurement of environmental influences on machines in frequency domain. *CIRP Annals - Manufacturing Technology*, v. 64, p. 479–482, 2015. Cited in page 47.

MAZUR, M.; LEARY, M.; SUBIC, A. Computer aided tolerancing (cat) platform for the design of assemblies under external and internal forces. *Computer-Aided Design*, v. 43, p. 707—719, 2011. Cited in page 20.

MCGRAW-HILL. *Dictionary of Scientific and Technical Terms*. McGraw-Hill, 2003. Cited in page 153.

MECHANICAL vibration — Evaluation of machine vibration by measurements on non-rotating parts — Part I: General guidelines. Geneva, Switzerland, 1995. Cited in page 163.

MERRIAN-WEBSTER. *Merrian Webster Dictionary*. 2020. Last accessed 10 November 2020. Disponível em: <https://www.merriam-webster.com/dictionary>. Cited in page 61.

METHOD and apparatus for geometric variations to integrate parametric computer aided design with tolerance analyses and optimization. 2005. Cited in page 65.

METROLOGY, J. C. for Guides in. *Evaluation of measurement data — Guide to the expression of uncertainty in measurement*. JGCM2008, 2008. Cited in page 149.

METROPOLIS, N. The beginning of monte carlo method. *Los Alamos Science*, p. 125–130, Special issue 1987. Cited in page 182.

METROPOLIS, N.; ROSENBLUTH, A. W.; ROSENBLUTH, M. N.; TELLER, A. H. Equation of state calculations by fast computing machines. *The Journal of Chemical Physics*, v. 21-6, p. 1087–1092, June 1953. Cited in page 184.

METROPOLIS, N.; ULAM, S. The monte calrlo method. *Jounal of the American Statistical Association*, v. 44, p. 335–341, Sept. 1949. Cited in page 182.

MILLER, W. W.; SMITH, C. W.; MACKENZIE, D. S. Negative thermal expansion: a review. *Journal of Mater Science*, v. 44, p. 5441—5451, 2009. Cited in page 46.

MORONUKI, N.; LIANG, Y.; FURUKAWA, Y. Experiments on the effect of material properties on microcutting processes. *Precision Engineering*, v. 16-2, p. 124–131, Apr. 1994. Cited in page 163.

MOVAHEDI, M. M.; KHOUNSIAVASH, M.; OTADI, M.; MOSLEH, M. A new statistical method for design and analyses of component tolerance. *J. Ind. Eng. Int.*, p. 1–8, 2016. Cited in page 71.

MUJEZINOVIC, A.; DAVIDSON, J. K.; SHAH, J. J. A new mathematical model for geometric tolerances as applied to polygonal faces. *Transactions of the ASME*, v. 126, p. 504–518, May 2004. Cited in page 67.

MURRAY, F. J. *The theory of mathematical machines*. King's Crown Press, 1947. Cited in page 183.

NAKASAWA, H. *Principles of Precision Engineering*. Oxford University Press, 1994. Cited in page 151.

NAKASONE - Laminate type manifold gasket. 1991. Cited in page 108.

NEJAD, M. K.; DESROCHERS, A.; VILLENEUVE, F.; VIGNAT, F. Tolerance analysis in machining, an approach combining the model of manufactured part and the Jacobian-torsor model. In: *Proceedings of the ASME 2008 International Design Engineering Technical Conferences & Computers and Information in Engineering Conference IDETC/CIE 2008*. ASME, 2008. p. 1–10. Cited in page 54.

NEJAD, M. K.; VIGNAT, F.; DESROCHERS, A.; VILLENEUVE, F. 3D simulation of manufacturing defects for tolerance analysis. *Journal of Computing and Information Science in Engineering*, v. 10, p. 1–13, Jun. 2010. Cited in page 61.

NEJAD, M. K.; VIGNAT, F.; VILLENEUVE, F. Tolerance analysis in machining using the model of manufactured part (mmp) – comparison and evaluation of three different approaches. *International Journal of Computer Integrated Manufacturing*, v. 25-2, p. 136–149, Feb. 2012. Cited in page 61.

NEYMAN, J. On a statistical problem arising in routine analyses and sampling inspections of mass production. *The Annals of Mathematical Statistics*, p. 46–76, 1941. Cited in page 175.

NISHIWAKI, N.; HORI, S. What is thermal deformation? In: ITO, Y. (Ed.). *Thermal Deformation in Machine Tools*. McGraw-Hill, 2010. p. 46–89. Cited 2 time in page 17 and 161.

OAKLAND, J. S. *Statistical Process Control - 5th. edition*. Butterworth-Heinemann, Oxford, 2003. Cited 3 time in page 18, 176, and 178.

OLWELL, D. H. *Topics in Statistical Process Control*. Tese (Doutorado) — University of Minnesota, USA, 1996. Cited in page 176.

OXFORD. *American Power Dictionary*. Oxford University Press, 1998. Cited in page 149.

PAHL, G.; BEITZ, W.; FELDHUSEN, J.; GROTE, K.-H. *Engineering Design: A Systematic Approach Third Edition*. Springer-Verlag London Limited, 2007. Cited in page 76.

PANDE, P. S.; NEUMAN, R. P.; CAVANAGH, R. R. *The Six Sigma Way: how GE, Motorola, and other top companies are honing their performance*. McGraw-Hill, 2000. Cited in page 44.

PARKINSON, D. B. Optimum sampling plans based on post-quality control reliability. *Reliability Engineering and System Safety*, v. 21, p. 59–75, 1988. Cited in page 176.

PARRA, C. A. F. *Heat Transfer Investigations in a Modern Diesel Engine*. Tese (Doutorado) — University of Bath, 2008. Cited 4 time in page 16, 112, 113, and 114.

PENG, H.; PENG, Z. Concurrent design and process tolerances determination in consideration of geometrical tolerances. *J Mechanical Engineering Science*, p. 1–14, 2019. Cited in page 21.

PENG, H.; WANG, B. A statistical approach for three-dimensional tolerance redesign of mechanical assemblies. *J Mechanical Engineering Science*, v. 0-0, p. 1–13, 2017. Cited in page 55.

PENG, H.; WANG, B. A statistical approach for three-dimensional tolerance redesign of mechanical assemblies. In: *Proc IMechE Part C: J Mechanical Engineering Science*. Institution of Mechanical Engineers, 2017. p. 1–13. Cited in page 55.

PIERRE, L.; TEISSANDIER, D.; NADEAU, J. P. Integration of thermomechanical strains into tolerancing analysis. *Int J Interact Des Manuf*, v. 3, p. 247–263, 2009. Cited in page 70.

POYTHRESS, V. S. *Chance and the Sovereignty of God: A God-Centered Approach to Probability and Random Events*. Crossway, Wheaton, Illinois, 2014. Cited in page 181.

QUALITY, A. A. S. for. *Glossary of quality terms*. 2020. Last accessed 18 September 2020. Disponível em: <http://asq.org/glossary/index.html>. Cited in page 175.

QUESENBERRY, C. P. An spc approach to compensating a tool-wear process. *Journal of Quality Technology*, v. 20-4, p. 220–229,, 1988. Cited in page 176.

RABINOVICH, S. G. *Measurement Errors and Uncertainties Theory and Practice - Third Edition*. Springer Science and Media, Inc., 2005. Cited in page 154.

RAMESH, R.; MANNAN, M. A.; POO, A. N. Error compensation in machine tools — a review - part i: geometric, cutting-force induced and fixture dependent errors. *International Journal of Machine Tools & Manufacture*, v. 40, p. 1235–1256, 2000. Cited in page 165.

RAMESH, R.; MANNAN, M. A.; POO, A. N. Error compensation in machine tools — a review - part ii: thermal errors. *International Journal of Machine Tools & Manufacture*, v. 40, p. 1257–1284, 2000. Cited 2 time in page 162 and 165.

RAMESH, R.; MANNAN, M. A.; POO, A. N. Thermal error measurement and modelling in machine tools. part i. influence of varying operating conditions. *International Journal of Machine Tools & Manufacture*, v. 43, p. 391–404, 2003. Cited in page 162.

RENZI, C. C.; CERUTI, A.; LEALI, F. Integrated geometrical and dimensional tolerances stack-up analysis for the design of mechanical assemblies: an application on marine engineering. *Computer-Aided Design & Applications*, p. 1–12, Mar. 2018. Cited in page 21.

REQUICHA, A. A. G. Representations for rigid solids: Theory, methods, and systems. *Computing Surveys*, v. 12-4, p. 437–464, Dec. 1980. Cited in page 56.

REQUICHA, A. A. G. Representation of geometric eatures, tolerances, and attributes in solid modelers based on constructive geometry. *Journal of Robotics and Automation*, RA-2-3, p. 156–166, Sept. 1986. Cited in page 56.

RICE, W. B. *Control charts in factory management*. London, England: John Wiley & Sons, Inc. Chapman & Hall, 1947. Cited in page 175.

SALOMONS, O. W.; POERINK, H. J. J.; HAALBOOM, F. J.; SLOOTEN, F. van; HOUTEN, F. van; KALS, H. A computer aided tolerancing tool i: Tolerance specification. *Computers in Industry*, v. 31, p. 161–174, 1996. Cited 2 time in page 69 and 71.

SALOMONS, W.; BEGELINGER, R.; POST, E.; HOUTEN, F. v. Application of ttrs method in industrial practice tolerance specification for industrial cooling water pumps. In: *Proceedings of the 6th CIRP International Seminar on Computer-Aided Tolerancing*. Springer-Science + Business Media, B.V., 1999. p. 251–260. Cited in page 65.

SCHLEICH, B.; WARTZACK, S. Evaluation of geometric tolerances and generation of variational part representatives for tolerance analysis. *International Journal of Advanced Manufacturing Technology*, v. 79, p. 959–983, 2015. Cited in page 20.

SHAPIRO, S. S.; GROSS, A. J. *Statistical modeling techniques*. Marcel Dekker Inc., 1981. Cited 2 time in page 152 and 185.

SHEWHART, W. A. *Economic Control of Quality of Manufactured Product*. American Society for Quality Control, 1931. Cited 2 time in page 41 and 176.

SHEWHART, W. A.; DEMING, W. E. *Statistical method from the viewpoint of quality control*. The Graduate School - The Department of Agriculture - Washington, 1939. Cited in page 176.

SIGMETRIX. *Incorporating Thermal Expansion into CAD-Based 3-Dimensional Assembly Variation Analysis*. 2016. Last acessed 2021/11/10. Disponível em: <www.sigmetrix.com>. Cited in page 70.

SINAPIUS, J. M. *Adaptronics – Smart Structures and Materials*. Springer, 2021. Cited in page 165.

SIVAKUMAR, K.; BALAMURUGAN, C.; RAMABALAN, S. Simultaneous optimal selection of design and manufacturing tolerances with alternative manufacturing process selection. *Computer-Aided Design*, v. 43, p. 207–218, 2011. Cited in page 158.

SKOWRONSKI, V. J. Calculating derivatives in statistical tolerance analysis. *Computer-Aided Design*, v. 30, n. 5, p. 367–375, 1998. Cited in page 186.

SKOWRONSKI, V. J.; TURNER, J. U. Using Monte-Carlo variance reduction in statistical tolerance synthesis. *Computer-Aided Design*, v. 29, n. 1, p. 63–69, 1997. Cited 2 time in page 185 and 186.

SLOCUM, A. H. *Precision Machine Design*. Prentice Hall, Englewood Cliffs, NJ, 1992. Cited 3 time in page 17, 151, and 153.

SMITH, E. S. *Control charts: an introduction to statistical quality control*. Mcgraw Hill Book Company Inc., 1947. Cited in page 175.

SMITHSON, M. *Ignorance and uncertainty emerging paradigms*. Springer-Verlag, 1988. Cited 2 time in page 149 and 150.

SPOTTS, M. F. *Dimensioning and tolerancing for quantity production*. Prentice-Hall, 1983. Cited 2 time in page 42 and 176.

SPRUEGEL, T. C.; WALTER, M.; WARTZACK, S. Robust tolerance design of systems with varying ambient temperature influence due to worldwide manufacturing and operation. In: *International Design Conference - Design 2014 Dubrivnik - Kroatia*. Design 2014, 2014. p. 1189–1198. Cited 2 time in page 47 and 70.

SPUR, G.; DENCKER, B. Heat generation and heat exchange on machine tools (in german. *Werhstattstechnik*, v. 58, p. 260–264, 1968. Cited in page 161.

SRIVASTAVA, A. K.; VELDHUIS, S. C.; ELBESTAWIT, M. A. Modelling geometric and thermal errors in a five-axis cnc machine tool. *Int. J. Mach. Tools Manufact.*, v. 35-9, p. 1321–1337, 1995. Cited in page 162.

STEVENSON, A. *Oxford dictionary of english - 3rd. edition*. Oxford University Press, 2010. Cited in page 153.

SUH, C. S.; LIU, M.-K. *Control of cutting vibration and machining instability : a time-frequency approach for precision, micro and nano machining*. John Wiley & Sons, Ltd., 2013. Cited in page 163.

TAGUCHI, G.; CHOWDHURY, S.; WU, Y. *Taguchi's Quality Engineering Handbook*. New Jersey, USA: John Wiley & Sons, Inc., 2005. Cited in page 178.

TARNG, Y. S.; KAO, J. Y.; LEE, E. C. Chatter suppression in turning operations with a tuned vibration absorber. *Journal of Materials Processing Technology*, v. 105, p. 55–60, 2000. Cited in page 164.

TAYLOR, J. R. *An introduction to error analysis*. University Science Books, 1997. Cited 2 time in page 149 and 153.

TEBBY, S.; BARARI, A.; ESMAILZADEH, E. Analysis and optimization of the automotive structure's bending stiffness using bean elements. In: *Proceedings of the ASME 2012 International Design Engineering Technical Conferences & Computers and Information in Engineering Conference*. ASME, 2012. p. 1–8. Cited in page 48.

TEISSANDIER, D.; COUéTARD, Y.; GéRARD, A. A computer aided tolerancing model:proportioned assembly clearance volume. *Computer-Aided Design*, v. 31, p. 805–817, 1999. Cited 3 time in page 13, 50, and 51.

THOMPSON J, R.; KORONACKI, J. *Statistical process control: the Deming paradigm and beyond*. Chapman & Hall/CRC, 2002. Cited in page 176.

THOMSON, W. *Popular Lecturers and Addresses - Vol. 1 – Constitution of Matter – 2nd. Edition – page 101*. Macmillan and Co. – London (Digitized by Google), 1891. Cited in page 151.

THOMSON, W. *Treatyse on Natural Phylosophy - Part 1*. Cambridge University Press – London (Digitized by Google), 1912. Cited in page 182.

TIAN, Y.; SHU, Q.; LIU, Z.; JI, Y. Vibration characteristics of heavy-duty cnc machine tool-foundation systems. *Shock and Vibration*, v. 2018, p. 1–12, 2018. Cited in page 163.

TING, L.; ZUOWEI, Z.; YANLONG, C.; ANWER, N.; Y., Y. Consideration of working conditions in assembly tolerance analysis. In: *15th CIRP Conference on Computer Aided Tolerancing – CIRP CAT 2018*. Procedia CIRP, 2018. p. 226–231. Cited in page 53.

TJAHJONO, B.; BALL, P. Six sigma: a literature review. *International Journal of Lean Six Sigma*, v. 1-3, p. 216–233, 2010. Cited in page 45.

TOULOUKIAN, V. S.; KIRBY, R. K.; TAYLOR, R. E.; DESAI, P. D. *Thermal expansion - metallic elements and alloys*. Springer Science + Business Media New York, 1975. Cited 2 time in page 45 and 112.

TOULOUKIAN, V. S.; KIRBY, R. K.; TAYLOR, R. E.; LEE, T. Y. R. *Thermal expansion - non metallic solids*. Springer Science + Business Media New York, 1977. Cited in page 45.

UMARAS, E.; BARARI, A.; TSUZUKI, M. S. G. Intelligent design tolerance allocation for optimum adaptability to manufacturing using a monte carlo approach. *IFAC-PapersOnLine*, v. 52-10, p. 165–170, 2019. Cited in page 174.

UMARAS, E.; BARARI, A.; TSUZUKI, M. S. G. Tolerance analysis based on monte carlo simulation: a case of an automotive water pump design optimization. *Journal of Intelligent Manufacturing*, On line, p. 1–15, Nov. 2020. Cited 2 time in page 92 and 174.

UMARAS, E.; TSUZUKI, M. S. G. Research on the factors of influence in the dimensional and form precision of stamping processes. In: *ABCM Symposium Series in Mechatronics - Vol. 5*. ABCM, 2012. p. 694–703. Cited in page 159.

UMARAS, E.; TSUZUKI, M. S. G. Additive manufacturing - considerations on geometric accuracy and factors of influence. *IFAC-PapersOnLine*, v. 50-1, p. 14940–14945, 2017. Cited in page 159.

VANNONI, M.; MOLESINI, G. Joint interferometric measurement of planarity and parallelism. *Optical Engineering*, v. 43-5, p. 1215–1220, May 2004. Cited in page 156.

VENKATESH, V. C.; IZMAN, S. *Precision Engineering*. Tata McGraw-Hill Publishing Company Limited, 2007. Cited 3 time in page 17, 151, and 157.

VIGNAT, F.; VILLENEUVE, F.; NEJAD, M. K. Analysis of the deviations of a casting and machining process using a model of manufactured parts. *CIRP Journal of Manufacturing Science and Technology*, v. 2, p. 198–207, 2010. Cited in page 61.

VILLENEUVE, F.; LEGOFF, O.; LANDON, Y. Tolerancing for manufacturing: a three-dimensional model. *International Journal of Production Research*, v. 39-8, p. 1625–1648, 2001. Cited in page 60.

WADA, R. Ultra-precision machine and elements therefor. In: *Proceedings of the 1st International Machine Tool Engineers' Conference (IMEC)*. Japan Machine Tool Builders' Association (JMTBA), 1984. p. 36–60. Cited in page 160.

WAGNER, G. P.; ALTENBERG, L. Perspective: complex adaptations and the evolution evolvability. *Iternational Journal of Organic Evolution*, v. 50-3, p. 967–976, Jun. 1996. Cited in page 152.

WANG, J. J.; SO, H. The effects of thermal deformation on flatness in precision grinding. *Journal of Thermal Stresses*, v. 34, p. 394–409, 2011. Cited in page 162.

WANG, Y.; LI, L.; HARTMAN, N. W.; SUTHERLAND, J. W. Allocation of assembly tolerances to minimize costs. *CIRP Annals - Manufacturing Technology*, p. 1–4, 2019. Cited in page 20.

WARNOCK, T. Random number generators. *Los Alamos Science*, p. 137–141, Special issue 1987. Cited in page 183.

WEISSKOPF, V. F.; BERNSTEIN, H. Search for simplicity - thermal expansion. *American Journal of Physics*, v. 53, p. 1140–1141, 1985. Cited in page 46.

WHEELER, D.; CHAMBERS, D. *Understanding Statistical Process Control*. SPC Press, 1992. Cited in page 176.

WHITNEY, D. E. The role of key characteristics in the design of mechanical assemblies. *Assembly Automation*, v. 26-4, p. 315–322, 2006. Cited in page 20.

WILKS, S. S. Determination of sample sizes for setting tolerance limits. In: *The Annals of Mathematical Statistics*. Institute of Mathematical Statistics, 1941. p. 91–96. Cited in page 176.

WILLYARD, C. H.; MCCLEES, C. W. Motorola's technology roadmap process. *Research Management*, v. 30-5, p. 13–19, 1987. Cited in page 45.

WIRTZ, A. Vektorielle tolerierung zur qualitatssteuerung in der mechanischen fertigung. *Annals of the CIRP Vol. 37/1/1988*, v. 37, p. 493–498, 1988. Cited in page 59.

WITHERS, P. J. Residual stress and its role in failure. *Reports on Progress in Physics*, v. 70, p. 2211–2264, 2007. Cited in page 166.

XIE, K.; WELLS, L.; CAMELIO, J. A.; YOUN, B. D. Variation propagation analysis on compliant assemblies considering contact interaction. *Transactions of the ASME*, v. 129, p. 934–942, Oct. 2007. Cited in page 48.

YAN, H.; CAO, Y.; YANG, J. Statistical tolerance analysis based on good point set and homogeneous transform matrix. *Procedia CIRP*, v. 43, p. 178–183, 2016. Cited 2 time in page 69 and 71.

YANG, Y.-l.; CAO, Z.-y.; LIAN, Z.-s.; YU, H.-x. Thermal fatigue behavior and cracking characteristics of high si-mo nodular cast iron for exhaust manifolds. *Journal of Iron and Steel Research, International*, v. 20-6, p. 52–57, 2013. Cited 3 time in page 16, 114, and 115.

YANG, Z.; SUN, M.; LI, W.; LIANG, W. Modified elman network for thermal deformation compensation modeling in machine tools. *International Journal of Advanced Manufacturing Technology*, v. 54, p. 669–676, 2011. Cited in page 165.

ZALEWSKI, D. J. *Methods of monitoring statistical process control in the presence of autocorrelation*. Doutorado — USAF, 1995. Cited in page 176.

ZENG, W.; RAO, Y.; WANG, P.; YI, W. A solution of worst-case tolerance analysis for partial parallel chainsbased on the unified jacobian-torsor model. *Precision Engineering*, v. 47, p. 276–291, 2017. Cited in page 55.

ZHANG, Z.; ZHANG, Z.; JIN, X.; ZHANG, Q. A novel modelling method of geometric errors for precision assembly. *International Journal of Advanced Manufacturing Technology*, v. 94, p. 1139—1160, 2018. Cited 4 time in page 13, 20, 58, and 59.

ZHAO, J.; SANG, Y.; DUAN, F.; JI, X.; LINA, Z. High-precision surface parallelism measurement sing digital image correlation method. *Optical Engineering*, v. 58-9, p. 1–9, Sept. 2019. Cited 2 time in page 154 and 155.

ZHAO, Z.; BEZDECNY, M.; LEE, B.; WU, Y.; ROBINSON, D.; BAUER, L.; SLAGLE, M.; COLEMAN, D.; BARNES, J.; WALLS, S. Prediction of assembly variation during early design. *Journal of Computing and Information Science in Engineering*, v. 9, p. 1–11, Sep. 2009. Cited in page 152.

ZIEHER, F.; LANGMAYR F. JELATANCEV, A.; WIESER, K. Thermal mechanical fatigue simulation of cast iron cylinder heads. *SAE Technical Papers*, v. 2005-01-0796, p. 1–13, Apr. 2005. Cited 3 time in page 16, 112, and 113.

ZUO, X.-Y.; LI, B.; YANG, J.; JIANG, X. Application of the jacobian–torsor theory into error propagation analysis for machining processes. *International Journal of Advanced Manufacturing Technology*, v. 69, p. 1557—1568, 2013. Cited in page 55.

A DT concepts

The flow chart presented in Figure 97 is an overview of concepts related to DT. However, as can be seen, the approach of all of them would be impracticable in any single work. In this Appendix some of the items are approached, the ones that are not essential, but that can support the understanding of the concepts in the main text of this thesis. The gray-marked elements of the flow chart are beyond the scope of the text. The content of each item is described following the logical sequence indicated in the flowchart, but some of them are applicable to more than one path and, so, are described just once. As can be observed, there are up-to-date and some very old references: the reason for this is that the straight link to each basic theoretical concept involved has been pursued, since the further works are developments of the original ideas. The historical development of each item was considered important because, without this, the explanation could be troublesome for some readers not directly involved with the theme.

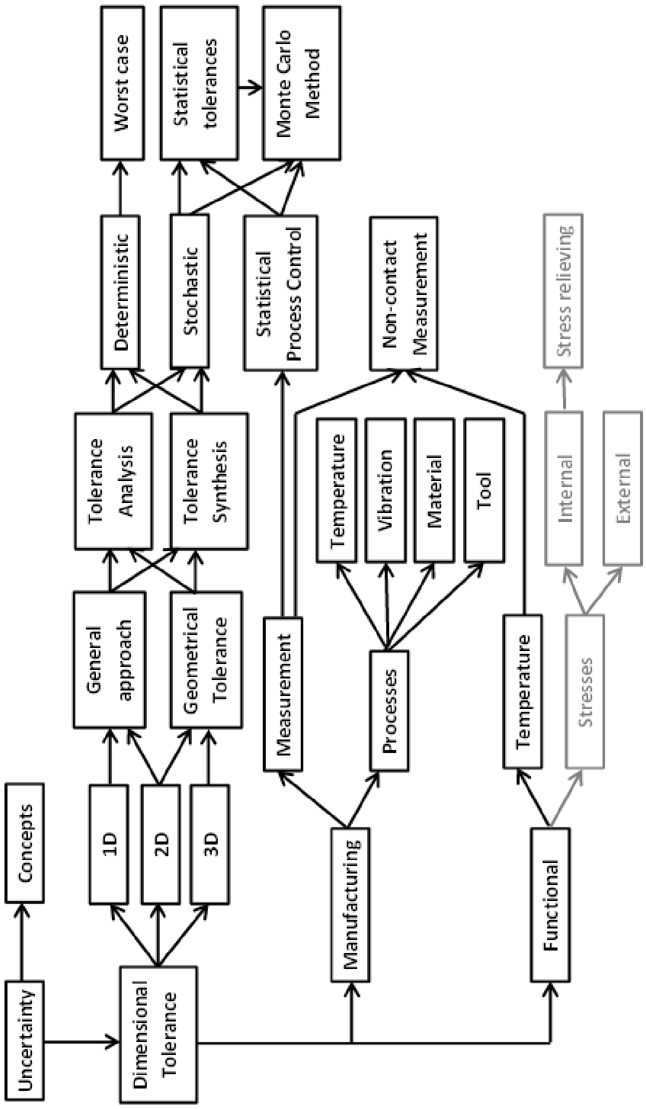

Figure 97 – Flowchart showing the sequence of items presentation. (Source: the author).

The concept of DT has its origin on the concept of uncertainty, and so, this is the first flowchart element.

A.1 The Uncertainty Concept

A direct definition of uncertainty is better found in Oxford [1998]: "The quality or state of not being certainly known, questionable and not determined". The word uncertainty has different meanings in the literature, such as error [TAYLOR, 1997]. Other authors link uncertainty in a taxonomy of ignorance as a result of incompleteness [SMITHSON, 1988] or use its concept as the opposite of predictability in risk assessment and sensitivity analysis. Krause and Clark [1993] view uncertainty either as a "frequentistic measure of randomness or in terms of a subjective measure of confidence that satisfies well-circuited propositions". The word "uncertainty" also means doubt [METROLOGY, 2008, p. 2]. Klir [2006] states: "Uncertainty is viewed as a manifestation of some information deficiency, while information is viewed as the ability to reduce uncertainty". Smithson [1988, p. 1] declares that "uncertainty is generally treated as some form of incompleteness in information or knowledge".

A more pragmatic approach to the concept of uncertainty shows that studies of its influence in each parameter of a system can lead to a decision on which is more significant or which can be ignored, depending on its degree of magnitude. Bury [1999, p. 5] presents a clear discussion of uncertainty. He defines at least four types of uncertainties with respect to their sources. A brief description is included:

1. Data uncertainty: an inherent variability is featured in each measured quantity. The measured value is caused or influenced by many chance factors whose effects aggregate to produce a measured value, and variability among measured values is an inherent reality, irrespective of the care taken in their acquisition;

2. Statistical uncertainty: limited information implies uncertainty about the true nature of the quantity, due to the limited amount of information that is typically available on a measurable quantity (sample) caused by time and cost constraints;

3. Event uncertainty: effects of unfavorable events that may rarely occur, leading to little information available on their likely occurrence;

4. Model uncertainty: the model's description of a real problem is often an idealization and represents a restricted version of reality. Important features of the physical phenomenon can be ignored.

A.1.1 The Concepts of Accuracy, Precision, Resolution and Smoothness

The referenced terms are used in metrology, and the correct interpretation of their meanings is important to prevent misunderstandings:

1. **Accuracy and Precision**: According to Black and Kohser [2008, p. 219]:

   - Accuracy refers to the ability to hit what is aimed at, a target;
   - Precision refers to the repeatability of a process.

   A simple illustration in Figure 98, originally from Black and Kohser [2008, p. 219] and referenced by other authors can better explain the difference between accuracy and precision:

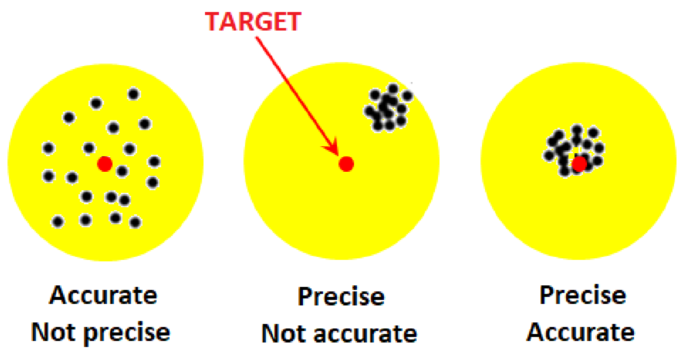

Figure 98 – The difference between accuracy and precision. (Source: based on [KUZNETSOV, 2017, p. 172], [VENKATESH; IZMAN, 2007, p. 4], [SLOCUM, 1992, p. 61]).

2. **Resolution**: According to Dornfeld and Lee [2008, p. 54]: Resolution can be defined as "the finest resolvable increment of measurement or motion". For example, it is not possible to take a measurement of 1 μm if the instrument used has a resolution lower than this value, for example 2 μm. Additionally, the accuracy and repeatability of this instrument must also be evaluated for reliable measurement.

3. **Smoothness**: Nakasawa [1994, p. 6] defines: Smoothness refers to an object's size regardless of accuracy or precision. It is used to describe microscopic dimensions. The magnitude of the smoothness dimension is much lower than with regard to accuracy and precision. The same author suggests the term precision as a combination of the above definitions of accuracy and precision (and smoothness in some cases), that is, in some fields such as in the design of precision machines, the combined term may be used, provided that the separate meanings are correctly understood.

The cited features are also important factors in machine design and process design. Regarding the study of DT, the accuracy and precision are important for defining the shape of the probability distributions (mean and variance), as described in the main text.

A.1.2 Measurement Uncertainty

The first statement about the importance of the measurement uncertainty was perhaps made by Lord Kelvin (Thomson [1891, p. 101]), regarding the general concept of measurement: *"In physical science a first essential step in the direction of learning any subject is to find principles of numerical reckoning and practicable methods for measuring some quality connected with it. I often say that when you can measure what you are talking about and express it in numbers, you know something about it; but when you cannot measure it, when you cannot express it in numbers, your knowledge is of a meager and unsatisfactory kind...".*

Hocken and Pereira [2012, p. 185] also state: *"The uncertainty of a measurement includes all factors that influence the result of the measurement"* and *"an uncertainty statement expresses one's ignorance about the true value of a measurement"*.

Fridman [2012, p. 6] authored reference work on measurement. According to him, "Measurement is the act of comparing a physical quantity with the unit or scale of that quantity using specialized equipment".

A good definition that references measurements has been given by Shapiro and Gross [1981, p. 6]: "A measuring device is said to be unbiased if the average measurement is zero".

Figliola and Beasley [2011] address the theoretical and practical concepts of measurement in engineering.

A.2 The Variation Concept

The variation is caused by, but not limited to:

- Machine accuracy;
- Type of process;
- Process variables, such as temperature;
- Tool wear;
- Operator's behavior.

Before discussing variation, it is necessary to make some important distinctions among different words which involve similar but different concepts. It can be seen that the terms *variation* and *variability* are often used synonymously in the literature. As the two terms are derived from the same root, few references are found displaying their appropriate meaning. A deeper investigation was conducted for this clarification and the best and most accurate definition of the two terms was found in the work of Wagner and Altenberg [1996, p. 969]:

- **variation** referring to the actual differences between individuals in a population or a sample, variation can be observed directly as a property of a collection of items;
- **variability** is a term that describes the potential or propensity to vary.

A good illustration of the two terms is found in Zhao et al. [2009, p. 1]: "unavoidable and unexpected variations introduced during the manufacture and assembly of parts are one of the main causes of product variability leading to failure to meet requirements".

Another definition of variation is “a change or slight difference in condition, quantity or level, typically within certain limits” [STEVENSON, 2010].

$$V = \frac{\sigma}{\mu} \quad [\%] \tag{A.1}$$

Here, $\sigma =$ is the standard deviation and $\mu =$ the mean.

The concept of **error** can be found in the literature with different meanings. According to McGraw-Hill [2003] on science and technology, *error* is defined as “Any discrepancy between a calculated, observed, or measured quantity and the true, specified, or theoretically correct value of that quantity”. Taylor [1997, p. 3] states that the terms error and uncertainty can be used interchangeably.

We prefer McGraw-Hill’s single meaning. In this sense and in this text, the term error is used to compare a measured quantity with its nominal (or specified) value.

Slocum [SLOCUM, 1992, p. 74] identifies three common types of error:

1. Random - which, under apparently equal conditions at a given position, does not always have the same value and can only be expressed statistically;

2. Systematic - which always have the same value and sign at a given position and under given circumstances. Wherever systematic errors have been established, they may be used for correcting the value measured;

3. Hysteresis - is a systematic error (which in this instance is separated out for convenience). It is usually highly reproducible, has a sign depending on the direction of approach, and a value partly dependent on the travel;

This classification is important in the monitoring of statistical process control (SPC), as referenced in the following.

In this text, the concept of dimensional variation is mainly considered for the purpose of the work.

A.2.1 The Measurement of Variation

The evaluation of the variation of a physical quantity is carried out by means of a measurement process. A good overview of this process is presented by Beckwith T. et al. [2011], which consists of a quantitative comparison of a measurand with a standardized value, for example, the meter, defined as a standard of length. The process is represented in Figure 99. The word *measurand* is used to designate the particular physical parameter that is observed and quantified. The standard of comparison must be of the same character as the measurand and are generally defined by a legal or recognized institute, for example: The

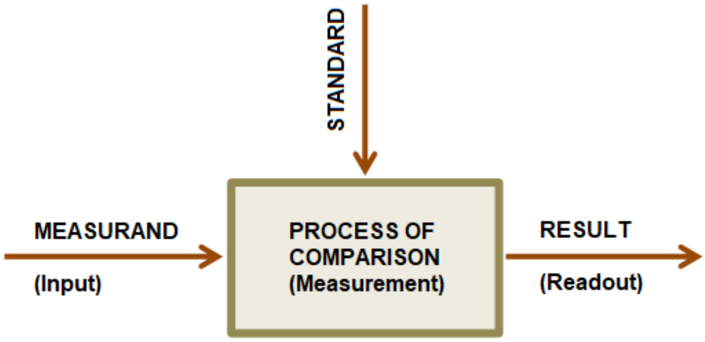

Figure 99 – The measuring process - based on [BECKWITH T. et al., 2011, p. 3]

National Institute of Standards and Technology (NIST), the International Organization for Standardization (ISO), and the American National Standards Institute (ANSI).

Rabinovich [2005] developed a comprehensive description of the measurement of physical quantities, their errors and uncertainties.

Regarding the dimensional measurements, some work is worth noting. Curtis and Farago [2014], in their Handbook of Dimensional Measurement, developed a comprehensive overview of measurement instruments and equipment. Colosimo and Senin [2011] addressed the evaluation of geometric tolerances; concepts of geometric features and their measurements are developed in the book. As already cited, any measurement procedure involves its inherent uncertainty, which must be taken into account in its result analysis. In this work, the measurement processes involving geometric variations are mainly addressed due to their scope. Two types of measurement system are considered: contact and non-contact. Destructive systems, applicable to the analysis of internal features, are not considered.

A.2.1.1 Contact measurements

As its name explains, contact measurements are performed by means of the contact between a surface or a tip of a measuring device and the measurand. The measured value is taken from a specified reference. Several instruments are used to acquire dimension values.

Contact measurements can be used to inspect geometrical variations. The currently used methods are [ZHAO et al., 2019]:

- The type of trigger probe, based on the dial indicator device, is usually used to measure the range of 0.25 to 300 mm with a scale of 0.001 to 0.01 mm;
- The CMM measurement, which can incorporate the type of trigger probe. This configuration can reach a measurement resolution of up to 0.4 μ m.

An issue in measuring the geometrical deviations of a part is that **the tolerances of position, orientation, and form are interrelated** [ASME. . . , 2009]. Therefore, the measuring method must distinguish these tolerances in relation to the part datum prior to inspection. In CMM measurements, this is done using specific software integrated into the machine system. Several works have dealt with this subject.

Zhao et al. [2019] proposed an alternative low-cost trigger probe-based method to measure surface parallelism at the submicron level, consisting of the use of a mechanical contact probe, as well as a combination of digital image correlation (DIC) techniques and a USB digital microscope.

The CMMs and their systems were comprehensively described by Hocken and Pereira [2012] in a specific work.

A.2.1.2 Non-contact measurements

Noncontact measurement applications have been increasing in use in recent years, although they have already been mentioned in the past decades. A good reference on nondestructive evaluation is provided by the ASM Handbook Vol. 17 [ASM, 1992]. With respect to our scope, two measuring methods can be cited:

- The laser triangulation and
- the laser interferometer

According to the reference cited (p. 29): "Laser triangulation sensors provide a quick measurement of deviations due to changes in the surface. With two sensors, the method can be used to measure the thickness of the part or the diameter inside the bores. However, it may not be possible to probe the entire length of the hole. Laser triangulation sensors can also be used as a replacement for through-trigger probes on coordinate measuring machines. In this application, the sensor determines surface characteristics and surface locations using an edge-finding device". The system is illustrated in Figure 100. As light strikes the surface (points $A1, B1$), the lens images the point of illumination using a photosensor or CMOS. Variations in the surface cause the image dot to move laterally along the photosensor (points $A2, B2$).

The application of the laser interferometer was better mentioned by Konkel et al. [1991], in a parallelism measurement. They describe the basic operating principle of an interferometer as illustrated in Figure 101: *An interferometer is a beam splitter that allows a portion of the laser light to continue unimpeded while the remainder is reflected at a right angle. The two beams are then passed through retroreflectors and focused on a photodetector. One of the beams is used as a reference and is reflected from a retroreflector, whose position is fixed relative to the interferometer. As the remote retro-reflector is moved, the phase relationship between the reference beam and the measurement beam will change. When the peaks of the two waves coincide, the resulting amplitude will be twice that of a single wave. When the waves are* 180 *degrees out of phase, the resulting amplitude will be zero. A one-fourth-wavelength movement of the moveable retroreflector*

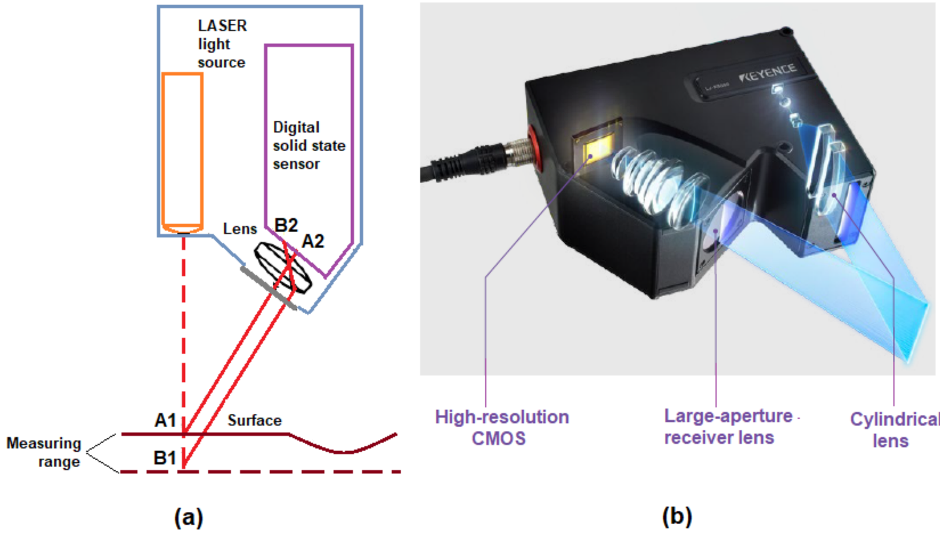

Figure 100 – (a)Schematic of laser triangulation method of measurement. Based on [ASM, 1992, p. 29]; (b) A laser profiler [KEYENCE, 2019b].

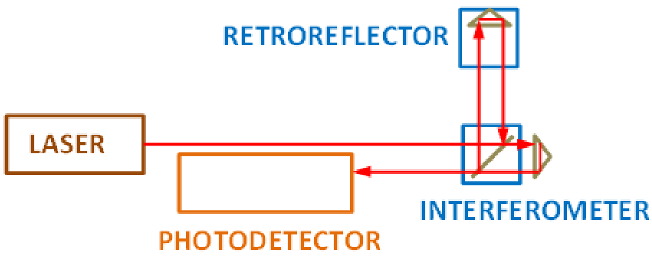

Figure 101 – The interferometer functioning principle [KONKEL et al., 1991].

will result in a half-wavelength movement, as seen by the photodetector. Phase changes seen by the photodetector are counted and an appropriate multiplier is used to display the change in relative distance between the two retroreflectors in engineering units [mm]. The resulting resolution obtainable with this system is one-quarter of the wavelength of the laser used in the instrument. For example, the wavelength of an NE-HE laser light is about $0.92 \times 10^{-6}mm$, and the specified resolution is one-fourth of a wavelength of $0.23 \times 10^{-6}mm$.

A good explanation of the measurement of geometric features is provided by Keyence [2019a]. Vannoni and Molesini [2004] approached the joint variation of flatness and parallelism by means of an interferometric measurement. According to the authors, typical tolerances of the order of 0.1μ m can be achieved for planarity and 0.3μ m for parallelism.

A.2.2 Manufacturing variation

As previously commented, variation affects both the quality and the functional behavior of a product. In addition, the lower the achievable variation, the higher the manufacturing and inspection costs of a part (as shown in Subsection A.2.2.1). Following this evidence,

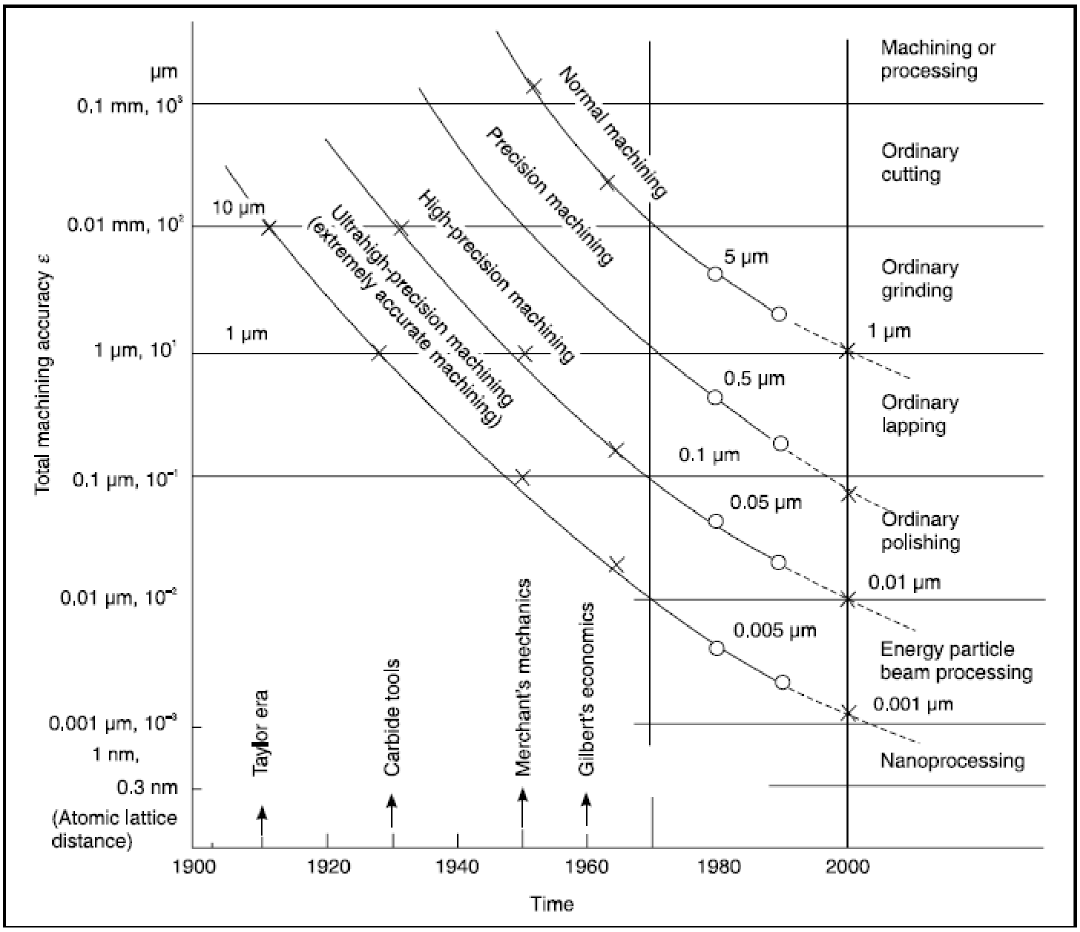

Figure 102 – The machining accuracy evolution in a century [VENKATESH; IZMAN, 2007, p. 7].

forms of improving quality by increasing manufacturing accuracy and simultaneously maintaining or even reducing the cost of a product must be pursued continuously. In this way, the identification and treatment of the causes of manufacturing variation is of fundamental importance.

This Appendix aims to deal with this issue, firstly describing the results of a research on the causes and, in the sequence, addressing the forms in which the control of important product features can be conducted. According to Venkatesh and Izman [2007]: *is seen nowadays that emphasis is on manufacturing high-precision products cheaply and quickly. The history of increasing machining precision also suggests that there is a growing demand to create value-added products.* Figure 102 shows the reduction in the variation in machining in the last century. It is worth noting that the normal machining, used in most of the products, showed a variation reduction of approximately ten times in fifty years!

A.2.2.1 Manufacturing costs

The manufacturing cost of a product is affected by several factors, such as the material, facilities, labor and design specifications of the parts [GREWAL, 2011]. Dimensional

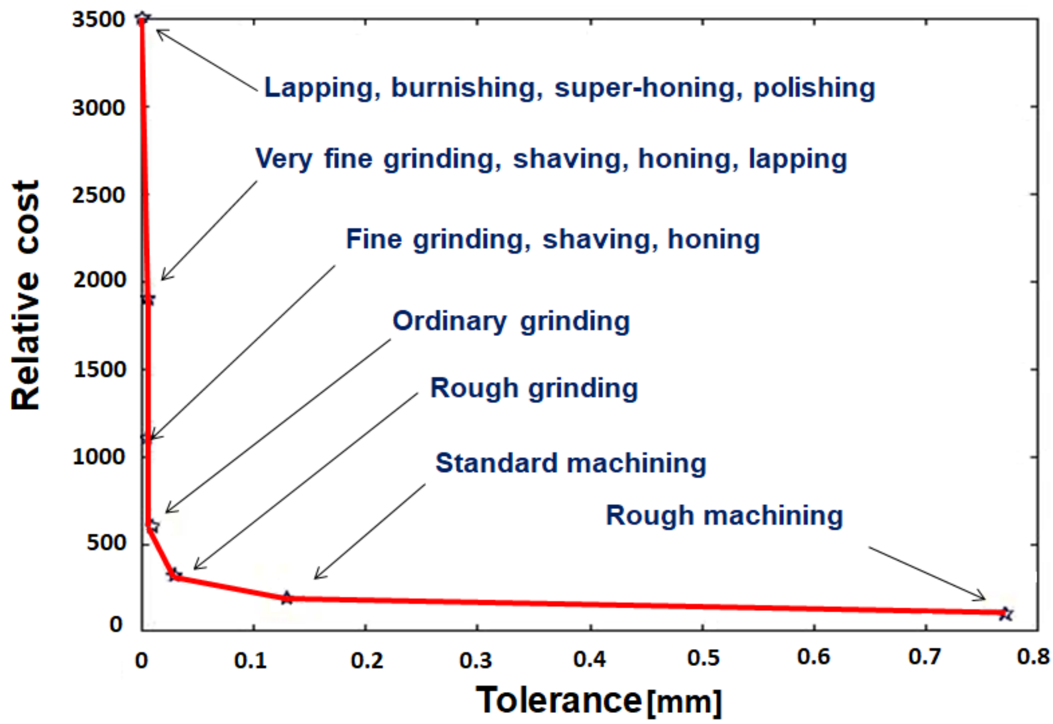

Figure 103 – Relative cost vs. tolerance vs. process type, based on [EL-HOFY, 2014].

tolerances play an important role in this aspect: Manufacturing cost increases with the specified accuracy and/or precision [BLACK; KOHSER, 2008]. There is general agreement that tight tolerances increase production costs [DIMITRELLOU et al., 2007; SIVAKUMAR et al., 2011]. This is especially verified below a certain value, as illustrated in Figure 103. The same behavior occurs with respect to the quality of the machined surfaces, as illustrated in Table A.8.

Table A.8 – Relative Cost (RC) for Machining Tolerances and Surface Finishes

	Tolerance		Roughness	
	$\pm mm$	RC	μm	RC
Rough machining	0.77	100	6.25	100
Standard machining	0.13	190	3.12	200
Fine machining	0.03	320	1.56	440
Ordinary grinding	0.01	600	0.8	720
Fine grinding	0.005	1100	0.4	1400
Very fine grinding	0.003	1900	0.2	2400
Polishing	0.001	3500	0.18	4500

Source: El-Hofy [EL-HOFY, 2014, p.486]

Tolerance-related manufacturing costs depend on the production site and are generally considered proprietary information and therefore not reported. In practice, the cost-tolerance function is usually represented by several linear functions, as in the case of Figure 103, plotted from discrete tabular values.

Some references were selected to show different ways in which the cost of dimensional tolerances can affect the product, including design, manufacturing, and even application. Curran et al. [2003] proposed the consideration of components as a function of the operating costs of the product. As an example, they reported the effect of expanding manufacturing tolerances on the aerodynamic behavior of an aircraft nacelle to reduce costs. Etienne et al. [2009] proposed the evaluation of the tolerance cost based on design and process selection activities, a concept called activity-based tolerance allocation. Chiang et al. [2015] reported the use of the skew normal distribution optimization strategy (SNDOS) as an approach to treating tolerance cost. An example they cited was the reduction in the rate of car seat rework. Generally, normal distributions are taken as symmetric. Armillotta [2020] presented a review of the tolerance cost functions used in tolerance synthesis processes. He highlighted especially the importance of the parameters used in cost functions, which in his opinion can cause result inconsistencies when not properly selected. Hallmann et al. [2020b] proposed a cost optimization with interrelated KCs.

A.2.2.2 Causes of manufacturing variation

Manufacturing (MFG) variation is caused by the characteristics inherent to each specific MFG process.

Due to functional requirements, in the great majority of cases, contact between mechanical components in an assembly is made through finished surfaces obtained by material removal. Material removal is obtained by stamping and different machining processes, the main ones being turning, milling, grinding, and drilling. Processes which present the higher variation are drilling and milling. Other material removal processes are not representative in high-volume production. Structural components are generally manufactured by cutting and forming processes and assembled by welding.

Additive manufacturing (AM) is a relatively recent manufacturing concept in which components of different materials can be produced and assembled in the same process and, because of this, it is beyond the scope of this work. Few works on the subject can be cited:

Barari [2012a] developed an unified methodology capable of analyzing complex surfaces and geometries with a practical approach to predict the actual profile tolerances of AM parts manufactured by AM. The methodology can be used to allocate profile tolerances for the rapid prototyping process and can also be used to select the optimum uniform layer thicknesses that compromise between the number of layers and the desired accuracy of the final surfaces. Umaras and Tsuzuki [2017] studied the factors that influence the geometric precision of AM. Regarding other processes, the same authors reported factors that influence the precision of the dimensions and form of the stamping processes [UMARAS; TSUZUKI, 2012].

The manufacturing variation of the components of an assembly is caused by noise factors. These noise factors induce dimensional errors, which can be reduced in two ways:

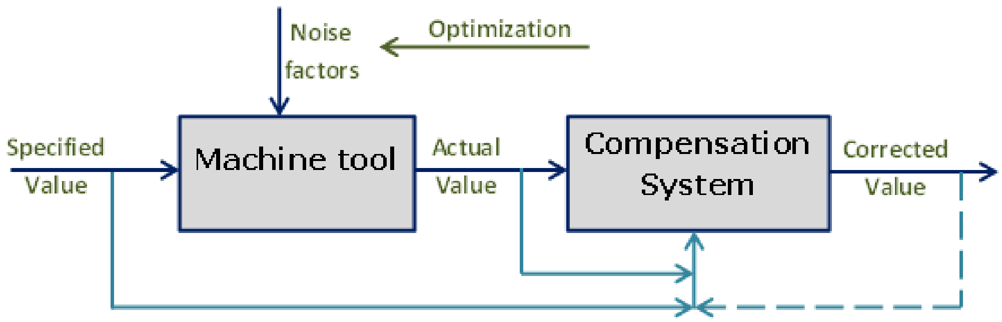

Figure 104 – The procedure for reducing manufacturing errors.

1. Through design improvements in the machine tool to reduce machining errors. This optimization of the machine tool design is a function of the technological development shown in Figure 102;

2. by means of a compensation system, which is activated by comparing the output errors of the process and the specified value. Figure 104 illustrates this procedure to improve accuracy.

Therefore, instead of being only minimized by machine toll design improvements, errors caused by the induced effects by the manufacturing process can be compensated for the achievement of maximum process accuracy. In this way, research in the area is focused on the development of methods to evaluate these errors and create mechanisms for their compensation. Several works are available with these tasks and are commented on in the text.

An excellent approach to the generation of machining errors was given by Wada [1984] apud Dornfeld and Lee [2008], illustrated in Figure 105. It can be seen that the major causes are the machine tool, the workpiece and the tool.

According to Ito [2010, p. 8] "Within a machine tool context, there are two crucial technological issues. One is *thermal deformation* and the other is *chatter*". Therefore, in relation to equipment, the main sources of errors are temperature and vibration.

Temperature

The effects of temperature on the manufacturing of mechanical components play an important role in their dimensional variation. According to Bryan [1990, p. 645], thermal errors account for approximately $40 - 70\%$ of the total error remaining in machine tools. Thermal sources cannot be eliminated because they are consequences of the operation of several systems and are induced by different origins, such as friction, fluid flow losses, and magnetic fields.

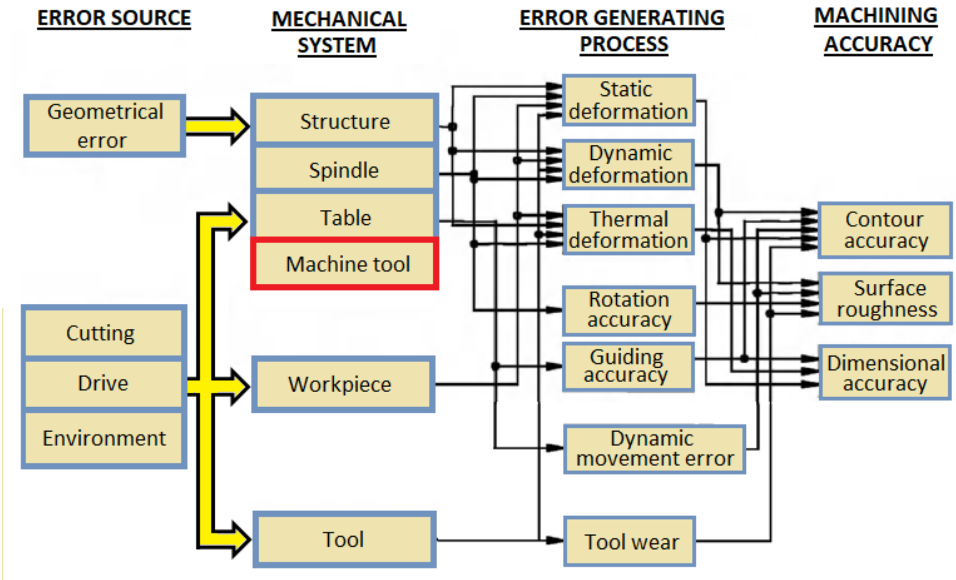

Figure 105 – Machining error generating process. The main components of the machine tool responsible for generating errors are the structure, the spindle and the table (Based on [DORNFELD; LEE, 2008, p. 46].

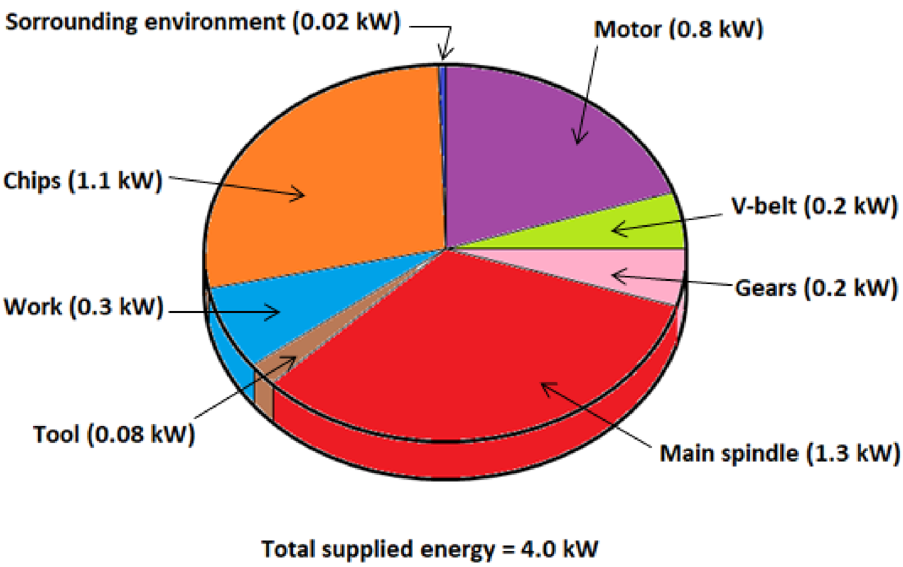

Figure 106 – Energy dissipation proportion during a machining operation of a manual lathe. Based on [NISHIWAKI; HORI, 2010, p. 46].

Spur and Dencker [1968] apud Nishiwaki and Hori [2010] studied the proportion of energy shared between the various components of a conventional manual lathe during a machining operation, as illustrated in Figure 106. As the structures of the machining tools are similar, this figure can serve as a reference for other machining processes.

There are three main ways to deal with thermal errors in manufacturing processes:

1. To ensure that parts are produced within a nearly stabilized temperature, it is suggested:

- waiting for the machine to warm up before initiating the process and
- keeping the machine running during production shifts and breaks, such as lunchtime.

This is common practice in industrial facilities, by the author's experience;

2. To try to reduce the thermal effects on design of machine tools. Ito [2010, p. 8], states that the principle of precision machine tool design to reduce thermal effects is based on a lightweight structural body and materials with a smaller thermal expansion coefficient and separation of heat sources as much as possible. Ramesh et al. [2000b, p. 1258] state: "One of the techniques used to solve the problem of errors caused by temperature variation is to use materials such as cement concrete, fiber-reinforced plastics, etc. in the construction of the machine tool"and, "..although these methods do reduce the deformation of the structure due to changes in temperature, this technique of removing errors by careful design tends to be very expensive".

3. Measure errors in samples of parts produced under a stabilized working condition (machine, setup, environment) and compensate for the errors in relation to the specified values. This procedure consists in measuring the temperatures of critical points on the machine and the respective errors induced in the machine as well. Analyzes of the readings allow the construction of a predictive model that can map the error data. Therefore, this model is capable of predicting machine tool error for any specific temperature condition, and based on predicted data, the necessary compensation values are calculated and incorporated into the respective axes to effect compensation [RAMESH et al., 2000b]. Other forms of compensation are described below.

Srivastava et al. [1995] developed a systematic approach to the development of geometrical and thermal errors based on the kinematic analysis of the machine structure for a five-axis CNC machine, in which additional sources of error are introduced by the added degrees of freedom in relation to conventional three-axis machines. The authors cited the interaction of all axes that complicates the relationship between the sources of error and the final error at the tool tip.

Wang and So [2011] presented an interesting theoretical model for estimating the transient temperature distributions and the corresponding thermal deflections of a workpiece in a precision grinding process. FEM is applied to compute the thermally induced deformation of the workpiece over time, predicting the transient convex expansion and subsequent overcut of a ground surface.

Ramesh et al. [2003] conducted an experimental investigation on a three-axis vertical machining center equipped with a PC-based open architecture controller. They concluded that thermal errors are affected by the temperature of the drive motor and also by the ball screws on the axes. The temperature of these components increased with load (part mass) and speed: a change in 300 kg of load and a half-time reduction in speed affected the error in $+24\mu$m and -15μm.

Vibration

The vibration measurement of machine nonrotating parts is covered by a collection of ISO standards. General guidelines are provided by ISO 10816-1 [MECHANICAL..., 1995]. Listewnik et al. [2015] performed a diagnostic application for the evaluation of machine vibration according to this standard.

Suh and Liu [2013] provided a comprehensive work on the analysis of cutting vibration and machine instability as input to its control.

Tian et al. [2018] studied the influence of CNC machine tool foundation systems on their vibration behavior.

Part material

Liang et al. [1994] analyzed the structure of a material with respect to the degree of magnitude of the cutting depth. They considered the effects of crystal orientation and grain boundaries on the microcutting process using FEA. They also reported that the concept of material homogeneity depends on the relation between the crystallographic characteristics and the cutting depth; that is, the same material may be considered homogeneous or not depending on the type of machining process. In another paper, the same authors [MORONUKI et al., 1994] conducted experiments and concluded that, in microcutting processes, the formation of the chips depends on the anisotropy of the material and the surface integrity depends on the crystal orientation.

Kundrak et al. [2008] compared the machining accuracy of hard materials between the turning and grinding processes. The results of this study were considered important due to the significant cost difference of these processes.

Tool and fixture

The tool and its holder are responsible for generating machining errors. The main factors are tool wear, tool holder displacement, deformation, and/or instability. The following articles report research in this area.

Barari et al. [2009] proposed a NURBS representation of estimated surfaces resulting from machining errors. This surface representation explicitly expresses the geometry and topology of the final product and increases the clarity in the mathematical representation of quasi-static machining errors. According to the authors, the proposed model can be utilized in virtual machining and simulation of the real process, modification of the design within a design for the manufacturing platform, and also in online error compensation during the machining process.

Darwish [1995] studied the impact of the assembly technique on the dimensional accuracy and geometric tolerances of the machined workpieces. Different techniques used for the assembly of metal cutting tool insert holders were considered, such as mechanical clamping, brazing, and adhesive bonding, which are common techniques for the assembly of metal cutting tool insert holders. Tests carried out on mild steel specimens cutting using different insert-holder assembly techniques revealed that the bonded assembly ranked ahead in preserving dimensional accuracy and geometrical tolerances compared to mechanically clamped and brazed assemblies.

Andolfatto et al. [2011] presented a method to evaluate the effect of high speed and high dynamic load on volumetric errors in the center of the tool. According to the authors, the method proposition was to decompose the geometric errors into two categories: the quasi-static geometric errors independent from the speed of the trajectory and the dynamic geometric errors, dependent on the programmed feed rate and resulting from the machine structure deflection during the acceleration of its axes.

Li et al. [2016] proposed an error modeling method based on a multibody system used to construct an error mapping among the error sources and the position error of the cutting tool for a five-axis machine tool. An error sensitivity was performed and the results were used to perform a precision design of the angular error components through numerical simulation.

In turning operations, chatter is a dynamic instability of the cutting process that can affect the accuracy of the surface of the machined part and damage the cutting tool. Tarng et al. [2000] developed a piezoelectric inertia actuator mounted on the cutting tool. This device acted as a tuned vibration absorber to suppress chatter in turning operations, improving cutting stability.

Choudhury and Srinivas [2004] developed a method to predict flank wear precisely in a turning process using a mathematical model. It was compared with the experimental results to prove its effectiveness. Factors that influence flank wear, such as diffusion index, wear coefficient, rate of increase in normal load with respect to flank wear, and tool hardness, were used as input parameters for the mathematical model.

Li et al. [1999] developed a method to generate wear maps that represent the wear rates of tools in a two-dimensional space defined by the machining conditions in metal cutting. The predicted rates of tool wear are then used to generate wear maps, which can be used in the development of an integrated predictive system for tool wear in metal cutting. This predictive system can be used to estimate the dimensional variation with machining time.

ElHakim et al. [2011] studied the wear resistance performance of mixed and coated cutting tools. They found that the high chemical and thermal stability of Al_2O_3 tribofilms protects the tool substrate because it prevents heat generated at the tool/chip interface from entering the tool core.

Compensation

As mentioned above, when the causes of MFG errors are identified and quantified, a compensation system can be developed to improve accuracy. Some works have been selected to illustrate this possibility.

According to Fleischer et al. [2012], *The geometrical accuracy of the manufactured work pieces thus depends on the accuracy of all the feed axes of a machine tool.* They proposed an adaptronical compensation of geometrical machine errors. *Adaptronics* is an artificial word composed of *adaptive* and *electronics*. According to a VDI working group, the term describes a system in which at least one element of a control loop is multifunctional, on the one hand, and, on the other, the process of generating intelligent structures on the basis of multifunctional elements (Neumann apud Sinapius [SINAPIUS, 2021]). This definition distinguishes adaptronics fundamentally from *mechatronic* systems in which the multifunctionality of a system element is not assumed ([p. 2][SINAPIUS, 2021]).

Ramesh, Mannan, and Poo made a comprehensive review of the causes and compensation of machine tools in two articles. In the first [RAMESH et al., 2000a], geometric errors were considered, induced by cutting force and dependent on fixture. In the second [RAMESH et al., 2000b], the influence of thermal errors was discussed.

Donmez et al. [1986] reported an experimental improvement in accuracy (up to 20 times) when their error correction methodology was applied. This methodology considered a flexible, modular, and structured software system that compensates for predicted errors in real time.

Yang et al. [2011] proposed a modified *Elman network* (EN) to improve the thermal error compensation model in machine tools. The improved EN can be regarded as a feedforward neural network with feedback from the hidden layer and the output layer as an additional set of inputs. Its structure determines the dynamic characteristic of the system with the memory function. As the machine tool spindle contributes the largest part of thermal errors, the authors established a precise finite element model of this component in the study.

Material Internal Stresses Remaining from Manufacturing Processes

The internal stresses of the material remaining from manufacturing processes may also have a favorable or unfavorable effect on the mechanical loading and deformation of the material and can affect the specified dimensions of the component. External stresses can be effectively calculated as a function of static or dynamic component loading. However, internal stresses are not easily determined. Contrary to other material defects, such as voids and porosity, their measurement and prediction are generally not easily determined. Their prediction a priori is difficult because they are the result of almost every stage of manufacturing processing (residual stresses) and subsequently evolve during their life in service. Their measurement is hampered by the fact that they do not leave outward sign [WITHERS, 2007, p. 2213]. Residual stresses (eigenstrains) are the stresses that are retained within a body when no external forces are acting. Residual stresses arise because of misfits (incompatibilities) between different regions of the material component or assembly. Withers [2007] gives an example: "perhaps the simplest residual stress field is due to an oversized sphere placed inside a spherical cavity in a large homogeneous body of the same material". This might occur by cooling a body containing a sphere that has a smaller coefficient of thermal expansion, but the same elastic constants. For the sole elastic accommodation, the included sphere experiences uniform residual compression and the stress in the matrix decreases with the distance, r, from the center of the sphere according to $\frac{1}{r^3}$."

As failures due to material overstressing are not the objective of this work but only the effects of material deformation, the causes of residual stresses will be briefly considered. The possible process of eliminating detrimental internal stresses can be made by thermal treatment by heating the stressed parts at a determined temperature and cooling at a slow rate.

Origin of residual stresses

As mentioned above, residual stresses can have favorable or unfavorable effects on material behavior. Those that originate from manufacturing processes generally have a detrimental effect and must be removed or attenuated. However, in some cases, residual stresses have a beneficial effect and are promoted to modify the properties of the local material. Residual stresses can arise from various transformations of material processes [WITHERS, 2007, p. 2227], [GRZESIK, 2017]. From these references, three main items can be summarized:

1. Plastic deformation
2. Thermal phase transformation
3. Thermal/plastic deformation

Plastic deformation

A simpler way to introduce the concept of residual stress is to consider the bending of a flat body, such as a bar or plate. Figure 107 illustrates the example, which is the following sequence:

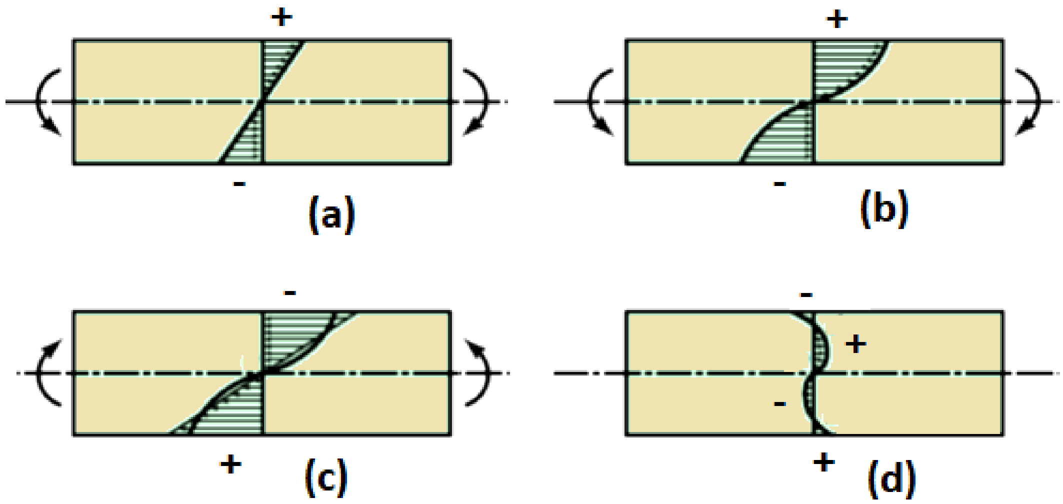

Figure 107 – The bending and unbending process of a bar. (Source: based on [KALPAKJIAN; SCHMID, 2010, p. 81]).

a) A moment is applied in one direction, elastic region;

b) The moment application continues beyond the elastic limit, the plastic region. The bar is then permanently deformed with the stress distribution;

c) A moment is further applied in the reverse direction - elastic region;

d) The moment continues in the reverse direction beyond the elastic limit, the plastic region.

The bar is permanently deformed in the opposite direction in an attempt to reach the original shape. The remaining residual stresses distribution is shown.

Groover [2013, p. 60] presents a clear explanation on the stress-strain behavior of materials used in industrial processes in the plastic region.

$$\sigma = K\epsilon^n \tag{A.2}$$

where σ = true stress, [MPa]; ϵ = true strain; K = strength coefficient, [MPa]; and n = strain hardening exponent.

The values of K and n are given in the tables for different materials [GROOVER, 2013, p. 60]. In metal formation, the flow stress Y_f is defined as the instantaneous value of the stress required to continue deforming the material to keep the metal flowing. It is the yield strength of the metal as a function of strain, which can be expressed as

$$Y_f = K\epsilon^n. \tag{A.3}$$

As a result of this characteristic of the steel sheet stamping (forming) processes, the final condition of the material behaves as item (B) of Figure 107. Residual stresses generally cause the "spring back effect ", that is, the tendency of the material to partially recover under the original condition.

Grzesik [2017, p. 556] proposed a model for residual stresses, according to Figure 108. His proposal is based on machining processes, but the model can be adapted to other manufacturing processes.

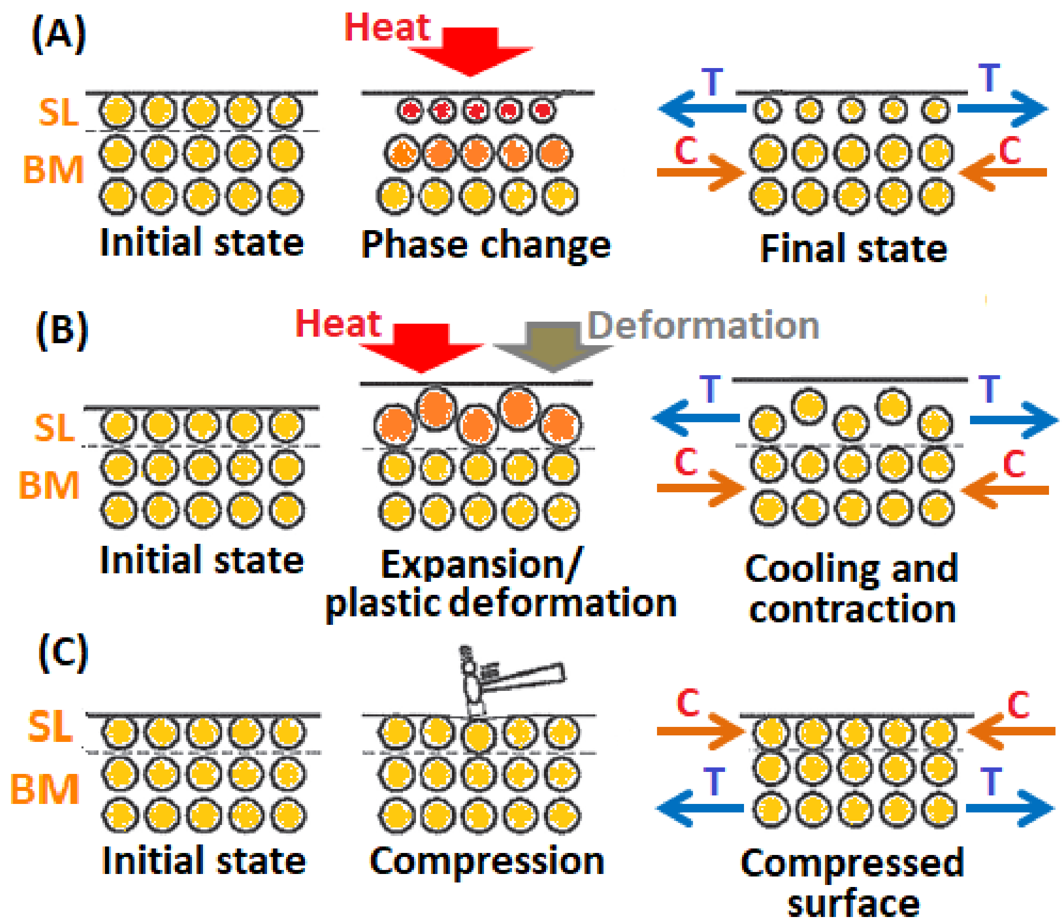

Figure 108 – Models for residual stresses. (Source: based on [GRZESIK, 2017, p. 556]).

An explanation of Figure 108 follows:

- In case (A), the thermal phase transformation mechanism is also called thermal or hot model, and the residual stress is caused by a volume change. If the change in phase causes a decrease in volume, the surface layer is under tension, and a tensile residual stress is induced;
- Case (B) represents a thermal/plastic deformation, also called mixed model. The heat supply causes the surface layer to expand, and this expansion is relieved by the limited plastic flow to the surface layer. During cooling, the surface layer contracts, resulting in a tensile residual stress;
- In case (C), there is a predominant mechanical plastic deformation, called a mechanical or cold model. The residual stress is compressive because the surface layer is compacted by mechanical action. This model applies mainly to burnishing in which

significant tangential compressive stresses with a maximum value at a certain depth below the surface are generated.

The case (A) model is suitable for the conventional heat treatment of steel. Welding can also use this model;

In a drawing, the cross section of a long rod or wire is reduced or changed by pulling (hence the term drawing) through a die called a draw die. Because they undergo non-uniform deformation during the drawing, cold-drawn products usually have residual stresses. For light reductions, such as only a few percent, the longitudinal surface residual stresses are compressive (while the bulk is in tension), and the fatigue life is thus improved. In contrast, heavier reductions induce tensile surface stresses (while the bulk is in compression). Residual stresses can be significant in causing cracking of the part due to stress corrosion over time. Furthermore, they cause the component to warp if a layer of material is removed subsequently, such as by slitting, machining, or grinding [KALPAKJIAN; SCHMID, 2010, p. 377].

Beneficial surface plastic deformation is promoted to improve the mechanical characteristics of the material, such as fatigue strength, by developing compressive stresses in a layer adjacent the surface of the part. In shot peening, a high-speed stream of small cast steel pellets (called shot) is directed at a metallic surface with the effect of cold working and inducing compressive stresses in the surface layer. Shot peening is used primarily to improve the fatigue strength of metal parts [GROOVER, 2013, p. 724]. Figure 109 illustrates the effect.

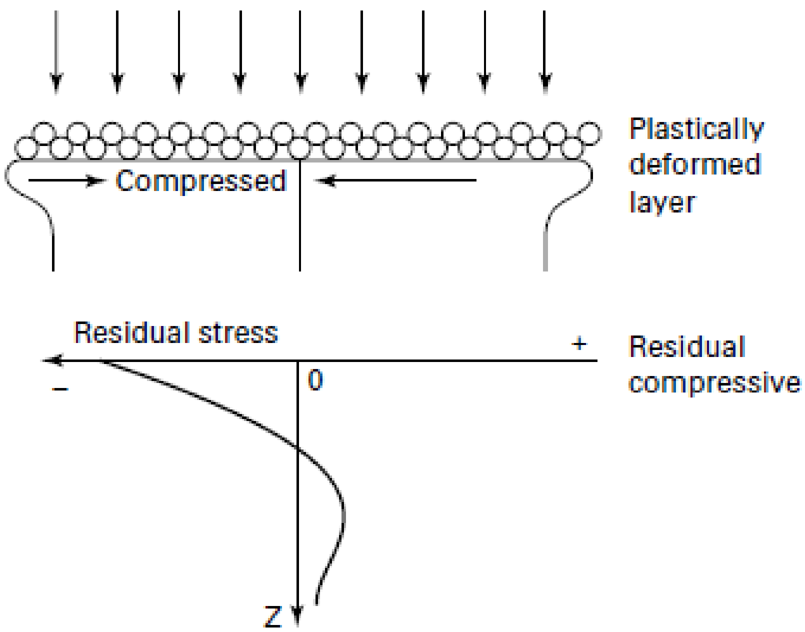

Figure 109 – Surface layer residual compressive stresses by shot peening. (Source: based on [BLACK; KOHSER, 2008, p. 963])

.

Roller burnishing can be used to improve the size and finish of internal and external cylindrical and conical surfaces. The hardened rolls of a burnishing tool press on the surface and deform the protrusions to a more nearly flat geometry. The resulting surfaces have improved wear and fatigue resistance, as they have been cold worked, and are now in residual compression [BLACK; KOHSER, 2008, p. 417], as shows Figure 110.

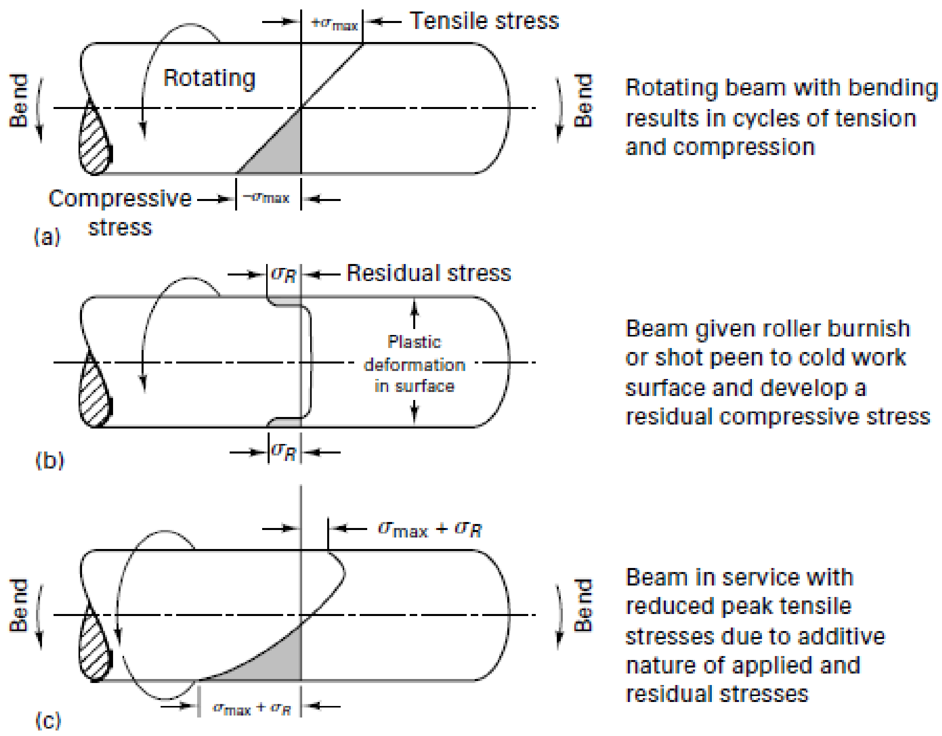

Figure 110 – Surface layer residual compressive stresses by roller burnishing. (Source: based on [BLACK; KOHSER, 2008, p. 964]).

Ground surfaces can have residual tension or residual compression, depending on the mix between chip formation and plowing or rubbing during the grinding operation. If sufficient heat is generated, phase transformations can occur in the surface and subsurface regions [BLACK; KOHSER, 2008, p. 962].

Thermal origins

For illustration, an engine block is shown in Figures 111 and 112 showing both the residual tensile and compressive stresses that remain from the casting process.

Figure 111 – Tensile residual stresses on a engine block casting at room temperature. (Source: based on [MAGMA, 2020]).

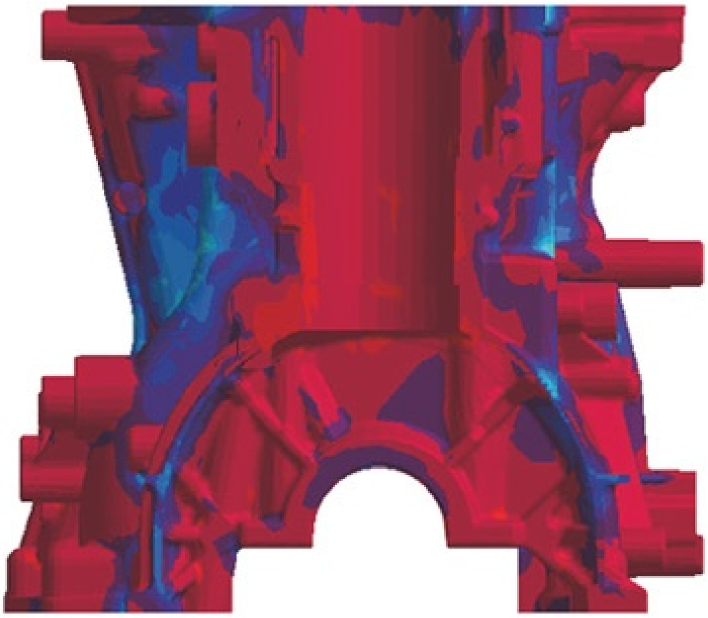

Figure 112 – Compressive residual stresses on a engine block casting at room temperature. (Source: based on [MAGMA, 2020]).

Methods for measuring residual stresses can be destructive or nondestructive and are described in the Measurement section.

A.2.3 Control of the manufacturing variation: quality control

The objective of quality control is to ensure that the dimensions of the components and assemblies are in accordance with the specified design values in a desired and acceptable proportion. As discussed above, this is not a technical decision, but an economical one, since the tighter the accuracy of the MFG process, the higher the cost of the part. Furthermore, quality concerns bring functional concerns with their consequences.

The potential of the process to produce parts within the design specification is called **process capability** (PC). Black and Kohser [2008, p. 979] presented a good discussion on this matter, as follows:

1. "If the PC is on the order of two-thirds to three-fourths of the design tolerance, there is a high probability that the process will produce all good parts over a long period of time";

2. "If the PC is on the order of one-half or less of the design tolerance, the selected process may be considered too good; in this case, it may be possible to trade off some precision in this process for looser specifications elsewhere, resulting in an overall economic gain";

3. "Quality in well-behaved processes can be maintained by checking the first, middle and last parts of a lot or production run. If these parts are good, then the lot is certain to be good. This is called $n = 3$. Naturally, if the lot size is 3 or less, this is a 100% inspection. Sampling and control charts are also used under these conditions to maintain the objective and variability of the process".

The statement of item 1 supports the proposal of our thesis on the statistical approach. Alternatives for non-capable processes could be:

1. Shift the job to another machine with greater process capability.

2. Getting a review of the specifications to see if they may be relaxed.

3. Sorting of the product to separate the good from the bad. This involves 100% inspection of the product, which may not be a feasible economic alternative unless it can be done automatically. Automatic sorting of the product on a 100% basis can ensure near-perfect quality of all accepted parts, but, even in these cases, a cost issue is still present, because the production of defects had already been paid. Furthermore, automated sorting does not determine the causes of defects, leading to a simple "automated defect finder";

4. Determining whether the precision (repeatability) of the process can be improved by:

   a) Switching cutting tools, workholding devices, or materials;

   b) Overhauling the existing process and/or developing a preventive maintenance program;

c) Finding and eliminating the causes of variability, using cause-and-effect diagrams;

d) Combinations of (a), (b), and (c);

e) Using designed experiments and Taguchi methods to reduce the variability of the process.

The solution to this problem was reached by statistical quality control (SQC). As variability may be affected by several factors, as already mentioned, the probabilistic distribution of each of these factors can take any shape so that the variability distribution of each measured quantity could be determined. This could be considered troublesome as the statistical behavior of each factor is not known.

However, a solution was found to deal with this problem: the concept of the central limit theorem ([FISCHER, 2010]). The essence of this concept is that: "if a population has a finite variance σ^2 and a mean value μ, then the distribution of the mean of the sample approaches the normal distribution with variance $[\sigma^2/n]$ and mean μ as the sample size n increases", and "nothing is said about the form of the population distribution function" ([HAUGEN, 1968, p. 53]). Based on this consideration, the normal distribution is acceptable for any measured value provided that the sample size is chosen adequately. Perhaps the first and most comprehensive study on sampling theory in general statistics applications has been conducted by Deming [1950], which has been used as a reference in several subsequent works.

Quality control and statistical tolerancing are important in preventing drifts and shifts in the distribution mean, as discussed below. Gradual drift can occur, for example, due to tool wear in a machining process. Shifts can be caused by a change in suppliers or differences in raw material hardness ([EVANS, 1975b, p. 73]). In the last case, acceptance sampling tests can be used on incoming material lots for this purpose and then incorporated into an existing quality control program ([DUNCAN, 1959, p. 215]).

Statistical Distributions

Properly controlled manufacturing processes produce parts with continuously distributed random dimensions. The collection of data of these dimensions allows the calculation of the mean and variance of a statistical distribution of each component; the type of statistical distribution depends on the acceptance inspection of the produced parts. According to Bury [1975, p. 446]:

- In case of a 100 % inspection, for example, by a fixed gauge checking [CURTIS; FARAGO, 2014, p. 33], the dimensions are certainly within the design specification; otherwise, the parts are rejected. In this case, the beta distribution is indicated because the variation limits are contained in a finite range. However, such an inspection type is indicated only for low production volumes, for cost reasons, or when critical safety design constraints are involved. An example of this case can be found in [UMARAS et al., 2019];

- When statistical sampling is used for inspection [COLOSIMO; SENIN, 2011, p. 237], as in the case of medium-high manufacturing volumes, mainly in the case of material removal processes, the normal distribution is recommended. In this case, some specimens may have dimensions beyond the tolerance limits. Theoretically, this behavior indicates a distribution with unlimited tails.

The general range of a probability distribution for a manufacturing process presents little statistical significance because an infinite number of parts would be considered in part production, which is beyond reality. To overcome this problem, the Monte Carlo Method (MCM) [HAMMERSLEY; HANDSCOMB, 1964; KALOS; WITHLOC, 2004] is used for the production simulation by generating random numbers. The power of the method is to consider only the most probable statistical values, disregarding the values that approximate the infinite tails of the distribution. Theoretically, values tending to infinite are only to be accessed when the production volume also tends to infinite. The probability distribution may then more accurately reflect the intended number of parts to be produced. In fact, the method is also used to estimate the uncertainty of the coordinate measurement machine (CMM) uncertainty [HOCKEN; PEREIRA, 2012, p. 256], as illustrates Figure 113. An example of an application can be found in [UMARAS et al., 2020].

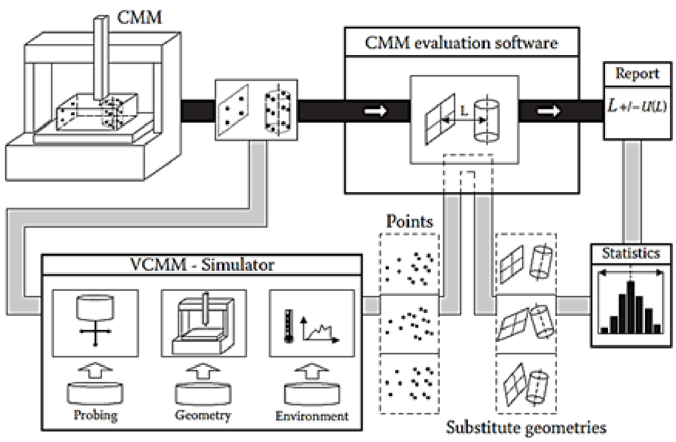

Figure 113 – The virtual CMM concept. (Source: based on [HOCKEN; PEREIRA, 2012, p. 373]).

A.2.3.1 Data acquisition and analysis

High-production data acquisition is currently performed by automated or sampling inspection, depending on the characteristics of the product and the degree of confidence needed. Curtis and Farago [2014, Chapter 19], presented an overview of automated inspection, which can be carried out using the contact or non-contact inspection procedures already discussed. The sampling procedures are discussed in the following section. Regarding the sampling of mass production, Neyman [1941] raised interesting issues in dealing with this statistical procedure.

Sampling

For industrial processes, measurements are made by statistical sampling at a rate determined by the importance of quantity (dimension) for the functional requirements of the product. The results of data acquisition are recorded and analyzed using *control charts*. A control chart consists of the upper control limit (**UCL**) and the lower control limit (**LCL**), on which the values of some statistical measure are plotted for a series of samples or subgroups. The chart frequently shows a central line to help detect a trend of plotted values toward either control limit [QUALITY, 2020]. A great development in this area was observed on the occasion of the Second World War. Smith [1947] and Rice [1947] developed two original works specifically for this purpose. Figure 114 illustrates an example of a generic control chart, where the zone between the LCL and UCL lines represents the specified range of values, that is, the lower specification limit (**LSL**) and the upper specification limit (**USL**).

Perhaps the first comprehensive and specific work on sampling has been done by Deming [1950] with his "Some Theory of Sampling".

Buescher [1984] discussed the issue of errors in the sampling process and provided suggestions to prevent them. Black and Kohser [2008, p. 987] also treated the sampling errors with two examples:

- When the process is running perfectly, but the sample data indicate that something

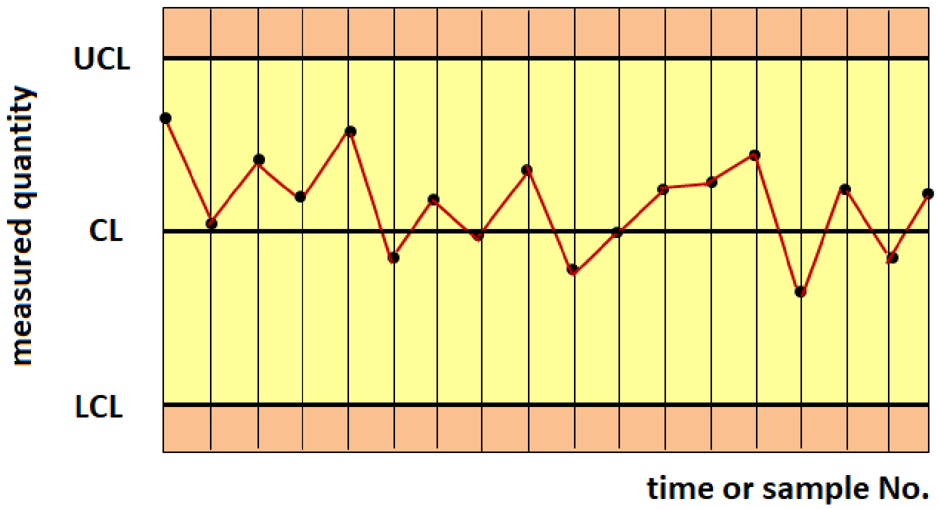

Figure 114 – A control chart.

is wrong, the decision is to stop the process to make adjustments;

- when the process is not running perfectly and is making defective products, but the sample data do not indicate anything wrong, and the process is not stopped to set it right.

Another interesting approach was proposed by Parkinson [1988], based on the reliability of post-quality control.

Wilks [1941] reported the importance of determining the sample size by setting tolerance limits. In another different approach, Belle [2008, Chapter 2.1] suggested calculation of a sample size using the "rule of thumb".

Evans [1963] introduced the concept of "multiplex sampling" as *a method for estimating characteristics of the response by a sampling technique when the response is a function of several independent variables and each of the several variables is available in a variety of completely known distributions.* In other words, he proposed calculating an estimate by appropriately weighting the observations and then reusing the sample, instead of sampling from a fictitious distribution, as done by the Monte Carlo method.

A.2.3.2 Statistical Process Control

The control chart is the basis for statistical process control (SPC). It seems that SPC has its origin in the work of Shewhart [1931] on quality control. In the following work [SHEWHART; DEMING, 1939], the same author, in partnership with W. E. Deming deepened the statistical content of quality control. Several works have been published since then, focusing on the analysis of the control charts to keep the process under control and to search for causes of deviations from the specified target value. Some of them are Wheeler and Chambers [1992], Oakland [2003], [THOMPSON J; KORONACKI, 2002]; Dissertations and Ph.D. theses have also been written on the subject: [ZALEWSKI, 1995], [OLWELL, 1996]. Andrássyová et al. [2012] deal with nonnormal data in the automotive industry; Jeang and Chung [2008] considered the influence of deterioration of product usage during its useful life in the SPC analysis; Quesenberry [1988] and Jagadeesh and Babu [1994] describe an approach to SPC that includes a tool wear process.

SPC monitoring during production is necessary to prevent the shipment of defective products. The process capability concept is described in this way.

The SPC task is to monitor the output of the process by means of measurements and registering the specified features of the part. Regarding dimensional variation, (Spotts [1983, Chapter 7] cited important concepts on the reason for the variability of a process:

- *Assignable causes*: A small modification in the process can cause variations in a dimension. A slight change in the properties (e.g. hardness) of the raw material can cause the dimension to vary. Tools will wear and must be reset. Changes can

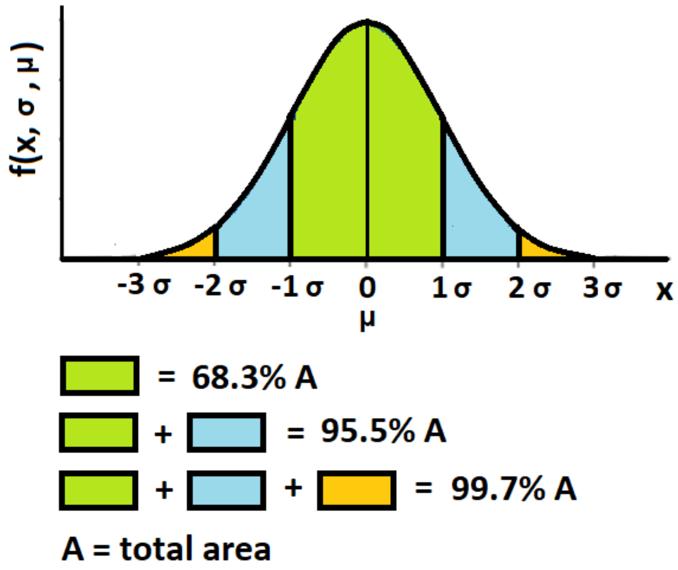

Figure 115 – Probabilities given by a normal distribution in standard deviation intervals (based on [HAHN; SHAPIRO, 1967, p. 72]).

occur in speed, lubricant, temperature, operator, and other conditions. A systematic search will generally bring these causes to light, and steps can be taken to have them eliminated;

- *Chance causes*, on the other hand, occur at random and arise from vague and elusive forces that can be neither traced nor measured. They are inherent in production equipment and occur even though all other conditions have been kept as constant as possible. Individually, a chance cause may be very small, but the cumulative effect will cause variability in the product. A dimension may be controlled so that it falls within a tolerance limit, but the precise length that results is usually determined by chance causes.

The concept of process capability

The normal (or Gaussian) distribution is the statistical model most commonly used ([HAHN; SHAPIRO, 1967]- p.69). Its probability density function is given by:

$$f(x; \mu, \sigma) = \frac{1}{\sigma\sqrt{2\pi}} exp\left[-\frac{(x-\mu)^2}{2\sigma^2}\right] \tag{A.4}$$

Here μ and σ are the mean and standard deviation of the distribution, respectively. The standard deviation is the square root of the variance σ^2.

The probability defined by a probability density function *pdf* is given by the area delimited by an interval of x, as illustrated in Figure 115.

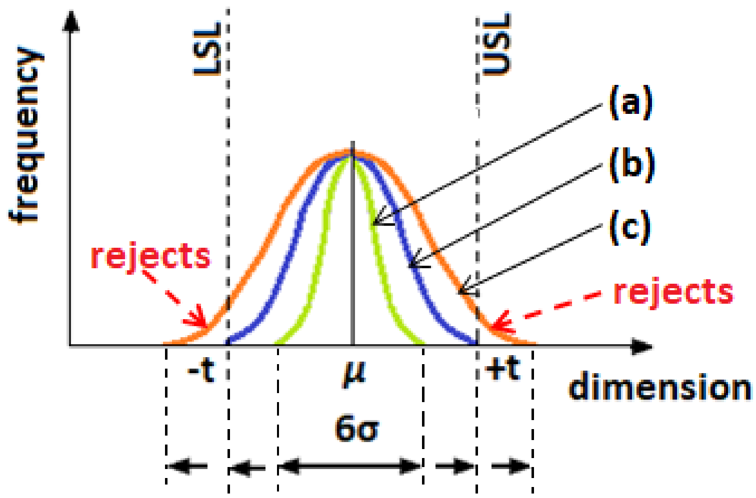

Figure 116 – Possibilities of precision of a process (based on [OAKLAND, 2003, p. 260])

As can be seen in the figure, the area below the probability density function of a normal distribution in the range of $\pm 3\sigma$ corresponds to the probability of 99.7%. This observation gives rise to three possibilities between the differences in the values of the difference between the specification limits $(USL - LSL)$ and 6σ, as illustrated in Figure 116.

In the figure, three levels of process precision ([OAKLAND, 2003, p. 261]) are identified:

a) High Relative Precision, where $(USL - LSL) >> 6\sigma$;

b) Medium Relative Precision, where $(USL - LSL) > 6\sigma$;

c) Low Relative Precision, where $(USL - LSL) < 6\sigma$.

Process capability indexes

A process capability index is a measure that relates the actual performance of a process to its specified performance [OAKLAND, 2003] - p. 261.

The index Cp was created as a forecast of nondefective products delivered to the customer [TAGUCHI et al., 2005]. It is calculated as the ratio of the dimensional tolerance range to six standard deviations:

$$Cp = \frac{tolerance}{6\sigma} \tag{A.5}$$

In Figure 116 the rejected fraction of the production is shown on both sides of the normal distribution. In this case, $Cp < 1.0$, and the process is considered incapable. In the opposite direction, the greater the Cp value above unity, the greater the capability of the process. The index is effective in evaluating the process capability when the process has a mean centered on the specification limits. A better illustration of the process capability was provided by Groover [2013]. Table A.9 shows the defective ppm versus Cp.

Table A.9 – Defective parts per million versus the process capability index

No. of σ	Cp	Defective ppm
±1.0	0.333	317.400
±2.0	0.667	45.600
±3.0	1.0	2.700
±4.0	1.333	63
±5.0	1.667	0.57
±6.0	2.0	0.002

Source: Groover [2013, p. 1061].

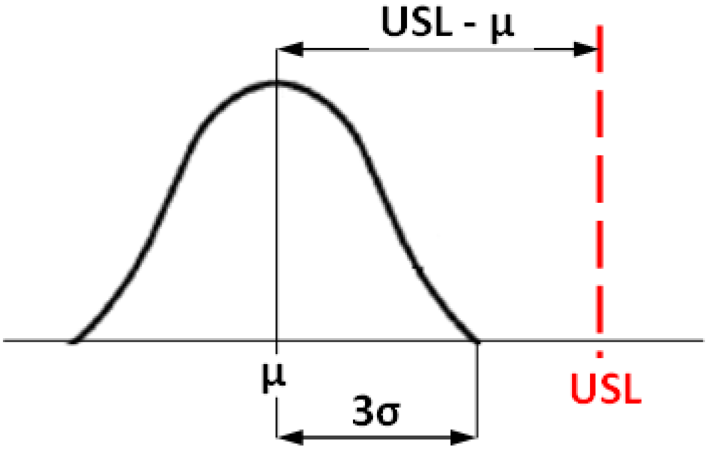

Figure 117 – Illustration of the variables for Cpk_u calculation

The index Cpk was developed to overcome the limitations of the index Cp and considers both the comparison of the specification with 6σ and the position of the distribution mean. The value of Cpk, or "overall Cpk" is defined as the lower value between the other two indexes Cpk_u and Cpk_l:

$$Cpk_u = \frac{USL - \mu}{3\sigma} \qquad Cpk_l = \frac{LSL - \mu}{3\sigma} \tag{A.6}$$

Figure 117 illustrates the meaning of Cpk_u for a capable process.

The characteristics of Cpk are as follows:

1. If $Cpk \leq 1$ the process is incapable because its variation and centering are such that at least one of the tolerance limits are exceeded;

2. The process capability increases with increasing values of Cpk above 1.0 (as in the case of Cp);

3. The Cpk value may be increased by neighboring the mean of the process with the mid-specification value;

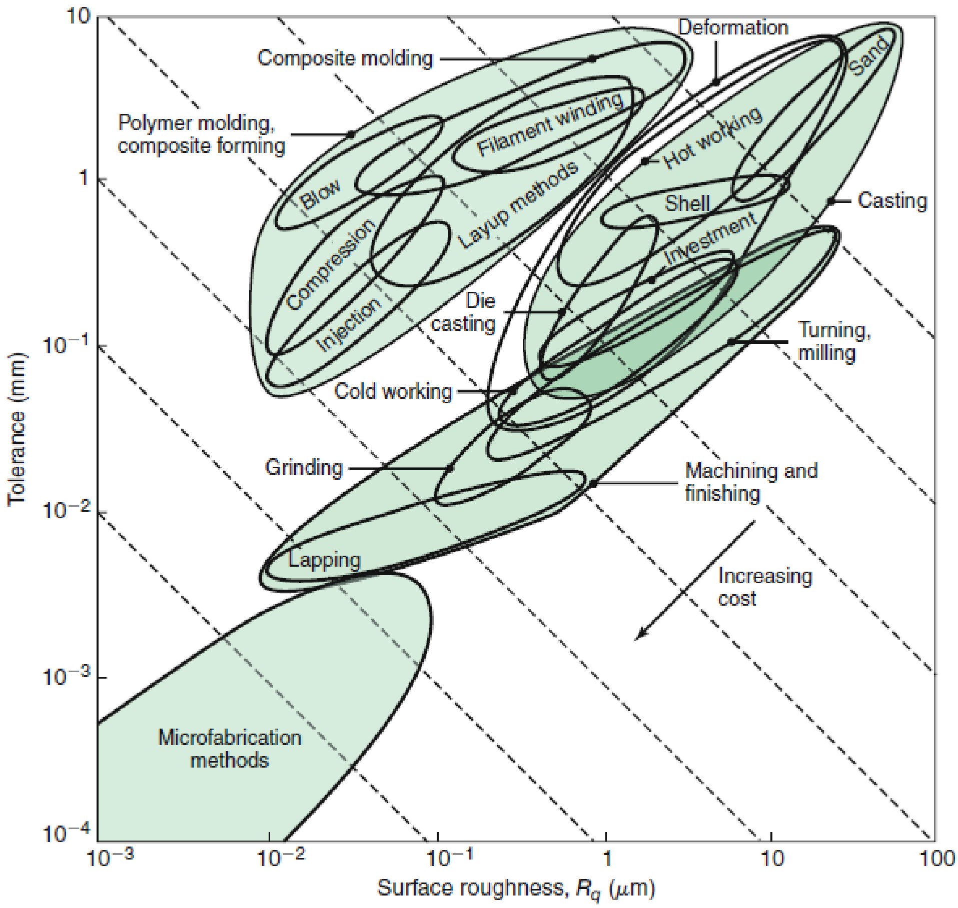

Figure 118 – Achievable tolerance vs. surface roughness for several MFG processes. Source: [KALPAKJIAN; SCHMID, 2010, p. 1150].

4. The difference $Cp - Cpk = 0$ when the mean of the process is centered with the mid value of the specification.

Capability of manufacturing processes

After discussing the process capability and its indexes, the remaining issue is raised from the characteristic variation of different available processes. This information is important to designers when specifying the feasible design tolerance range, that is, the limits USL and LSL. Fortunately, the values are available in the specific literature. Kalpakjian and Schmid [2010] supply useful values, as shown in Figure 118, where the dashed lines indicate cost factors.

A.2.4 The Monte Carlo Method (MCM)

The Monte Carlo method, or better methods, deals with generating random variables (or simply "variates" [HAHN; SHAPIRO, 1967, p. 23]) using probability density functions to estimate unknown parameters or general functions of unknown parameters and to compute their expected values, variances, and covariances [KOCH, 2018]. Due to the importance of MCM, a historical description was researched and presented in the next section.

Random and Deterministic Data

In this text, the term random has a statistical meaning. Other approaches cited in non-scientific references [POYTHRESS, 2014] are not applicable due to conflicting interpretations.

An interesting early work from Kuznets [1929] cites the behavior of random events, but in an opposite way, that is, according to the author, the summation of random events can transform random events into a cumulative series of ordered behaviors, such as oscillatory fluctuations. In our work, these considerations are not approached due to its scope.

Bendat and Piersol [2010, Chapter 1] define and cite examples to illustrate the differentiation between deterministic and nondeterministic (random) data:

1. "Deterministic data are those that can be described by an explicit mathematical relationship". Examples: a mass-spring system can be represented by a periodic mathematical equation in function of the mass, the spring constant, and the time; the motion of a satellite in orbit about the earth; the potential across a condenser as it discharges through a resistor; the vibration response of an unbalanced rotating machine; the temperature of water as heat is applied;

2. Random data are those that it is impossible to predict an exact value at a future instant of time; each observation is unique - and must be described in terms of probability statements and statistical averages. Examples: the height of waves in a confused sea; the acoustic pressures generated by air rushing through a pipe; the electrical output of a noise generator.

According to the same authors, a single time history representing a random phenomenon is called a "sample function" or a "sample record" (when observed over a finite time interval). The collection of all possible sample functions produced by the random phenomenon is called a "random process" or a "stochastic process". Therefore, a sample record of data for a random physical phenomenon represents the physical realization of a random process. Figure 119 shows a sample record example. In a previous section, a record of dimensional measurements was treated as random data in a manufacturing statistical process control.

Figure 119 – A sample record of a random event. (Source: based on [BENDAT; PIERSOL, 2010, p. 9]).

The authors also classify the random data into two groups:

1. Stationary:
   - Ergodic
   - non-ergodic
2. Nonstationary:

This classification is used when the sample record properties of a collection of sample records are compared in relation to the mean and autocorrelation in a fixed time interval. As these concepts are not used in this work, a comprehensive description will not be developed.

MCM General Description

According to Metropolis [1987, pp. 126,127], the MCM started in 1946 at Los Alamos Laboratory with the availability of the first electronic computer, the ENIAC, although statistical sampling techniques already existed at that time, but their applications were very time consuming due to the need of tedious and most of the time impracticable manual calculations. The name Monte Carlo seems to be derived from an analogy of a card-playing game - the solitaire - due to its random behavior. Stam Ulam suggested the name for a possible statistical approach to solving the problem of neutron diffusion in fissionable materials. The method idea had been developed more than ten years earlier by Enrico Fermi when he was studying the moderation of neutrons in Rome, but, due to the calculation constraints, it had not succeeded. Compilation of all documents that reference the beginning of MCM was carried out by Eckhardt [1987] and the first description of the method was carried out by Metropolis and Ulam [1949].

It is worth mentioning that mechanical continuous calculation machines have already been developed long before, as described by Thomson [1912, Appendix B], for the calculation of simultaneous linear equations, tide prediction, and for the calculation of the integral of the product of two given functions. Other very interesting work that focused specifically on mechanical calculation machines was written by Murray [1947], which also included some electrical devices. However, only the development of electronic machines allowed the speed necessary for developing an intensive simulation process. A concern reported by Hammersley and Morton [1954] was the computation time required by the MCM simulation due to the level of development of electronic devices at that time: in the paper "Poor Man's Monte Carlo" they proposed a manual calculation, giving some application numerical examples, since the availability of electronic computers was prohibitive due to their lack of availability and cost for an ordinary man. The simulation has been carried out with extremely hard work by means of the random generation of numbers by different methods [WARNOCK, 1987] and published tables [KENDALL; SMITH, 1939; FISCHER; YATES, 1943]. In the following work [HAMMERSLEY; MORTON, 1956], the same authors raise concerns about achieving a small standard error in the final result of the MCM simulation. They also reported on the limitations of electronic computers at that time and gave an example: To reduce a standard error by a factor of k, the labor involved must be increased by k^2, and it is stated: "The remedy lies in a skillful choice of sampling technique and the substitution of analytical methods for random processes where possible. The efficiency of an MCM process can be taken as inversely proportional to the product of the sampling variance of the final estimate and the amount of labor expended in obtaining this estimate; and it is profitable to allow some increase in labor if this produces an overwhelming decrease in the variance. In a parallel work, Hammersley and Mauldon [1956] introduced the concept of antithetic variates. They distinguished two desirable properties of an MCM: reliability and precision. The antithetic variate method consists of choosing a functional or stochastic dependence between the variates in such a way that precision is improved without sacrificing reliability. The MCM, started with nuclear physics, has been developed since that time, has been revealed to be a powerful simulation tool, and has proven its effectiveness for decades in several areas of knowledge, such as mathematics, general physics, economy, and biology. This range of applications can be seen in a bibliography between the years 1949 and 1963, compiled by the University of California [KRAFT; WENSRICH, 1964]. Indeed, not just one but several MCMs may be considered, depending on how and under what conditions they are applied. Hammersley and Handscomb [1964, p. 2], define: "MCM comprises that branch of experimental mathematics that is concerned with experiments with random numbers. The problems handled by MCMs are of two types, called probabilistic or deterministic, depending on whether or not they are directly concerned with the behavior and outcome of random processes". The simplest MCM approach is probabilistic in which random numbers are observed and chosen in such a way that they directly simulate the physical random processes of the original problem. The desired solution is found by inference from the behavior of these random numbers (this was used in our case study). On the other hand, the idea behind the MCM approach to deterministic problems is to exploit the strength of theoretical mathematics, its abstraction and generality, while avoiding its associated weakness by replacing the theory by experiment whenever the former falters. The inherent weakness can be explained by the fact that the more general and formal language, the less the theory is ready to provide a numerical solution in a particular application. Thus, the deterministic problem can be solved numerically by an MCM simulation, as a probabilistic problem. Perhaps the first mention of the solution of a deterministic problem is the calculation of number π [KALOS; WITHLOC, 2004, p. 4].

Features and Application

As already mentioned, stochastic MCM was originally developed in Los Alamos Laboratory, which has spread over several methods and applications. Doolen and Hendricks [1987] report the two originally derived methods: 1. The Monte Carlo Neutron and Proton Transport Code (MCNP) and 2. The Metropolis method. The MCNP code features a general 3D geometry, a continuous energy or multigroup physics package, and sophisticated variance reduction techniques. Even very complex geometry and particle transport can be modeled almost exactly. The Metropolis method [METROPOLIS et al., 1953] intends to find an energy equilibrium solution for any physical system as follows:

1. In the general procedure for finding the lowest energy state of a system of many particles, the system energy is calculated, then the particles are randomly moved a small distance and the energy is recalculated; if the energy has decreased, the new position is accepted, and the procedure continues until the energy no longer changes;

2. When a move results in an increased energy, the new position is accepted with probability $\exp(-\Delta E/T)$, where ΔE is the change in energy and T is the temperature. This procedure gives the equilibrium for any physical system. A system with many particles can be solved with only a few lines of code on a fast computer.

After the 1960s, several MCM features were developed, and the range of their application has been widened. Kroese et al. [2011] display a general overview and systematic development of several MCM resources and application possibilities. The most important of them are also specifically developed by other authors, although more than one resource can be applied in the same application:

- Mathé and Novak [2007] analyze the integration error of optimal algorithms using a simple MCM and the Metropolis Method;

- Bardenet [2013] describes the MCM sampling methods: the inverse cumulative distribution function (cfd) method; the transformation method, rejection sampling, and importance sampling;

Hahn and Shapiro [1967, p. 236] describe the use of MCM simulation as a method to obtain information on the performance of the system from component data and refer to it as synthetic sampling or empirical sampling. They suggest an example of the procedure of MCM application to evaluate system performance by building mathematical models of their behavior and evaluate the performance of these synthesized systems:

1. Consider a system made up of several components;

2. Consider the availability of $1,000$ of each component that makes up the system;

3. So, it is possible to build $1,000$ systems and obtain $1,000$ measurements of system performance.

This can represent a probabilistic approach to system performance. However, if the structure of the system is known, that is, the relationship between the component variables and the performance of the system, this performance can be calculated from the measurements of the components without actually building the system. Moreover, if the distribution of each component variable is known, it is possible to obtain synthetic measurements of these components by drawing 1000 random values from each distribution, without having $1,000$ samples of each component. These random values can then be used to calculate the performance of $1,000$ synthetic systems. This procedure is called MCM according to the authors, but as mentioned before, this is a reference to the deterministic form of MCM.

Shapiro and Gross [1981, p. 273] compare the MCM with the gambling operations in Monte Carlo, the capital of Monaco: in the simulation study, the "game" is a functional or mathematical representation of the system, and chance factors are the random variables used to represent the components of the system. They present some application examples. This is also a case of a deterministic problem, since a distribution is needed to represent the system. Haugen [1968, p. 178] also distinguishes the probabilistic and deterministic forms of MCMs.

Skowronski and Turner [1997] describe a MCM variance reduction technique, cite the features of the method, and raise its main issue: an increase in accuracy by a factor of 10 requires that the number of simulation samples be increased by a factor of 100 and invokes the computation time and cost. However, nowadays this issue is of lower importance due to the current power of available CPU processors. An example is used to illustrate the efficacy and accuracy of MCM in calculating integrals of functions. To avoid a large number of samples, two methods for variance reduction are presented:

1. The correlation method, which replaces the function being evaluated by an approximation or correlation function. An MCM calculation estimates the error between the approximation and the actual function. Since the error term is smaller than the

actual function value, the variance is smaller in relation to the total calculation than using MCM on the actual function;

2. Importance sampling, where a large fraction of the samples are drawn from regions where the function being evaluated has a small value relative to the rest of the probability space. Samples from such a region contribute little to the total MCM, so the technique avoids sampling these regions and makes better use of the available samples.

Skowronski [1998] provide formulas for estimating the derivatives of the acceptance fraction with respect to the parameters of the manufacturing variation distribution. According to the authors, the formulas have been shown to be more accurate than the finite-difference technique for computing derivatives. The authors also found that a combination of correlation and importance sampling techniques proposed by Skowronski and Turner [1997] provides the greatest accuracy.